The Development of a Catalytic Asymmetric Bromination Reaction of Alkenes

A thesis submitted by

Mrs Joanna Redmond

to Imperial College London in partial fulfilment of
the requirements of the degree of

Doctor of Philosophy

Department of Chemistry
Imperial College London
South Kensington
London SW7 2AZ
United Kingdon

December 2007

Abstract

This thesis describes our investigations into the development of a general method for the catalytic, asymmetric bromination of alkenes. The bromination catalysts employed in the research are *ortho*-substituted iodobenzenes, which are hypothesised to deliver Br^+ to the alkene substrate *via* a hypervalent I(III)-Br bond.

Initially, endeavours to achieve a large scale preparation of our asymmetric bromination catalyst, 2,6-di-[(4*R*,5*R*)-4,5-diphenyl-4,5-dihydro-1*H*-imidazol-2-yl]iodobenzene, or *R*-IBAM, are detailed. In order to facilitate this, a large quantity of enantiopure 1,2-diphenylethylene diamine was required to form the chiral amidine moieties of our *R*-IBAM catalyst. Thus, the development of two novel methods for the synthesis and resolution of 1,2-diphenylethylene diamine are described and the subsequent application of each route to a large scale preparation of the enantiopure diamine. The subsequent novel and optimised preparation of our catalyst to produce 25 g of *R*-IBAM is detailed.

The following studies into the catalytic asymmetric bromination of alkenes include the screening of the various reaction conditions, stoichiometric addition of *N*-bromosuccinimide to the catalysts and the synthesis and screening of a range of *R*-IBAM derivatives and analogues. An improved understanding of the catalytic cycle and the possible mechanisms of loss of enantioexcess in our brominated product is detailed.

The final section of the thesis describes research into the exchange of Br^+ between enantiopure bromonium ions and alkenes. The generation of an enantiopure bromonium ion in the absence of alkene was achieved *via* the rearrangement of enantiopure bromohydrin, (2*S*)-1-bromo-1-phenylpropan-2-ol. The intermediate bromonium ion was trapped by chloride to produce the enantiopure bromochlorinated product. This, to the best of our knowledge, represents the first example of the generation and trapping of an enantiopure bromonium ion. Our subsequent investigations into Br^+ transfer from the bromonium ion to added alkene are described.

Contents

Acknowledgements

First and foremost, my thanks to my supervisor, Dr. Chris Braddock for devising and driving forward such a fascinating project. I sincerely appreciate both the opportunity to work in his group, along with his time, ideas and encouragement over the past three years. I would also like to thank my industrial supervisor, Steve Hermitage, for his unfailing enthusiasm for the project and the invaluable insights from a fresh perspective. Thanks also for the careers advice and for all the help on my CASE placement; most especially for helping the big pot of IBAM to happen!

I am grateful to GSK for the CASE funding, the various chemicals that they have supplied me with along the way and for the opportunity to work in GSK laboratories in Stevenage for three months. Along these lines, thanks also to all the occupants of lab 2G 121 for welcoming me on my CASE placement, in particular Yui and Andy for sharing their wealth of GSK and chemistry knowledge!

My colleagues from the Braddock group have made working in the lab far more enjoyable (and challenging…) than it would have been without them. Thanks is due to Gemma, for easing my transition into the lab, and also to Simon A., Kiyo, Sav, Romain, Yolanda, Anna and Bingli for all their help and their friendship. Particular thanks are due to Sav and Anna for all the presentation practice, nerve calming and the proof reading.

The other groups within the Imperial Synthesis Section also deserve aknowledgement for their generosity in sharing resources. Thanks is especially due to the Barrett, Gibson and Spivey groups for the loan of chemicals, HPLC columns and the use of the Spivey HPLC machine (and to Paula, Sarah, Gill and Gordon for usually being the people to do the loaning!).

I am extremely grateful to the analytical services at Imperial College London; to Dick Shephard and Pete Haycock for NMR analysis, John Barton for mass spectroscopy and Andrew White for X-ray crystallography. Also thanks to Asha at GSK for her time and her chiral HPLC expertise; her input has proved invaluable over this final year.

I am deeply grateful to my parents for their support, advice (the “eight hour plan” still stands me in good stead), love and friendship. This thesis and all the work which has gone into it is dedicated to them. Thanks also to Jonathan, Susanna, Daniel and Josie for being wonderful big brothers and sisters in law; I have appreciated and continue to appreciate all your advice and kindness.

Kate and Sarah also deserve a special thank you; from Oxford to London, it would have been no where near as fun without you both. And to Jenny, Natalie, Claire, Katy, Anna and Kathryn: thank you for your friendship over so many years and for all the welcome weekends away from London and chemistry over the last three.

And finally thank you to Chris, my lovely husband, for the huge amount of love and support he has given me, particularly over the last three months. Thank you for putting up with the long and unpredictable hours, the chemistry-rants, the bad moods when it’s gone wrong and, more generally, thank you for making the last three years so wonderful. Here’s to the next sixty, hubby.

Abbreviations

*	Chiral centre or chiral group
Ac	Acetyl
AM	*Trans*-4,5-dihydro-2,4,5-triphenyl-1*H*-imidazole
Anal.	Analysis
aq.	Aqueous
Ar	Aryl
BAM	1,3-Di-(4,5-diphenyl-4,5-dihydro-1*H*-imidazol-2-yl)benzene
Bn	Benzyl
Boc	*t*-Butyloxycarbonyl
b.p.	Boiling point
br	Broad
Bs	Brosyl
c	Concentration
ºC	Degrees Celsius
calcd	Calculated
CI	Chemical ionisation
cm^{-1}	Wavenumbers
Cy	Cyclohexyl
d	Doublet
DCC	*N,N'*-Dicyclohexylcarbodiimide
dd	Doublet of doublets
de	Diastereomeric excess
DIB	(Diacetoxy)iodobenzene
DIBAL-H	Diisobutylaluminium Hydride
DMAP	4-Dimethylaminopyridine
DMF	*N*,*N*-Dimethylformamide
DMSO	Dimethylsulfoxide
dt	Doublet of triplets
E	Energy
E^+	Electrophile
ee	Enantiomeric excess
EI	Electron ionisation

eq.	Equivalent
ES	Electrospray
Et	Ethyl
FAB	Fast Atom Bombardment
FT	Fourier Transform
g	Gram(s)
GC-MS	Gas Chromatography – Mass Spectrometry
h	Hour(s)
HMDS	Hexamethyldisilazane
HPLC	High Performance Liquid Chromatography
HRMS	High Resolution Mass Spectrometry
Hz	Hertz
IAM	2-(2-Iodophenyl)-4,5-diphenyl-4,5-dihydro-1*H*-imidazole
IBAM	2,6-Di-(4,5-diphenyl-4,5-dihydro-1*H*-imidazol-2-yl)iodobenzene
IR	Infra-red
J	Coupling constant
L	Litre(s)
L*	Chiral ligand
Lit.	Literature
m-	*meta*
m	Multiplet
M	Molar
*m*CPBA	3-Chloroperoxybenzoic acid
Me	Methyl
mg	Milligram(s)
min	Minute(s)
mL	Millilitre(s)
µL	Microlitre(s)
mmol	Millimole(s)
mol%	Molar percent
m.p.	Melting point
Ms	Methanesulfonyl (Mesyl)
MS	Mass Spectrometry
mTHF	2-Methyltetrahydrofuran

m/z	Mass to charge ratio
NBS	*N*-Bromosuccinimide
NIS	*N*-Iodosuccinimide
nm	Nanometre
NMR	Nuclear magnetic resonance
Nuc	Nucleophile
o-	*ortho*
p-	*para*
Ph	Phenyl
ppm	Parts per million
Pr	Propyl
q	Quartet
R	General substituent
RT	Room temperature
s	Singlet
S_N	Nucleophilic Substitution
t	Triplet
TBCO	2,4,4,6-Tetrabromocyclohexa-2,5-dienone
TES	Triethylsilyl
Tf	Trifluoromethylsulfonyl (Trifyl)
THF	Tetrahydrofuran
TIPS	Triisopropylsilyl
TLC	Thin layer chromatography
TMG	*N*,*N*,*N'*,*N'*-Tetramethylguanidine
TMS	Trimethylsilyl
Tol	Tolyl
Ts	Tosyl
UV	Ultra violet

1. Introduction: Asymmetric Electrophilic Bromination and the Bromonium Ion

1.1. A History of the Bromonium Ion

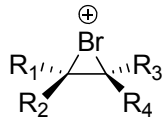

1

Figure 1: the bromonium ion as proposed by Roberts and Kimball

The bromonium ion, **1**, was first proposed as an intermediate in the electrophilic bromination of alkenes by Roberts and Kimball in 1937.[1] Previously, work by Bartlett and Tarbell[2] had demonstrated that the first step in the reaction of halogen molecules with olefins led to the formation of a negative halide ion and a positively charged organic ion. Roberts and Kimball invoked a bridged cationic intermediate (**1**) rather than an open *β*-bromocarbonium ion (**2**) to account for the well-established stereochemistry of the addition of molecular bromine to olefins.[3] They argued that the initial formation of a bromonium ion (preventing free rotation around the carbon-carbon bond), followed by its opening with bromide in an S_N2 manner, could account for the predominantly *trans* addition of bromine across the alkene.

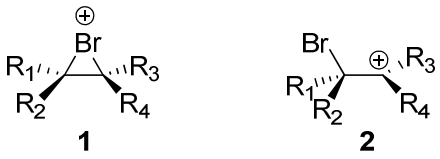

1 **2**

Figure 2: bromonium ion (1) or *β*-bromocarbonium ion (2)

It is interesting to note that even Roberts' and Kimball's original paper indicated that the "actual structure is undoubtedly an intermediate between **1** and **2**", due to the very small difference between the ionisation potentials of carbon (11.22 volts) and bromine (11.80 volts). This uncertainty in the nature of a bromonium ion has fuelled a scientific debate that has spanned almost six decades and, despite the emergence of much new evidence, has still not been satisfactorily resolved.

*1.1.1. Structure of the "Bromonium Ion"; Cyclic Bromonium Ion (**1**) or β-Bromocarbonium Ion (**2**)*

Subsequently to Roberts' and Kimball's proposal of a 3-membered cyclic bromonium ion intermediate, Winstein published a series of elegant investigations into bridging bromine in the reactions of 3-bromo-2-butanols.[4,5] Winstein and Lucas noted that when 2,3-diacetoxybutane is converted into 2,3-dibromobutane by the action of fuming hydrobromic acid, the transformation is accompanied by an odd number of inversions.[6] Thus, racemic (*R**,*R**)-diacetate **3** affords the *meso* (*R**,*S**)-dibromide **4** and the *meso* (*R**,*S**)-diacetate **5** affords the racemic (*R**,*R**)-dibromide **6** (Scheme 1).

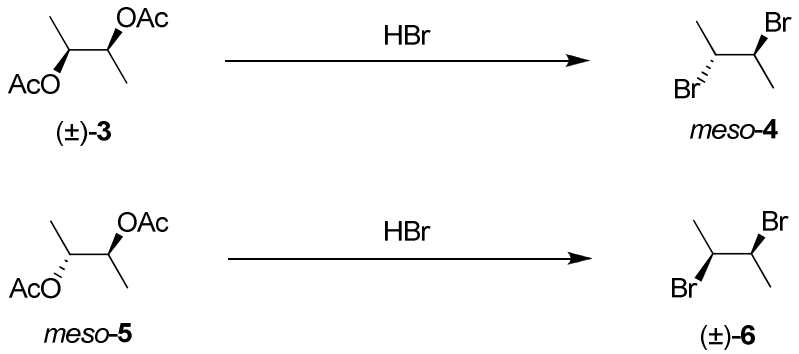

Scheme 1: reaction of 2,3-diacetoxybutanes with hydrobromic acid

The substitution reactions were demonstrated to proceed with complete stereoselectivity, each proceeding to give a single product. This unexpected phenomenon prompted Winstein and Lucas to investigate the reaction in greater detail in an attempt to elucidate its mechanism. It was found that 3-bromo-2-butanol (**7** and **8**) was the last of the intermediates in the reaction profile[7] and that it was the conversion of this to the dibromide that gave rise to the unexpected stereochemistry of the products. Winstein and Lucas observed that the reaction of racemic (*R**,*S**)-3-bromo-2-butanol (**7**) with hydrobromic acid affords pure *meso* (*R**,*S**)-2,3-dibromobutane (**4**), whilst racemic (*R**,*R**)-3-bromo-2-butanol (**8**) yields pure racemic (*R**,*R**)-2,3-dibromobutane (**6**) (Scheme 2).[4]

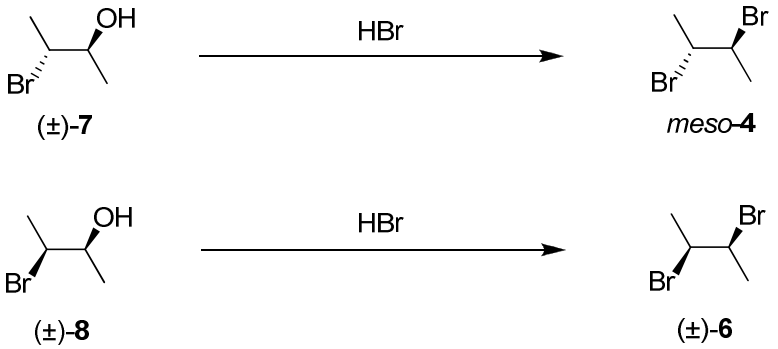

Scheme 2: reaction of 3-bromo-2-butanols with hydrobromic acid

As a possible explanation for the observed retention of configuration in the above reactions, Winstein and Lucas proposed a cyclic bromonium ion intermediate **10** (Scheme 3).

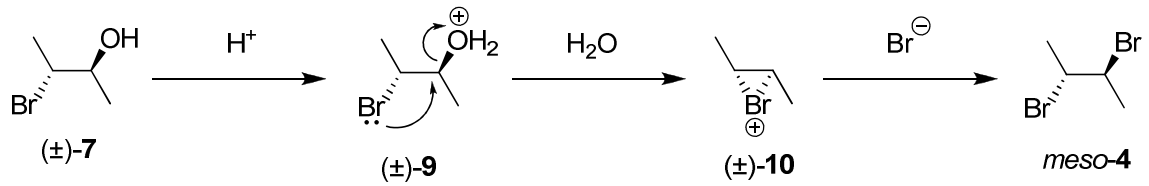

Scheme 3: Winstein's proposed bromonium ion mechanism

The proposed mechanism involves a double inversion, *via* neighbouring group participation of the bromine to expel water, followed by opening of the bromonium ion with bromide to afford the product with complete stereospecificity. Furthermore, Winstein hypothesised that this cyclic bromonium ion was analogous to that proposed by Roberts and Kimball as an intermediate in the electrophilic bromination of olefins.

As further confirmation of their proposed mechanism Winstein and Lucas repeated their experiments with optically active 3-bromo-2-butanols.[5] As expected, the optically enriched (+)-(*R**,*S**)-3-bromo-2-butanol (**7**) afforded the optically inactive *meso* dibromide **4**. Additionally, the optically enriched (-)-(*R**,*R**)-3-bromo-2-butanol **8** gave racemic (*R**,*R**)-2,3-dibromobutane **6** due to the progression of the reaction through a *meso* cyclic bromonium ion **11** (Scheme 4), resulting in the loss of any enantioexcess in the product.

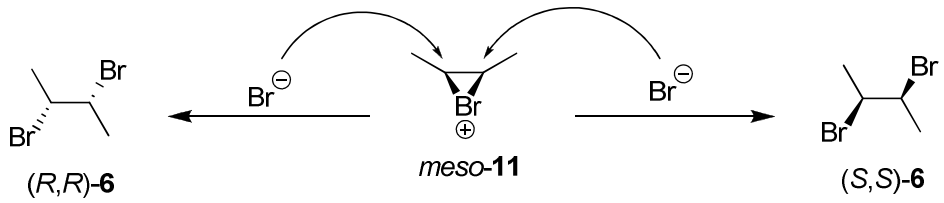

Scheme 4: formation of racemic dibromide

Winstein reasoned that if the intermediate was not a bromonium ion (**1**), but an open *β*-bromocarbonium ion (**2**) both starting materials should afford a mixture of *meso* (*R**,*S**)-2,3-dibromobutane (**4**) and optically active (*R**,*R**)-2,3-dibromobutane (**6**); an observation which is not recorded and thus a reaction pathway which can be ruled out. The other proposed forms for the cationic intermediate are an open *β*-bromocarbonium ion where the configuration is stabilised in the pyramidal form, or an asymmetric, weakly bridged bromonium ion. If either such route is operating, the resulting dibromide produced from the optically active (-)-(*R**,*R**)-3-bromo-2-butanol (**6**) should retain some degree of its enantio-enrichment, due the reaction proceeding *via* an intermediate which is not completely symmetrical (and thus is not *meso*). Therefore, with two beautifully simple experiments, Winstein had unequivocally proven the existence of a cyclic bromonium ion in his symmetrical aliphatic system.

However, despite Winstein's excellent progress in determining the identity of the cationic intermediate, a number of questions were still left unanswered. Firstly, Winstein's and Lucas' investigation is limited to a symmetrical aliphatic bromonium ion. It is very likely that the cationic intermediate in question may change with the structure of the carbon framework. Secondly, whilst Winstein's and Lucas' work proved the existence of a symmetrical bromonium ion, it does not ascertain whether this is a true intermediate or simply a short lived transition state. It is feasible that such a transition state may form and subsequently collapse to form a one-to-one distribution of the two possible open *β*-bromocarbonium ions. These could go on to react in a stereospecific manner to each afford a single diastereomer of the dibromide. There is a precedent in the literature for the stereospecific reaction of certain carbonium ions[8] and thus, such a mechanism was proposed as a plausible alternative by Winstein's contemporaries.[9]

In 1942, Winstein and Buckles went on to demonstrate the phenomenon of bromide bridging in the reaction of *meso* (*R**,*S**)- and racemic (*R**,*R**)-2,3-dibromobutanes (**4** and **6**) and

trans-1,2-dibromocyclohexane with silver acetate.[10] Winstein, Grunwald and Ingraham also investigated the relative rates of acetolysis of a range of 2-substituted cyclohexyl benzenesulfonates[11,12] providing further evidence for the neighbouring group participation of the bromine in the expulsion of the leaving group and for the formation of a bridged bromonium ion. The acetolysis of *trans*-2-bromoester **12** is 800 times faster than that of the *cis*-2-bromoester **14** (Scheme 5), strongly suggesting that the trans-2-bromine atom furnishes a nucleophilic driving force in the reaction.[12]

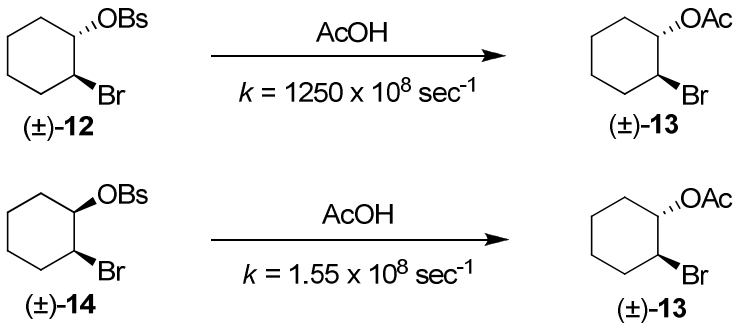

Scheme 5: acetolysis of 2-bromocyclohexyl benzenesulfonates

In 1951 Buckles and Long reported the bromochlorination of alkenes with bromine chloride (generated by a mixture of *N*-bromoacetamide and hydrochloric acid).[13] Under the reaction conditions styrene, *trans*-cinnamic acid, *trans*-stilbene and *cis*-stilbene all afford the bromochlorinated products in which addition was demonstrated to be both *trans* and consistent with Markovikov's rule. Thus the stereo- and regio-chemistry were consistent with initial bromonium ion formation followed by ring opening by chloride.

Henbest and Wilson noted the stereochemistry of the addition of hypobromous acid to steroid **15** in 1959.[14] This proceeded to give the bromohydrin (**17**) in a *trans*-diaxial manner (Scheme 6), suggesting the initial formation of a bromonium ion and its subsequent opening in keeping with the stereochemical requirements of attack on a three-membered ring.

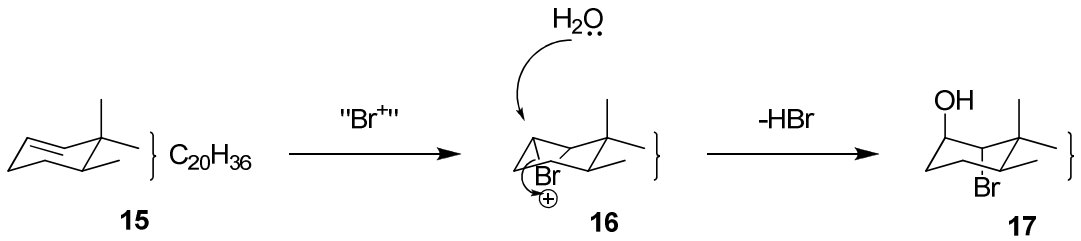

Scheme 6: addition of hypobromous acid to steroid 15

Thus, by the early 1960s, evidence in favour of the bromonium ion accumulated to the point where it was well established as an intermediate in the electrophilic bromination of alkenes.[9] However, since its initial proposal and Winstein's and co workers' proof of concept, the nature the bromonium ion over a more general range over of substrates has been subject of much scrutiny. Whilst Winstein had, at the very least, proven the transient existence of a cyclic bromonium ion in his symmetrical, aliphatic system, evidence for open transition states and intermediates in olefin bromination was also accumulating. In 1968, Fahey and Schneider reported that the electrophilic bromination of *cis*- and *trans*-β-methylstyrenes (**18**) and *trans*-anethole **21** proceeded in a non-stereospecific manner (Scheme 7).[15]

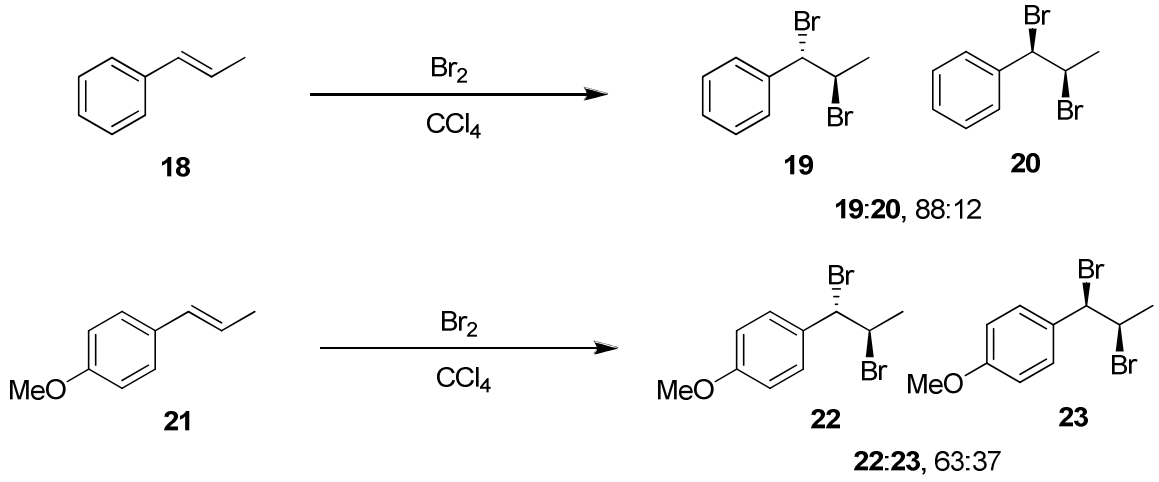

Scheme 7: nonstereospecific bromination of *trans*-β-methylstyrene (18) *trans*-anethole (21)

The product mixtures obtained suggest that, in such non-symmetrical substrates capable of forming resonance stabilised benzylic carbocations, the intermediate resembles an open benzylic carbocation more than a bromonium ion. The decrease in the stereoselectivity of the reaction on the introduction of a *p*-methoxy group on the phenyl ring is consistent with an intermediate of considerable benzylic carbocation character. The electron donating effect

of the *p*-methoxy group further stabilises a *β*-bromo benzylic carbocation, reducing any bridged character and thus decreasing selectivity for *trans* addition of bromine.

Rolston and Yates[16] investigated the bromination of a range of α- and β-methyl-substituted styrenes and demonstrated that all such additions were also not completely *trans* selective. They compared the non-stereospecific bromination of *cis*- and *trans*-2-phenyl-2-butene, which proceeded with 63% and 68% *trans* addition respectively, with the 100% trans dibromide obtained with *cis*- and *trans*-2-butene under analogous conditions.

In addition to analysing the product stereochemistry to draw inferences about the intermediate, Yates *et al*[17,18] and Dubois and Schwarcz[19] investigated the relative rates of bromine addition to aromatically substituted styrenes (**24**, Scheme 8) and analysed their findings by a Hammett plot.

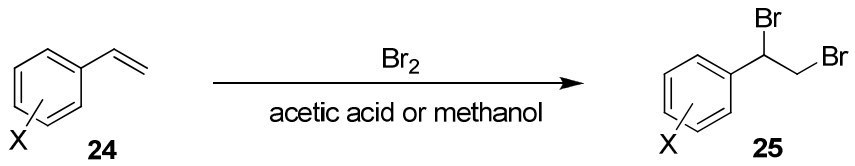

24 **25**

Scheme 8: bromination of aromatically substituted styrenes

In almost all cases the rates demonstrated a better correlation with σ^+ values than σ and all the plots demonstrated a negative ρ value, indicating a transition state in which positive charge is developed at the benzylic carbon. However, substantially different ρ values were calculated in different studies, possibly as a consequence of different experimental techniques and reaction conditions.

Yates and Wright[17] initially calculated a ρ value of -2.23 for the bromination of a range of styrenes, **24**, substituted with electron withdrawing groups (X = 3-F, 3-Cl, 3-Br, 3,4-Cl, 3-NO_2, 4-NO_2) in acetic acid. The reactions were followed by changes in bromine absorption at 450 nm and the rate data was correlated against σ values. Rolston and Yates[18] later used a potentiometric method, requiring the presence of a large concentration of bromide, to analyse the rates of a similar range of styrene derivatives. The results were correlated to σ^+ and gave a ρ value of -2.65. However, Rolston and Yates noted that the presence of bromide can increase the rate of bromination and ascribed this to the occurrence of an additional mechanism (and thus transition state) proceeding *via* tribromide. They duly

separated the rate constants into k_{Br2} and k_{Br3-} terms. The ρ values from the plots of these separate terms were -4.21 for the molecular bromine process and -2.02 for the tribromide process, indicating the former is more than 100 times as sensitive to the effects of ring substituents. On comparing this ρ value of -4.21 to Yates' previously obtained value of -2.23 a large difference was obvious. In an attempt to explain such inconsistency, Yates and Rolston replotted the earlier rate data against σ^+ and noted a marked curvature in the new plot.

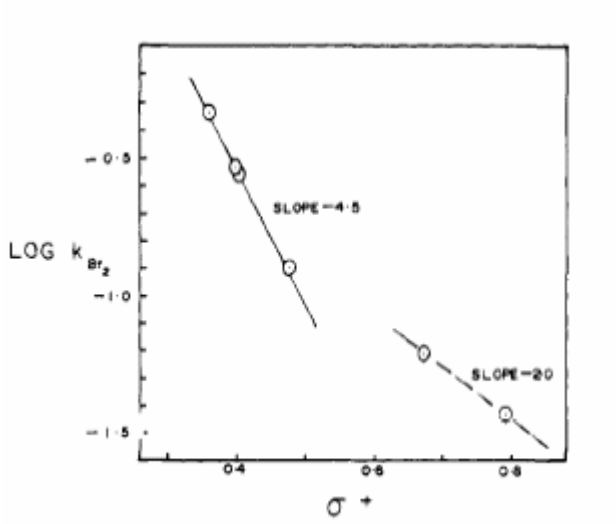

Figure 3: plot of rate constants versus σ^+ for bromination of substituted styrenes (by molecular bromine only) in acetic acid at room temperature[18]

Yates ascribed this curvature to a change of mechanism in the reaction series due to the presence of two possible methods of stabilisation of the positive charge, i.e. delocalisation into the ring and participation of by the neighbouring bromine. It was hypothesised that the points to the right hand side of the plot (X = 3-NO_2, 4-NO_2) proceed *via* a transition state which has considerably more stabilisation of the positive charge by assistance of the neighbouring bromine and thus has a much lower dependency on the σ^+ value for the aromatic substituent. However, less electron poor styrenes proceed *via* a transition state more characteristic of a benzylic carbocation than a bromonium ion. Thus, these styrenes to the left hand side of the Hammett plot exhibit a greater dependence on σ^+.

Dubois' and Schwarcz's[19] Hammett treatment of the bromination of styrenes also employed a similar potentiometric method to Rolston and Yates, using a Br_2/Br^- mixture. However, they conducted the study in methanol, in which the rate acceleration by added bromide has been demonstrated to be absent.[20] They also correlated their results to σ^+ and calculated an

overall ρ value of -4.30. This marked difference from Rolston's and Yates' overall ρ value was ascribed by Yates to different solvent/Br^- effects. However, Dubois' and Schwarcz's investigations mainly used styrenes substituted with electron donating groups (X = 3-H, 4-F, 3-Me, 4-Me, 4-MeO) which, if Yates' theory of a variable mechanism is correct, should proceed *via* a benzylic carbocation-like transition state. As such, it is no surprise that Dubois' and Schwarcz's electron rich substrates demonstrated a higher degree of dependence on σ^+ than Yates' electron deficient styrenes.

Typical ρ values for solvolysis reactions involving a benzylic carbonium ion intermediate are in the range of -4.0 to -4.7. Thus, these Hammett investigations of styrene bromination suggest a highly asymmetrical intermediate with a large amount of positive charge placed on the benzylic carbon. However, the nature of the intermediate also appears to be strongly dependent on the structure of the starting olefin, such that an array exists between essentially open *β*-bromocarbocations in the styrene intermediates bearing an electron donating substituent, to substantially bridged bromonium ions in the styrene intermediates bearing electron withdrawing groups. In 1971 Yates generalised this qualitative theory for all olefins, proposing a spectrum of possible cationic intermediates, of which **26** and **28** are extremes.[21]

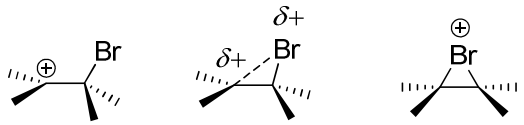

26 **27** **28**

Figure 4: Yates' qualitative description of the "bromonium ion"

In 1973, Yates and McDonald[22] conducted a thermochemical-kinetic study of the transition state structure of olefin bromination and found that, in all of the alkenes studied, the initial enthalpy difference between *cis* and *trans* isomers increased on moving into the transition state. This indicates an increase in unfavourable steric interactions in the *cis* alkene upon formation of the transition state. It is hypothesised that this originates in the movement of the substituents into closer proximity to each other on formation of a bridged intermediate. Surprisingly, this energy difference was observed over a range of alkenes including both symmetric and non-symmetric alkenes and aliphatically and aromatically substituted substrates. Their findings, combined with previous observations in the literature, led Yates and McDonald to conclude that, although there is a spectrum of intermediates ranging from

symmetrically bridged bromonium ions to open *β*-bromocarbonium ions, an initial bridged transition state was involved in all cases.

There is a plethora in the literature of further kinetic and stereochemical investigations into the nature of the bromonium ion. Their findings, depending on the alkene in question and the reaction conditions, support open,[23] closed[24] and weakly bridged[25] intermediates encompassing characteristics of both. An extremely thorough and more quantitative analysis of the structure of the cationic intermediate of bromination was undertaken by Dubois, Rausse and co-workers.[26] Their analysis was based on rate-product relationships and encompassed a range of substituted stilbenes. Dubois and Rausse reasoned that a stilbene system can follow three pathways in bromination; the Br, C_α or C_β pathways in which the intermediate is a bromonium ion (**30**) or a carbocation with the positive charge localised on either C_α (**31**) or C_β (**32**) respectively (Figure 5).

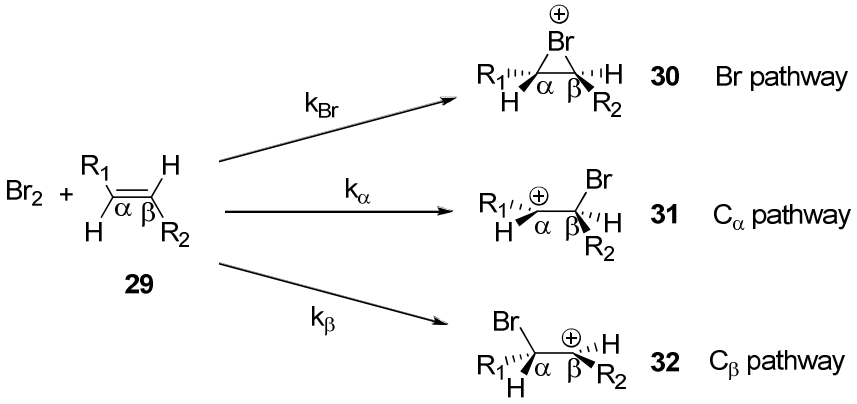

Figure 5: pathways of stilbene bromination

The Hammett plot for monosubstituted stilbenes has a marked curvature (Figure 6), demonstrating unambiguous competition between two pathways.

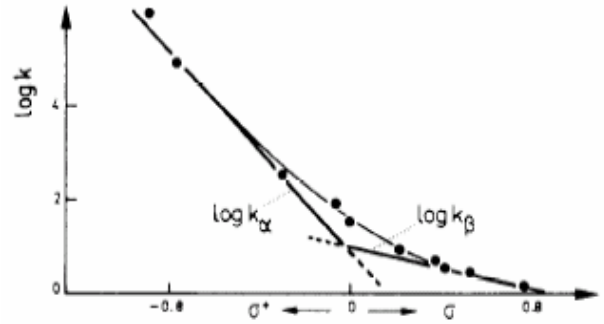

Figure 6: the curved Hammett plot for the bromination of monosubstituted stilbenes in methanol[26]

Additionally, Dubois and Rausse reported that in X,Y-disubstituted stilbenes (**33** and **34**, Figure 7), when both X and Y are electron donating, the kinetic effects of the two substituents are not additive. This is indicative of a highly asymmetric charge distribution in the transition state. In contrast, additivity is observed when the two substituents are both electron withdrawing.

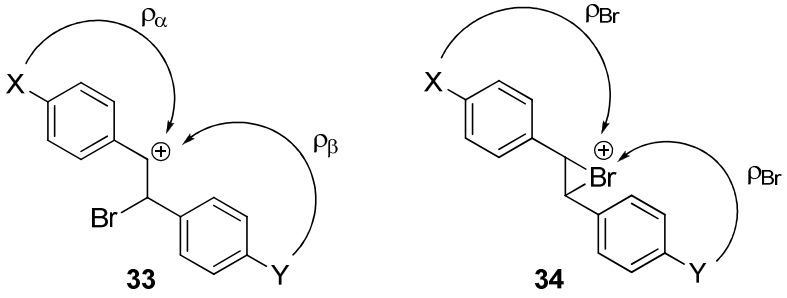

Figure 7: kinetic effects of substituents in X,Y-disubstituted stilbenes

Dubois and Rausse concluded that electron-donating groups favour the C_α *β*-bromocarbonium ion pathway, whilst electron withdrawing groups promote the formation of a bromonium ion. The ρ values obtained from the Hammett analysis (-1.0 for Br pathway, -5.4 for C_α pathway, -1.6 for C_β pathway) were used to calculate the preferred pathways depending on substituents and were compared to the observed regiochemistry of addition (Table 1). A good correlation was observed between Dubois' and Rausee's predictions and the experimental product ratios obtained.

Table 1: bromination of stilbenes in methanol; comparison of the experimental and calculated rates, and of the regiochemistry[26]

X[a]	Y[a]	Log *k*[b]	Predominant paths[c]			% MeOH attack on C_α[d]
			C_α	C_β	Br	
4-OH	4-OMe	5.97 (5.73)	+	+		
4-Me	H	1.88 (1.91)	+	+		97 (95)
H	H	1.04 (0.56)	+	+	+	50 (50)
4-Cl	H	0.29 (0.11)	+	+	+	34 (35)
3-CF_3	H	-0.07 (-0.31)		+	+	0 (0)
4-NO_2	3-Cl	-1.57 (-1.58)			+	

a - X and Y at C_α and C_β, respectively. b - *k* in litres per mole per second at 25 ºC; experimental and, in parentheses, calculated data. c - The sign "+" means the corresponding pathway is significant. d - Experimentally measured percentage (%) and, in parentheses, calculated percentage (%).

Thus, Dubois and Rausse concluded that the degree of bridging in the intermediate is intimately related to the substituents around the bromonium ion and their ability to stabilise an adjacent partial positive change. In short, Yates' hypothesis appears to be an excellent qualitative description of the cationic intermediate in the bromination of alkenes.

Ruasse and Dubois also investigated the effects of solvent in the electrophilic addition of bromine to olefins and whether, as had previously been hypothesised, solvent can exert an influence on the structure of the cationic intermediate.[26] McManus and co-workers,[27] Modro *et al*[28] and Rolston and Yates[29] had all postulated that there is greater bromonium ion character, as opposed to *β*-bromocarbonium ion character, as the solvent polarity decreases. They proposed that this occurs as a consequence of the differential solvation requirements of the two extreme structures of the intermediate. However, in contradiction to this, Rausse and Dubois reported that in the rate determining step of bromination (i.e. the formation of the bromonium ion) the solvent exerts a high polar effect and strong electrophilic assistance, but little or no nucleophilic involvement. This led them to the conclusion that solvent changes cannot lead to significant variation in bromine bridging. They therefore invoke the relative ease of rotation of the *β*-bromocarbonium ion conformers

and the lifetime of the intermediate to explain the differences in *trans* stereoselectivity observed in different solvents.

More recently, a number of quantum mechanical studies have been employed to assess the relative stabilities of the cyclic bromonium ion and the open *β*-bromocarbonium ion. Hamilton and Schnaefer[30] calculated the cyclic ethylene bromonium ion to be more stable than the 1-bromoethyl cation by 1.5 kcal mol^{-1}, in good agreement with experimental results. Rausse and co-workers[31] calculated the energy profiles for six bromonium ions with varying methyl substitution (Figure 8). They found very shallow or flat minima corresponding to symmetrical or highly asymmetric bridged structures, depending on the symmetry of the substitution.

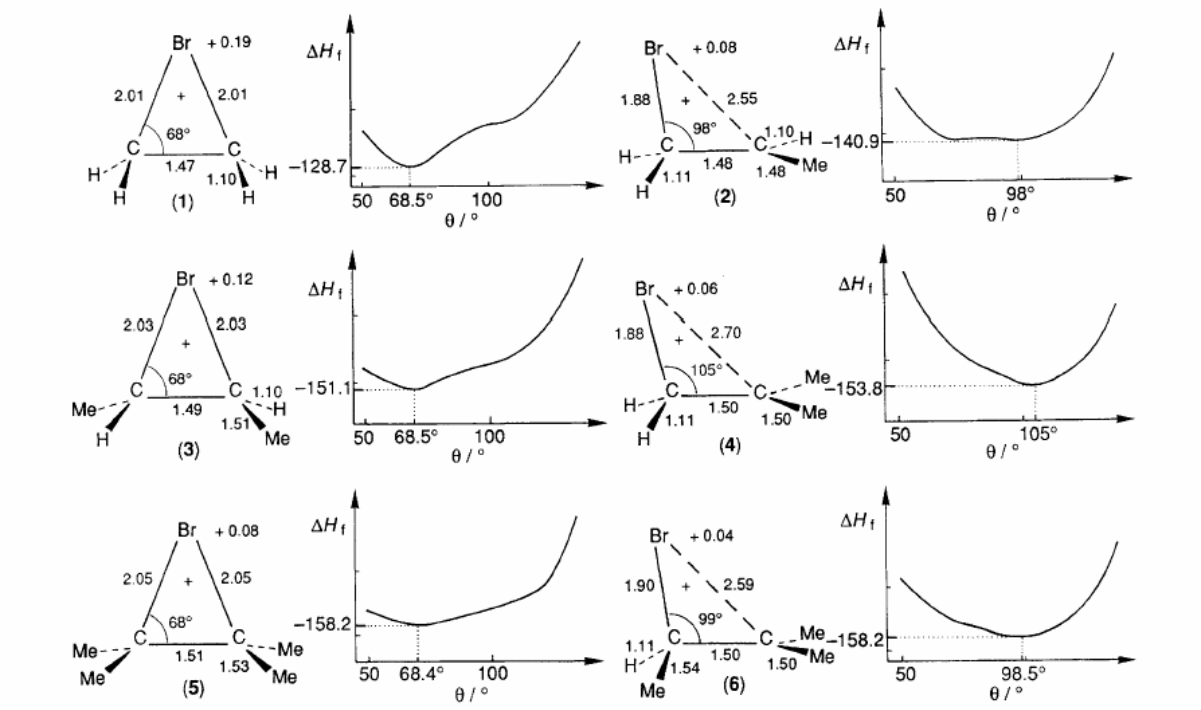

Figure 8: Rausse's energy profiles for bromonium ion formation[31]

These results provide further insight into the complexities of the intermediate and reaction profile of bromination. However, it was noted by Brown and Klobukowski[32] that the magnitude of the asymmetry calculated for the bromonium ion is markedly dependent on the computational method used. Brown commented that the structure of the ion becomes more symmetric as the quality of the computational method improves and thus casts some doubt

upon the high degree of asymmetry of the substituted bromonium ions in Rausse's earlier calculations.

NMR studies have also been used to probe the structure of bromonium ions. Olah and co-workers[33] were the first to observe a stable bromonium ion and study it by NMR spectroscopy. Treatment of 1-2-bromo-2-fluoroethane (**35**) with antimony pentafluoride resulted in the loss of fluoride to afford the ethylene bromonium ion (**36**).

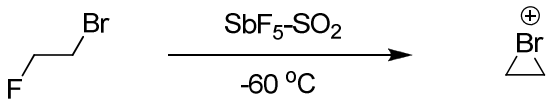

35 **36**

Scheme 9: formation of stable bromonium ion

In the absence of any nucleophile, this ion was stable in sulphur dioxide at -60 ºC and its ^{1}H NMR was spectrum was recorded. This demonstrated the coalescence of the two doublets of triplets of **35** (at 3.49 ppm and 4.61 ppm) to a broad singlet at 5.53 ppm, indicating the formation of an electron deficient symmetrical intermediate.

In 1985, Servis and Domenick[34] observed the deuterium isotope effects on the ^{13}C chemical shifts of the bromonium ion derived from 2,3-dimethyl-2-butene-d_6 (**37**, Figure 9). They observed a large downfield (positive) shift of the resonance of the carbon proximal to the deuteria and ascribed this to a *β*-deuterium isotope effect. The *β*-deuterium isotope effect occurs as a consequence of the perturbation of the vibrational motion caused by deuterium substitution. Vibrational perturbation results in a reduced C-D bond length and increased electron density at the sp^3 hybridized carbon atom. This reduces the degree to which the C-D bond can stabilise an adjacent carbocation by hyperconjugation and results in a small downfield (positive) shift in an adjacent electron deficient sp^2 hybridised carbon. Servis and Domenick proposed that a three-membered cyclic bromonium ion, in which all bonds are of the two-electron two centre type, best fitted their findings.

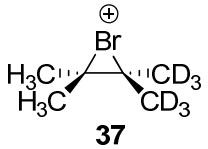

37

Figure 9: Servis' and Domenick's NMR substrate

However, Ohta *et al*[β5] recently applied a similar analysis to chloronium ions with surprisingly different observations. In addition to the intrinsic isotopic shifts reported by Servis and Domenick, it is possible for an additional isotopic ^{13}C shift to be caused by the isotopic perturbation of a degenerate equilibrium (Scheme 10).

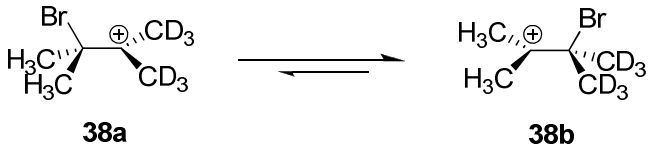

38a **38b**

Scheme 10: isotopic perturbation of a degenerate *β*-bromocarbocation equilibrium

Due to the relative destabilisation (as described above) of a carbocation adjacent to the site of deuterium substitution, if the cation is asymmetrically substituted with deuterium, the two isotopomers **38a** and **38b** of the *β*-bromocarbocation are no longer degenerate. Thus, the equilibrium favours the isotopomer with deuteria placed distal to the carbonium ion (**38b**) rather than proximal (**38a**). The result of this isotopic perturbation is that the time averaged ^{13}C signal for the distal quaternary carbon should appear downfield (positively shifted) from the **37**-d_0 signal, whilst the proximal carbon signal should appear upfield. Such equilibrium isotope shifts (Δ_{eq}) are typically large and temperature dependent.

Ohta *et al* reported such equilibrium isotope shifts in their chloronium ion system and concluded from their observations that chloronium ions are better described as equilibrium of *β*-chlorocarbonium ions. Additionally, they found evidence for the occurrence of 1,2-methyl shifts in the sample mixture. If such shifts occurred in Servis' and Domenick's system, they would have generated a mixture of isotopomers with both geminal and vicinal orientations of the methyl-d_3 groups. Based on these findings, Ohta re-examined Servis's and Domenick's work and reported that the cationic brominated intermediate of 2,3-dimethyl-2-butene-d_6 also demonstrates equilibrium isotope shifts, a phenomenon which was missed by Servis and Domenick due to the complication of the spectrum by the occurrence of a mixture of isotopomers formed *via* the 1,2-methyl shifts. Ohta provides a full description of the observed signals within the framework of an isotopic perturbation of an equilibrium on a mixture of isotopomers. Thus they conclude that **28** is also better described as an equilibrium of *β*-bromocarbonium ions than a cyclic bromonium ion (Figure 10).

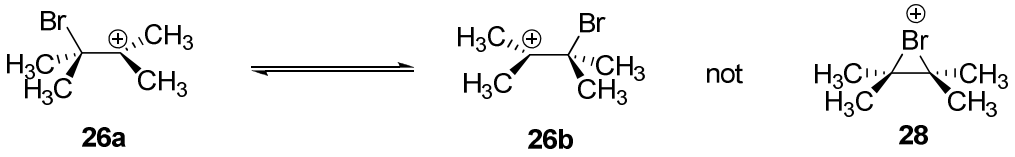

Figure 10: Ohta *et al*'s conclusions on the nature of the bromonium ion

However, Ohta *et al* note the absence of any temperature dependence of the observed equilibrium isotopic shift; an observation which is inconsistent with the proposal of an equilibrium. A perhaps more plausible explanation for their observations is the isotopic perturbation of the symmetric bromonium ion structure to give an asymmetrically bridged intermediate (**38c**).

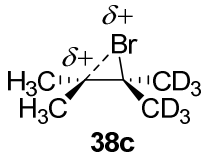

Figure 11: isotopically perturbed bromonium ion

The sensitivity of the degree of bromine bridging to the asymmetric substitution of the double bond is well established.[15-21] Thus, it is reasonable to assume that deuterium substitution will, *via* the *β*-deuterium isotope effect, destabilise a completely symmetric bromonium ion (**28**) in favour of an asymmetrically bridged structure (**38c**). The partial positive charge is now no longer equally distributed over the quaternary carbon atoms and thus an analogous downfield shift of the carbon distal to the deuteria and an upfield shift of the proximal carbon should be observed. This distortion would not be expected to be temperature dependent and thus this hypothesis seems to more accurately agree with Ohta's experimental results than that of an equilibrium between *β*-bromocarbocations.

1.1.2. Isolation and Characterisation of Stable Bromonium Ions

A major breakthrough in the field was made in 1969 when Wynberg and co-workers[36] reported that when adamantylideneadamantane (**39**) is treated with bromine in carbon tetrachloride, a yellow precipitate is obtained. Wynberg formulated this as the world's first example of an isolable three membered bromonium ion - bromide salt (**39**Br^+/Br_3^-, Scheme 11).

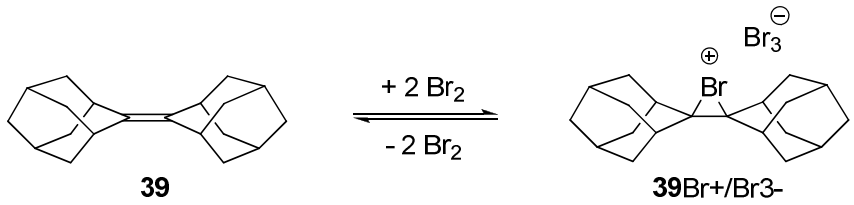

Scheme 11: reaction of adamantylideneadamantane and bromine

The identity of this yellow precipitate was confirmed in 1985 when Brown and co-workers[37] reported the crystal structure of **39**Br^+/Br_3^- (Figure 12). The salt was revealed to contain the proposed three membered cyclic bromonium ion. The unique structure of adamantylideneadamantane precludes any *trans* attack due to severe crowding at the opposite side of the molecule of the bromonium ion. It also cannot undergo loss of a proton to form an allylic bromide due to the only available protons lying at bridgehead carbons. It is interesting to note that even from the completely symmetrical adamantylideneadamantane (**39**), the adduct **39**Br^+/Br_3^- contains a slightly asymmetrical bromonium ion with C-Br bond lengths of 2.166 (6) and 2.194 (6) Á. It was hypothesised that this distortion could be a result of the interaction between the Br_3^- counter ion and the bromine of the bromonium ion.

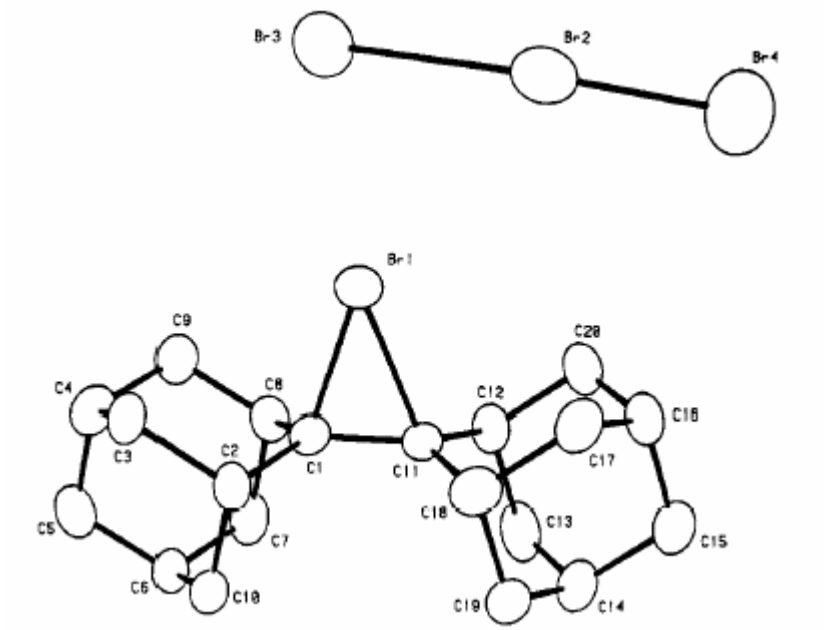

Figure 12: X-ray crystal structure of 39Br^+/Br_3^- (hydrogen atoms omitted for clarity)[37]

In 1991, Brown and co-workers further reported the formation of a **39**Br^+/TfO^- salt on the sonication of **39**Br^+/Br_3^- in the presence of methyl triflate.[38,39] After removal of the volatiles (CH_3Br, Br_2), a white solid was obtained which was characterised by NMR and, following re-crystallisation from dichloromethane, X-ray crystallography (Figure 13).

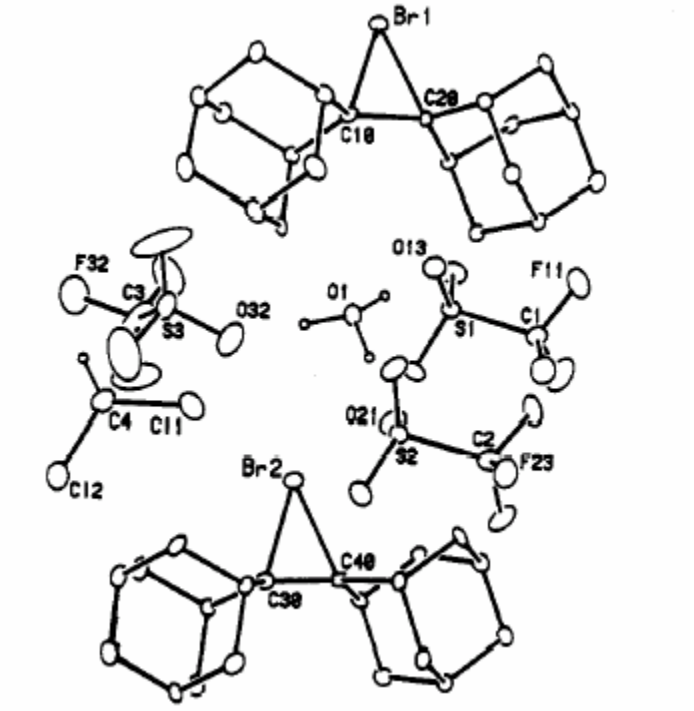

Figure 13: the asymmetric unit in the X-ray crystal structure of 39Br^+/TfO^- (all hydrogen atoms omitted for clarity)[39]

The X-ray crystal structure of the **39**Br^+/TfO^- salt revealed the presence of a completely symmetrical bromonium ion with C-Br bond lengths of 2.118 (10) and 2.136 (10) Á. This is presumably due to the considerably weaker interaction with the less nucleophilic triflate counterion relative to that with Br_3^-.

These advancements in the isolation of a stable bromonium ion not only confirmed its structure and existence as an intermediate, but also facilitated subsequent detailed investigations into the mechanism of the electrophilic bromination of olefins.

1.1.3. Intermediates in the Electrophilic Bromination of Alkenes: the Bromonium Ion and the Charge Transfer Complex

The existence of a charge transfer complex (CTC) in the early stages of the electrophilic bromination of alkenes has long been well established in the literature.[40] Spectroscopic, kinetic and thermodynamic studies support the role of one or two π complexes (**40** and **41**, Figure 14) as intermediates in bromine addition.

40 **41**

Figure 14: charge transfer complexes (CTCs)

It is generally accepted that *via* either solvent or bromide assisted dissociation the CTC goes on to form the bromonium/*β*-bromocarbonium ion intermediate. However, in some cases, depending upon the olefin structure and the attacking nucleophile, it has been proposed that bromination may occur through *via* the nucleophilic attack on the CTC complex itself.[40,41]

Following Brown's isolation of the stable **39**Br^+/Br_3^- salt, Brown, Bellucci and co-workers undertook a study of the solution behaviour of adamantylideneadamantane (**39**) and bromine in 1,2-dichloroethane.[42] They reported that equilibrium is instantaneously established between 1:1, 1:2 and 1:3 olefin-Br_2 complexes (Scheme 12).

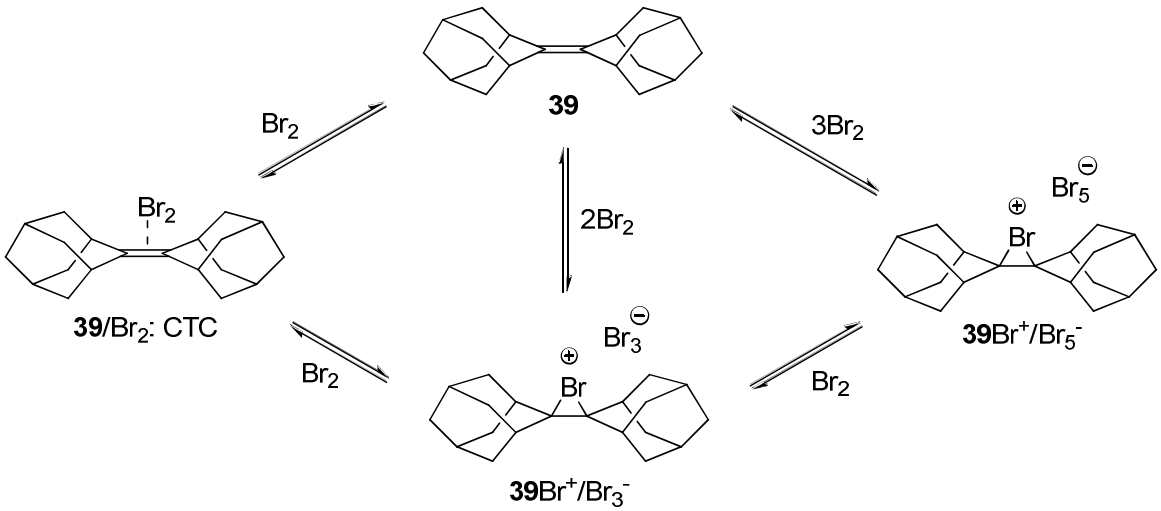

Scheme 12: adamantylideneadamantane/bromine equilibrium[42]

The mixtures obtained were highly variable and closely dependent upon the relative concentrations of the reagents, as would be expected for a rapidly exchanging system. Brown's and Bellucci's studies revealed the rate of formation of the CTC to be related to the substitution pattern and electron-donating ability of the alkene as well as steric crowding around the double bond. Comparison of the formation constant of the CTC of adamantylideneadamantane (**39**/Br_2) with those of other alkenes which can proceed beyond the formation of the bromonium ion demonstrated that it is by no means an atypical alkene with respect to the generation of a CTC.[42] Thus, the conclusions that can be drawn from studying the reaction of bromine with **39** can be taken as directly applicable to the bromination of reactive alkenes. Therefore, as a result of their findings in their studies of **39**, Brown and Bellucci were able to propose a general scheme summarising the various mechanistic pathways for the electrophilic bromination of olefins (Scheme 13).[43]

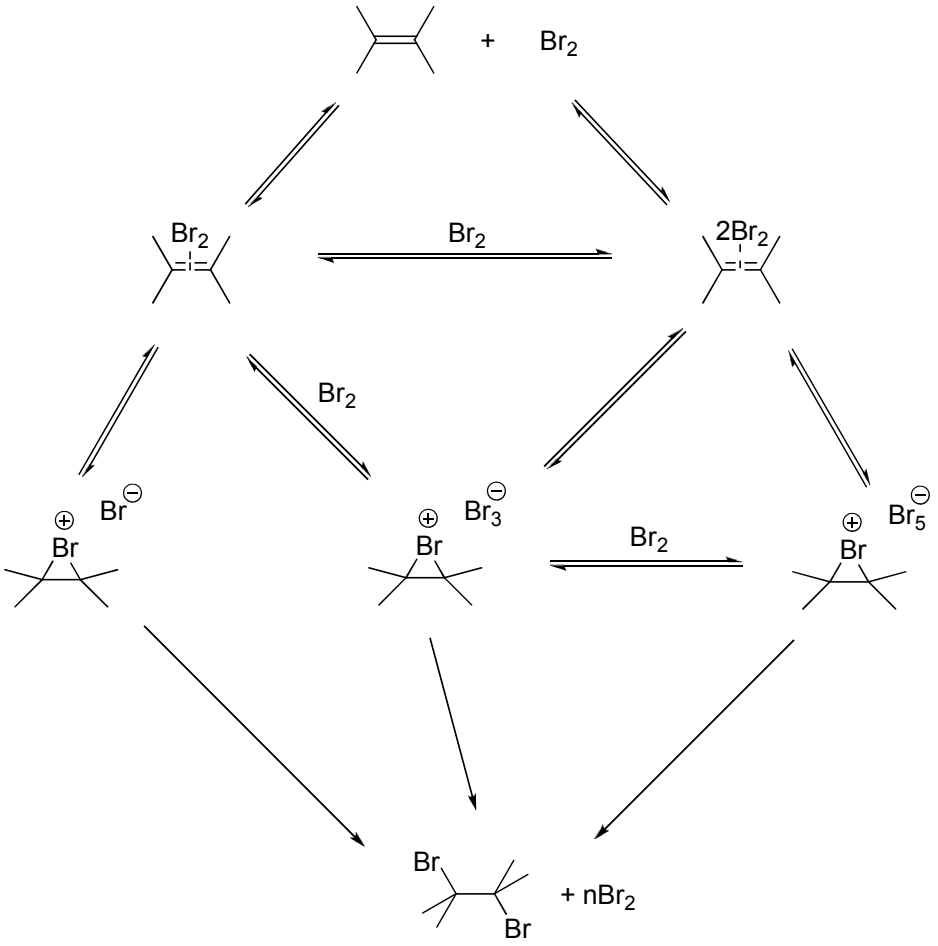

Scheme 13: Brown's and Bellucci's proposed mechanism of electrophilic bromination[43]

1.2. Reversible Bromination Ion Formation

The question of whether of not bromonium ion formation was reversible was one which, until the 1980's, had received very little attention. In 1984, Brown *et al*'s studies on the solvolysis of the *trans*-bromobrosylates of cyclohexene (**12**) and cyclopentene was the first indication that such a phenomenon may exist.[44] A series of experiments were conducted in which the *trans*-bromobrosylates of cyclohexene (**12**, Scheme 14) and cyclopentene were solvolysed at 75 ºC in acetic acid containing Br^- and an acceptor olefin, namely cyclopentene and cyclohexene, respectively.

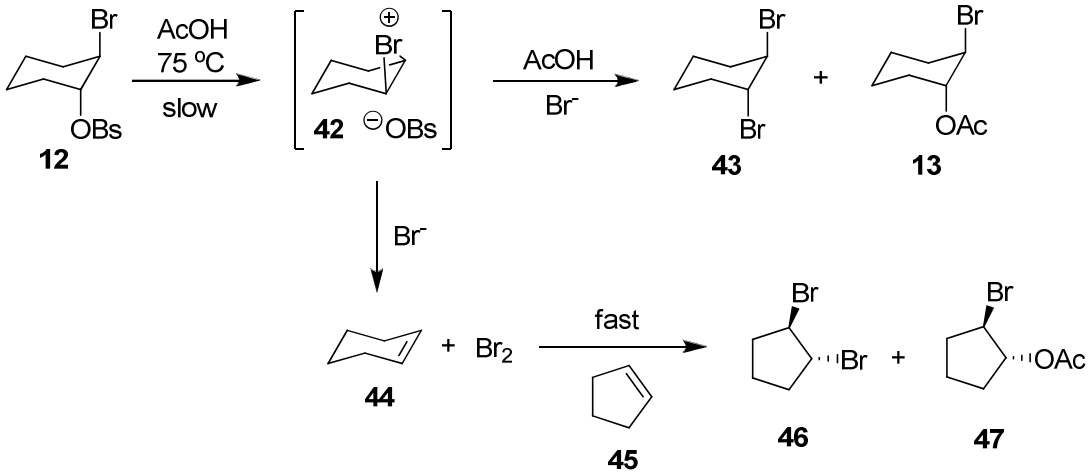

Scheme 14: Brown's solvolysis of the trans-bromobrosylate of cyclohexane 12 in the presence of cyclopentene 45

It was hypothesised that, in a similar manner to Winstein's early experiments, the bromine assists the exit of the leaving group and produces the intermediate bromonium ion **42**. This could then be opened by either solvent or bromide to form the corresponding *trans* product, or the Br^+ of the bromonium ion is captured by bromide to liberate molecular bromine and the free alkene. The so produced molecular bromine would then go on to react with excess scavenger olefin to produce its normal addition products. It was observed by Brown and co-workers that, in the presence of bromide and cyclopentene, the products of the solvolysis of **12** consist of the dibromide and bromosolvates of *both* cyclohexane and cyclopentane. Likewise, the solvolysis of the *trans*-bromobrosylate of cyclopentene in the presence of bromide and cyclohexene led to a similar product mixture (though differing greatly in the relative amounts of the components). Brown's observations led him to propose the

reversible formation of bromonium ions *via* the attack of the bromide anion on the bromine of the bromonium ion.

Four years later, Bellucci *et al* reported the slow debromination of dibromide **48** back to the olefin and molecular bromide (Scheme 15) when stirred at room temperature in acetonitrile in the presence *cis*-stilbene (**50**).[45]

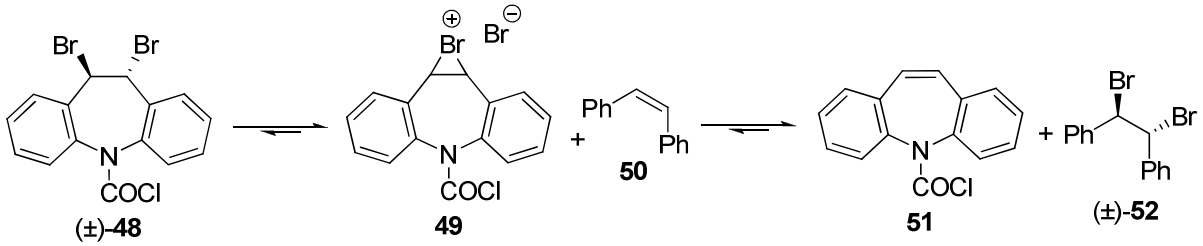

Scheme 15: Bellucci's debromination of dibromide 48

Like Brown, Bellucci ascribed the debromination to occur *via* reformation of the bromonium-bromide ion pair **49**, followed by attack of the bromide on the bromine atom of the bromonium ion to re-form olefin and molecular bromide, which is scavenged by *cis*-stilbene (**50**).

A subsequent collaboration between the two authors resulted in the publication of a kinetic isotope effect study in the bromination of sterically encumbered alkene tetraisobutylethylene (**53**).[46]

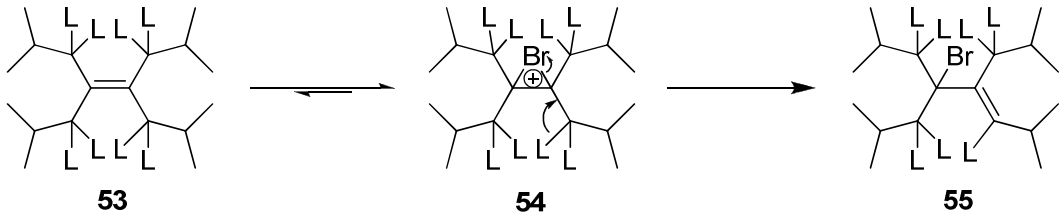

Scheme 16: bromination of tetraisobutylethylene (53)

Due to severe steric hindrance to *trans* attack on bromonium ion **54**, the alkene reacts with bromine in acetic acid to form the double bond rearranged allylic bromide **55**. Brown, Bellucci and co-workers reported a large kinetic isotope effect (2.3) in the reactions of **53**-H8 (L=H) and **53**-D8 (L=D) in which the eight allylic positions are isotopically substituted. They demonstrated that this value was too large for any imaginable *β*-secondary kinetic isotope

effect on the bromonium ion and was most consistent with a primary effect in which a C-L bond is removed in a rate limiting or partially rate limiting elimination. The observation of such a primary kinetic isotope effect requires that all steps preceding the rate limiting one must have lower activation energies. Consequently, the bromonium ion intermediate is likely to be reversibly formed.

However, the first unequivocal proof for the reversibility of formation of the bromonium ion was reported by Brown in 1991 from his studies on the bromonium ion salt of adamantylideneadamantane, **39**Br^+/TfO^-.[38,39]

1.2.1. Adamantylideneadamantane and Reversible Bromonium Ion Formation

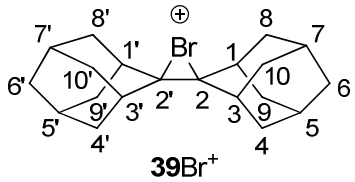

39Br^+

Figure 15: Bromonium ion of adamantylideneadamantane, 39Br^+

Brown *et al* found that ^{13}C NMR was an effective tool in the study of **39**Br^+/TfO^- in solution.[38,39] At -80 ºC, the ^{13}C NMR spectra demonstrated that the bromonium ion contained two perpendicular planes of symmetry. One plane contains the C_2, $C_{2'}$ and Br atoms of the bromonium ion, whilst the other plane contains the Br atom and bisects the C_2-$C_{2'}$ bond. The ^{13}C resonances for the carbons on the top side of the molecule ($C_{8,8',10,10'}$) are distinct and are shifted downfield from their counterparts ($C_{4,4',9,9'}$) on the bottom side. However, addition of a small amount of adamantylideneadamantane, or Ad=Ad, to the mixture resulted in the broadening and ultimately the coalescence of the $C_{8,8',10,10}$ and $C_{4,4',9,9'}$ peaks to give a single narrow line for $C_{8,8',10,10,4,4',9,9'}$. From these observations, Brown deduced that a fast, 2-step exchange process is occurring which translates Br^+ from the top to the bottom side of the **39**Br^+ molecule *via* the intervention of a second molecule of Ad=Ad.

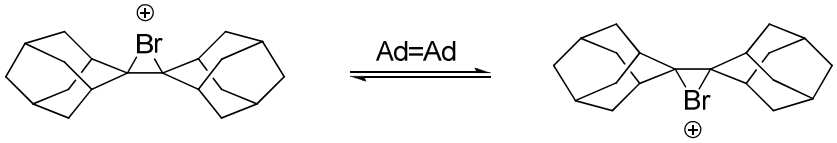

Scheme 17: Br^+ exchange between Ad=Ad molecules

The second order rate constant for this Br^+ exchange was calculated as 2 x 10^6 $M^{-1}s^{-1}$ at -80 ºC, with an activation parameter of $\Delta H^{\ddagger}$ = 1.8 ± 0.2 kcal mol^{-1}, indicating an extremely facile process. As a simple model for the bromonium ion-alkene Br^+ exchange, Brown *et al* calculated the energies of the Br^+ transfer between two ethylenes. Their results indicated that the lowest energy conformation for the exchange was the approach of the two ethylene molecules with their C-C bonds orientated at an angle of 90º (Figure 16).The calculated potential energy profiles demonstrated the existence of three intermediate states in the reaction coordinate; two degenerate olefin-bromonium complexes and a single D_{2d} transition state.

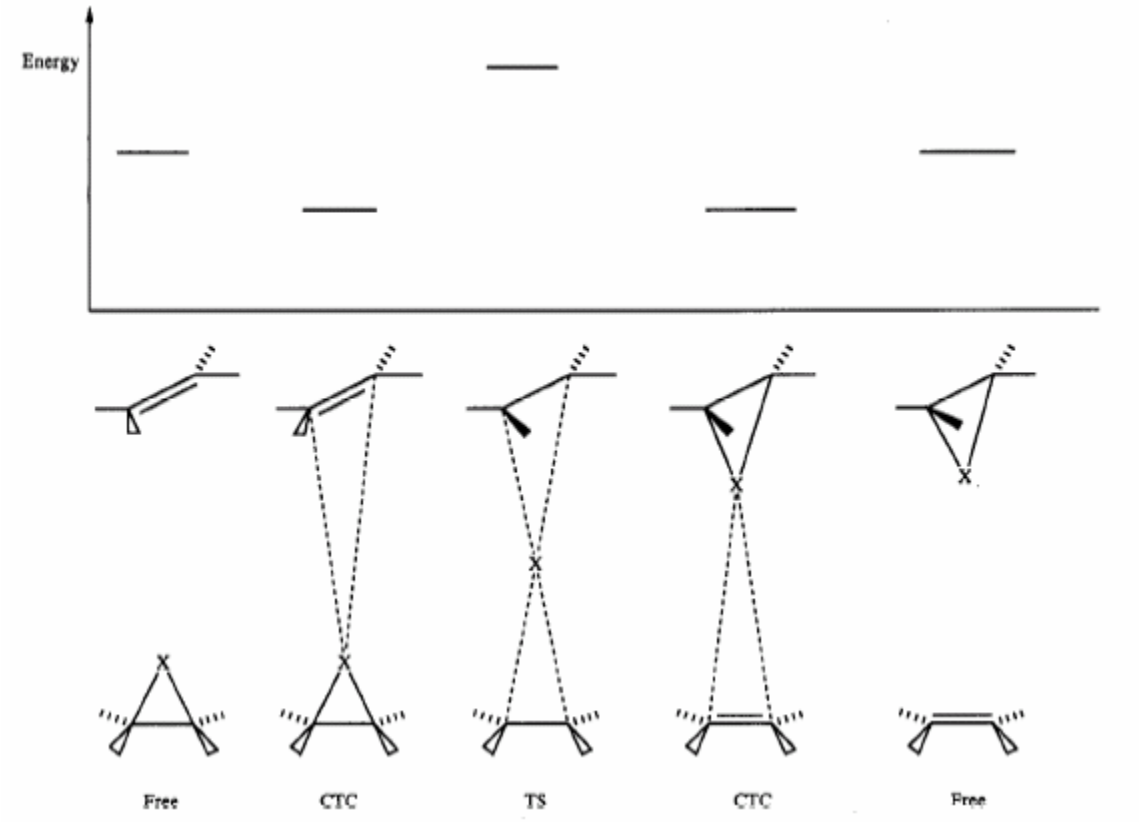

Figure 16: classical potential energy profile for Br^+ (X^+) exchange between two ethylene moieties[39]

Further calculations by Braddock, Rzepa and co-workers considered the possibility of an inverted non-classical potential energy profile (Figure 17) in which the equidistant point for the bromine atom, **57**, is an energy minimum.[47]

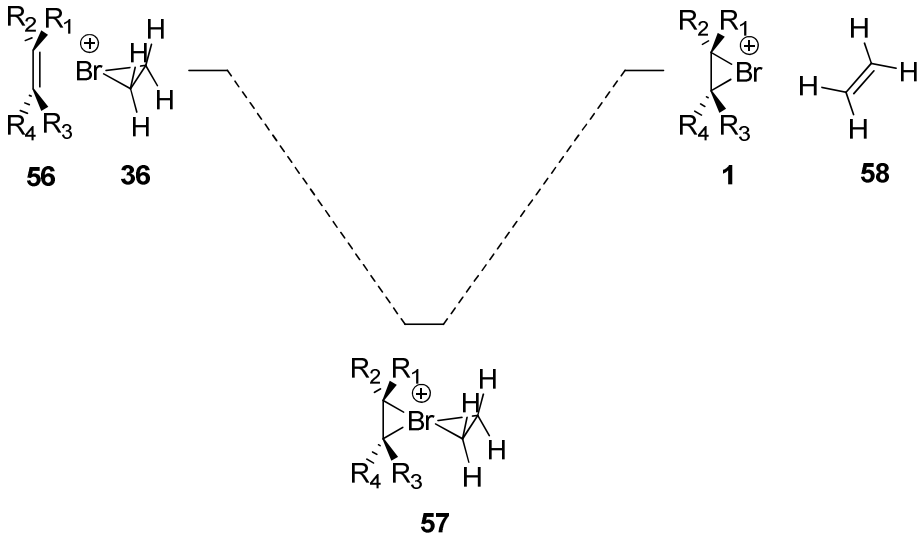

Figure 17: inverted non-classical energy potential profile for Br^+ exchange between two alkenes

Braddock and Rzepa's calculations suggested that, in the gas phase at least, the inverted energy potential was a better model for Br^+ transfer between alkenes. As the four-coordinate species **57** exists in a potential well, the rate of bromonium ion transfer would be determined by entropic rather than energetic considerations, which is in good agreement with the extremely facile exchange observed by Brown. The calculations also indicated very little energetic discrimination between a tetrahedral (**57**) and planar (**59**) central bromine atom, suggesting a less rigid geometry for the transition state than Brown previously predicted.

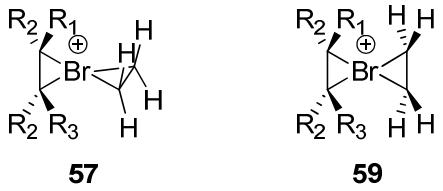

Figure 18: D_{2d} (57) and D_{2h} (59) intermediates

The computational theoretical studies on Br^+ transfer and the observed ease with which such exchange occurs in the sterically hindered Ad=Ad systems suggests that Br^+ transfer from **39**Br^+ to other acceptor olefins should also occur readily. Thus, Brown and co-workers went on to investigate such a possibility.

Brown, Bellucci and co-workers initially probed the transfer of Br^+ from **39**Br^+ to acceptor olefins by the addition of cyclohexene-d_{10} to a solution of **39**Br^+/TfO^- in dichloromethane. ^2H

NMR of the solution demonstrated the conversion of cyclohexene-d_{10} into *trans*-2-bromocyclohexyl trifluoromethanesulfonate-d_{10}. Neverov and Brown extended the scope of Br^+ transfer from **39**Br^+/TfO^- by studying the process with a wide range of acceptor olefins in the bromocyclisation reaction (Figure 19).[48]

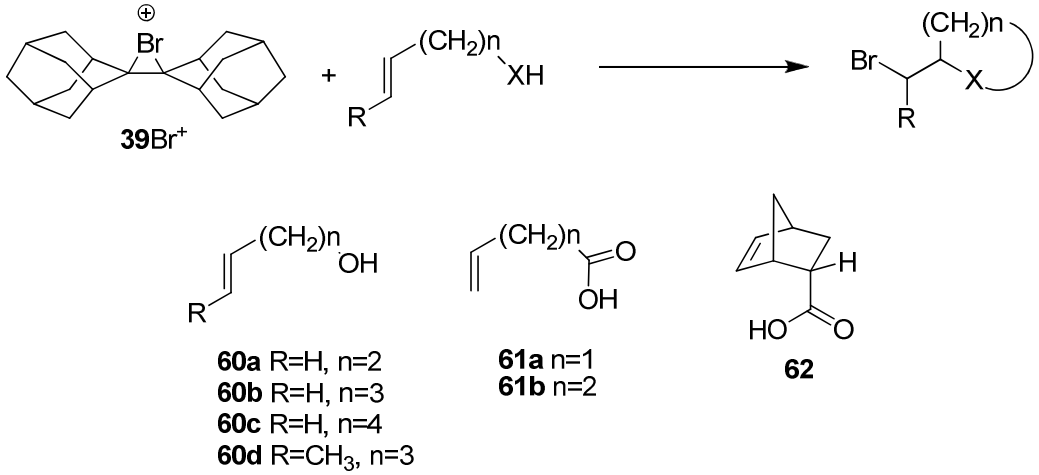

Figure 19: bromocyclisation substrates

In all cases the products were formed in essentially quantitative yield and were those expected from an electrophilic bromocyclisation reaction. The kinetics of these reactions were conveniently monitored by observing the decrease in absorbance of the bromonium ion triflates, **39**Br^+/TfO^- at 250 nm in dichloroethane containing an excess of olefin. Brown and Neverov reported several observations of note. Firstly, they demonstrated that Br^+ transfer and subsequent cyclisation is fastest for the formation of five-membered rings. This was accounted for by invoking the anchimeric assistance by oxygen of the Br^+ addition to the π-bond which is optimised when the assisting group can react to form a five-membered ring (Figure 20).

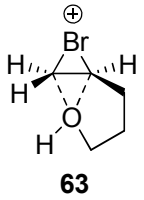

Figure 20: internal stabalisation of the bromonium ion by lone pairs on oxygen

Brown and Neverov also noted that addition is faster for more highly substituted olefins and, for a given ring size, ether cyclisation is faster than lactonisation. This was ascribed to the greater inductive electron withdrawing effect of the COOH group relative to the OH, which

decreases the reactivity of the π-bond to electrophilic attack. This effect could also be due to the greater nucleophilicity of the alcohol oxygen compared to that of the carboxylic acid and thus its greater contribution to the anchimeric assistance of the addition of Br^+ to the olefin.

Unexpectedly, Brown and Neverov noted that addition of Ad=Ad markedly suppressed the reaction rate in all cases. With certain olefins (**60b** and **61b**) the reaction is completely suppressed at high Ad=Ad concentrations. With others, the added Ad=Ad suppresses the reaction to a certain point, but no further. Additionally, it was reported that in some cases (e.g. **60b**-**d**) the bromocyclisation exhibited kinetic terms which were second order with respect to the concentration of alkenol. In fact, for these cases, added propanol or pentanol catalysed the reaction. Brown and Neverov rationalised this behaviour by a general mechanism involving two reversibly formed intermediates **64** and **65** (Scheme 18).

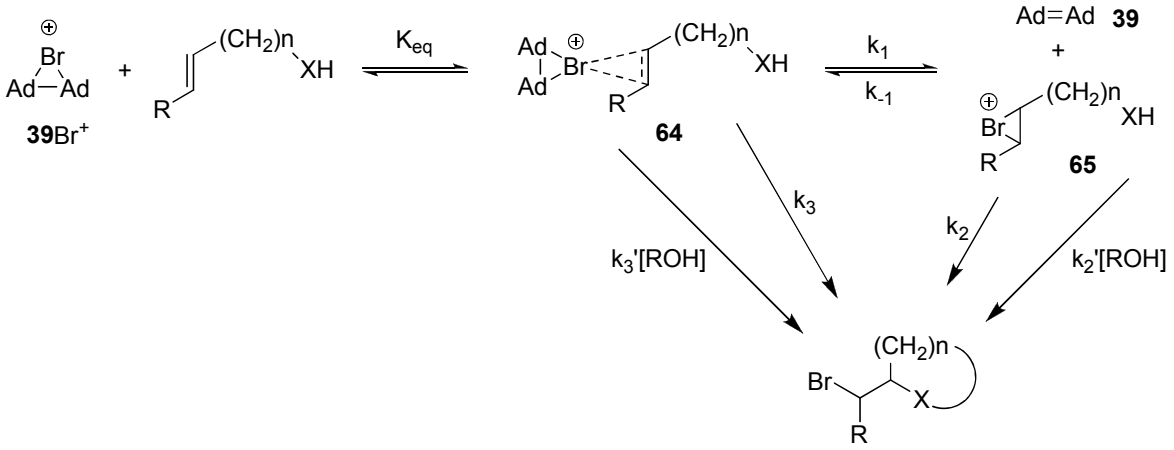

Scheme 18: $39Br^+$ promoted bromocyclisation of alkenols

The addition of Ad=Ad will cause the second equilibrium k_1/k_{-1} to lie towards intermediate **64**, added Ad=Ad recapturing the alkenol bromonium ion **65** to reform the CTC **64**. This would result in the observed suppression of rate noted by Brown and Neverov. The suppression of the rate of bromocyclisations by Ad=Ad to a certain point, but no further, suggests the existence of another channel for the formation of the product which does not proceed *via* bromonium ion **65**. It was suggested that this involved direct cyclisation within complex **64**. For the bromocyclisations which are catalysed by the addition of alcohol, it was proposed that product formation could occur *via* four alternative pathways. Two of these are the spontaneous cyclisation of either complex **64** (k_3) or bromonium ion **65** (k_2), whilst the

remaining two involve a second molecule of alkenol or added alcohol (k_3' and k_2'). It was suggested that the mechanism for this catalysis proceeds *via* the action of ROH as a base to remove the proton from the intramolecular nucleophile OH, thereby assisting ring closure. Thus, Brown's and Neverov's studies in the use of **39**Br^+/TfO^- as a Br^+ transfer agent allowed a much deeper insight into the mechanistic subtleties of halocyclisations than had previously been achieved. However, most significantly, it was demonstrated that Br^+ transfer from a bromonium ion kinetically competes with nucleophilic attack on the carbons of the bromonium ion, even when the nucleophile in question is already tethered to the alkene to facilitate an intramolecular cyclisation. Although the Ad=Ad system can be described as a special case due to the unprecidented unreactivity of **39**Br^+, it seems logical to apply the findings from such examples of facile Br^+ exchange to the bromination of reactive olefins. The ease of Br^+ transfer from, or to, such a sterically encumbered system as **39**Br^+/Ad=Ad suggests that Br^+ transfer involving two less hindered alkenes should occur readily.

1.2.2. Normal Bromonium Ions and Reversible Bromonium Ion Formation

As described earlier, the first indication that reversible bromonium ion formation in normally reactive systems may be more prevalent than previously believed was reported by Brown and co-workers in 1984 with the solvolysis of *trans*-bromobrosylates in the presence of a scavenger alkene.[44] However, it was contended[26] that this evidence was obtained under "more or less drastic conditions", i.e. at elevated temperatures and in solvents such as acetic acid or chlorinated solvents, in which the fates of the bromonium ions were different from what occurs in aqueous or alcoholic media. It was suggested that under such, more "normal" conditions, there is an absence of reversal unless the olefin is highly congested.[49] Thus, in 1993, Brown and co-workers repeated similar experiments using the *trans*-bromotriflate of cyclohexene (**66**), which was solvolysed at room temperature in both acetic acid and methanol (Scheme 19).[50]

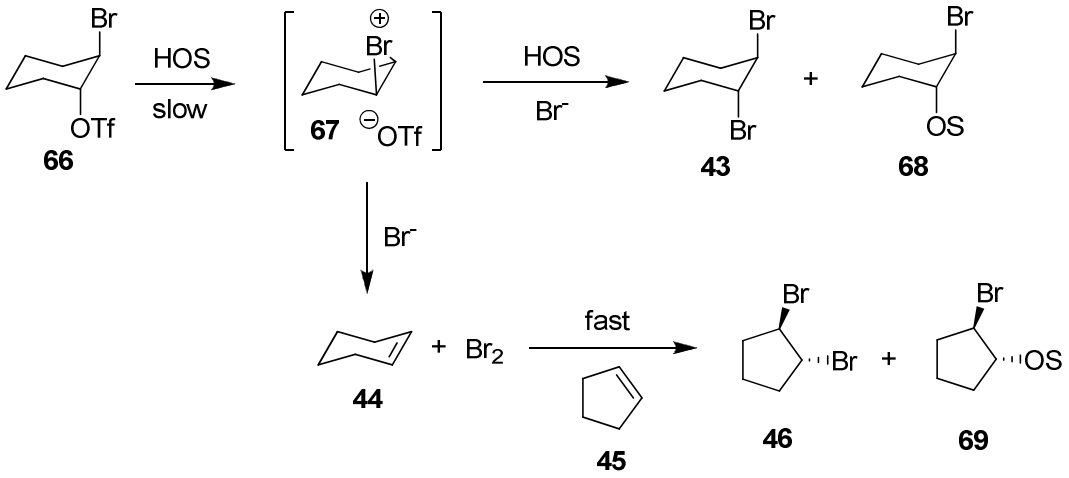

Scheme 19: Brown's solvolysis of *trans*-bromotriflates of cyclohexane

Analogously to the brosylate system (Scheme 14), Brown and co-workers observed a product mixture that consisted of the dibromide and bromosolvates of both cyclohexane (**43** and **68**) and cyclopentane (**46** and **69**), indicative of reversible bromonium ion formation. Control experiments established that no direct attack of bromide on **66**, which leads to elimination, is occurring and that free molecular bromine is formed over the course of the reaction. Significantly, in the absence of bromide, no cyclopentyl products were observed during the solvolysis of bromotriflate **66**. Thus, no direct transfer of Br^+ from bromonium ion to alkene was observed under these conditions. The degree of reversibility and subsequent Br_2 liberation was also demonstrated to be dependent on the solvent; far more cyclopentyl products are produced from solvolysis of bromotriflate **66** in methanol/Br^- than in acetic acid/Br^-.

Subsequently to Brown and co-workers' investigations in this field, Rodebaugh and Fraiser-Reid reported evidence to support the direct transfer of Br^+ from the bromonium ion intermediate to an acceptor alkene.[51] Rodebaugh and Fraiser-Reid observed that, upon treatment with NBS in aqueous acetonitrile, n-pentenyl glycoside **70c** underwent oxidative hydrolysis to the corresponding hemi-acetal **71**, whilst allyl (**70a**), butenyl (**70b**) and hexenyl (**70d**) analogues gave bromohydrin addition products **73** and **74** (Scheme 20).

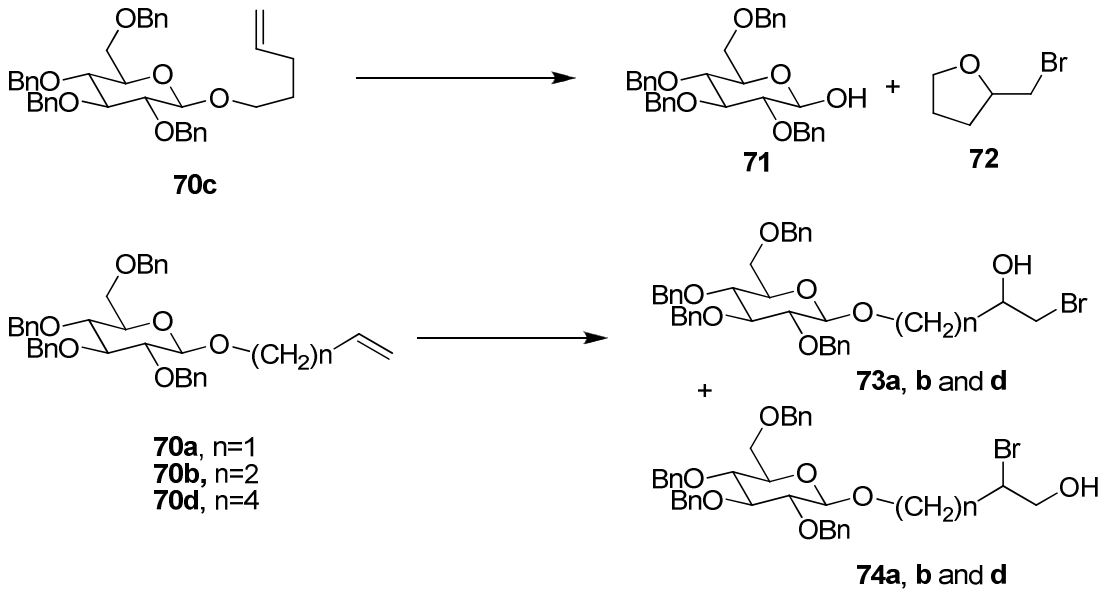

Scheme 20: reaction of ω-alkenyl glycosides with aqueous NBS

Furthermore, it was found that when the n-pentenyl (**70c**) and n-hexenyl (**70d**) glycosides were made to compete for an insufficient amount of NBS, a product ratio of 23:1 was obtained in favour of the products derived from pentenyl species (**71** and **72**). This was unexpected, due to the similar rates displayed by the two analogues when they are reacted independently (product ratio predicted by the pseudo-first order rate constants; 2.6:1). Upon further investigation, the product distribution of this competition reaction was found to be concentration dependent, the ratio of hemiacetal **71** to bromohydrins **73** and **74** decreasing with decreasing concentration. Rodebaugh and Fraiser-Reid rationalised these results by invoking the extremely facile, diffusion controlled transfer of Br^+ between bromonium ions and alkenes in the reaction mixture (Scheme 21). It was proposed that both **70c** and **70d** react to give the corresponding bromonium ions **75c** and **75d**, respectively, the former progressing rapidly to the hydrolysis products, **71** and **72**. Transfer of Br^+ from the less reactive bromonium ion **75d** to excess alkene, before it is trapped by a nucleophile, is set against the more rapid nucleophilic trapping of bromonium ion **75c**. This results in a product distribution weighted hugely in favour of the products resulting from the hydrolysis of the more reactive intermediate, **75c**.

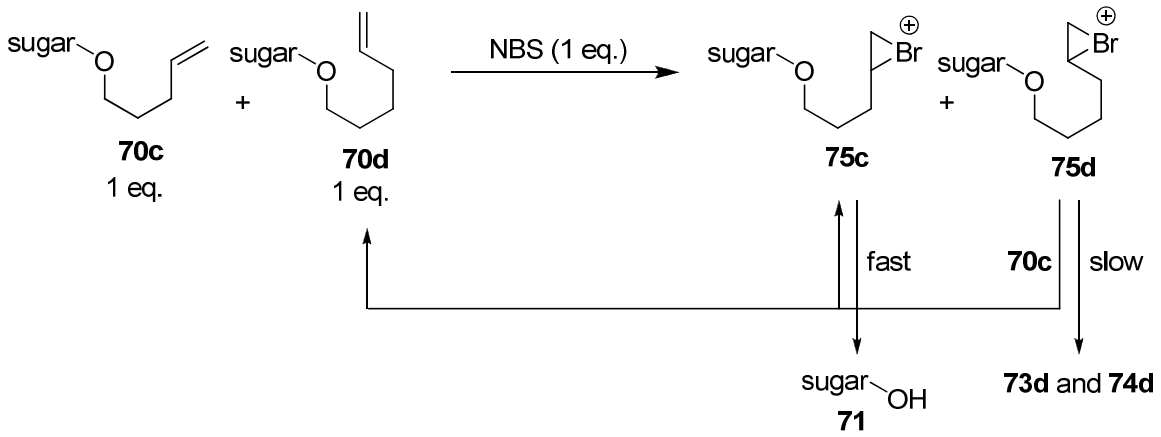

Scheme 21: Br^+ exchange in the bromination of ω-alkenyl glycosides

Rodebaugh and Fraiser-Reid concluded that Brown's observation of facile transfer within the **39**Br^+/TfO^--alkene system could also be applied to ordinary, unhindered, electronically similar and (nearly) equivalently reactive alkenes.

The generality of a reversible bromonium ion mechanism and of bromonium ion-alkene Br^+ exchange in the electrophilic bromination of olefins is still debated in the literature. Evidence which contests the reversible formation of bromonium ions has also been reported. Much of this evidence is derived from studies of solvent effects as reported by Rausse and Dubois.[26,49] More recently, in 1999, Merrigan and Singleton reported their findings of kinetic isotope effects in the bromination of 1-pentene (**76**) in carbon tetrachloride.[52] They demonstrated the presence of an inverse ^2H kinetic isotope effect for the vinylic protons and a relatively small, but significant ^{13}C kinetic isotope effect for both olefinic carbons (Scheme 22).

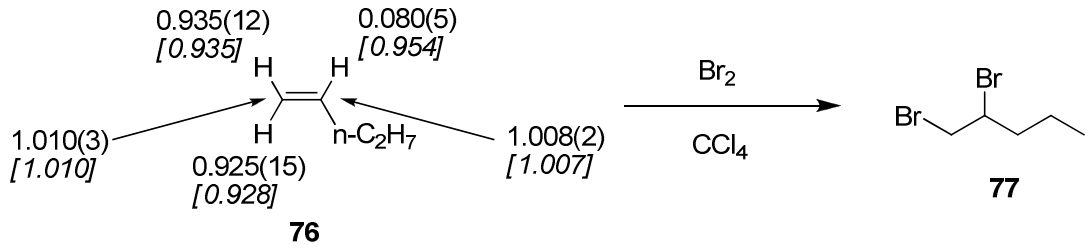

Scheme 22: ^{13}C and ^2H kinetic isotope effects for the bromination of 1-pentene 76
(theoretically predicted kinetic isotope effects in parentheses)

These observations matched the calculated predicted kinetic isotope effects for the formation of a bridged bromonium ion at the rate determining step. This led Merrigan and

Singleton to conclude that the formation of the bromonium ion was irreversible (i.e. rate determining).

It is possible that some of the conflicting evidence originates in differing degrees of reversibility of the bromonium ion formation depending on the cyclic bromonium ion or *β*-bromocarbonium ion character of the intermediate. In 1991 Brown, Bellucci and co-workers reported that the degree of reversibility of bromonium ion formation in a series of substituted *cis*-stilbenes appeared to decrease with increasing *β*-bromocarbonium ion character of the intermediate.[53] An excess (2:1, olefin to bromine ratio) of the *cis*-stilbene (**78a**, **b**, **c** and **d**) was reacted with bromine in dichloromethane to give the dibromide. Whether the involved intermediate ions were symmetrically or asymmetrically bridged, or an open *β*-bromocarbonium ion, depended on the ability of the remote substituents to stabilise a positively charged benzylic cation. Brown and Bellucci reported a product mixture from the bromination which not only contained a mixture of the (*R**,*R**) and (*R**,*S**) dibromides, **82** and **83**, but also the corresponding *trans*-stilbene **79**. The observed product mixture was rationalized by the reversible formation of a partially bridged (the degree of bridging varying with substrate) bromonium ion (**80** and **81**, Scheme 23).

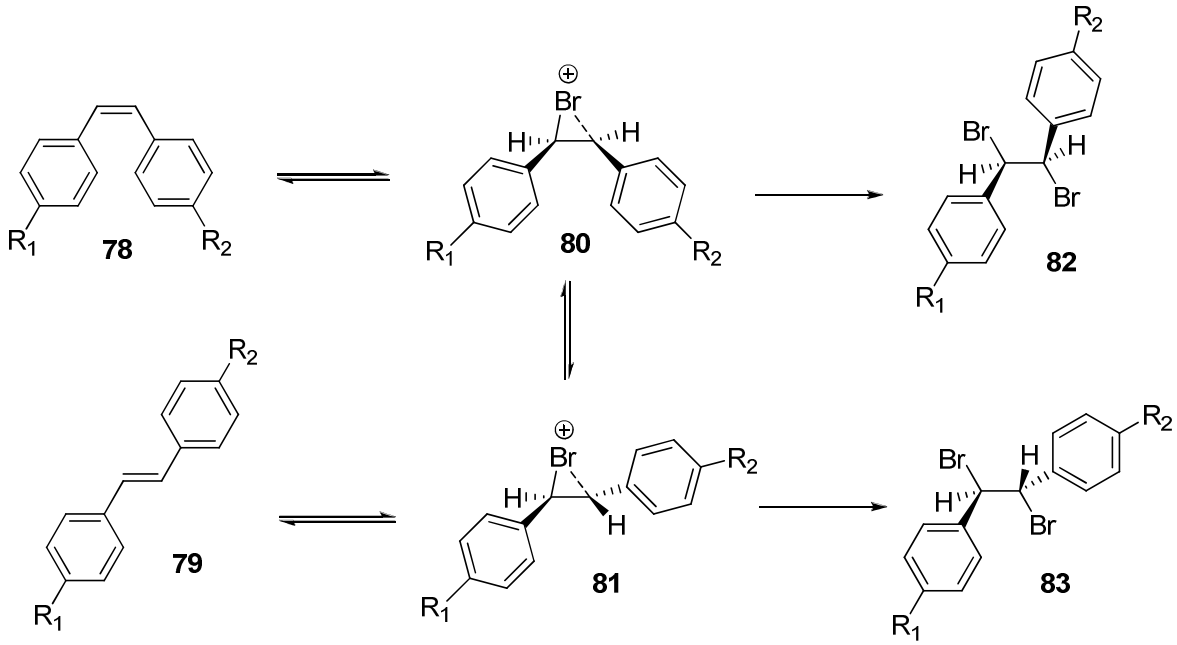

78a R_1=H, R_2=CH_3, **78b** R_1=R_2=H, **78c** R_1=CF_3, R_2=H, **78d** R_1=R_2=CF_3

Scheme 23: the reversible formation of a partially bridged bromonium ion in the bromination of *cis*-stilbenes

The degree of bridging in the intermediate was determined by the (*R**,*R**)/(*R**,*S**) (**82**/**83**) ratio of the dibromide products obtained, significant bridging leading to an increase in *trans* addition. The degree of reversibility was monitored by the *trans*-stilbene (**79**)/dibromide (**82** and **83**) ratio. It was reported that there was a strong correlation between increasing bromine bridging and increasing reversibility from **78a** through to **78d**. Thus, Brown and Bellucci deduced that open *β*-bromocarbonium ions do not significantly revert back to the olefin. However, symmetrically bridged bromonium ions are much more prone to reversal. This is consistent with considering the relative charge distribution in the two intermediates. Theoretical calculations have demonstrated that a symmetrically bridged bromonium ion will have a significant amount of charge located on the bromine atom,[54] which will thus be activated to attack by a nucleophile (e.g. bromide or alkene). On the other hand, an open *β*-bromocarbonium ion has the majority of positive charge localised in the carbon atom. Thus, nucleophilic attack is more likely to occur at the carbon than at bromine, leading to trapping of the intermediate to form addition products rather than undergoing Br^+ exchange.

The experimental and theoretical results obtained in favour of the Br^+ exchange mechanism lead to the conclusion that a general bromonium ion-alkene Br^+ exchange process certainly cannot be ruled out. Thus, the possibility of such a process must be given serious consideration when designing or interpreting reactions involving the electrophilic bromination of olefins.

1.3. Catalytic Asymmetric Electrophilic Bromination

1.3.1. Investigations into the Catalytic Asymmetric Bromination of Alkenes Reported in the Literature

The catalytic asymmetric transfer of a positively charged bromine atom to one face of a prochiral alkene, followed by regioselective attack of the bromonium ion by a nucleophile is unprecedented in the literature. This conclusion was reached after a review of asymmetric halogenation in 2004 by Cansell[55] and publications in the field since this date have been limited. A significant advancement in the area of asymmetric halogenation was reported in 2007 by Sakakura *et al* with the development of the reagent controlled asymmetric

iodolactonization of polyprenoids (for example, **84**, Scheme 24) with excellent enantioselectivity (91-99% ee over a range of polyprenoids).[56]

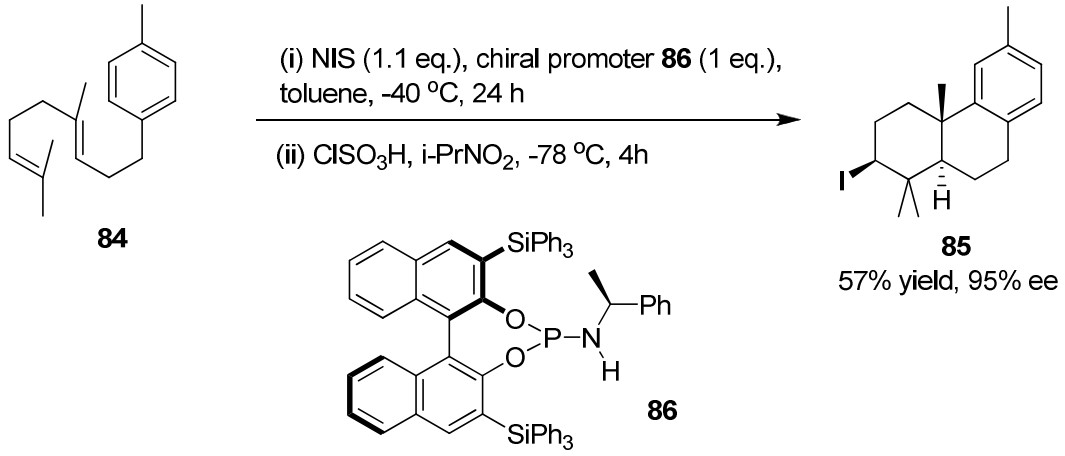

Scheme 24: Sakakura *et al*'s asymmetric iodocyclization of polyprenoids

Sakakura *et al* used phosphoramidite **86** as a chiral nucleophilic promoter to activate the iodinating agent, *N*-iodosuccinimide (**87**), and transfer "I^+" to the alkene substrate (Scheme 25).

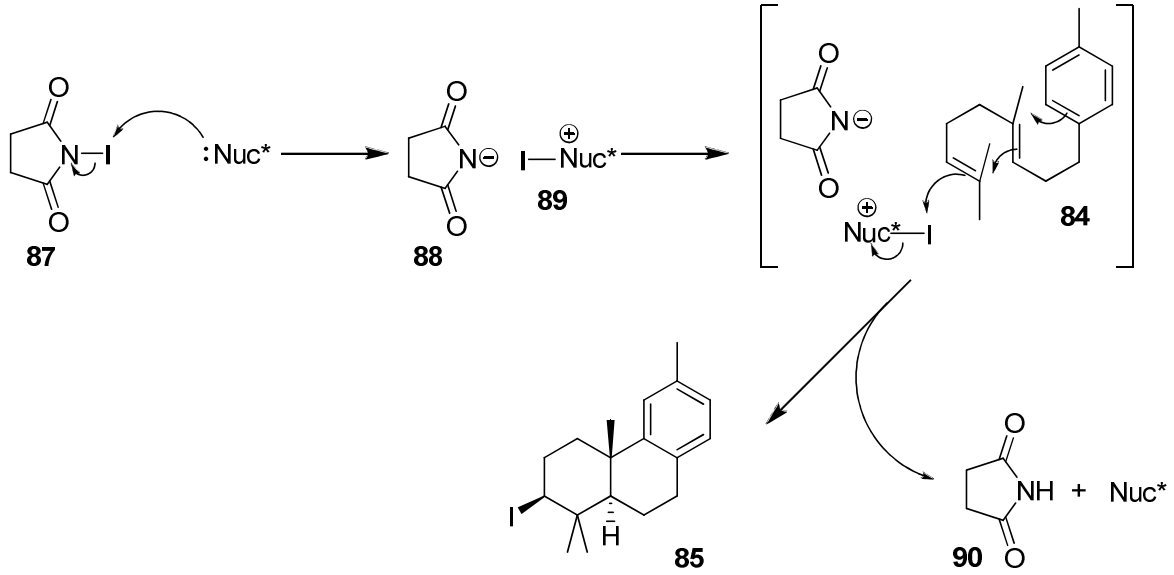

Scheme 25: nucleophilic promotion in the activation of *N*-iodosucciminde and halocyclisation of 4-(homogeranyl)toluene (84)

However, application of the same methodology to bromocyclisation (using NBS as the halogen source) afforded only 36% enantioexcess in the product. Attempts to render the

reaction catalytic in the nucleophilic promoter resulted in negligible enantioselectivity, yielding 29% product with an ee of 4%.

Thus, to date, a single example of a catalytic bromination reaction of an olefin exists, as developed by Henry and co-workers.[57] Henry used catalytic amounts (0.5-3.1 mol%) of chiral bidentate Pd(II) complexes (**91** and **92**) to control the stereochemistry in the dibromination of olefins by copper(II) bromide (Scheme 26).

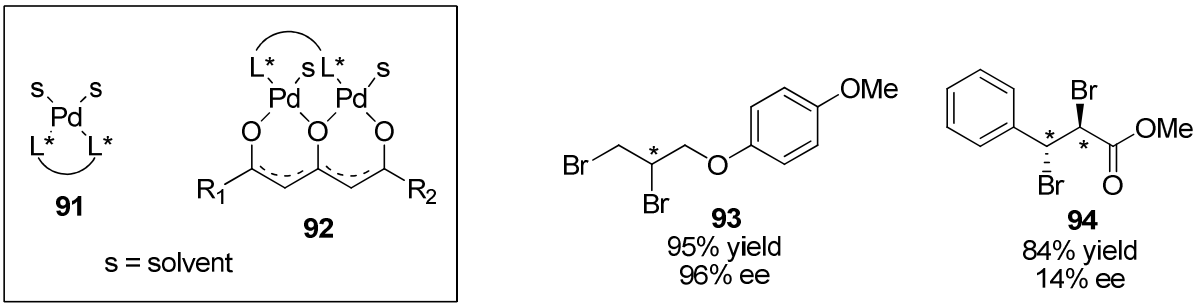

Scheme 26: Henry *et al*'s asymmetric dibromination of alkenes

Although yields and enantioselectivity were good for terminal α-olefins (*e.g.* (4-methoxy)-1-phenoxy-2,3-dibromopropane (**93**), 95% yield, 96% ee), the enantiocontrol showed a marked decrease in the bromination of internal olefins (*e.g.*, methyl 2,3-dibromo *trans*-cinnamate (**94**), 84% yield, 14% ee). A great degree of success had also been obtained in the field of catalytic asymmetric α-bromination of aldehydes and ketones,[58] but a comprehensive survey of this area is beyond the scope of this review. However, it is apparent that no successful catalytic asymmetric bromination reaction has been developed that proceeds *via* a chiral bromonium ion intermediate.

1.3.2. Catalytic Asymmetric Bromination of Alkenes and the Reversible Formation of Bromonium Ions

Our past and current research has been directed towards the development of a general catalytic asymmetric bromination reaction of alkenes. The successful development of such a protocol would provide a novel and extremely powerful synthetic tool. Subsequently to chiral bromonium ion formation and opening by a nucleophile, a number of transformations can be envisaged which utilise the newly incorporated chiral centres (Scheme 27)

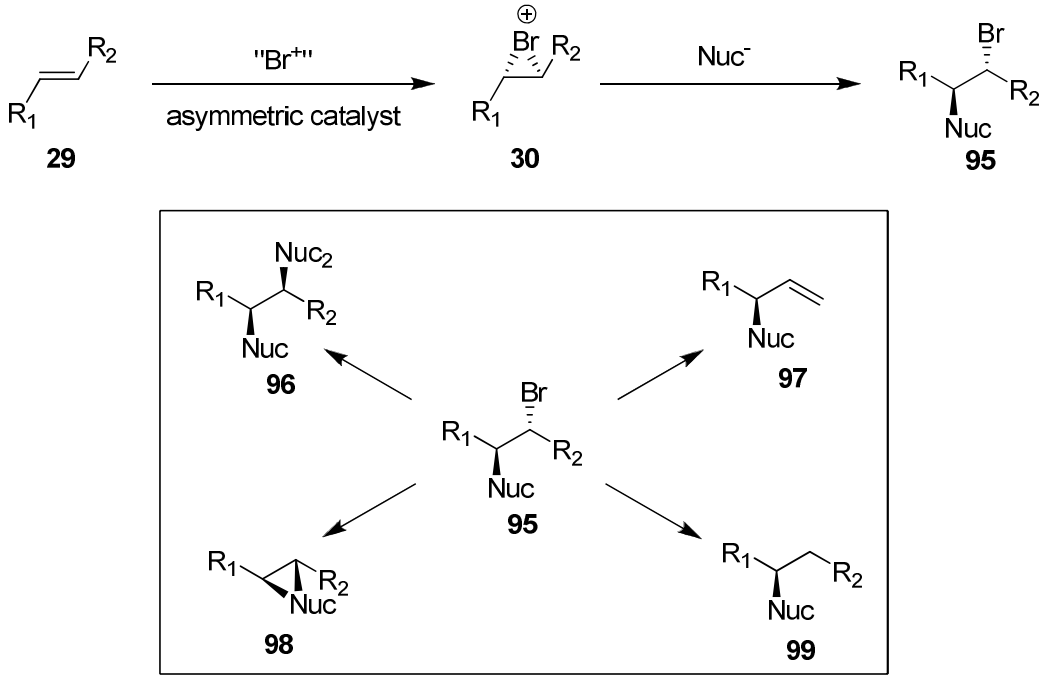

Scheme 27: catalytic asymmetric electrophilic bromination of alkenes and subsequent transformations

However, over the course of our current research, we had cause to re-examine the principles behind our ultimate goal of catalytic asymmetric bromination of olefins. In the light of the apparent reversibility of bromonium ion formation and the extremely facile transfer of Br^+ between bromonium ions and alkenes in some systems, we noted that the catalytic asymmetric bromination reaction may be considerably more complex and challenging than originally perceived. In theory, a chiral bromonium ion may be formed as the result of a chiral catalyst. However, if Br^+ exchange is a factor in the reaction mixture, in the presence of alkene starting material a chiral bromonium ion could go on to exchange Br^+ with another prochiral alkene molecule. If this occurs in a non-asymmetric manner, this would lead to the loss of any enantioexcess imparted by the asymmetric bromination catalyst.

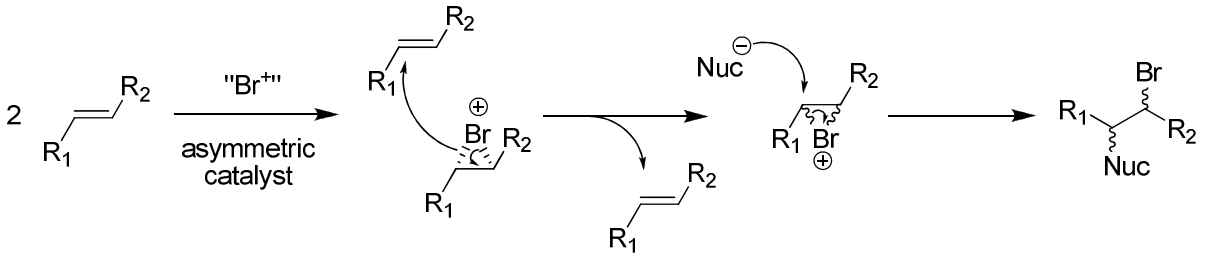

Scheme 28: racemisation of chiral bromonium ion *via* Br^+ exchange

Thus, after a review of the existing literature, we can more fully grasp the complexities of developing a catalytic asymmetric bromination reaction of alkenes.

1.3.3. Previous Work within the Braddock Group

Previous work within the Braddock group has focused on the development of organocatalysts in the asymmetric bromination of alkenes. The use of non-metal systems has advantages over the use of more common metal-based asymmetric catalysts (generally complexed with asymmetric ligands to allow enantiocontrol of the product)[59,60] both in purification of the products and in the handling and disposal of the catalysts. It is often difficult to remove all traces of metal based catalysts and in addition to this they are generally toxic, introducing the necessity of complex and costly waste disposal procedures.

1.3.3.1. Hypervalent Iodine as a Stoichiometric Electrophilic Bromine Transfer Reagent

It had previously come to our attention over the course of our investigations into bromination that there are a number of instances of hypervalent iodine acting as a stoichiometric Br^+ transfer agent in the use of (diacetoxyiodo)benzene, or DIB (**100**), with a bromide source.[61] On further research it was found that a stoichiometric combination of DIB (**100**) and LiBr in THF smoothly brominates a variety of substrates in less than 30 min at room temperature.[62]

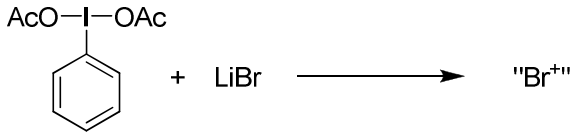

100

Scheme 29: DIB and LiBr as a source of "Br^+"

It was proposed that electrophilic bromine is generated *in situ* by the reaction of the bromide anion with DIB (**100**) and the displacement of acetate to give the intermediate **101** (Scheme 30). The resulting I(III)-Br bond renders the bromide atom electrophilic and thus open to attack by the alkene moiety.

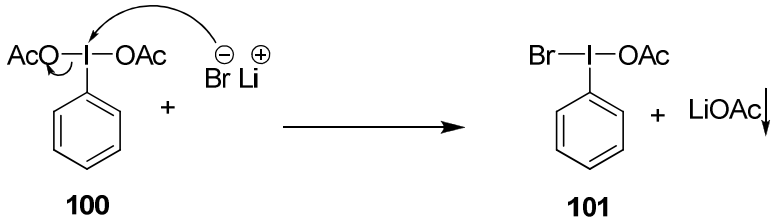

Scheme 30: formation of intermediate 101 containing hypervalent I(III)-Br bond

In an attempt to gain evidence to support both the existence of such I(III)-Br bonds and their ability to act as an electrophilic bromine source, the bromoiodinanes **103** and **105** were selected as suitable targets. Although similar species had been previously synthesised[63] there was incomplete characterisation of their structure, and no investigations had been carried out into the ability of such compounds to act as a source of electrophilic bromine (instead their reactivity in free-radical brominations had been explored). It was found that the bromoiodinanes of interest (**103** and **105**) were formed cleanly and in good yield by the addition of NBS to the corresponding carbinol precursor (**102** and **104**, Scheme 31).

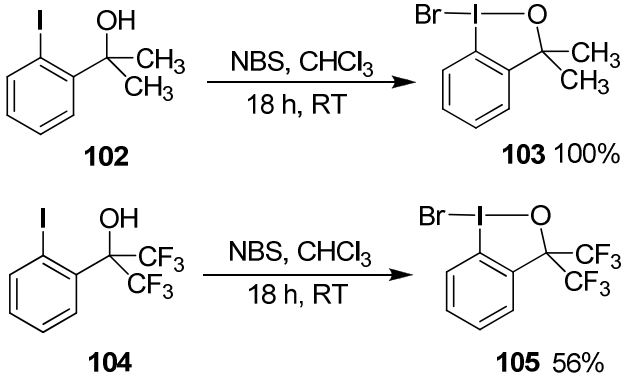

Scheme 31: formation of bromoiodinanes

The structures of the iodinanes **103** and **105** and consequently the presence of the I(III)-Br bonds were confirmed by single crystal X-ray diffraction.[64] Screening of the bromoiodinanes with electron-rich olefin substrates confirmed their ability to act as a source of electrophilic bromine (Scheme 32).

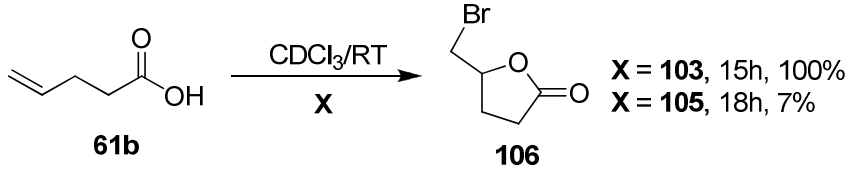

Scheme 32: bromolactonisation with bromoiodinanes as a source of Br^+

1.3.3.2. Catalytic Hypervalent Iodine-Mediated Bromination

A significant observation of the above bromination reactions is that the only observable by-products were the carbinol precursors (**102** and **104**) to the bromoiodinanes (**103** and **105**). In addition to this, the rate of bromination *via* the dimethylbromoiodinane (**105**) is considerably faster than bromination of substrate by NBS. These observations allowed the process to be rendered catalytic using a stoichiometric amount of NBS and 25 mol% of carbinol **105**. Thus, catalytic hypervalent iodine-mediated bromination was achieved, opening up extensive possibilities for the development of asymmetric catalysts based on hypervalent iodine.

A screen of iodine-based catalysts containing an electronegative heteroatom in the *ortho* substituent to the iodine revealed that increasing the nucleophilicity of the heteroatom increases the catalytic activity. Thus the rate of conversion of substrate **61b** increases dramatically as the apical group is changed in the order alcohol < carboxylic acid < amide < amidine (Scheme 33 and Table 2)

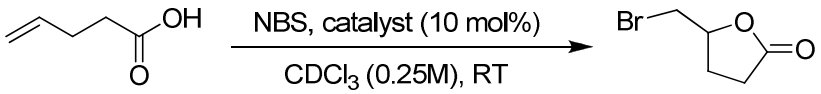

61b **106**

Scheme 33 and Table 2: catalytic hypervalent iodine-mediated bromination

Catalyst	Time	Conversion
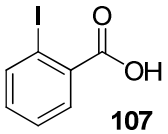 **107**	6 h	100%
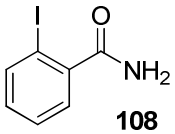 **108**	2 h	72%
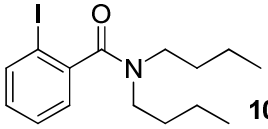 **109**	20 min	100%
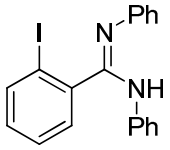 **110**	10 min	100%

These results led to the selection of an iodine/amidine based catalyst with stoichiometric NBS as the most potent catalytic system. After this optimisation of the system, steps were taken to render the reaction asymmetric.

1.3.3.3. Introduction of Asymmetry to the System

The original modification made to the amidine based catalyst introduced chiral centres adjacent to the amidine nitrogens in (4*R*,5*R*)-2-(2-iodophenyl)-4,5-diphenyl-4,5-dihydro-1*H*-imidazole, or IAM (**111*R***).

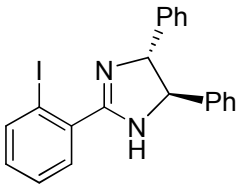

111*R*

Figure 21: (4*R*,5*R*)-2-(2-iodophenyl)-4,5-diphenyl-4,5-dihydro-1*H*-imidazole, or IAM

Screening of this catalyst with a variety of unsaturated carboxylic acid substrates produced excellent yields of lactone but, unfortunately, with no enantiocontrol. It was reasoned that this lack of enantioselectivity was due to the remoteness of the chiral centres from the site of bromine delivery in the hypothesized I(III)-Br intermediate, (**112**, Figure 22). The electronically required linearity of the N-I(III)-Br bond orientates the bromine away from the chiral cyclic amidine.

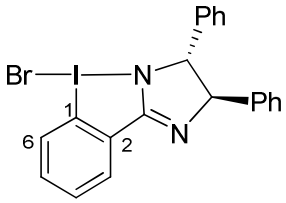

112

Figure 22: I(III)-Br catalytic intermediate of IAM

It was hypothesized that a chiral group in the 6-position on the benzene ring, *ortho* to the iodine, should lie closer in space to the "Br^+" in the catalytic intermediate than the group in the 2-position. This is confirmed by the observation that a sp^3 group in the 6-position diminishes the catalytic activity of iodobenzoic acid (**107**) (53%, 19 h, *c.f.* 100%, 6 h) indicating the high sensitivity of "Br^+" delivery to substituents in this position.

The C_2 symmetric structure of 2,6-di-[(4*R*,5*R*)-4,5-diphenyl-4,5-dihydro-1*H*-imidazol-2-yl]iodobenzene (IBAM, **113*R***, Figure 23) was settled on as a suitable candidate for an asymmetric bromination catalyst. This structure was desirable as the C_2 symmetric design results in the I(III)-Br bond sitting in the same chiral pocket irrespective of free rotation. In addition to this, the cyclic amidine moiety places a sp^2 centre at the C-6 position. This should allow introduction of chiral groups in close proximity without significantly diminishing catalytic activity (which the introduction of a sp^3 centre at C-6 undoubtedly would).

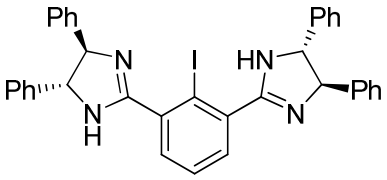

113R

Figure 23: 2,6-di-[(4*R*,5*R*)-4,5-diphenyl-4,5-dihydro-1*H*-imidazol-2-yl]iodobenzene or IBAM

The catalyst IBAM (**113*R***) demonstrated excellent activity and at 1 mol% loadings facilitated the complete conversion of pentenoic acid (**61b**) to the corresponding bromolactone **106** in less than 15 min at room temperature. However, extensive screening of the catalyst with various substrates and temperatures resulted in only limited success in terms of enantioselectivity. Most substrates were converted to lactone with no measurable enantioselectivity under the conditions employed. However, a reproducible enantioexcess was observed with the catalytic asymmetric bromination of cyclopenten-2-yl acetic acid (**114**) (Scheme 34).

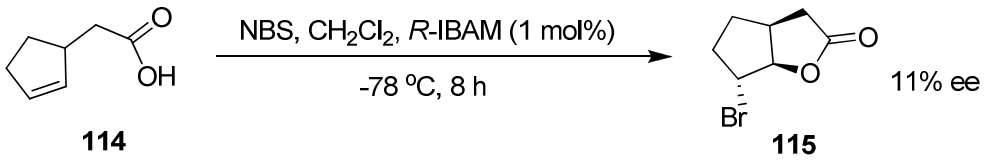

114 **115**

Scheme 34: enantioselective bromolactonisation with *R*-IBAM

The (*S*)-enantiomer the IBAM catalyst (**113*S***) was confirmed to produce the opposite asymmetric induction in the isolated bromolactone product. This result was extremely encouraging, representing the first example of a metal-free catalytic asymmetric alkene bromination reaction.

Attempts were made to increase the enantiomeric excess of the product by changing the solvent and catalyst loading, but with no reproducible success. Due to a large amount of background variation in the results it was deduced that the enantioexcess observed is extremely sensitive to external factors such as small variations in temperature, solvent purity or localised heating during quenching.

Another complication in this catalytic system became apparent on carrying out control reactions carried out with the iodine-free mono-amidine analogue, AM (**116*R***).

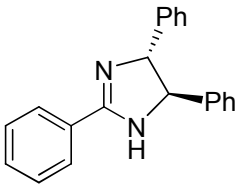

116*R*

Figure 24: iodine-free catalyst analogue, AM (116*R*)

Under identical reaction conditions, with low temperature quenching, lactone was produced in a similar yield to that seen with *R*,*R*-IBAM, **113*R*** (50% *c.f.* 55-65%). This implies that in the catalytic reaction of IBAM (**113**) there is a significant background reaction occurring involving bromine transfer *via* the amidine moiety alone. As catalysis with iodine free species **116*R*** produced lactone with no enantiocontrol, it is suspected that this background reaction in IBAM may account for the low enantioexcess observed. It is likely that the observed variations in enantioexcess due to external factors, such as small variations in temperature, are occurring due to such factors affecting the ratio of "Br^+" delivered from iodine and nitrogen (Figure 25).

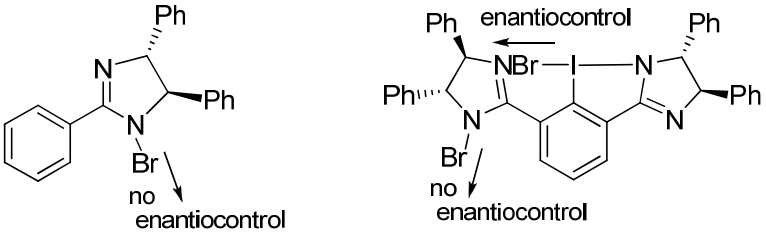

117*R* **118*R***

Figure 25: N-Br and I-Br catalytic intermediates

1.3.3.4. Attempted Structural Elucidation of Active Catalytic Intermediates

In order to gain further information on the site of bromine transfer, attempts were made to isolate the species formed on addition of stoichiometric NBS to IBAM (**113*R***) (Scheme 35). Such additions, at room temperature in deuterated chloroform, resulted in the reaction mixture changing from a colourless to a bright green solution. Subsequent analysis by ^{1}H NMR after stirring for 40 min indicated the complete conversion of NBS to succinimide. Overlapping peaks in the aromatic region prevented identification of any changes in the resonances belonging to the catalyst, although considerable line broadening was observed in both the ^{1}H and ^{13}C spectra.

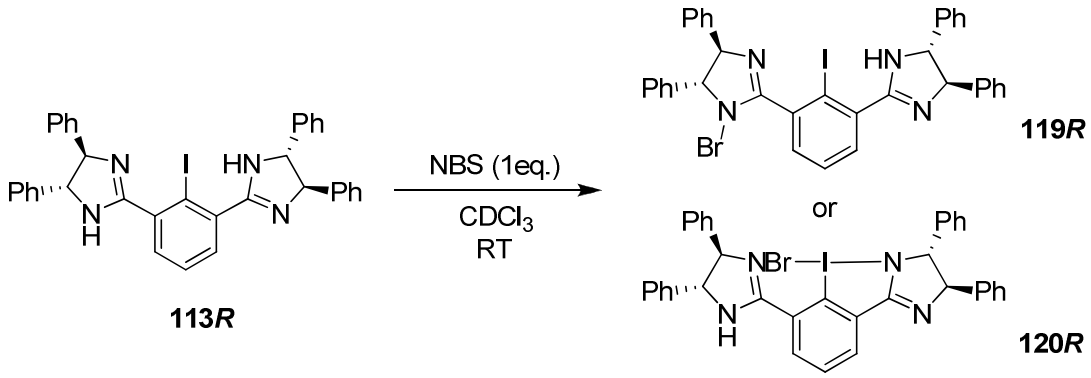

Scheme 35: stoichiometric addition of NBS to IBAM (113*R*)

Attempts at isolation of the active catalytic species **119*R*** or **120*R*** were unsuccessful, as were mass spectrometry experiments to confirm the existence of a catalyst-Br^+ adduct.

Similar stoichiometric additions were also carried out with both IAM (**111**) and AM (**116**). The reactions proceeded in the same fashion as observed with IBAM (**113*R***), both solutions changing from colourless to yellow/green on addition of NBS, and ^{1}H NMR analysis revealing complete conversion of NBS to succinimide. Line broadening was again observed in both the ^{1}H and ^{13}C spectra, to the extent that certain ^{13}C resonances (142.6 ppm in **111** and 143.5 in **116**, belonging to the quaternary carbons on the phenyl rings (NCH*C*), and the H*C*N peak at 76.7 ppm in **111**) no longer appeared as measurable peaks. This broadening was attributed to the formation of a new catalytic species containing a "Br^+" moiety.

Unfortunately, the methods employed failed to either isolate or fully characterize the intermediates concerned or to establish whether electrophilic bromine is bonded to the iodine in a hypervalent species or to the nitrogen of the amidine.

In conclusion, past work conducted in the Braddock group has resulted in the successful development of a highly active non-metal catalyst for the bromination of alkenes, which demonstrates the ability to deliver Br^+ with some degree of enantiocontrol. However, the level of enantioselectivity proved to be sensitive to a number of factors such as substrate, temperature, solvent and background reaction, and much scope exists for further investigations in this field.

1.4. Proposed Further Investigations into Asymmetric Catalytic Hypervalent Iodine-Mediated Bromination: General Objectives

The objective of our continued research into asymmetric bromination is to gain a better understanding of the catalytic system and the action of the catalyst IBAM (**113**). It is envisaged that we can use such knowledge to increase the enantioselectivity of the reaction and to develop a synthetically useful protocol.

It was initially proposed that our investigations should focus on continuing and broadening our studies into the existing IBAM (**113**) catalyst. This would include further stoichiometric additions of NBS to the catalyst to determine the nature of the catalytic intermediate, more detailed investigations into the effects of temperature, solvent and catalyst loading and the synthesis and screening of modified IBAM-based catalysts. Additionally, over the course of our investigations, it became apparent that bromonium ion-alkene Br^+ exchange within our catalytic bromination system also was a key factor which warranted our attention.

In order to satisfy our research aims, it was apparent to us that considerably larger quantities of our catalysts IBAM (**113**) and IAM (**111**), and their iodine-free analogues BAM (**121**) and AM (**116**), were required than we had been previously been able to synthesise.

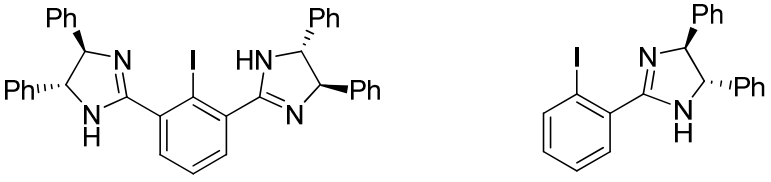

113 (IBAM)

111 (IAM)

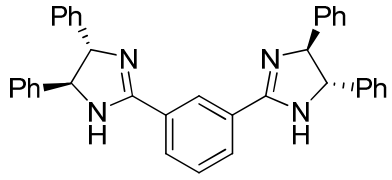

121 (BAM)

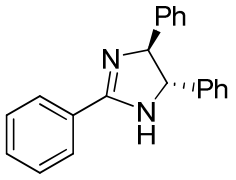

116 (AM)

Figure 26: asymmetric bromination catalysts and their iodine-free analogues

The limiting factors in the previous synthesises of such cyclic amidine based catalysts had been two-fold. The extremely high cost of the (1*R*,2*R*)- and (1*S*,2*S*)-1,2-diphenylethylene

diamine (**124*R*** and **124*S***) resulted in the availability of only milligram amounts of chiral starting material. In addition to this, formation of the chiral cyclic amidine moieties *via* an intermediate imidate (**123**, Scheme 36) has always proved to be a low yielding and capricious reaction, often affording inseparable mixtures of products and resulting in the loss of the valuable diamine starting material.

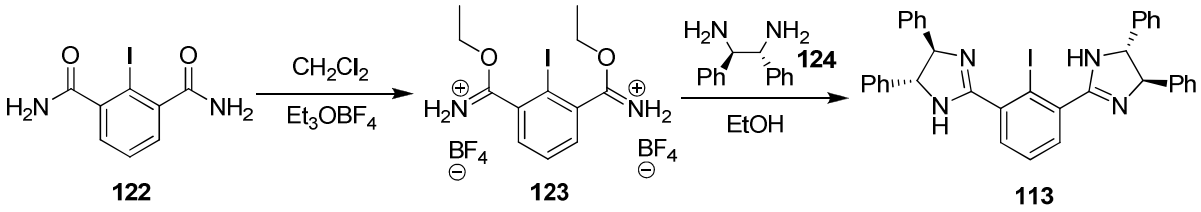

122 **123** **113**

Scheme 36: original IBAM (122) synthesis

As such, the route to IBAM (**122**) was unsuitable for a large scale synthesis and required modification. Thus, our first goal was to synthesise gram amounts of optically pure diamines **124*R*** and **124*S*** and, on achieving this, to optimise catalyst synthesis, minimizing the loss of the chiral diamine.

2. Synthesis and Resolution of (+)-(1*R*,2*R*)- and (–)-(1*S*,2*S*)-1,2-Diphenylethylenediamine (124*R* and 124*S*)

2.1. Introduction

*2.1.1. 1,2-Diphenylethylenediamine (**124**) in Asymmetric Synthesis*

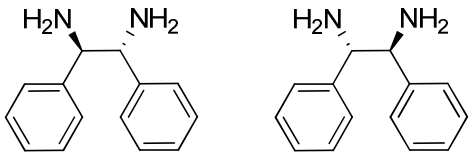

124*R* **124*S***

Figure 27: (+)-(1*R*,2*R*)- and (–)-(1*S*,2*S*)-1,2-Diphenylethylenediamine (124*R* and 124*S*)

Asymmetric synthesis continues to be a rapidly developing field within organic chemistry. Enantiopure chiral diamines have been extensively utilized as a convenient source of chirality when incorporating a chiral motif into reagents and catalysts for asymmetric synthesis. As the applications of asymmetric methodology expand, the need for cheap and simple routes towards the chiral components of the catalysts and reagents become of increasing importance.

The C_2 symmetric (+)-(1*R*,2*R*)- and (–)-(1*S*,2*S*)-1,2-diphenylethylenediamines (**124*R*** and **124*S***) and their *N*-modified derivatives have been widely incorporated into reagents for various asymmetric transformations. The chiral ligand **125** (Scheme 37), derived from chiral diamine **124*S***, has been demonstrated by Corey to be an excellent ligand for the enantioselective dihydroxylation of olefins by osmium tetraoxide, with enantiomeric excesses of 82-98% for olefins ranging from styrene to *trans*-3-hexene.[65]

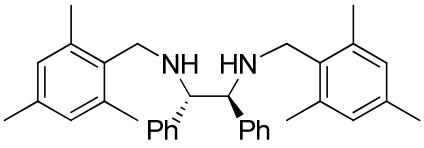

125

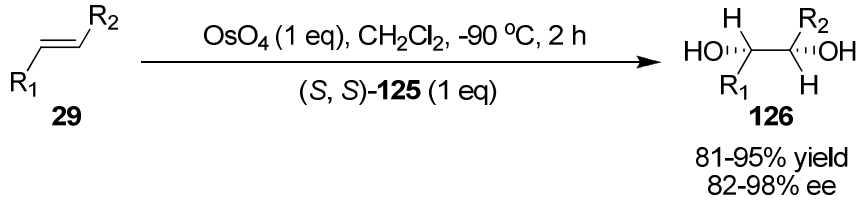

29 **126**

81-95% yield
82-98% ee

Scheme 37: asymmetric dihydroxylation

Corey has also employed similar *N*-modified diamines to form chiral boron reagents (**127**, Figure 28) for enantioselective propargylation,[66] propadienylation,[66] allylation[67] and aldol[68] reactions. All such reactions demonstrate excellent enantiocontrol (see Scheme 38, for an example of asymmetric propadienylation), and have proved valuable tools in the field of asymmetric synthesis.

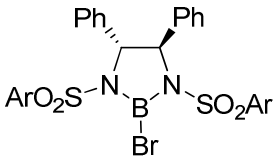

127

Figure 28: general structure of chiral bromoborane reagent

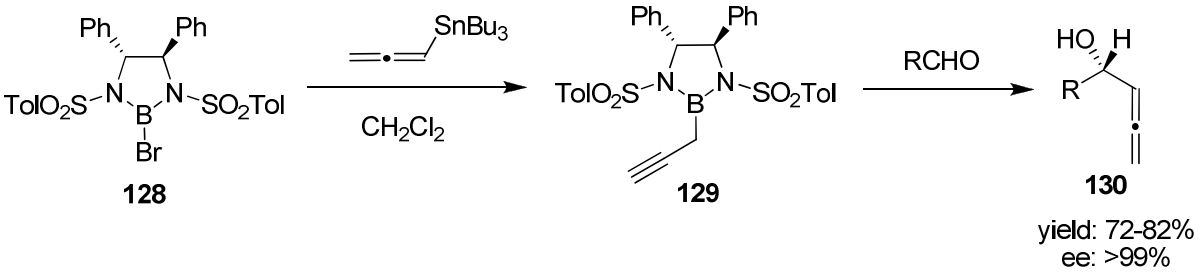

128 **129** **130**

yield: 72-82%
ee: >99%

Scheme 38: asymmetric propa-1,2-dienylation

Chiral ligands based on our target diamine **124** have also been used in a number of important catalytic asymmetric processes. Corey has synthesised chiral Lewis acids in which the boron atom in **127** is replaced with aluminium. These were demonstrated to be highly enantioselective catalysts in the Diels Alder reaction.[69]

An extremely significant recent advancement in the field of asymmetric catalysis was made by Noyori on the introduction of chiral diarylethylenediamine ligands into his already well-precedented BINAP-Ruthenium asymmetric hydrogenation catalyst.[60] The inclusion of the chiral diamine to form a [$RuCl_2$(phosphane)$_2$(diamine)] complex such as **131** (Figure 29) allowed the extension of Noyori's methodology to simple ketones. Catalyst **131** facilitated the reduction of a range of simple aromatic and heteroaromatic ketones with excellent enantiofacial differentiation; hydrogenation of acetophenone and its derivatives proceeding to give the secondary alcohols quantitatively in up to 99% ee. The methodology also tolerated a wide range of functional groups, including F, Cl, Br, I, CF_3, OCH_3, $COOCH(CH_3)_2$, NO_2, NH_2, and NRCOR.

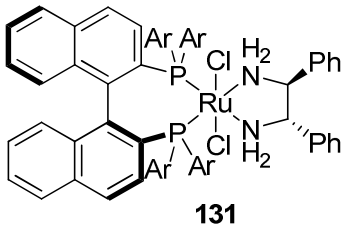

131

Figure 29: (*S*)-BINAP/(*S*)-diamine-Ru^{II} catalyst

Further investigations by Noyori and co-workers found that [RuCl(diamine)(η^6-arene)] complexes such as **132** (Scheme 39) catalyse asymmetric transfer hydrogenation of aromatic and acetylenic carbonyl compounds in a 2-propanol/alkaline-base system. The asymmetric reduction is thought to proceed *via* the 18-electron hydride intermediate, **134**, which undergoes the enantioselective transfer of H_2 to reform the 16 electron true catalyst **133** (Scheme 39).[70]

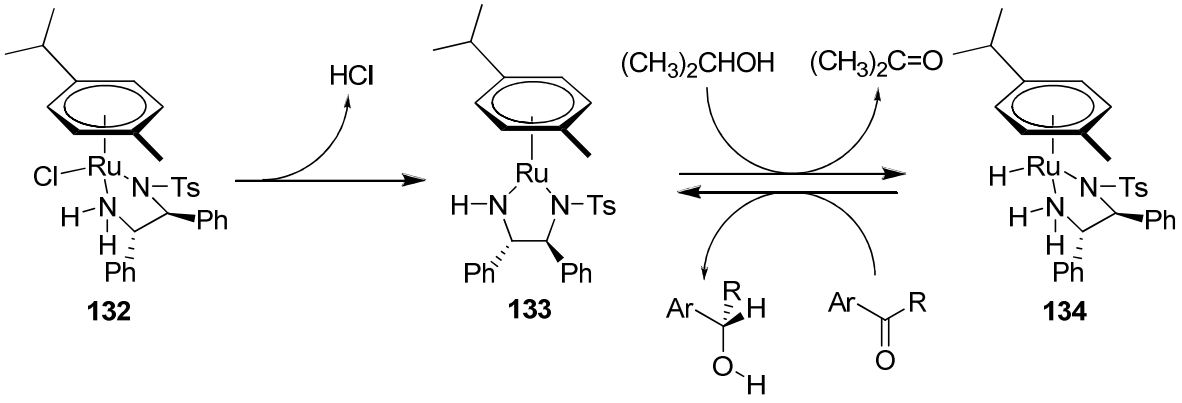

132 **133** **134**

Scheme 39: asymmetric hydrogenation

Noyori's unprecedented discoveries in this field have prompted an abundance of further work by other groups. Whilst the ruthenium/diamine combination has been retained, a number of modifications have been made to the diphosphine ligand. Recent developments include the synthesis and screening of 4,4'-substituted-xylBINAPS,[71] these ligands imparting the highest enantioselectivity reported to date in the hydrogenation of ketones. A number of cheaper and easier-to-prepare alternatives to BINAP have also been investigated, including monodentate phosphines[72] and "achiral" benzophenone-based diphoshines, to which chirality is imparted within the ruthenium complex by the chiral diamine.[73] The substrate range of Ru/diamine hydrogenation catalysts has been expanded to include the dynamic reductive kinetic resolution of racemic α-branched aldehydes to optically active primary alcohols[74] and the enantioselective reduction of activated C=C bonds.[75]

Jacobsen demonstrated the use of manganese (III) complexes of chiral Schiff bases in the asymmetric epoxidation of unfunctionalised olefins.[76] The epoxidation catalysts **135** and **136** (Figure 30) were easily prepared from diamine **124** and, in 1-8 mol% loadings with a stoichiometric amount of iodosylmesitylene, gave good yields in moderate to good enantioexcess of the desired epoxide product.

The inclusion of a glycol chain to form macrocyclic chiral manganese (III) salen complex **137** was demonstrated to further increase the enantioselectivity of the epoxidation reaction.[77]

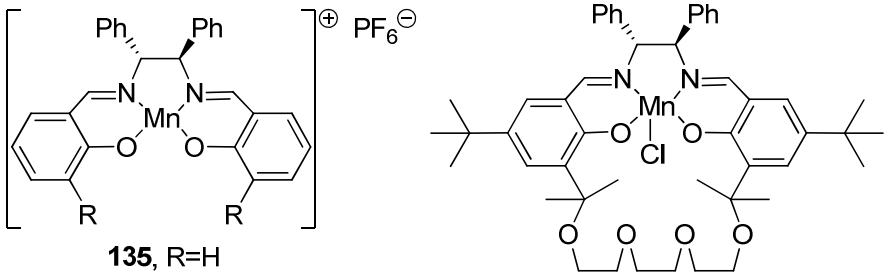

Figure 30: asymmetric epoxidation catalysts

Similar manganese/Schiff base complexes have also been demonstrated to catalyse the asymmetric cyclopropanation of simple alkenes[78] and the silylcyanation of aldehydes with good to moderate enantioselectivity.[79]

Magnesium, complexed with *N*-substituted diamine **124,** was used by Evans in 10 mol% loadings to enantioselectively catalyse the merged enolization and amination of *N*-acyloxazolidiones (**138**) (Scheme 40).[80] This presumably proceeds *via* a chelated magnesium enolate complex, in which the chirality is derived from the diamine ligand rather than the oxazolidinone auxiliary, thus reducing ten fold the amount of enantiopure reagent necessary to impart chirality to the product. The reaction proceeded with excellent enantiocontrol, enantioexcesses being observed in the range of 96->99% for a range of aryl substituted *N*-acyl groups.

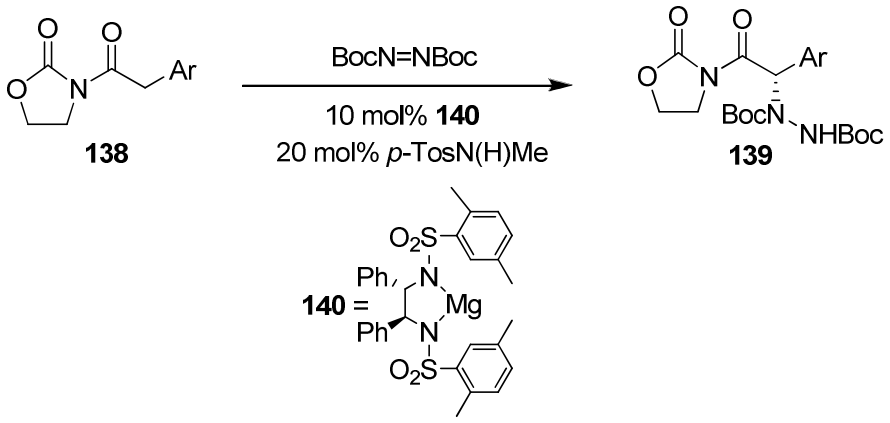

138 **139**

140 =

Scheme 40

Enantiopure 1,2-diphenylethylenediamine (**124**) has also been used to form C_2 symmetric chiral heterocyclic imidazoline moieties in ligands for asymmetric catalysis. Peters and co-workers developed a ferrocenyl-imidazoline palladacyle (**141**), capable of catalysing Aza-Claisen rearrangements with excellent enantioselectivity.[81] Buscacca employed phosphoimidazolines (**142**) as electronically tuneable ligands to explore electronic effects in the asymmetric Heck reaction.[82] Beller and co-workers demonstrated the ability of C_2 symmetric pyridine bisimidazoline ligand **143** to impart moderate to good enantioexcesses to the products of the ruthenium catalysed asymmetric epoxidation of aromatic olefins.[83]

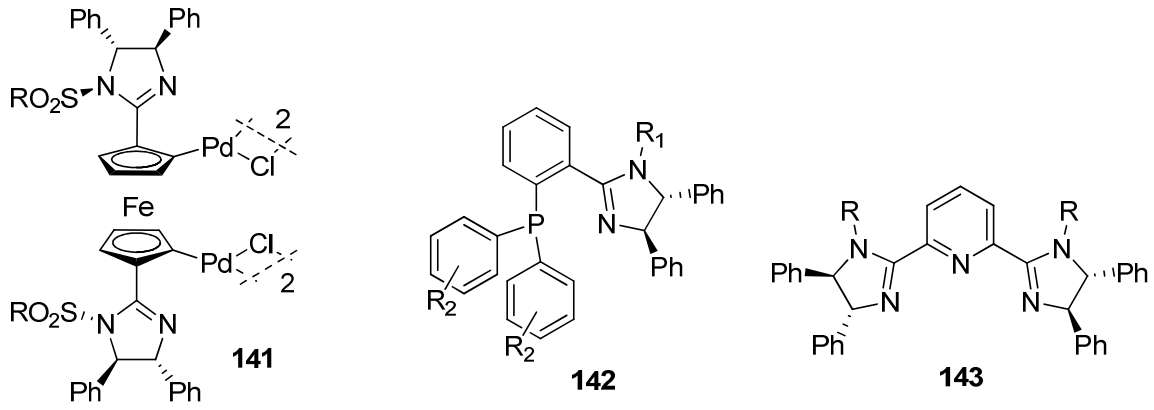

Figure 31: selection of 4,5-diphenyl-imidazoline-containing chiral ligands

Chiral N-hetereocyclic carbenes (NHCs); a relatively new class of ligand within asymmetric synthesis; are also commonly derived from enantiopure 1,2-diphenylethylenediamine. Both Grubbs[84,85] and Hoveyda[86] have recently reported the use of NHCs as ligands in ruthenium catalysed asymmetric olefin metathesis reactions. Hoveyda and co-workers have developed a bidentate asymmetric NHC ligand which, when complexed to ruthenium in catalyst **146**, facilitates asymmetric ring opening cross metathesis with excellent enantioselectivity (83-98% ee) (Scheme 41).[86]

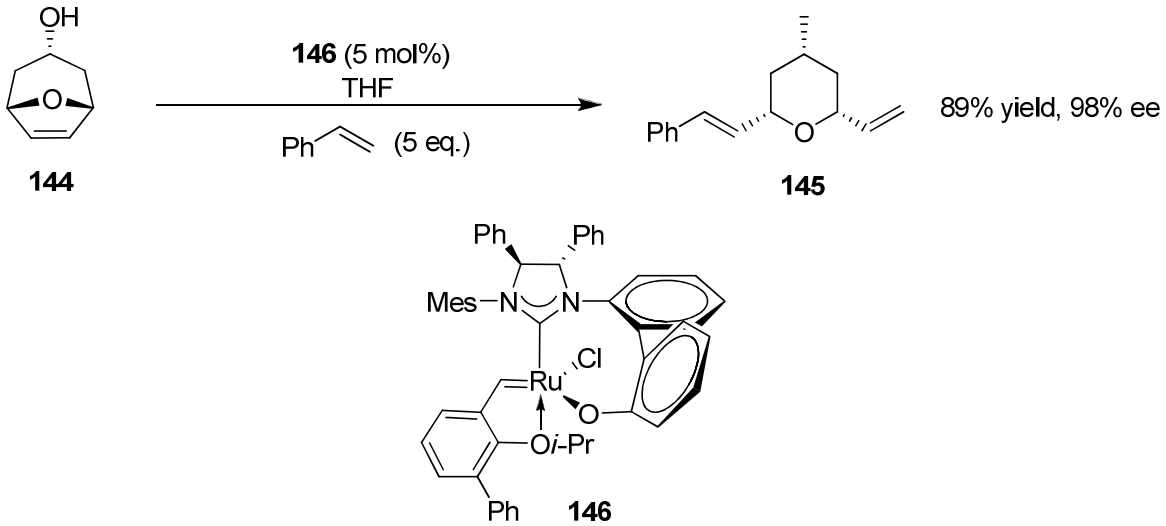

Scheme 41: asymmetric ring opening cross metathesis

Grubbs and co-workers demonstrated the ability of a range of catalysts of the general structure **147** (Figure 32) to afford the de-symmetrised products of ring closing metathesis in good ee (76-92% ee).[84] Additionally, it was demonstrated by Grubbs that these catalysts

could be used to facilitate asymmetric cross and ring opening cross metathesis with moderate to good enantioselectivity.[85]

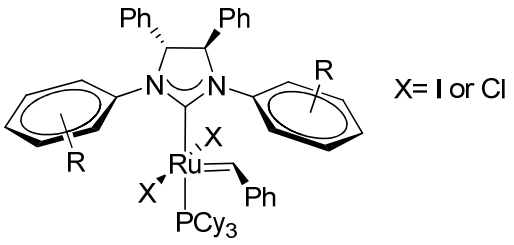

147

Figure 32: Grubbs' asymmetric olefin metathesis catalyst

Hoveyda has also developed the application of 1,2-diphenylethylenediamine-derived NHC ligands in the copper catalysed asymmetric addition of diethyl zinc to α,β-unsaturated ketones[87] and to allylic phosphates.[86] Faller and Fontaine have extended the use of NHC ligands into the field of rhodium catalysed asymmetric hydrosilylation, yielding 1-phenylethanol in up to 58% enantiomeric excess from the hydrosilylation of acetophenone.[88] In almost all of the examples given above of the uses of NHC ligands in asymmetric catalysis, the ligands' electronic and steric properties have been tuned *via N*-functionalisation to optimise catalyst activity and enantioselectivity. It is evident that such asymmetric N-heterocyclic carbenes are extremely versatile and it is probable that we have not yet seen the full extent of their applications within asymmetric synthesis.

A further group of asymmetric catalysts derived from the chiral diamine **124** are enantiopure amides and thioamides. Feng and co workers screened a range of amide-based bifunctional catalysts for the enantioselective cyanosilylation of ketones.[89] As is the case with many such bifunctional catalysts, Feng's catalyst was designed to mimic natural enzymatic processes, bringing two activated components together within an "active site". Feng found that, of all the variations screened, a bisamide ligand derived from 1,2-diethylenediamine, complexed to titanium(IV) (**148**, Scheme 42), afforded the optimum enantioexcesses in the cyanohydrin products.

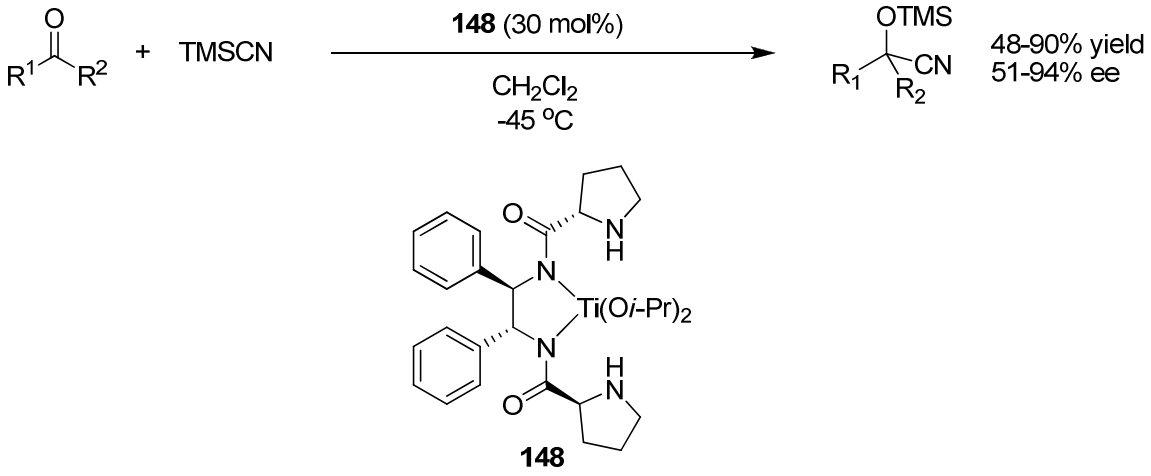

Scheme 42: asymmetric cyanosilylation of ketones

Tsogoeva and Wei recently reported a bifunctional thiourea/primary amine organocatalyst (**149**, Figure 33) for the asymmetric Michael addition of ketones to nitroalkenes.[90] Jacobsen and co-workers subsequently demonstrated the application of similar catalysts (**150**, Figure 33) to the Michael addition of aldehydes to nitroalkenes.[91] In both Tsogoeva's and Jacobsen's catalysts the C_2 symmetry of the diamine is lost; one nitrogen atom forming part of the thiourea moiety and one remaining as a free primary amine. Both authors report that the bifunctional catalysts, which simultaneously activate both nucleophile and electrophile, facilitate the Micheal additions with high yields and excellent enantioselectivity.

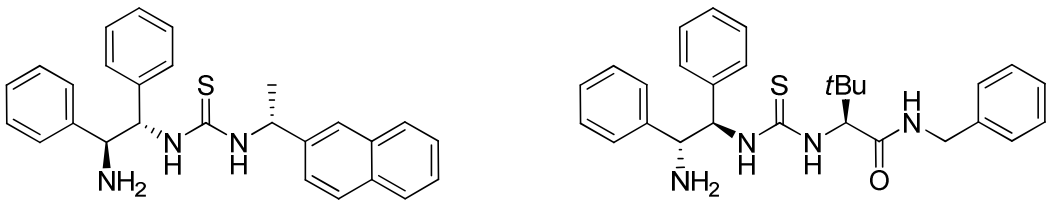

Figure 33: Tsogoeva's (149) and Jacobsen's (150) catalysts

From such numerous examples, it is evident that enantiopure diamine **124** is an extremely useful and versatile source of chirality in asymmetric synthesis in many systems. As such, a short and efficient route for the formation and resolution of gram amounts of diamine is extremely desirable.

*2.1.2. Existing Synthesis and Resolution of 1,2-Diphenylethylenediamine (**124**)*

Racemic diamine (±)-**124** can be resolved into its enantiomers by diastereomeric salt formation with chiral carboxylic acids. A number of such resolutions have been achieved using tartaric acid,[92,93,94] yielding the enantiopure diamine in moderate yields (49-66% after decomplexation, based on half the amount of diamine used). A higher yielding resolution employing mandelic acid[95] to form the diastereomeric salt has also been reported (72% after decomplexation).

However, the synthesis of the diamine, either in its enantiopure or racemic form, has proved more problematic and a number of different strategies have been employed. An enantioselective reduction of *N*-protected 1,2-diimines has been achieved using stoichiometric BH_3.THF and catalytic chiral oxazoborolidine to give the *N*-protected diamine species.[96] However, subsequent purification is required to separate the undesired *meso* compound from its enantiopure diastereomer. This has proved typical of such chemistry, reductive couplings of *N*-protected aromatic imines generally giving mixtures of *meso* and racemic *N*-protected diamines. A notable exception to this is Corey's dissolving metal reduction of spiroimidazole **151** (Scheme 43).[93] This successfully gave the desired racemic diamine after hydrolysis with no formation of *meso* the diasteromer observed.

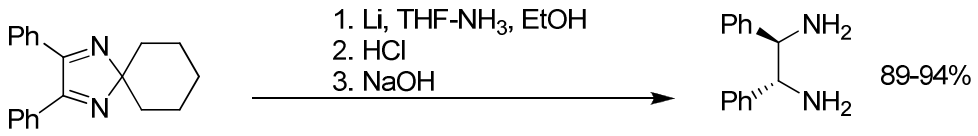

151 (±)-**124**

Scheme 43: dissolving metal reduction of spiroimidazole 151

Two examples of direct asymmetric synthesis of enantiopure diamine **124** have also been reported, both of which commence with a Sharpless asymmetric dihydroxylation of stilbene. Salvadori converted chiral diol **152** to the diamide *via* diazide **153**. This proceeded with an inversion of stereochemistry due to the S_N2 displacement of the tosyl leaving group by azide (Scheme 44).[97]

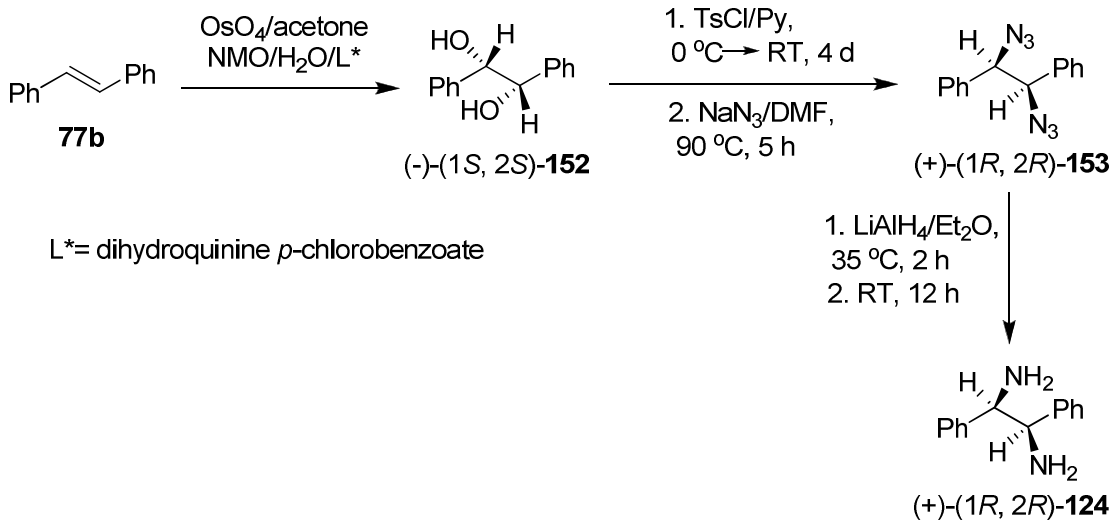

Scheme 44: Salvadori's asymmetric diamine synthesis

Sharpless also achieved the transformation with inversion of stereochemistry of the diol *via* cyclic sulfate **154** and its subsequent reaction with an amidine to form enantiopure imidazoline **116**.[98] Hydrolysis yields the desired chiral diamine (Scheme 45).

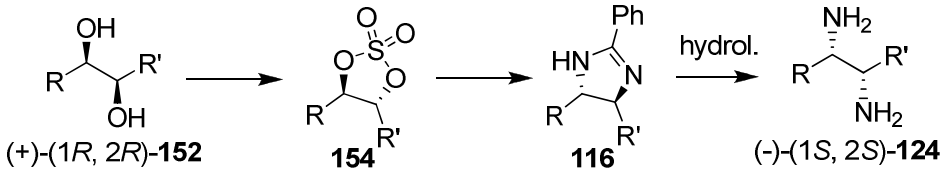

Scheme 45: Sharpless' asymmetric diamine synthesis

However, neither of these asymmetric syntheses are suitable for our aim of a large scale, low cost synthesis of enantiopure diamine **124** due to the high cost of the chiral reagents required to achieve the initial asymmetric dihydroxylation.

Since the commencement of our own work in this area, an expedient asymmetric synthesis of diamine **124** has been reported by Deng and co-workers.[99] Deng synthesised (+)-(1*R*,2*R*)- and (–)-(1*S*,2*S*)-1,2-diphenylethylenediamine (**124*R*** and **124*S***) with high diastereo- and enantioselectivity *via* the addition of phenyllithium to the chiral C_2-symmetric bisimine **157** (Scheme 46). The authors had previously developed a method for the large scale production of both enantiomers of *tert*-butanesulfinamide **155** in good yield and high optical purity[100] and thus this method is viable as a large scale synthesis of the chiral diamine.

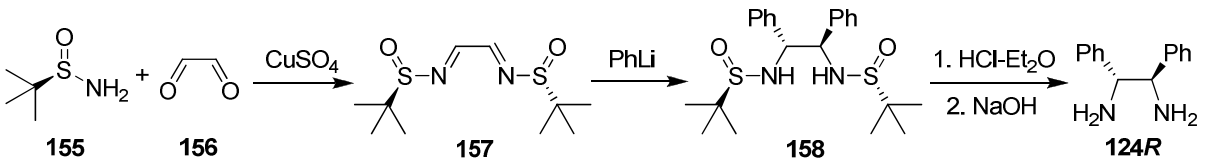

Scheme 46: Deng's diamine synthesis

The classical, and most widely used, route for the synthesis of diamine **124** involves the reaction of benzaldehyde (**159**) and liquid ammonia to give the diimine "hydrobenzamide" (**160**, Scheme 47). This is then followed by thermal cyclisation to "amarine" (**161**) by heating in an inert solvent (Scheme 47). Amarine is readily epimerised under basic conditions to "*iso*-amarine" (**116**) which, in principle, should liberate the desired racemic diamine on hydrolysis. However, due to strong conjugation, the cyclic amidine subunit is resistant to direct acid hydrolysis. Activation to attack by water is achieved by conversion to an *N*-acyl diamide and, once the conjugation is broken by acylation, the *N*-acyl *iso*-amarine (**162**) can be converted to the racemic diamine *via* a two-step hydrolysis procedure.

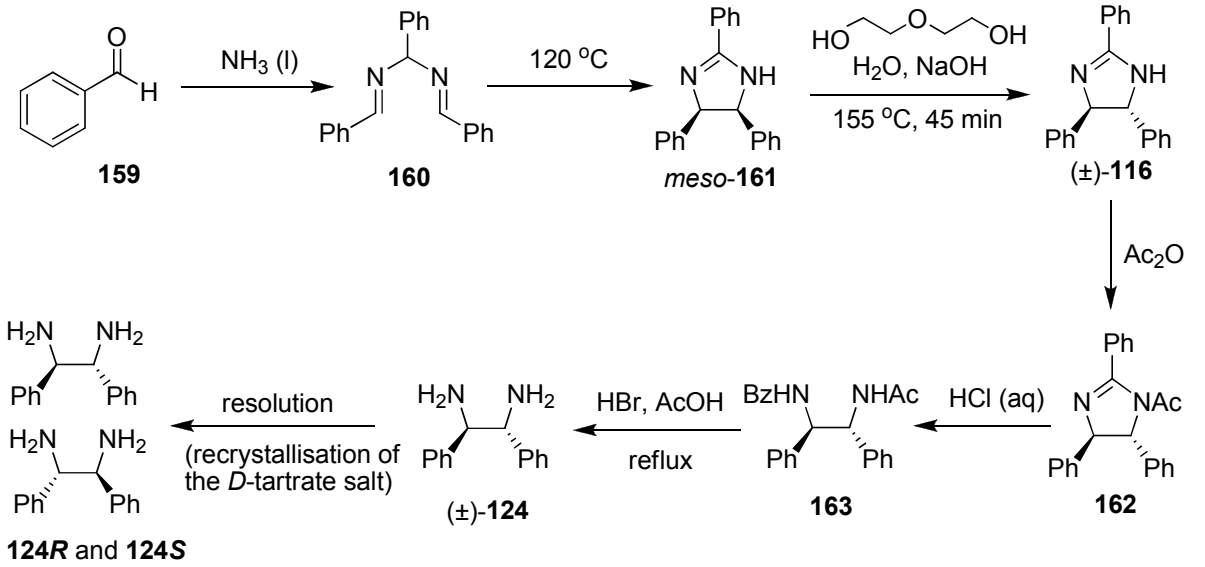

Scheme 47: Williams' and Bailar's diamine synthesis

This route was first developed by Williams and Bailar[92] in 1959 as a modification of the synthesis of enantiopure diamine **124** by Lifschitz and Bos.[101] They achieved a large scale synthesis of racemic diamine **124**, followed by resolution by recrystallisation with tartrate. Corey later confirmed the structures of the intermediates **160** and **161** by X-ray

crystallography, and suggested an alternative to the lengthy activation-hydrolysis procedure, using aluminium amalgam to achieve direct reduction to the diamine from *iso*-amarine.[102] Although this reduction considerably shortens the synthesis, this modification is unsuitable to apply to a large scale preparation as it uses large amounts of highly toxic reagents, requiring expensive and time consuming waste disposal procedures.

Due to the lack of any need for chromatographic purifications and the low cost of the starting materials and reagents, William and Bailar's route was selected as the most attractive for our large scale synthesis of enantiopure diamine, despite the lengthy activation-hydrolysis procedure. Thus this route was taken as a basis for our diamine synthesis, with a view to improving the procedure by combining the resolution and hydrolysis steps by protection of the amidine subunit with a chiral acyl group (Scheme 48). In this strategy two chemically distinguishable diastereoisomers **164** and **165** should be formed that are also activated to hydrolysis *via* nucleophilic attack at the amidine carbon.

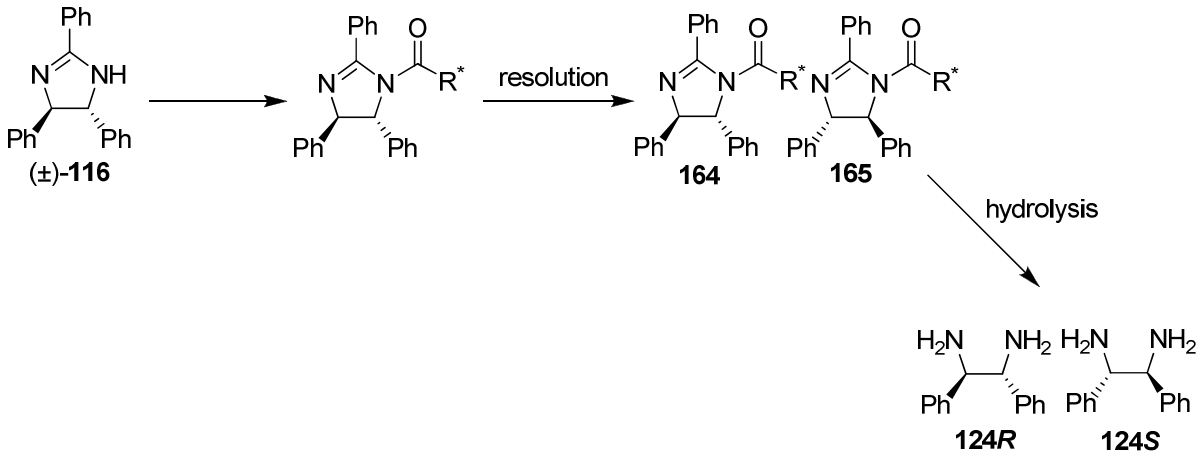

Scheme 48: proposed shortened diamine synthesis

In conclusion, our aim was to develop and apply a novel synthesis and resolution to obtain gram amounts of enantiopure diamine **124**, to be used to synthesise gram amounts of our catalytic targets AM (**116**), IAM (**111**), BAM (**121**) and IBAM (**113**).

2.2. Novel Synthesis and Resolution of (+)-(1*R*,2*R*)- and (–)-(1*S*,2*S*)-1,2-Diphenylethylenediamine (124*R* and 124*S*) *via* the Formation Diastereomeric *N*-Acylamidines[103]

2.2.1. Improved synthesis of amarine using HMDS and benzaldehyde

In previously reported syntheses of diamine **124** *via* the classical *iso*-amarine route, the amarine intermediate had been synthesised in two steps. Diimine **160**, or hydrobenzamide, is formed by the reaction of liquid ammonia and benzaldehyde and, after isolation, this is subsequently cyclised to amarine (**161**) by heating in an inert solvent. However, on investigation into existing literature on similar reactions, it was discovered that further improvements could be made in this route by condensing the first two steps in Williams' and Bailar's synthesis into a single reaction. Uchida *et al*[104] reported a one pot procedure using hexamethyldisilazane (HMDS) as a higher boiling alternative to liquid ammonia. The elevated boiling point facilitated heating of the reaction mixture and thus reduced the reaction time for formation of hydrobenzamide (**160**) from one week[105] to a matter of hours. Additionally, heating the reaction mixture meant that once the hydrobenzamide (**160**) is formed *in situ*, it subsequently cyclises under the reaction conditions in a thermally promoted disrotatory ring closure. Thus, the desired amarine product (**161**) is obtained in a single step, in a fraction of the time required by Williams' and Bailar's protocol. This is achieved in a solvent free procedure performed by heating benzaldehyde and HMDS in a sealed tube at 120 °C for 6 h (Scheme 49).

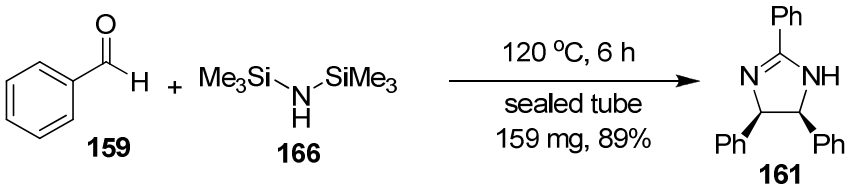

159 **166** **161**

Scheme 49: one pot formation of amarine

The use of a sealed tube is undesirable for our purposes, the build up of high pressure in the reaction vessel (due to the evolution of ammonia over the course of the reaction) being dangerous and impractical when working on a large scale. Thus, the reaction was attempted in a round bottomed flask with a reflux condenser fitted under an inert atmosphere of nitrogen.

The first attempts at this procedure proved partially successful, crude ^{1}H NMRs indicating the presence of some amarine (**161**) product in addition to unreacted starting material and a number of by-products. In an attempt to improve the reaction, the benzaldehyde (**159**) was distilled prior to reaction to ensure dryness and purity. However, this led to no reaction occurring at all; ^{1}H NMR analysis of the crude reaction mixture revealing only unreacted starting materials present after 6 h. This led us to the conclusion that the small amount of benzoic acid present in undistilled benzaldehyde was catalysing imine formation by providing the optimum, slightly acidic, pH for the reaction. This was confirmed when, on a 12 g scale, the addition of 1 mol% of benzoic acid led to the reaction proceeding smoothly over 17 h to give the amarine product (**161**) in 53% yield.

However, upon increasing the scale of the reaction to 100 g an extended reaction time of 36 h was necessary to observe completion of the cyclisation reaction. This resulted in a slightly reduced yield of 49%, with an increase in the number of by-products formed, possibly through decomposition of the amarine (**161**). It was thought that the added benzoic acid may be inhibiting the cyclisation step which proceeds *via* an anionic species (**167**, Scheme 50).

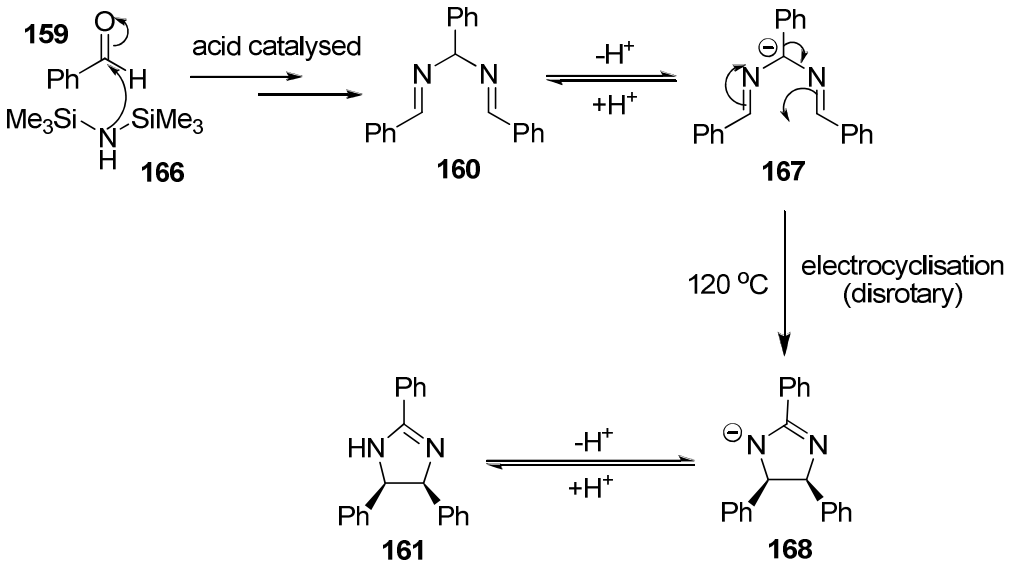

Scheme 50: one pot formation of amarine

Additional evidence was provided for this theory by the observation that the diimine **160** is rapidly consumed once the amarine product (**161**) has begun to form. It appears that the reaction may be autocatalytic, the strongly basic amidine product lowering the pH of the

system and promoting cyclisation. Evidently the reaction has a delicate pH dependence which may be affected by the differential rates of evaporation of reaction components on scaling up of the reaction. It is also possible that pressure differences on scaling up could affect yields. It was suggested that a reduction in the amount of benzoic acid may increase the overall reaction efficiency, and a series of smaller scale trial reactions were carried out to ascertain the optimum amount of catalyst (Table 3).

Table 3: benzoic acid catalysed amarine (161) formation

Mol% of benzoic acid added	Ratio of amidine **161** to imine **160** at time, t		
	t = 15 h	t = 18 h	t = 19 h
1mol%	25 : 75 (benzaldehyde still remaining in reaction mixture)	80 : 20	100 : 0
0.5 mol%	70 : 30	100 : 0	—
0.1mol%	40 : 60 (benzaldehyde still remaining in reaction mixture)	95 : 5	100 : 0

The amount of benzoic acid catalyst was thus set to 0.5 mol%, our results demonstrating that this provided the optimum pH for the reaction. It is also interesting to note from the results that the final step of the reaction indeed appears to be autocatalytic; the rate of cyclisation increasing as amarine is produced. In accordance with our findings, on scaling up to 100 g the reduction in the amount of benzoic acid added leads to a shorter reaction time (24 h) and an increase in isolated yield (61%).

2.2.2. Epimerisation of Amarine to Iso*-amarine*

The isomerisation of *meso* amarine (**161**) to racemic *trans*-4,5-dihydro-2,4,5-triphenyl-1*H*-imidazole (*iso*-amarine) (**116**) is performed in good yield (70%) following the procedure as published by Bailar and Williams.[92] The reaction is achieved by reversible deprotonation of the NC-*H* protons by heating with sodium hydroxide in water and diethylene glycol (Scheme 51). The major product of this thermodynamically controlled system is the more stable *iso*-amarine (**116**) with its phenyl groups placed in a less sterically demanding *trans* orientation.

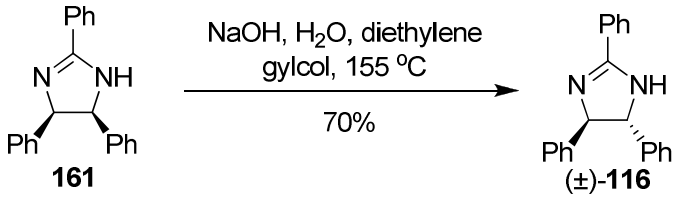

Scheme 51: isomerisation of *iso*-amarine

2.2.3. Acyl Chloride Mediated Acylation of Racemic Iso*-amarine*

As a trial for the formation of the diastereomeric *N*-acyl amidines, *iso*-amarine **116** was *N*-benzoylated by its reaction at room temperature with benzoyl chloride and triethylamine (Scheme 52).

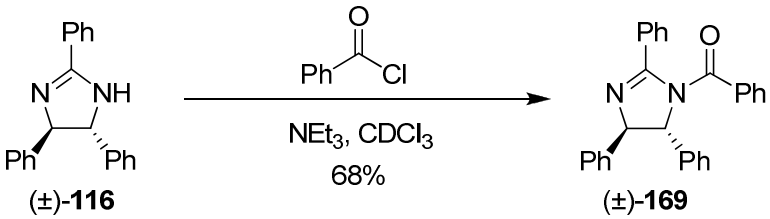

Scheme 52: benzoylation of *iso*-amarine

It was found that no nucleophilic catalyst (e.g. DMAP) was necessary for the benzoylation; the amidine itself being sufficiently nucleophilic to react rapidly and cleanly with benzoyl chloride. In fact, in a trial experiment exploring the use of tetramethylguanidine (TMG) as an acylation catalyst (in a continuation of previous work which found it to be an effective nucleophilic catalyst in electrophilic bromination),[106] it was found that the rate actually decreased if 0.1 eq of TMG were added in addition to the 2 eq of triethylamine (85% conversion of starting material after 30 min compared to 100% when no additional catalytic base added). This result is most likely due to the irreversible benzoylation of TMG by benzoyl chloride competing with the benzoylation of the *iso*-amarine rather than catalysing it. This is feasible due to the presence of the acidic proton in TMG allowing a neutral, stable benzoylated compound (**170**, Figure 34) to be formed on benzoylation with deprotonation. This differs from DMAP which, due to the absence of any acidic proton, forms an unstable cationic species upon benzoylation (**171**, Figure 34). This rapidly undergoes further reaction to transfer the benzoyl group to the starting material.

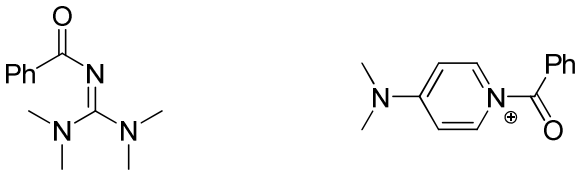

170 **171**

Figure 34

Once successful benzoylation had been achieved, the same conditions were applied to the protection of the amidine with a mandelic acid derivative. (*R*)-(+)-Acetyl-mandelic acid (**173**) was selected as a suitable, readily available chiral carboxylic acid to be used in the resolution and activation to hydrolysis of the amidine. This was synthesized from (*R*)-(+)-mandelic acid (**172**) following Singh's proceedure.[107]

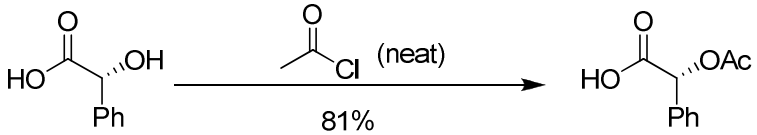

172 **173**

Scheme 53: acetylation of mandelic acid

The acetyl-mandelic acid was coupled to the racemic *iso*-amarine *via* the acyl chloride **174** (Scheme 54). This resulted in the formation of two diastereoisomers, (–)-(4*R*,5*R*)-1-[(*R*)-α-acetoxybenzeneacetyl]-4,5-dihydro-2,4,5-triphenylimidazole (**175**) and (+)-(4*S*,5*S*)-1-[(*R*)-α-acetoxybenzeneacetyl]-4,5-dihydro-2,4,5-triphenylimidazole (**176**). These diastereomers were found to be distinguishable by NMR and separable by both flash column chromatography and fractional recrystalisation.

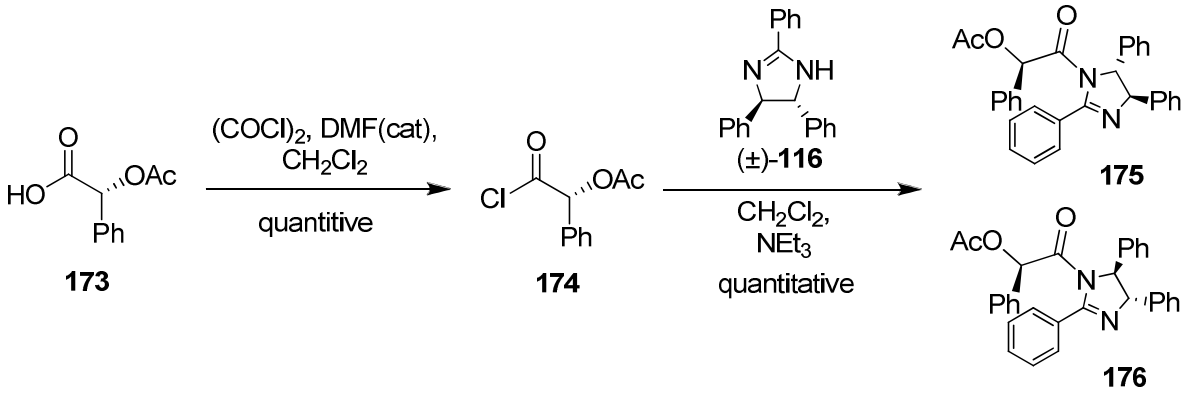

173 **174** **175** **176**

Scheme 54: acyl chloride mediated coupling of (±)-*iso*-amarine and (*R*)-acetyl-mandelic acid

This was carried out on a gram scale, and the synthesis was taken through to the diamine final product. However, a value of zero was obtained for all the optical rotations of all the intermediate single diastereomers, indicating racemisation had occurred in the acylation process. This was confirmed by analysis of the final product by polarimetry, which proved to be racemic diamine. It was suggested that racemisation occurs as a result of the amidine starting material being basic enough to remove the α-proton of acetyl-mandelic acyl chloride. This would form the ketene, followed by the addition of the acetyl-mandelic moiety as a racemate, resulting in the formation of the two racemic diastereomers **175** and **176** (Scheme 55).

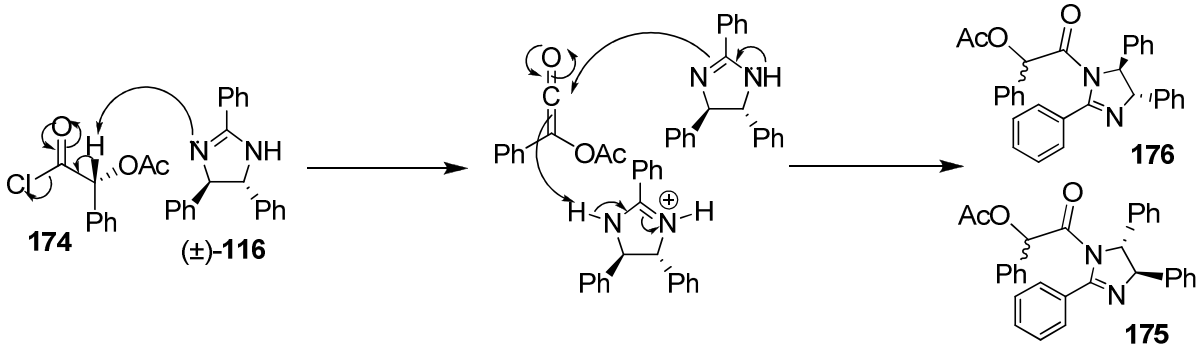

Scheme 55: racemisation of acetyl-mandelic acid

2.2.4. DCC Mediated Acylation of Racemic Iso-*amarine*

It was proposed that a solution to this problem would be to couple the acid and amidine *via* dicyclohexylcarbonimide (DCC) mediated coupling.[108] The pK_a of the α-proton in the acid will be significantly higher than in the acid chloride, reducing the possibility of addition of the acyl group by the ketene route. This was implemented with excellent results, producing optically pure diastereomers and ultimately producing diamines (**124*S***) and (**124*R***) as single enantiomers (Scheme 56).

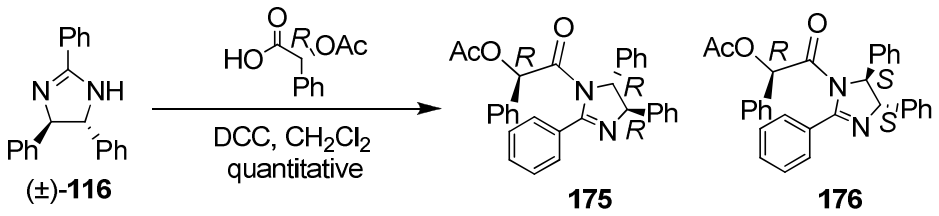

Scheme 56: DCC mediated coupling of isoamarine and acetyl-mandelic acid

2.2.5. Fractional Recrystalisation of Diastereomeric N*-acyl amidines*

After separation of the two diastereomers by flash column chromatography, solubility screens were carried out with a range of different solvents. These revealed a marked difference in crystallinity of the two diastereomers, particularly on recrystallisation from ethereal solvents. Thus, fractional crystallisation of (+)-(4*S*,5*S*)-1-[(*R*)-α-acetoxybenzeneacetyl]-4,5-dihydro-2,4,5-triphenylimidazole (**176**) was achieved from isopropyl ether, giving the pure diastereomer in 68% of the theoretical yield.

The structure and diastereomeric identity of this species were confirmed by X-ray crystallography (Figure 35).

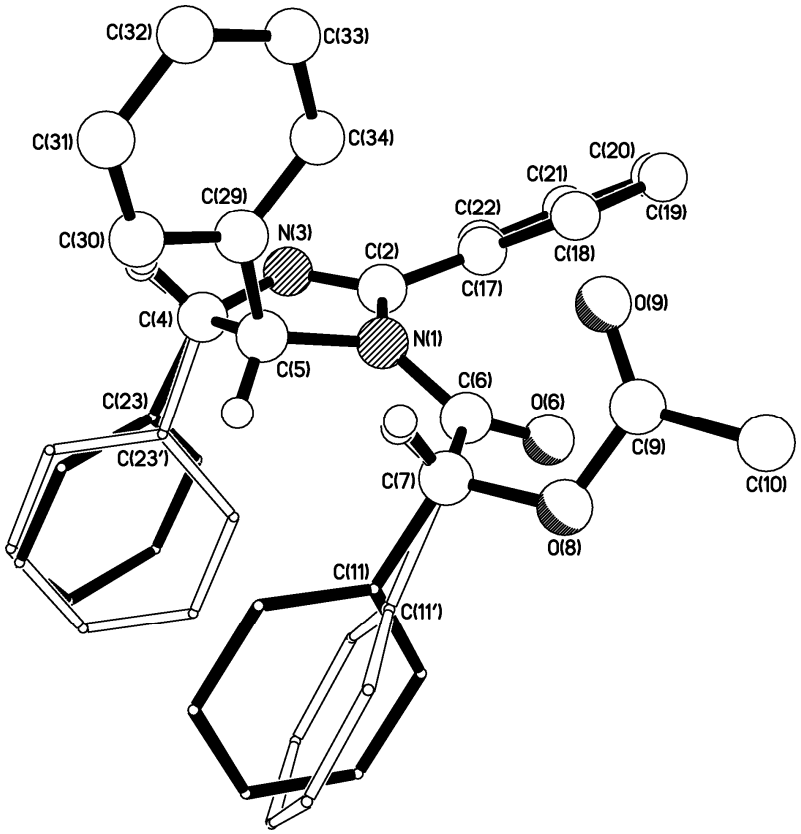

Figure 35: X-ray crystal structure of (+)-(4*S*,5*S*)-1-[(*R*)-α-acetoxybenzeneacetyl]-4,5-dihydro-2,4,5-triphenylimidazole (176)

Repeated attempts were made at fractional recrystallisation of the other diastereomer (+)-(4*R*,5*R*)-1-[(*R*)-α-acetoxybenzeneacetyl]-4,5-dihydro-2,4,5-triphenylimidazole (**175**) from the diastereomerically enriched filtrate. However, despite the testing of a large number of solvent systems all such trials were unsuccessful. It was therefore decided to hydrolyse the mixture of diastereomers enriched in **175** to the diamide stage with aqueous hydrochloric acid (Scheme 57) and to attempt the fractional crystallisation of this compound. This proceeded with some success, pure (+)-*N*-(*R*)-acetoxyphenylacetyl-*N'*-benzoyl-(1*R*,2*R*)-1,2-diphenylethylene diamine (**179**) crystallising from chloroform in 58% of the theoretical yield.

2.2.6. Hydrolysis of N*-Acyl Amidines to Enantiopure Diamines*

The *N*-acyl amidines **175** and **176** were hydrolysed in two steps to the enantiopure diamine products (**124*R*** and **124*S***) in modifications of the procedures developed by Williams and Bailar (Scheme 47). THF was added as an additional solvent to water in the hydrolysis to diamides **177** and **179** to improve solubility of the starting material. Further portions of aqueous hydrobromic and acetic acid were added in the diamide hydrolysis to the diamine to ensure complete hydrolysis and formation of hydrobromide **178** (Scheme 57).

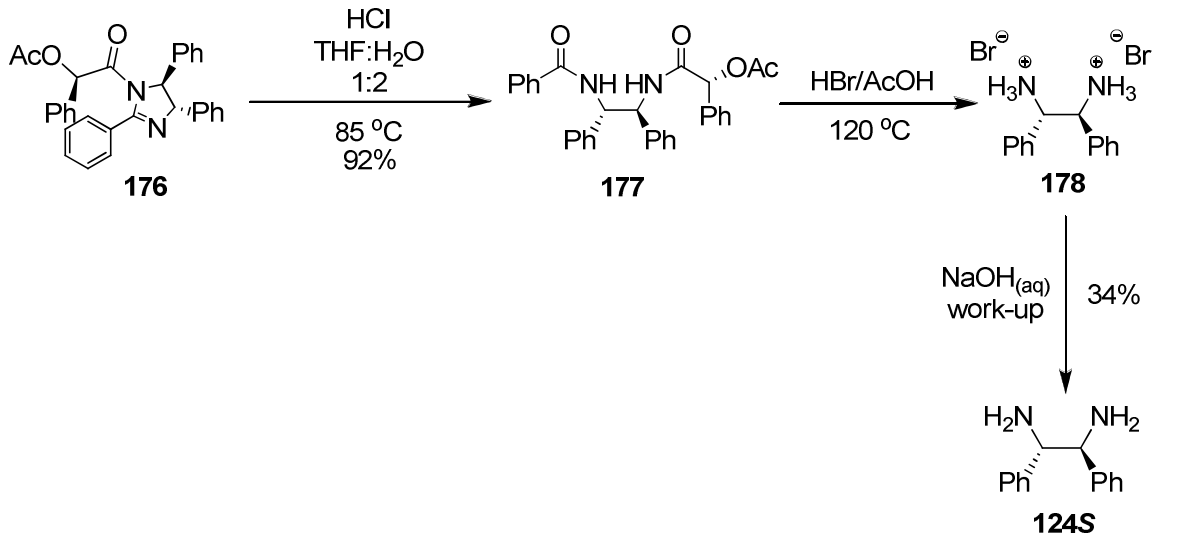

Scheme 57: hydrolysis of *N*-acyl amidine 176 to diamine 124*S*

In summary, we have developed a novel, shortened route to enantiopure 1,2-diphenylethylenediamine (**124**) (Scheme 58), and have successfully applied this to a large scale synthesis of both enantiomers of the desired diamine.

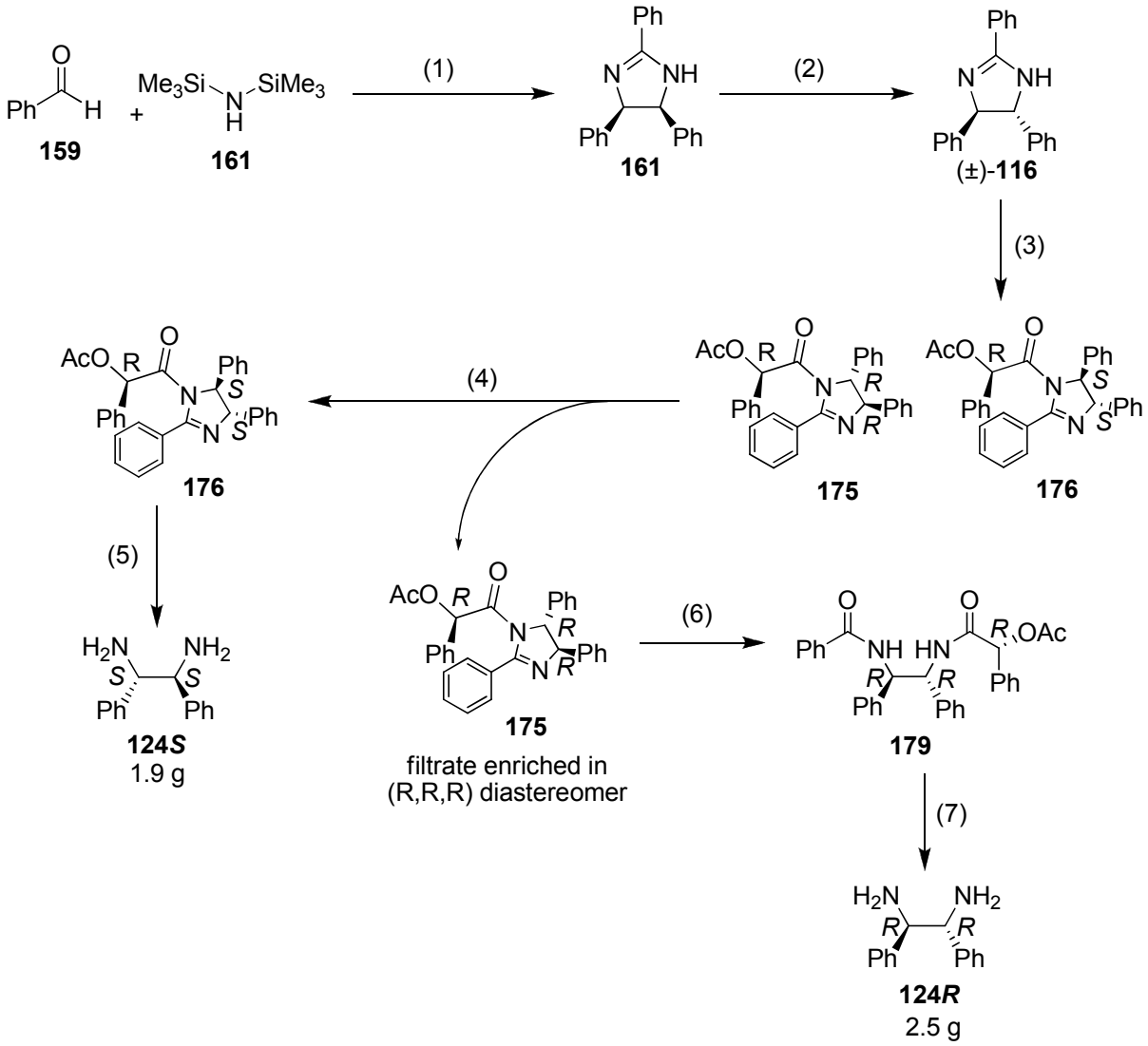

(1) 0.5 mol% benzoic acid, 120 °C, 61%; (2) NaOH, H_2O, diethylene glycol, 155 °C, 70%; (3) (*R*)-Acetyl mandelic acid (**173**), DCC, CH_2Cl_2, quantative; (4) *i*Pr_2O; (5) (i) THF/H_2O, HCl, reflux, 92% (ii) HBr(aq), AcOH, reflux, 34%; (6) (i) THF/H_2O, HCl, reflux, 79% (ii) $CHCl_3$, 58% pure *R*,*R*,*R*-**179**; (7) HBr(aq), AcOH, reflux, 46%.

Scheme 58: novel synthesis of enantiopure 1,2-diphenylethylenediamine 124

*2.2.7. Confirmation of Optical Purity of Diamine **124***

The optical purity of the diamine was explored by Snyder's ^{1}H NMR method,[109] using enantiopure mandelic acid as a chiral solvating agent. When the racemic diamine and enantiopure mandelic acid are mixed in a 1:2 ratio in deuterated chloroform (4 mg of diamine in 0.4 mL), the resulting ^{1}H NMR was reported by Synder to demonstrate

distinguishable shifted resonances for the *R*,*R* and *S*,*S* enantiomers. The *R*,*R* and *S*,*S* NC*H* protons were reported as being shifted up to 0.046 ppm apart, thus demonstrating base-line separation in a 400 MHz spectrometer.

Pleasingly, we found this result repeatable with the racemic diamine. However, we encountered problems when analogous conditions were applied to the enantiopure diamine. It was observed that the diastereomerically pure salts precipitated out from solution much more rapidly than the 1:1 diastereomeric mixture formed from the racemic diamine. The *S*,*S*,*S* and *R*,*R*,*R* salts precipitated out from deuterated chloroform almost instantaneously upon addition of the mandelic acid, whilst the *R*,*R*,*S* and *S*,*S*,*R*, though having slightly improved solubility, began to form crystals after ~30 seconds. This led to the practical necessity of forming only the *R*,*R*,*S* and *S*,*S*,*R* salts and running the spectra at 40°C to ensure full solvation (Scheme 59). Such raised temperatures lead to the loss of full, baseline separation for the NC*H* protons. However, when studying the aromatic region, baseline separation of a doublet at ~6.8 ppm was observed in the spectra of the racemic diamine recorded at 40°C (Figure 36). The two analogous spectra of the enantiopure diamine showed a single doublet in this region (Figure 37 and Figure 38), thus confirming optical purity of the *R*,*R* and *S*,*S* diamines to >96% enantiomeric excess (the detection limit of Synder's method being stated as <2%).

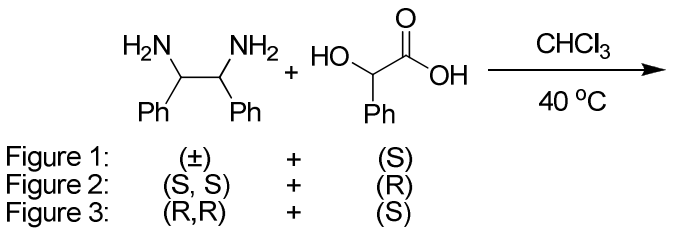

Scheme 59: determination of optical purity of diamine 124

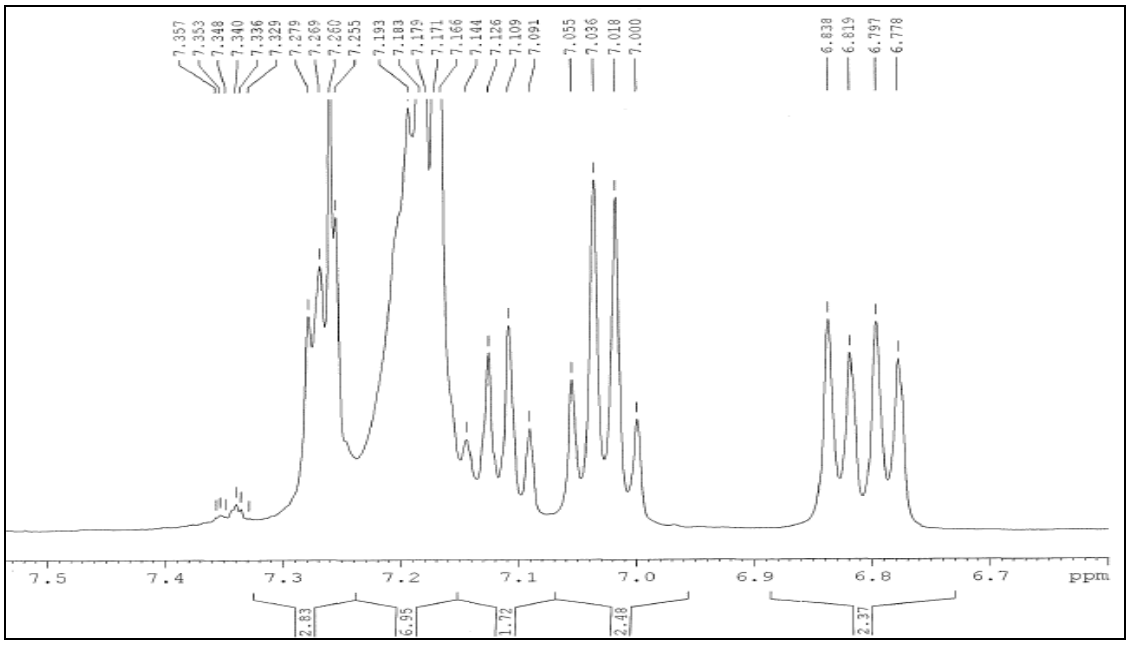

Figure 36: racemic diamine 124 with (*S*)-mandelic acid (172)

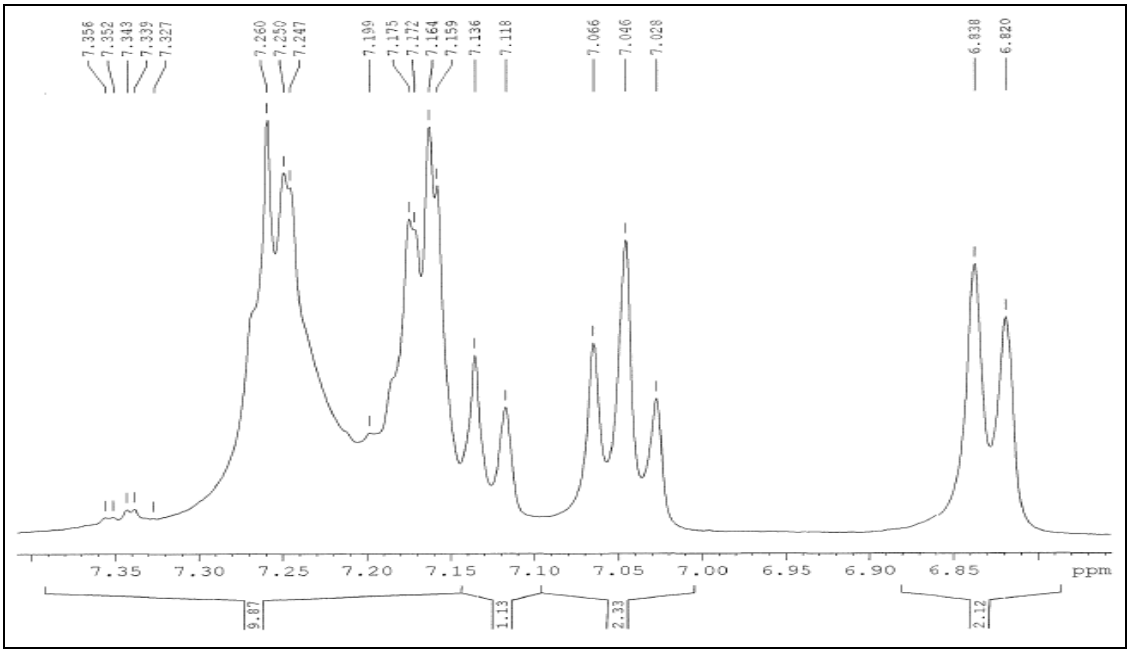

Figure 37: (*S*,*S*)-diamine 124 with (*R*)-mandelic acid (172)

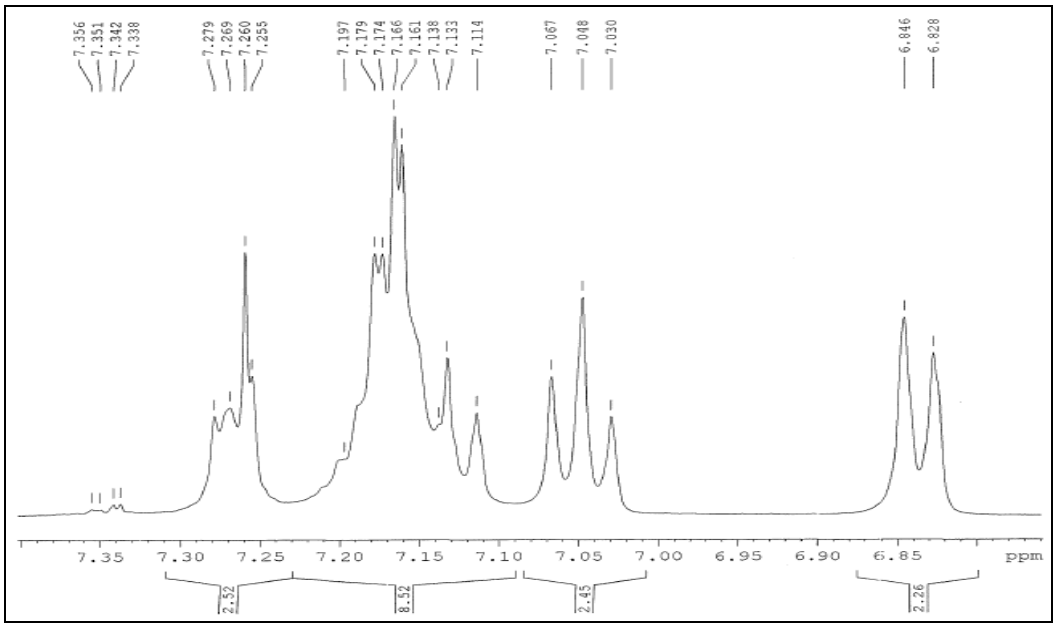

Figure 38: (*R*,*R*)-diamine 124 with (*S*)-mandelic acid (172)

2.3. Novel Synthesis and Resolution of (+)-(1*R*,2*R*)- and (–)-(1*S*,2*S*)-1,2-Diphenylethylenediamine (124*R* and 124*S*) *via* Fractional Crystallisation of (±)-*Iso*amarine with Enantiopure Mandelic acid[110]

2.3.1. Limitations of our initial diamine synthesis

Our novel synthesis and resolution of diamine **124** *via* our *N*-acylamidines proceeded with considerable success. Not only were gram amounts of both enantiomers of 1,2-diphenylethylenediamine synthesised in high optical purity, but we also gained access to a number of interesting optically pure chiral intermediates.

However, within the context of our work, our procedure had two major failings. Firstly, the final hydrolysis step of the diamide to the diamine was low to moderate yielding (34-46%), resulting in the loss of much of our valuable resolved material at this late stage of the synthesis. From analysis of the by-products of this step, it is hypothesised that the poor yields are a consequence of a side reaction involving the hydrolysis of the acetyl ester of the acetyl mandelic acid moiety. This produces alcohol **180** (Figure 39), which is isolated from the reaction mixture as a solid precipitate and is thought to undergo no further hydrolysis due to its extreme insolubility.

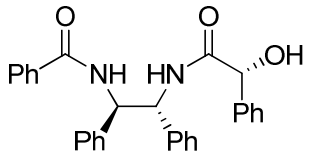

180

Figure 39: by-product in hydrolysis of diamide

Secondly, we had initially hoped to gain access to optically pure *iso*-amarine (**116**) (for use in our studies into asymmetric catalytic bromination) by removing the acyl group from the resolved *N*-acylamidine **175** and **176**. Unfortunately, **175** and **176** proved resistant to all our efforts of selective hydrolysis or reduction. Thus, despite us having developed an efficient procedure to form large amounts of racemic *iso*-amarine (**116**), we still had no simple method of obtaining a single enantiomer.

Thus, when a second batch of diamine was required and it was necessary to return to our synthesis, we turned our attention to solving the problems encountered in our initial procedure. It was decided that we would attempt a direct resolution of the *iso*-amarine **116** *via* diastereomeric salt formation. If successful this would give us access to enantiomerically pure *iso*-amarine in three steps from benzaldehyde and HMDS (after salt decomplexation). Additionally, this strategy should also eliminate our problems in the final hydrolysis step; Williams and Bailar report good yields[92] for their hydrolysis of racemic *iso*-amarine, a procedure which should be applicable to resolved *iso*-amarine to afford enantiopure diamine.

*2.3.2. Fractional crystallisation of 4,5-dihydro-2,4,5-triphenyl-1H-imidazole (*iso*-amarine, **116**)*

A range of chiral acids were screened in the fractional recrystallisation of *iso*-amarine. (*R*)-(+)-acetyl-mandelic acid (**173**) and (*R*)-(+)-mandelic acid (**172**) were selected due to the success of the mandelate structure in our existing diamine resolution, along with camphor sulphonic acid (**181**); a popular resolving agent due to its wide availability and greater acidity than carboxylic acids.

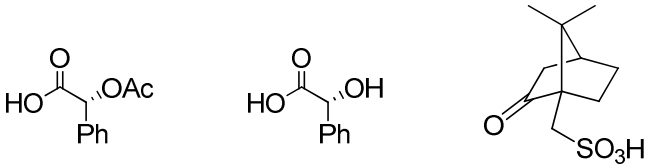

(*R*)-**173** (*R*)-**172** (*R*)-**181**

Figure 40: chiral acids

Addition of (*R*)-(+)-acetyl-mandelic acid (**173**) to the racemic *iso*-amarine (**116**) in ethanol did not result in the formation of any crystals; the salt formed presumably being too soluble to precipitate out. Camphor sulphonic acid (**181**) gave an excellent yield of salt (95% of theoretical yield based upon the precipitation of only one diastereomer). However, on decomplexation with sodium hydroxide, the *iso*-amarine (**116**) isolated had zero optical rotation. Comparative success was achieved with the use of (*R*)-(+)-mandelic acid (**172**). After diastereomeric salt (**182**) formation and decomplexation, *iso*-amarine (**116**) was isolated in 54% yield of theory, with an optical rotation of +43 (compared to a literature value of +46).[111] The procedure was optimised, with a solvent change from ethanol to isopropanol and the inclusion of a recrystallisation of the salt, to afford (*R*,*R*)-*iso*-amarine (**116*R***) in 80% yield with an optical rotation identical to the literature value (Scheme 60).

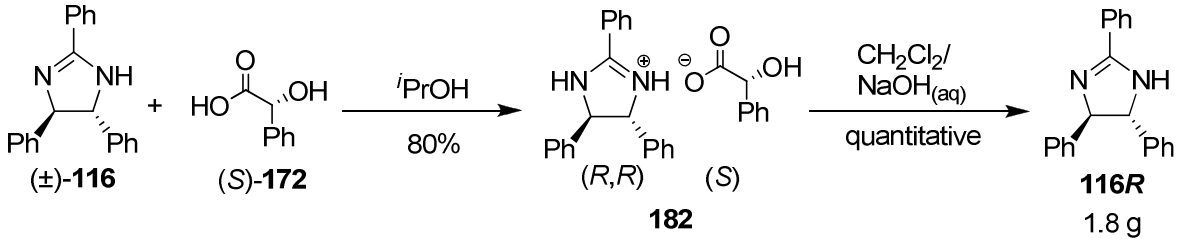

Scheme 60: fractional crystallistion of (*R*)-*iso*-amarine

The 1:1 composition and the diastereomeric purity of the salt (**182**) were confirmed by X-ray crystallography (Figure 41).

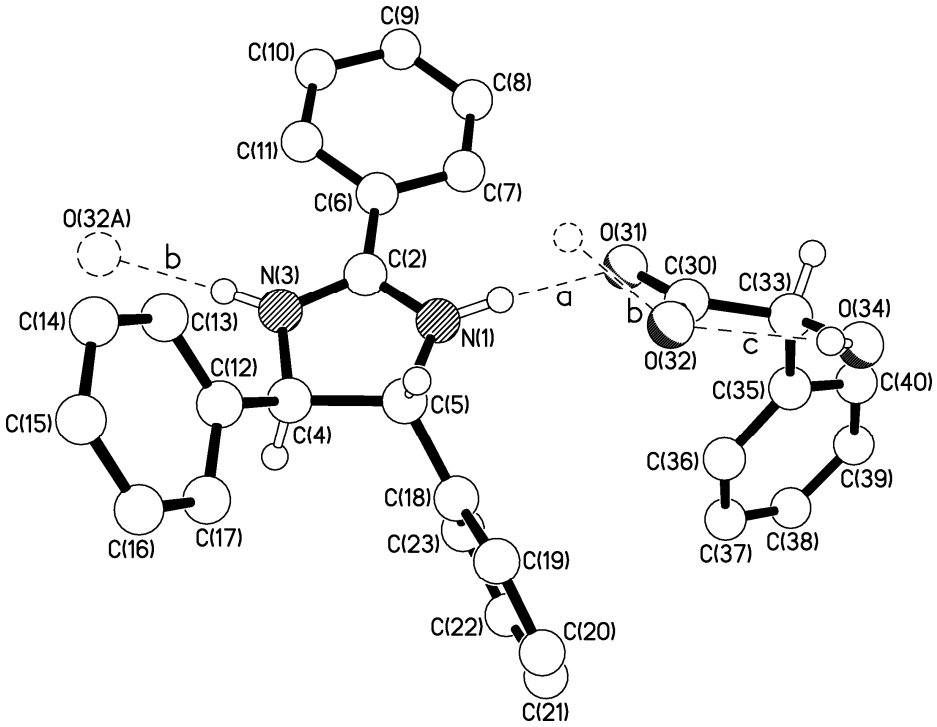

Figure 41: X-ray crystal structure of 1:1 (*S*)-mandelic acid-(*R*,*R*)-*iso*-amarine diastereomeric salt

The optical purity of the resulting (*R*,*R*)-*iso*-amarine (**116*R***) was confirmed by DCC mediated coupling with (*R*)-acetyl-mandelic acid. ^{1}H NMR analysis of the crude reaction mixture showed the presence of only the (*R*,*R*,*R*)-diastereomer, confirming both the efficiency of the resolution and of the absence of any racemisation in the DCC coupling.

A scaled up, analogous fractional crystallisation was performed with the (*R*) enantiomer of mandelic acid. This proceeded with identical yield to afford (*S*,*S*)-*iso*amarine (**116*S***) (5.5 g, 80% over salt formation/decomplexation). Furthermore, it was found that upon concentration of the basified aqueous phase after decomplexation of the salt, some of the mandelic acid starting material (1.7 g, 24%) crystallised and could be recovered by filtration. Thus, a portion of the chiral resolving agent can be recycled, increasing the efficiency and economy of the protocol.

*2.3.3. Hydrolysis of (+)-(4R,5R)-4,5-dihydro-2,4,5-triphenyl-1H-imidazole [(R,R)-*iso*-amarine, **116R**]*

Pleasingly, one-pot acetylation and hydrolysis under Lifschitz's and Bos' conditions[101] gave enantiomerically pure (*S*,*S*)-diamide **163*S***. Further hydrolysis using Williams' and Bailar's protocol[92] gave 1.4 g of enantiomericallly pure (*S*,*S*)-diamine **124*S*** (Scheme 61).

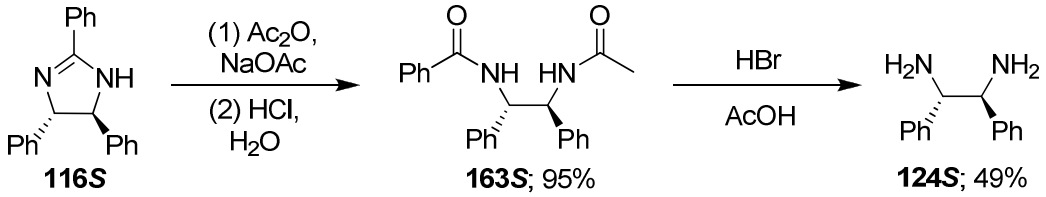

Scheme 61: hydrolysis of (*S*,*S*)-*iso*-amarine to (*S*,*S*)-diamine

As we had predicted, exchanging the mandelate group for a simple acetate group led to improved yields in the diamide to diamine hydrolysis step (49% from 34%).

2.3.4. Conclusion

We have developed two alternative novel syntheses of enantiopure 1,2-diphenylethylenediamine **124**; both of which give us access to gram amounts of the diamine and are arguably two of the best routes to the chiral diamine in the literature. After developing our initial protocol, we identified the limitations of our procedure and addressed these when returning to the synthesis. We have demonstrated that enantiopure *iso*-amarine can be accessed by the fractional crystallisation of the racemic *iso*-amarine and enantiopure mandelic acid. We have also improved the yield of the lowest yielding step in our procedure to increase the overall efficiency of the synthesis.

3. Catalytic Asymmetric Electrophilic Bromination

3.1. Catalyst Synthesis

With a large scale synthesis and resolution of 1,2-diphenylethylenediamine (**124**) completed, we turned our attention to the preparation of our asymmetric bromination catalysts IAM (**111**) and, more importantly, IBAM (**113**). Gram amounts of such catalysts were required to enable further screening of reaction conditions, derivatization of the catalyst and stoichiometric experiments.

*3.1.1. Synthesis of 2-(2-Iodophenyl)-4,5-diphenyl-4,5-dihydro-1*H*-imidazole or IAM (**111**)*

IAM (**111**) had previously been synthesised from 2-iodobenzoic acid (**107**) according to a literature proceedure.[55,82] The acid was converted into the amide (**108**) *via* the acyl chloride in good yield. The amide (**108**) was then treated with triethyloxonium tetrafluoroborate (BF_4OEt_3) to form the imidate (**183**), which was condensed with 1,2-diphenylethylenediamine (**124**) to form the chiral cyclic amidine moiety (Scheme 62).

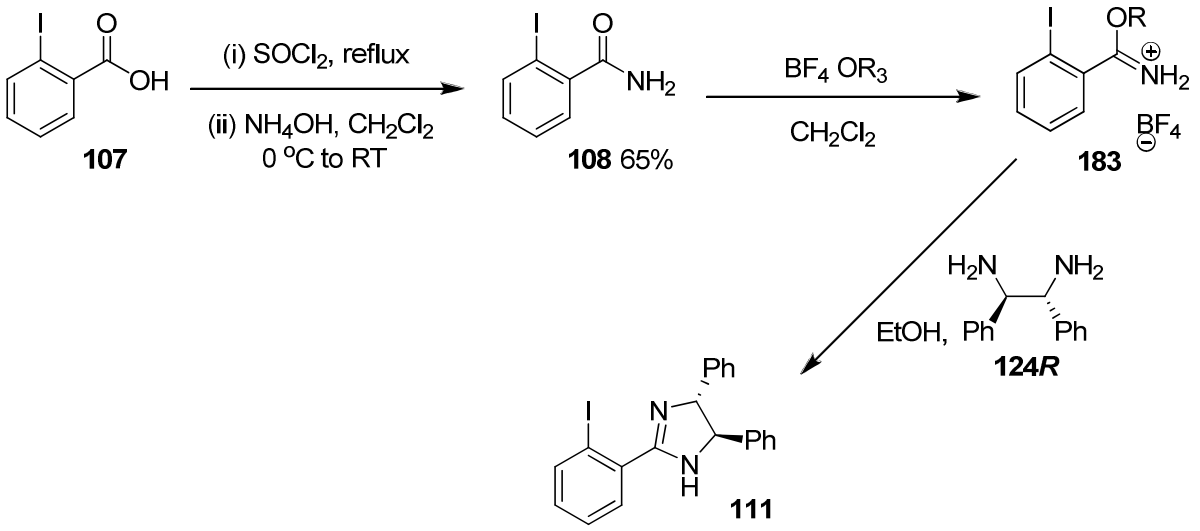

Scheme 62: synthesis of IAM (111)

The imidate formation proved to be an inconsistent and thus, problematic step. The best yield for the transformation was recorded as 56%, but more commonly yields of between 30 and 50% were observed. In our recent work, numerous attempts to form the ethyl imidate

resulted in failure to isolate the product and crude ^{1}H NMR demonstrated the presence of only ~40% imidate product in the best of cases.

It was hypothesized that the use of the analogous trimethyloxonium tetrafluoroborate (BF_4OMe_3) salt may improve the yield of the imidate formation. Not only is the trimethyl salt less hygroscopic than the triethyloxonium salt (thus reducing the possibility of water present in the reaction mixture), but its use eliminates the possibility of imidate decomposition back to the amide *via* β-elimination (Scheme 63).

184 **108**

Scheme 63: decomposition of imidate via β-elimination

As predicted, the use of trimethyloxonium tetrafluoroborate resulted in a considerable improvement in yield. On analysis of the reaction product after washing with diethyl ether, the imidate was observed to have formed in almost quantitive yield (99% by ^{1}H NMR of the product mixture), without the need for further purification. The crude imidate (characterised by a shift in the ^{13}C spectra from 171.3 ppm in the amide to 178.8 ppm in the *O*-methyl imidate) was taken through to the next step to form the amidine product, IAM (**111**), giving an overall yield for the two steps as 76%; a considerable improvement on the best results obtained with the triethyloxonium salt (53% over two steps).

*3.1.2. Synthesis of 2,6-Di-(4,5-diphenyl-4,5-dihydro-1*H*-imidazol-2-yl)iodobenzene or IBAM (**113**)*

The substitution of triethyloxonium tetrafluoroborate with the trimethyl analogue was also applied to the original synthesis of IBAM (**113**).[55] IBAM was synthesised from 2,6-dimethyl iodobenzene (**185**), which was oxidised to bis-acid **186** using a procedure previously reported for the bromo analogue,[112] employing $KMnO_4$ as oxidant in a mixture of *tert*-butanol and water (Scheme 64).

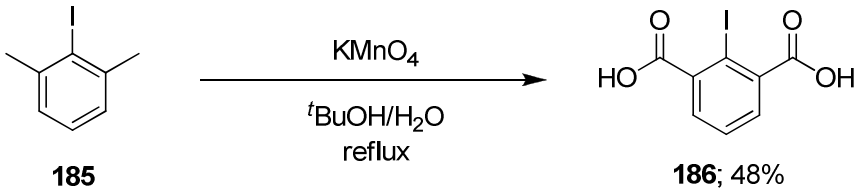

Scheme 64: oxidation of 2,6-dimethyliodobenzene (185) to 2-iodoisophthalic acid (186)

Bis-acid **186** was then converted to the bis-amide **122** by formation of the bis-acyl chloride followed by quenching with aqueous ammonia solution under biphasic conditions.

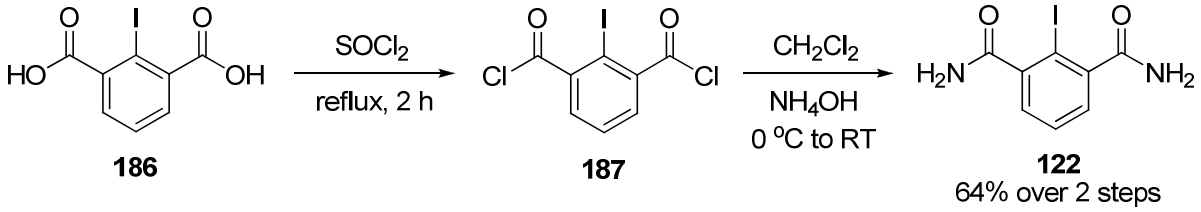

Scheme 65: formation of 2-iodoisophthalamide (122)

The bis-amidine, IBAM (**113**), was formed from the bis-amide *via* the intermediate imidate **188**, using a procedure similar to that employed with the mono-analogue. In previous syntheses of IBAM (**113**), using triethyloxonium tetrafluoroborate and stirring for 48 h at room temperature, the best yield obtained was 47% over the two steps.[55] Initially on substitution of the triethyloxonium salt with its trimethyl analogue we observed minimal reaction due to the limited solubility of both the bis-amide **122** and the trimethyloxonium salt in dichloromethane. However, it was found that heating the reaction mixture to reflux resulted in conversion to the bis-imidate **188** after 48 h (Scheme 66).On dissolving the crude imidate in ethanol and adding the chiral diamine (**124**), the bis-amidine product, IBAM (**113**) was formed in 68% yield over the two steps. This again is a considerable improvement on the poor to moderate yields obtained *via* the *O*-ethyl imidate salt.

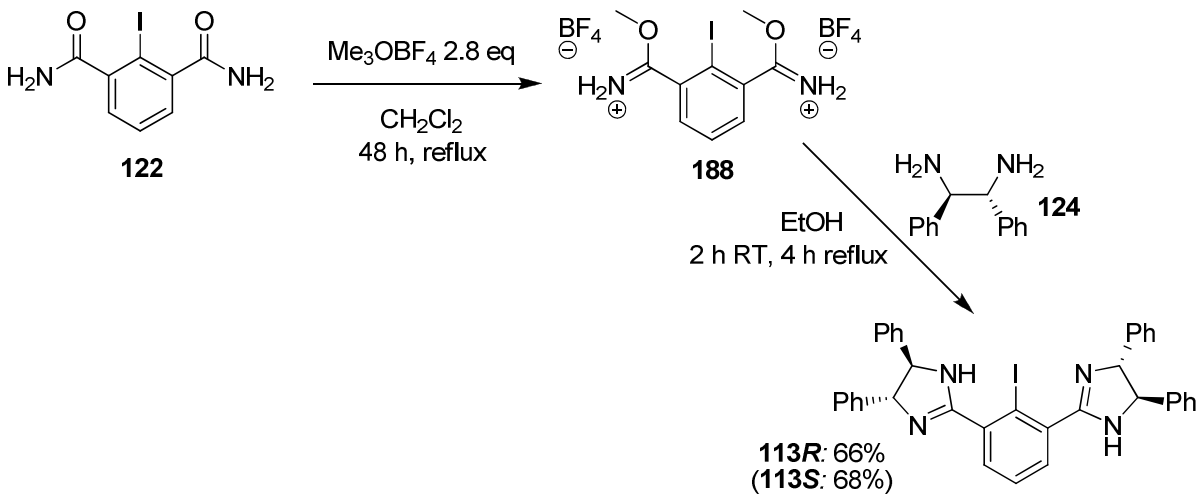

Scheme 66: formation of IBAM (113) *via* the *O*-methyl imidate salt (188)

However, despite the improved yield, the imidate (**188**) formation and subsequent diamine (**124**) condensation still proved to be a capricious reaction, occasionally failing and resulting in a large mixture of inseparable products. Thus, the existing IBAM (**113**) synthesis was still not deemed sufficiently robust to be used in a gram-scale preparation of our catalyst. It became clear that it would be necessary to formulate a completely new protocol if we were to ensure the success of a large scale procedure.

*3.1.3. Re-design of the synthesis of IBAM (**113**)*

We embarked on the re-design of the synthesis of IBAM (**113**) with the goal of producing a robust, high yielding procedure for synthesis of gram-amounts of our catalyst. Particular emphasis was placed on the final step to form the chiral amidine moieties, with an objective of minimizing loss of the valuable enantiopure diamine starting material (**124**).

After reviewing the various starting materials available to us, we selected 1,3-dicyanobenzene (**189**). Krizan and Martin[113] had demonstrated that when **189** was treated with lithium diisopropylamide (LDA) in THF at -96 ºC, it underwent a directed lithiation; the lithium-proton exchange occurs exclusively at the position *ortho* to the two cyano groups (Scheme 67). Subsequent low temperature quenching of the lithiated species with a range of electrophiles afforded the expected 2-substituted products in good yields (68-83%).

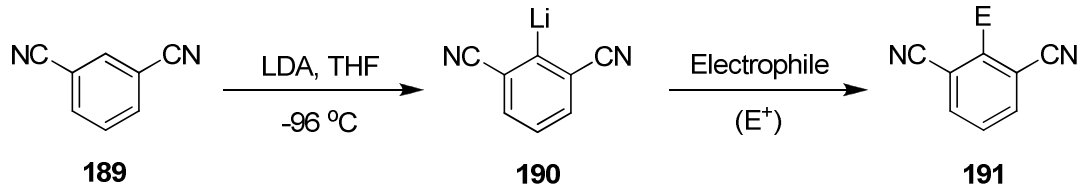

189 **190** **191**

Scheme 67: Krizan's and Martin's regiospecific functionalisation of 1,3-dicyanobenzene (189)

We utilized this procedure for the regioselective introduction of iodine to form 2,6-dicyano-1-iodobenzene (**192**) and in small scale trial reactions demonstrated the reproducibility of Krizan and Martin's reported yield (69% of 2,6-dicyano-1-iodobenzene (**192**) after recrystallisation compared to a reported 79% by Krizan and Martin).

However, we envisaged a number of modifications to Krizan's and Martin's protocol were necessary if we were to successfully apply the reaction to a large scale procedure:

The solvent was changed from tetrahydrofuran (THF) to 2-methyltetrahydrofuran (mTHF) to remove the need for a solvent change in the work up, thus improving the efficiency of the procedure. mTHF is not miscible with water, whilst it still retains the relatively high polarity (dielectric constant of 6.97, compared to 7.52 for THF) and ion solvating ability of THF. Thus, it can be used as a solvent in both the reaction itself and the subsequent aqueous work up.

The order of addition was reversed from Krizan's and Martin's procedure. In the original protocol it was reported that best results were obtained if a solution of **189** was added drop-wise to a stirred solution of LDA. However, **189** required a relatively large amount of solvent to fully dissolve it (minimum dilution; 0.25 M) and consequently, as the scale of the reaction increased, the volume of the solution and the time required for its addition became unmanageably large. The lengthy addition procedure resulted in considerable decomposition of the lithiated intermediate (**190**) prior to quenching with iodine. On the other hand, LDA was available as a 1.8M solution. Thus we elected to add the LDA to a stirred solution of 1,3-dicyanobenzene (**189**) in order to reduce the lifetime of the unstable intermediate **190**.

It was anticipated that achieving and maintaining a temperature of -96 ºC (by use of a liquid nitrogen/methanol bath) would be practically difficult on a large scale. Indeed, we had

planned to carry out the iododination in a controlled laboratory reactor (CLR) which operates at a minimum temperature of -30 ºC. However, investigations into the possibility of raising the temperature of the reaction demonstrated that substantial decomposition of the lithiated intermediate occurred at temperatures elevated considerably from -90 ºC. At -30 ºC a much reduced yield of 41% was obtained. The crude reaction mixture contained a high number of impurities and required purification *via* flash column chromatography; a time-consuming and wasteful procedure on a large scale. The possibility of adding a 1,3-dicyanobenzene/iodine mixture to a stirred solution of LDA was also investigated as a method of reducing the lifetime of the lithiated intermediate and thus facilitating a higher temperature procedure. However, this order of addition resulted in incomplete reaction, ^{1}H NMR analysis of the crude reaction mixture demonstrating approximately 20% conversion to the iodinated product. Thus, we were unable to increase the temperature of the reaction and were restricted to the use of a round bottomed flask and nitrogen/methanol bath for the reaction itself.

However, the changes made to the solvent and the order of addition facilitated the successful directed iodination of 65 g of 1,3-dicyanobenzene (**189**) to afford 2,6-dicyano-1-iodobenzene (**192**) in 64% yield (Scheme 68).

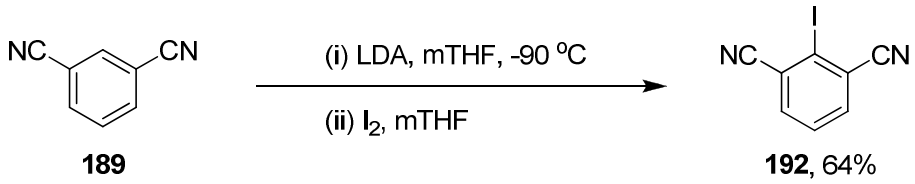

189 **192**, 64%

Scheme 68: large scale iodination of 1,3-dicyanobenzene (189)

The crude reaction mixture in mTHF was transferred directly to a CLR for the aqueous work-up. After the aqueous washes, the crude product was purified by filtration through a silica plug and the filtrate was concentrated to a volume of ~400 mL. The desired product precipitated out as a pale beige powder and was collected by filtration. Thus, the need for a lengthy large scale chromatographic procedure was eliminated and an efficient gram-scale synthesis accomplished.

With the bis-cyano compound **192** in hand, we examined a number of possibilities available to us to form the chiral imidazoline moieties in IBAM (**113**). Initially we explored the acid-

promoted formation of the bis-imidate salt *via* the *in situ* generation of hydrochloric acid in an alcohol solution.

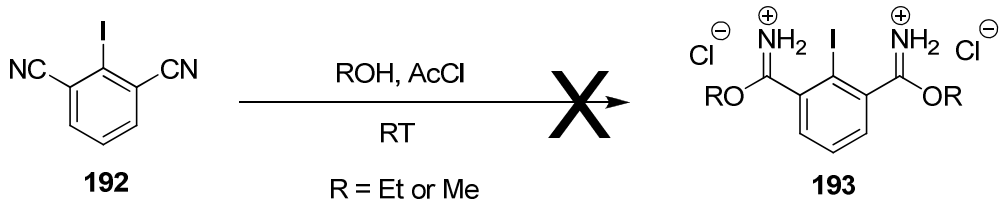

Figure 42: acid-promoted formation of imidate salt 193

However, our bis-cyano substrate **192** proved extremely unreactive to these conditions; stirring for one week produced a reaction mixture which was still mainly unreacted starting material. It was hypothesized that the two electron-withdrawing cyano groups on the benzene ring reduce the basicity of the nitrogens relative to that of a mono-substituted cyanobenzene. Thus the rate of acid promoted imidate formation is diminished.

Accordingly, we investigated the possibility of basic imidate formation, in a methoxide catalysed synthesis of the bis-imidazoline (Scheme 69).[114]

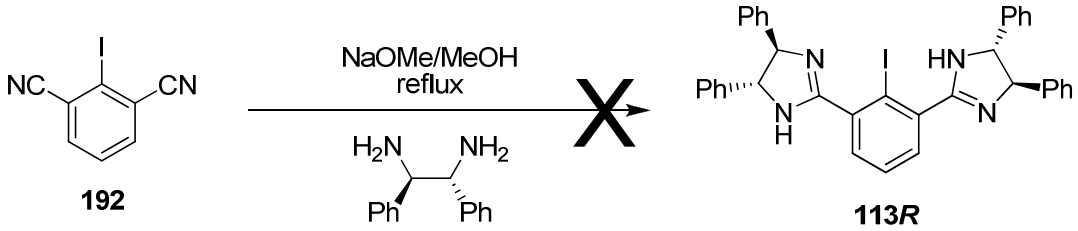

Scheme 69: attempted methoxide catalysed IBAM (113) formation

Although the starting material was consumed, a complex mixture of products was produced which demonstrated evidence of S_NAr at the position *ipso* to the iodine (Scheme 70).

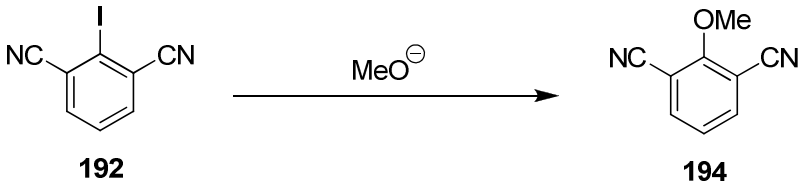

Scheme 70: S_NAr of iodine with methoxide in 2,6-dicyanoiodobenzene (192)

Our initial failures demonstrated the unsuitability of our substrate **192** for both acid and base promoted imidate formation. Thus, we turned our attention to alternative methods of forming our IBAM catalyst (**113**) from 2,6-dicyanoiodobenzene (**192**). An attractive protocol (Scheme 71) was published by Fujioka *et al*[115] which reported the synthesis of imidazolines (**198**) from aldehydes (**195**), *via* formation of an aminal, **196**, and its subsequent oxidation with NBS. The reaction presumably proceeds *via* an N-Br intermediate, **197**, which eliminates HBr to form the C=N bond of the amidine.

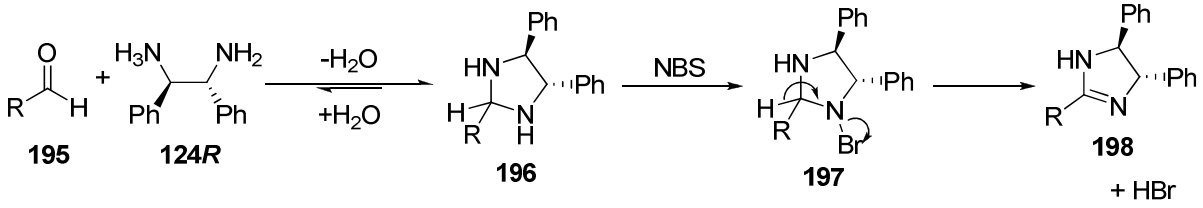

Scheme 71: Fujioka *et al*'s imidazoline synthesis

Fujioka's protocol was reported as clean and high-yielding for a range of aldehydes and was considered to be applicable to our electron deficient aromatic substrate.

We therefore reduced our 2,6-dicyanoiodobenzene (**192**) to the corresponding bis-aldehyde **199** with diisobutylaluminium hydride (DIBAL-H) (Scheme 72).

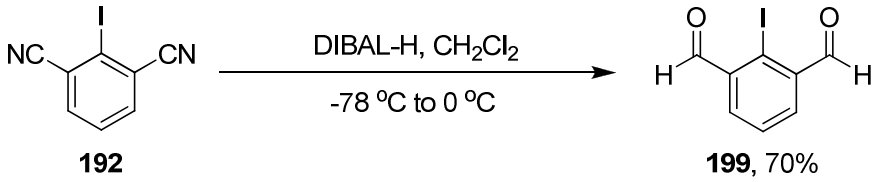

Scheme 72: DIBAL-H reduction of 2,6-dicyanoiodobenzene (192) to 2-iodoisophalaldehyde (199)

To remove the need for chromatography in a large scale procedure, the crude bis-aldehyde (**199**) was purified by formation of the bisulfite adduct (**200**, Scheme 73) and its precipitation from a solution of ethyl acetate, ethanol and water. Following filtration, washing and drying, the salt (**200**) was decomplexed with sodium hydroxide to afford the pure bis-aldehyde **199**.

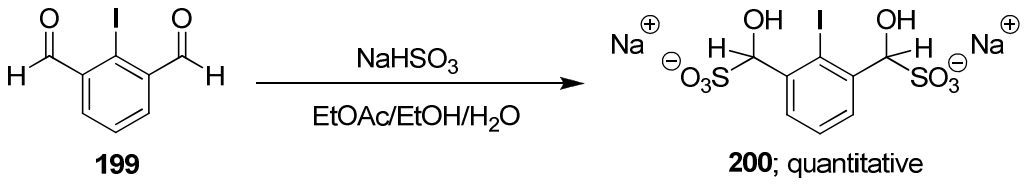

Scheme 73: formation of the bisulfite-aldehyde adduct, 200

The reduction and purification procedure was carried out on a multigram scale to produce 19 g of 2-iodoisophalaldehyde (**199**).

Trial reactions of the imidazoline formation using Fujioka's conditions were promising, yielding IBAM (**113**) in 51% yield after chromatography (Scheme 74).

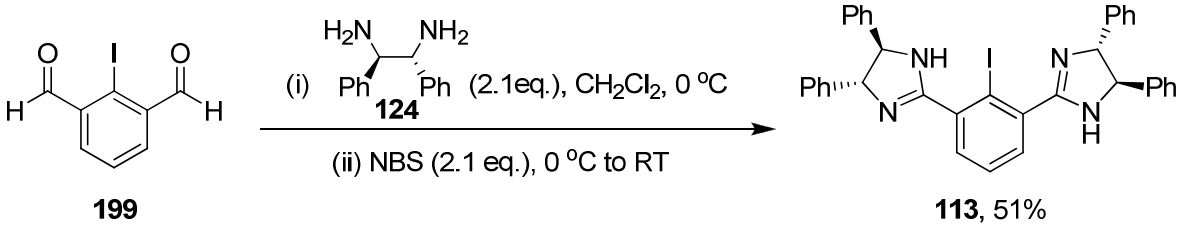

Scheme 74: initial attempt of IBAM (113) formation using Fujioka's conditions

However, analysis of the by-products revealed the presence of both unreacted starting material, **199**, mono-imidazoline, **201**, and, surprisingly, *iso*-amarine, **116** (Scheme 75).

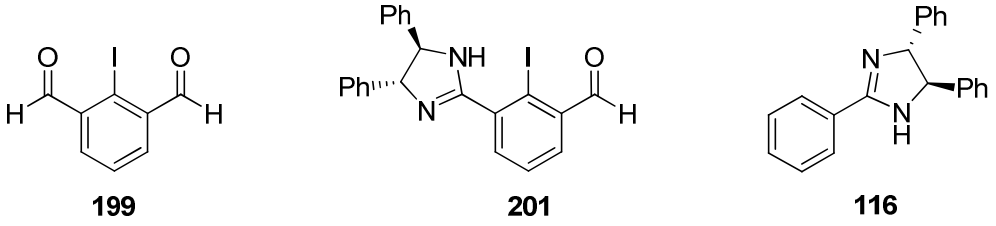

Scheme 75: by-products in IBAM (113) synthesis using Fujioka's method

It was apparent that much of diamine **124** had reacted to form the *iso*-amarine (**116**) impurity, leaving a portion of the aldehyde starting material unreacted. This resulted in only a moderate yield of IBAM (**113**). It was hypothesized that the *iso*-amarine or AM (**116**) was formed as a result of incomplete aminal (**206**) formation prior to the addition of NBS, thus leaving unreacted diamine **124** in the reaction mixture. It was proposed that this reacted with

the NBS to form “benzimine” (**203**), which rapidly coupled to further unreacted diamine **124** (Scheme 76).

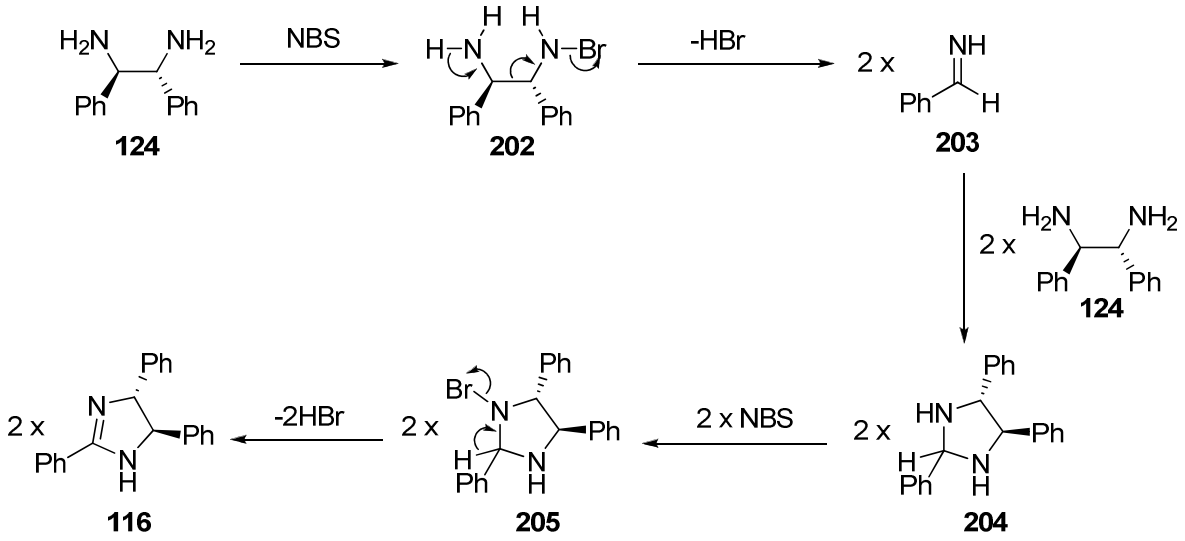

Scheme 76: formation of *iso*-amarine (116) from 1,2-diphenylethylene diamine (124)

In order to test this hypothesis, we stirred 1,2-diphenylethylene diamine (**124**) in deuterated chloroform with 1 equivalent of NBS. After stirring for 4 hours, crude *iso*-amarine (**116**) was obtained from the reaction mixture in 89% yield, thereby confirming our proposed mechanism. Thus, in order to reduce the *iso*-amarine (**116**) impurity, and thereby the efficiency of the reaction, full aminal (**206**) formation must be ensured before the addition of NBS.

We proposed that due to the greater steric encumbrance of aminal formation in our substrate relative to any of Fujioka’s examples,[115] the equilibrium between aldehyde (**199**) and aminal (**206**) does not lie as far to the right hand side (Scheme 77).

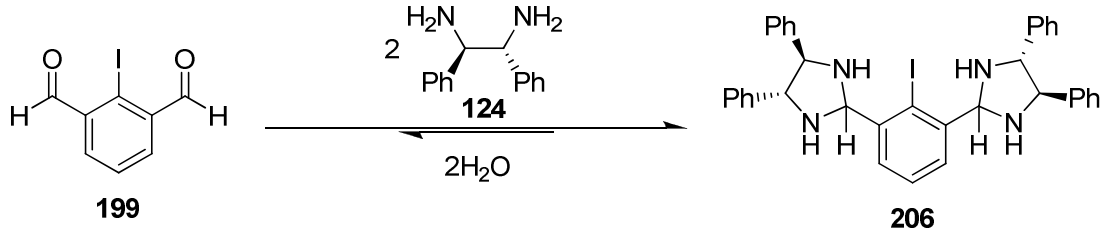

Scheme 77: aldehyde (199)/aminal (206) equilibrium

Indeed, Fujioka *et al* noted that *ortho* substituted aromatic aldehydes gave considerably lower yields than their *meta* and *para* substituted analogues, prompting Fujioka to conclude that "the steric factor is more important than the electronic factor in this reaction".[115] Therefore, although Fujioka did not find it necessary to remove water from the reaction, we hypothesized that in our system it was necessary in order to drive the equilibrium fully to the aminal product (**206**). We introduced an additional step in the reaction, conducting the initial aminal (**206**) formation in toluene, which was then concentrated *in vacuo* to remove the water by-product by formation of an azeotropic mixture. The resulting mixture was then taken up in dichloromethane and stirred with NBS. This two-step procedure eliminated the majority of the *iso*-amarine (**116**) by-product and resulted in the isolation of the desired IBAM product (**113**) in 83% yield (Scheme 78).

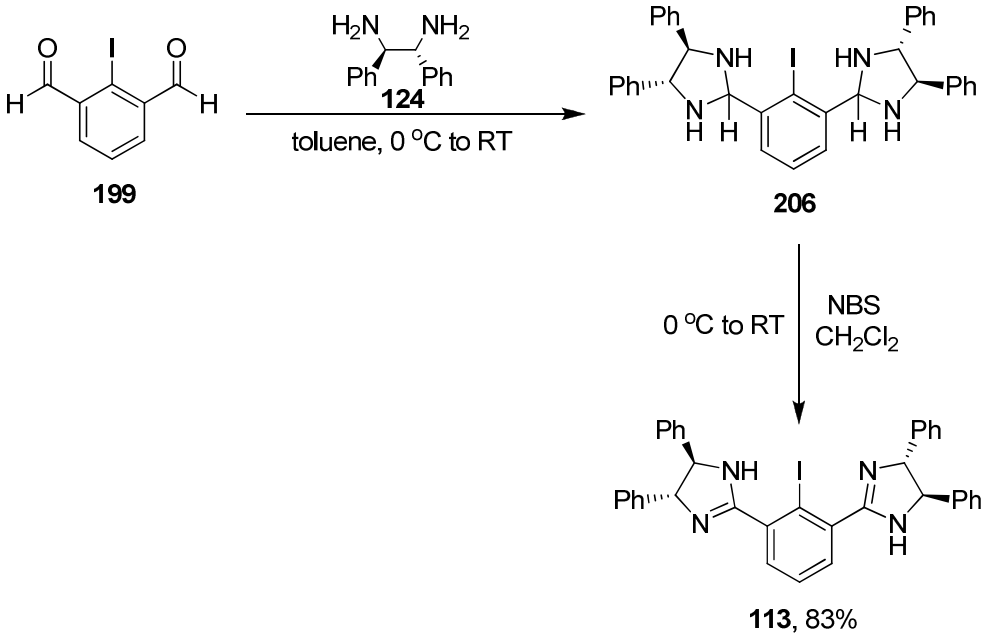

Scheme 78: optimised synthesis of IBAM (113) from aldehyde 119

Again, chromatography was eliminated in the purification procedure, the IBAM (**113**) instead being purified by recrystallisation from an ethanol/water mixture. This protocol was successfully applied to a large scale synthesis to produce 25 g of our catalyst (**113**).

Thus, by a complete re-design of the synthesis of our catalyst IBAM (**113**), we had successfully achieved an efficient large scale preparation (Scheme 79). We increased the overall yield of IBAM (**113**) from commercially available starting material from 14% to 37%

and, perhaps more significantly, we developed a high yielding and robust procedure for the incorporation of the chiral diamine **124** into the catalyst structure.

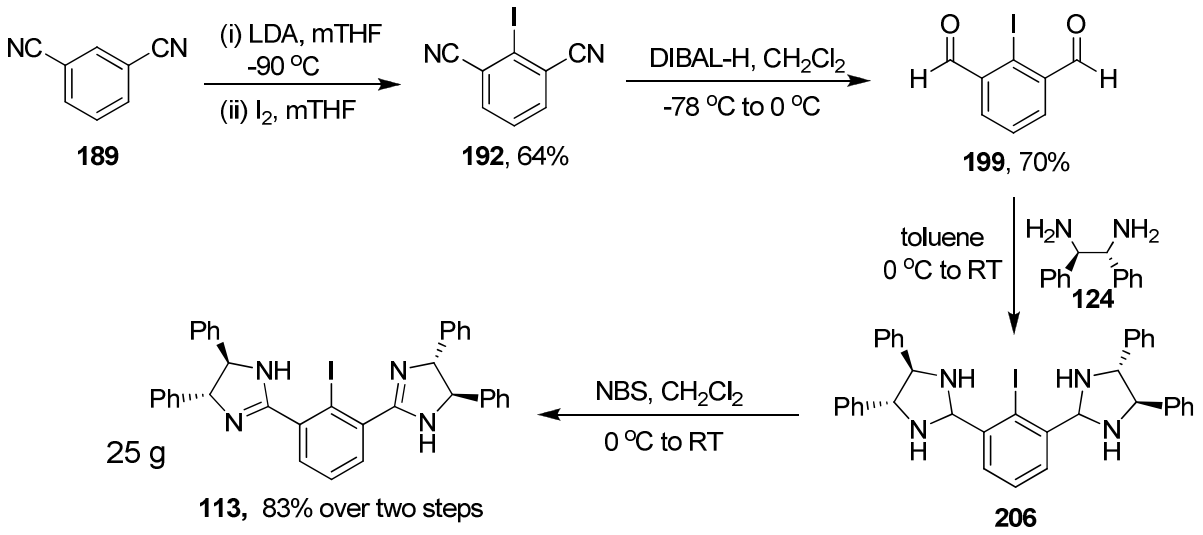

189 **192**, 64% **199**, 70% **124** **206** **113,** 83% over two steps

Scheme 79: re-designed IBAM (113) synthesis

We also explored the possibility of using this protocol for the synthesis of IBAM (**113**) analogues incorporating different diamines or amino-alcohols into the catalyst. Attempts to form the analogues **207** and **208** (Figure 43) from the bis-aldehyde intermediate, **199**, both resulted in imine formation (**212** and **214**, respectively, Scheme 80) on addition of (1*R*,2*R*)-1,2-diaminocyclohexane (**211**) or (1*R*,2*S*)-2-amino-1,2-diphenylethanol (**213**) rather than forming the desired aminal **209** or hemiaminal **210** (Figure 43). The imine and aminal species were distinguishable using ^{1}H NMR, by comparing the shift of the imine proton (8.64 and 8.24 ppm for **212** and **214**, respectively) to that of the aminal (5.81 ppm for **206**).

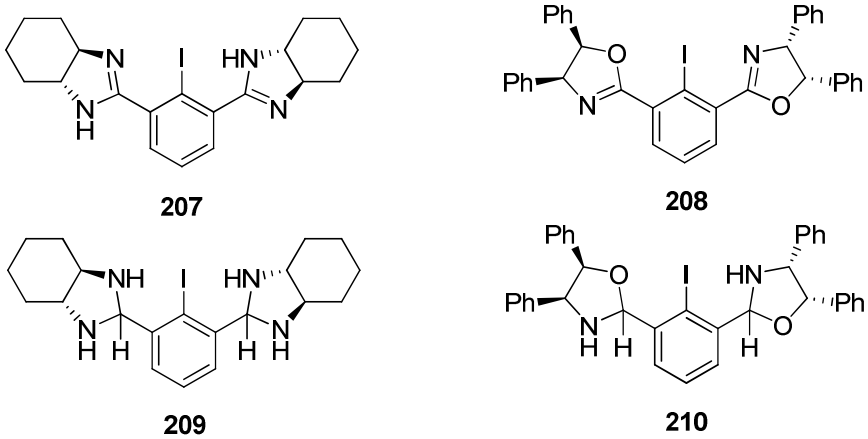

207 **208** **209** **210**

Figure 43: 1,2-diaminocyclohexane and 2-amino-1,2-diphenylethanol analogues of IBAM (207 and 208) and their aminal precursors (209 and 210)

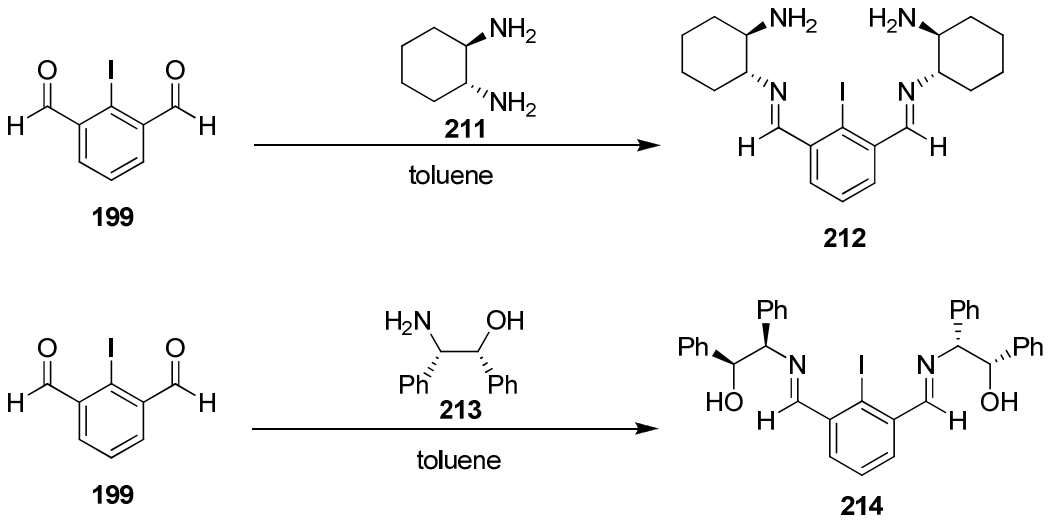

Scheme 80: attempted syntheses of IBAM analogues 207 and 208

Subsequent addition of NBS to the resulting imines, **212** and **214**, failed to afford the desired catalysts, **207** and **208**, but instead resulted in complex mixtures of products. In the case of (1*R*,2*R*)-1,2-diaminocyclohexane (**211**), the preferential formation of the imine is due to the high ring-strain introduced on formation of a *trans*-bicyclic aminal intermediate, **209**. The failure of 2-amino-1,2-diphenylethanol (**213**) to form the hemiaminal on reaction with aldehyde **199** may be a result of increased steric clashing between the *cis*-phenyl groups upon ring closure, or the reduced nucleophilicity of the oxygen relative to that of nitrogen.

However, further work by the Braddock group has demonstrated the successful application of the protocol to the synthesis of the (1*R*,2*R*)-1,2-di-*tert*-butylethylenediamine analogue (**215**, Figure 44) of IBAM (**113**).[116] This indicates that the procedure is successful for any diamine substrates which can undergo aminal formation without any significant increase in steric clashes or torsional strain.

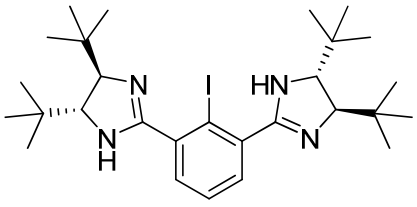

215

Figure 44: (1*R*,2*R*)-1,2-di-*tert*-butylethylenediamine analogue of IBAM

3.2. Investigations into hypervalent iodine mediated catalytic asymmetric bromination

In previous work,[55] enantioselectivity was only observed in IBAM (**113**) catalysed bromolactonisation on reaction of a 0.25 M or 0.025M solution of the substrate **114** in dichloromethane, at -78 ºC, with one equivalent of NBS and a catalyst loading of 1 mol% (Scheme 81).

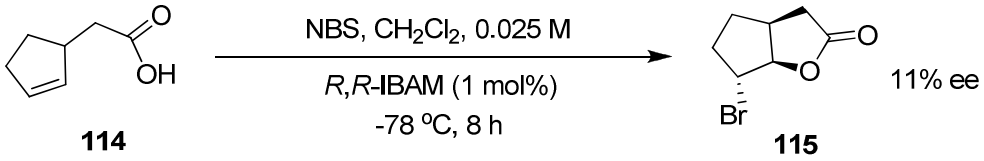

114 **115**

Scheme 81: enantioselective bromolactonisation with *R,R*-IBAM

Thus, these conditions were taken as the starting point for our investigations.

3.2.1. Extension of the substrate library

One of the initial goals in our investigations into catalytic asymmetric bromination was the extension of our substrate library for the bromolactonisation reaction to incorporate a wider range of unsaturated carboxylic acids.

4-Phenylpent-4-enoic acid (**216**, Figure 45) had been previously synthesized and screened as a possible substrate for the asymmetric bromolactonisation reaction. It was hypothesized that this was an attractive substrate for asymmetric induction on formation of the bromonium ion due to the greater steric bulk around the double bond. This should induce a greater differentiation between the diastereomeric transition states of Br^+ transfer to the alkene and thus lead to a higher degree of enantioselectivity. However, in previous work the racemic lactone had failed to separate into its enantiomers on the chiral HPLC, rendering the substrate unsuitable for screening in our asymmetric catalysis. However, by use of a different chiral HPLC system, we were able to achieve separation and could thereby screen the substrate **216** under asymmetric bromolactonisation conditions for enantioselectivity (Table 4).

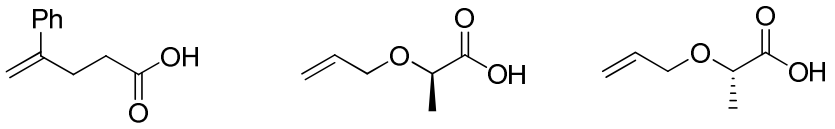

216 **217*R*** **217*S***

Figure 45: asymmetric bromolactonisation substrates

As an alternative method of analysis, we also proposed the synthesis of a substrate in which any asymmetric induction could be measured by ^{1}H NMR. We hypothesized that substrates **217*R*** and **217*S*** (Figure 45), which both already contained a chiral center, would afford a diastereomeric mixture of products upon bromolactonisation. The ratio of the diastereomers should, in theory, be measurable by integration of the ^{1}H NMR spectrum. When the bromolactonisation is catalysed by IBAM (**113**), any asymmetric induction in Br^+ delivery should result in a differential perturbation of the diastereomeric product ratio for the two enantiomers of the substrate. Thus, we hoped to develop a more efficient tool for screening any enantioselectivity in our catalytic bromination.

Accordingly, the (*R*)- and (*S*)-2-allyloxypropionic acids (**217*R*** and **217*S***) were synthesized from (*R*)- and (*S*)-ethyl lactate (**218*R*** and **218*S***) *via* the 2-allyloxypropionic acid ethyl esters (**219*R*** and **219*S***, Scheme 82).

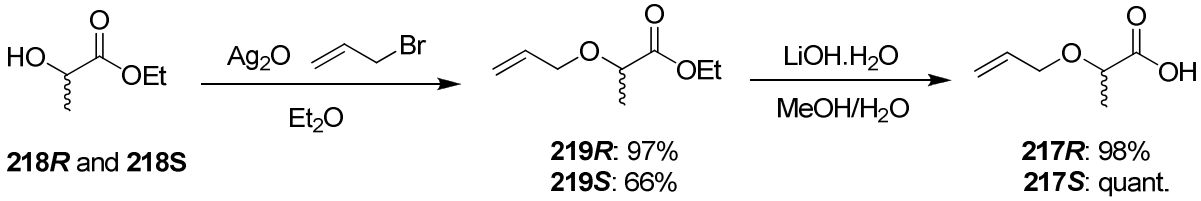

218*R* and **218S**

219*R*: 97%
219*S*: 66%

217*R*: 98%
217*S*: quant.

Scheme 82: synthesis of 2-allyloxypropionic acid substrates (217*R* and 217*S*)

The enantiopurity of the product was confirmed by re-esterification of the (*S*)-acid substrate (**217*S***) *via* a DCC mediated coupling (Scheme 83) and comparison of the resulting ester's optical rotation (-74.4, ethanol) to the literature value (-73.6, ethanol).[117]

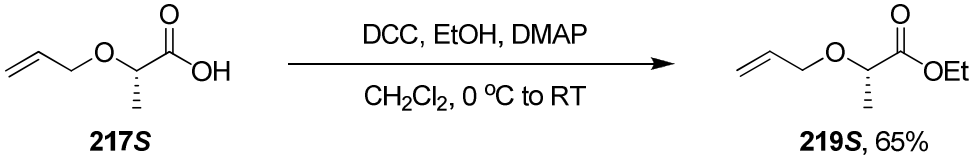

217*S*

219*S*, 65%

Scheme 83: DCC coupling to re-form (*S*)-2-allyloxypropionic acid ethyl ester (219*S*)

Pleasingly, on reaction with NBS, the substrate afforded the corresponding bromolactone as a diastereomeric mixture (**220** and **221**, Scheme 84). Both protons attached to the tri-substituted carbons (C-2 and C-5) of the ring appeared as distinct resonances for the two diastereomers and thus the diastereomeric excess was determinable by simple integration of the crude mixture.

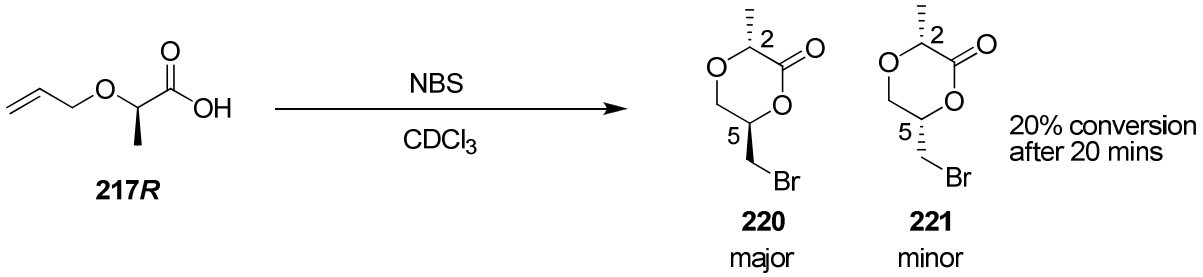

217*R*

220
major

221
minor

Scheme 84: bromolactonisation of (*R*)-2-allylpropanoic acid (217*R*)

On standing the (2*R*)-bromolactone product mixture at 0 ºC, a portion of the colourless oil solidified to form colourless needles. Isolation of these crystals and subsequent ^{1}H NMR analysis revealed them to be completely composed of the major diastereoisomer. X-ray crystallography identified the solid as the (2*R*,5*R*)-5-bromomethyl-3-oxa-2-methyl-δ-pentano-5-lactone (**220**, Figure 46), enabling us to assign our major and minor diastereomeric products in the bromolactonisation of either enantiomer of **217** as (2*R**,5*R**) and (2*R**,5*S**) respectively.

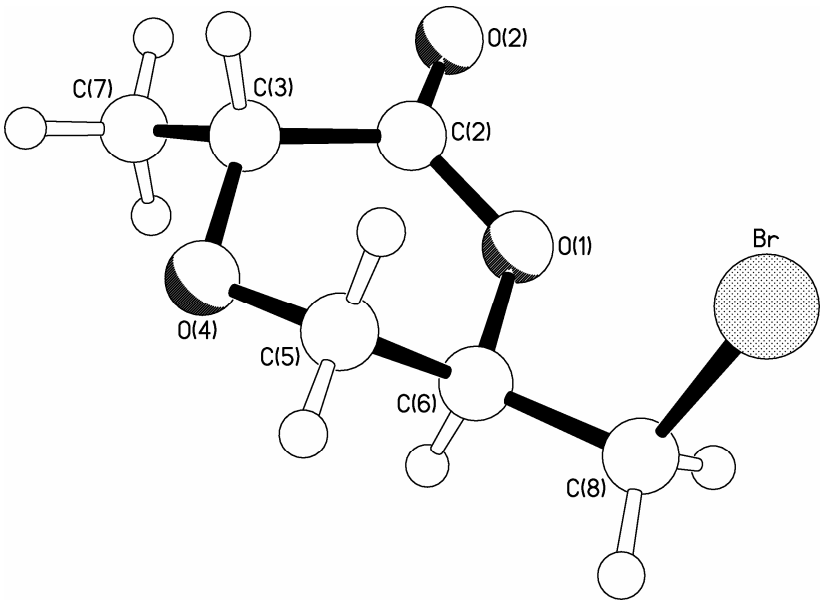

Figure 46: X-ray crystal structure of (2*R*,5*R*)-5-bromomethyl-3-oxa-2-methyl-δ-pentano-5-lactone (220)

The bromolactonisation was also appreciably catalysed by IBAM (**113**) at room temperature (Table 4), although no differentiation in the diastereomeric ratio was observed on using different hands of the catalyst. Thus (*R*)- and (*S*)-2-allyloxypropionic acids (**217*R*** and **217*S***) were also deemed suitable substrates to screen in the asymmetric catalytic bromination reaction.

Table 4: catalytic bromolactonisation of extended substrate library[a]

Entry	Substrate	Product	Catalyst (Loading)	Solvent (Conc.)	Temp.	Time	Yield	Ee or de
1	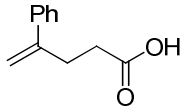 **216**	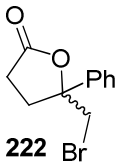 **222**	*R*-IBAM **113** (1 mol%)	CH_2Cl_2 (0.25M)	-78 ºC	8 h	81%	<5% ee
2	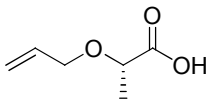 **217*S***	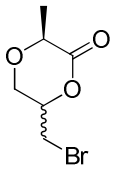 **220/221**	-	$CDCl_3$ (0.25M)	RT	20 min 1.5 h	20% 65%	21% de
3	**217*S***	**220/221**	*R*-IBAM **113** (1 mol%)	$CDCl_3$ (0.25M)	RT	20 min 1.5 h	60% 77%	28% de
4	**217*S***	**220/221**	*S*-IBAM **113** (1 mol%)	$CDCl_3$ (0.25M)	RT	1 h	70%	28% de
5	**217*S***	**220/221**	*R*-IBAM **113** (5 mol%)	CH_2Cl_2 (0.25M)	-78 ºC	8 h	17%	33% de
6	**217*S***	**220/221**	*S*-IBAM **133** (5 mol%)	CH_2Cl_2 (0.25M)	-78 ºC	8 h	18%	39% de

a - all reactions carried out using 1 eq. of NBS

Low temperature asymmetric bromolactonisation of substrate **217*S*** demonstrated a small perturbation of diastereomeric excess on changing from (R)-IBAM (**113*R***) to (S)-IBAM (**113*S***) (6%, c.f. entries 5 and 6, Table 4). Disappointingly the bromolactonisation product **222** of 4-phenylpent-4-enoic acid (**216**, entry 1) failed to demonstrate any evidence of

enantioselectivity. However, although no significant enantioselectivity was observed for the new substrates, we have successfully increased the range of unsaturated carboxylic acids available to us for screening purposes.

3.2.2. Further screening of catalytic bromination conditions

Although an extremely vigorous screening of the conditions for our catalytic bromination reaction had previously been undertaken,[55] there were a limited number of further variations which we wished to investigate. We desired a more thorough screen of temperatures, the catalytic bromination having in the past only been carried out at room temperature or -78 ºC (Table 5, entries 2-4). We also had identified toluene (Table 5, entry 5) as an attractive solvent for our catalysis reaction since Sakakura *et al* had demonstrated it to be an excellent choice of solvent for the asymmetric iodocyclisation of polyprenoids.[56] Finally, we wished to screen a range of concentrations for the IBAM (**113**) catalysis reaction, to ascertain the effect of dilution on the catalyst's asymmetric induction (Table 5, entries 6-9). Our screening of these variables focused on the bromolactonisation of **114**, which had previously yielded enantio-enriched bromolactone **115** after reaction under standard asymmetric catalytic bromination conditions (Table 5, entry 1).

Table 5: further screening of variables in IBAM (113)-catalysed bromolactonisation[a]

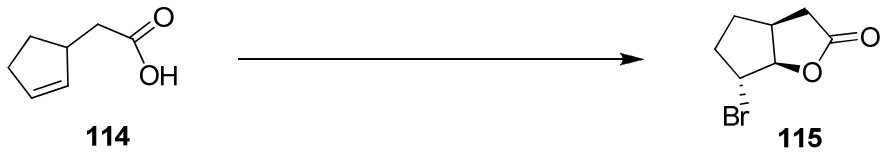

114 **115**

Entry	Catalyst	Loading	Solvent	Conc.	Temp.	Time	Yield	Ee
1	*R*-IBAM	1 mol%	CH_2Cl_2	0.25 M	- 78 ºC	8 h	43%	8%
2	*R*-IBAM	1 mol%	CH_2Cl_2	0.25 M	-45 ºC	15 h	60%	7%
3	*R*-IBAM	1 mol%	$CHCl_3$	0.25 M	-45 ºC	15 h	68%	8%
4	*S*-IBAM	1 mol%	acetone	0.25 M	- 45 ºC	8 h	52%	<5%
5	*R*-IBAM	5 mol%	toluene	0.025 M	- 78 ºC	8 h	44%	<5%
6	*R*-IBAM	1 mol%	CH_2Cl_2	0.25 M	- 78 ºC	8 h	55%	5%
7	*R*-IBAM	1 mol%	CH_2Cl_2	0.025 M	- 78 ºC	8 h	27%	11%
8[c]	*R*-IBAM	1 mol%	CH_2Cl_2	0.025 M	- 78 ºC	8 h	22%	8%
9	*R*-IBAM	5 mol%[b]	CH_2Cl_2	0.0025 M	- 78 ºC	24 h	51%	12%

a – all reactions were carried out using 0.5 eq. NBS
b - catalyst loading increased due to slow reaction rate at high dilution
c – repeat reaction

Disappointingly, our wider screen of conditions failed to highlight any significant increase in the asymmetric induction of our IBAM (**113**) catalysed bromination. A relationship between concentration and enantioexcess was noted, the ee increasing slightly at higher dilutions. Although no such inferences were drawn at the time, with retrospect it is apparent that this trend is in agreement with our proposed mechanism of racemisation *via* bromonium ion-alkene Br^+ exchange. It is to be expected that such exchange would be concentration dependent; the degree of Br^+ transfer decreasing as the dilution of the reaction mixture increases. Thus, the observed enantioexcess of the product would be expected to increase at lower concentrations. We selected a concentration of 0.025 M, representing compromise between observed enantioselectivity and practicality, as an optimum concentration for the IBAM (**113**) catalysed asymmetric bromination reaction.

3.2.3. Investigation of an alternative Br^+ source

2,4,4,6-Tetrabromo-2,5-cyclohexadienone (TBCO, **223**) was investigated as an alternative source of Br^+ to NBS in the catalytic bromination reaction. However, comparison of the IAM (**111**)-catalysed bromolactonisation to the uncatalysed control demonstrated almost no differentiation between the rates of the reactions (Table 6). Thus, due to the high background reaction, TBCO (**223**) was rejected as a possible alternative Br^+ source.

Table 6: investigation into the use of TBCO (223) as Br^+ source[a]

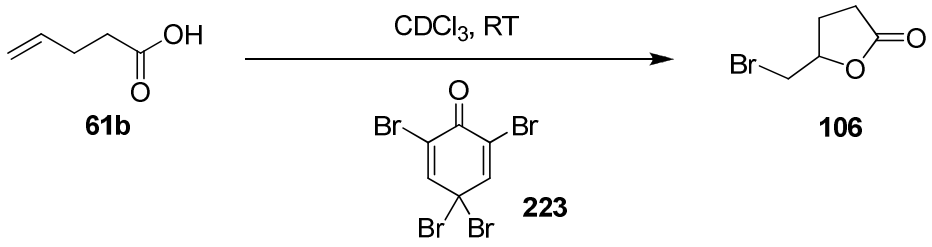

Catalyst	Loading	Concentration	Time	Conversion
-	-	0.25 M	17 min	51%
R-IAM (**111*R***)	1 mol%	0.25 M	18 min	49%

a – all reactions carried out using 1 eq. of TBCO

After failing to improve the enantioselectivity of the IBAM (**113**)-catalysed asymmetric bromination by extended screening of a wider range of variables, we returned to one of our original goals of developing a better understanding the nature of our catalytic intermediate. It was hoped that, on achieving this, we would be able to make more informed alterations to optimise our reaction conditions and catalyst structure.

3.3. Stoichiometric addition of NBS to the catalysts

As detailed earlier in the introduction, there is some ambiguity in our catalytic system as to whether the bromine is delivered from iodine, *via* a hypervalent I(III)-Br bond, or from the amidine nitrogen. As this appears to be of key importance to the degree of enantiocontrol observed, it is desirable that we understand the mechanism of bromine delivery in order to

effectively design a more enantioselective system. We had therefore synthesized our simplest hypervalent iodine-based bromination catalyst, IAM (**111**) and its iodine free analogue, *iso*-amarine (**116**), with a view to adding stoichiometric NBS and observing the catalyst-Br^+ adduct formed.

3.3.1. Stoichiometric addition of NBS to iso*-amarine (**116**)*

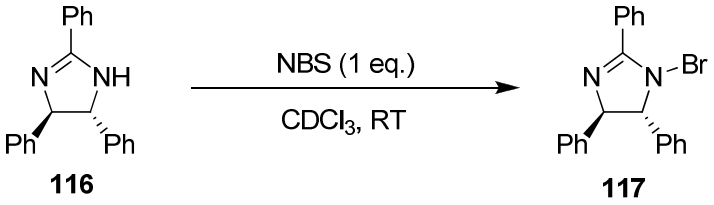

116 **117**

Scheme 85: stoichiometric addition of NBS to *iso*-amarine (116)

On addition of one equivalent of NBS to a solution of *iso*-amarine (**116**) in deuterated chloroform, a bright yellow/green solution was formed from the colourless starting materials. After stirring for 15 minutes, ^{1}H NMR analysis revealed the complete conversion of NBS to succinimide, indicating transferal of Br^+ to *iso*-amarine. However, due to an aromatic region which appears as an overlapping multiplet in the spectra of both *iso*-amarine (**116**) and the *iso*-amarine-Br^+ adduct (**117**), very little further information could be deduced from the ^{1}H NMR spectrum. The ^{13}C spectrum was more instructive, demonstrating extreme broadening of many of the peaks on addition of the NBS (Figure 47 and Figure 48).

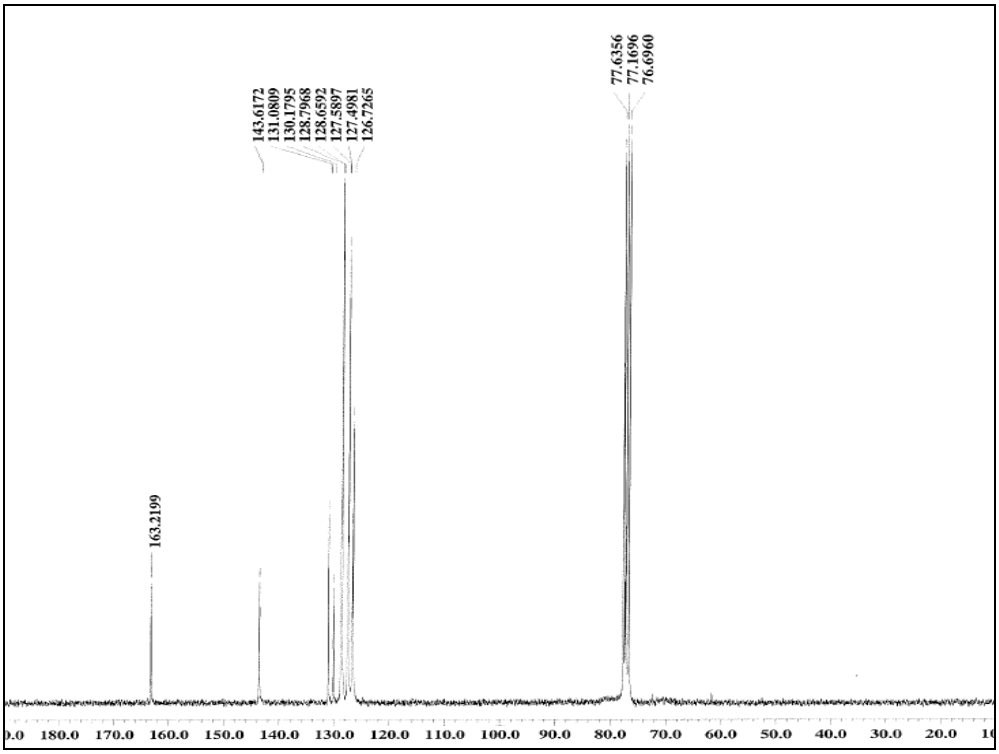

Figure 47: ^{13}C spectrum of *iso*-amarine (116) in CDCl3

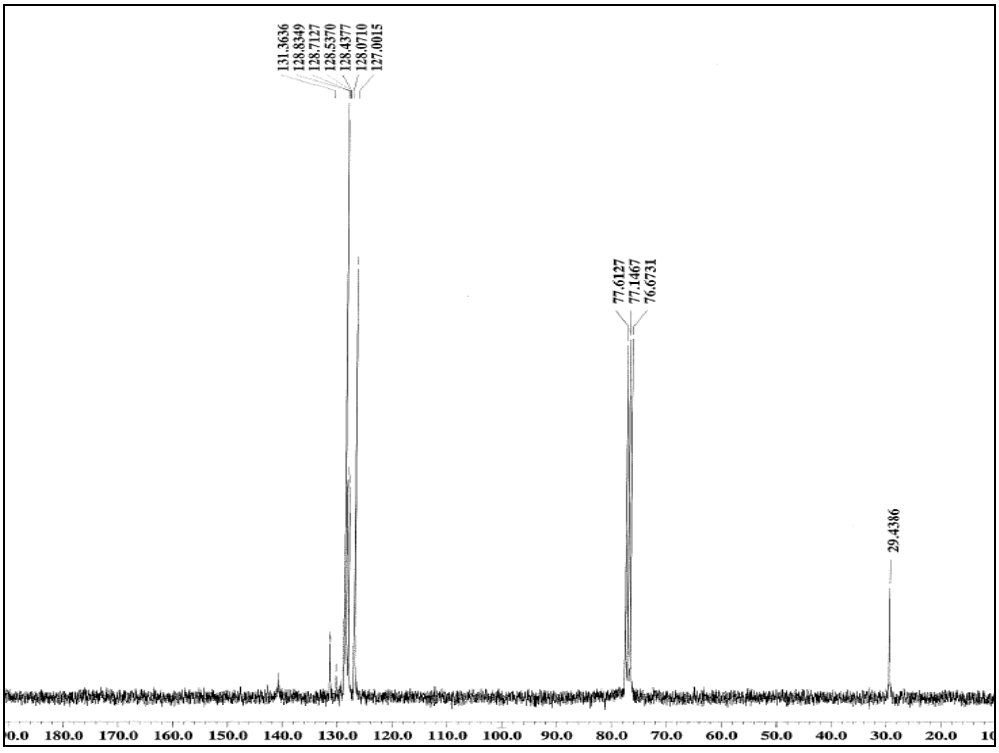

Figure 48: ^{13}C spectrum of *iso*-amarine (116) 15 mins after addition of NBS in $CDCl_3$

The broadening was most evident in the resonance belonging to the quaternary carbons on the phenyl rings, *C*CHN (143.0 ppm) and to a greater degree in the resonance of the amidine carbon (163.2 ppm), which was broadened to the extent where it was no longer detected in the spectra (Figure 49). The Ph*C*HN carbons are not evident in either spectra, presumably due to broadening of the peaks as a result of proton or Br^+ exchange between the amidine nitrogens on a timescale similar to that of the ^{13} C relaxation.

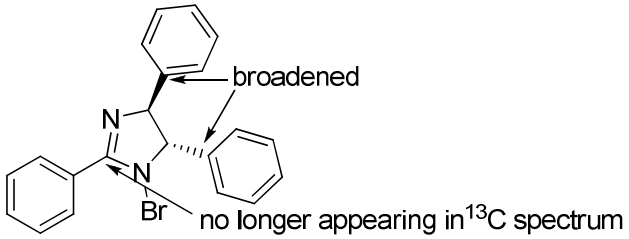

117

Figure 49: *iso*-amarine-Br^+ adduct (117)

3.3.2. Stoichiometric addition of NBS to IAM *(**111**)*

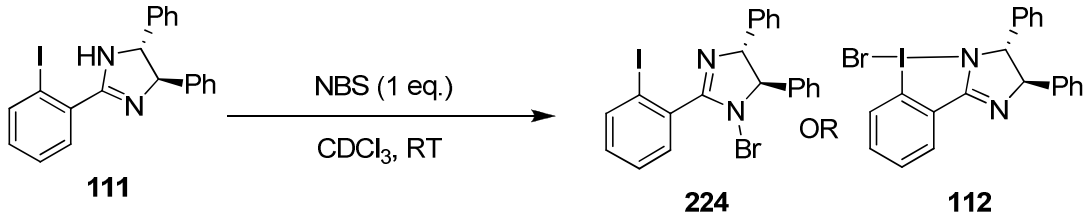

111 **224** **112**

Scheme 86: stoichiometric addition of NBS to IAM (111)

Stoichiometric NBS was added to IAM (**111**) in deuterated chloroform at room temperature. Again, the solution changed from colourless to bright yellow/green in colour on addition of NBS and ^{1}H NMR analysis demonstrated complete conversion of NBS to succinimide after 15 minutes. The resonances for the protons of the iodobenzene ring are out-lying from the rest of the aromatic resonances in the ^{1}H NMR spectrum of IAM (**111**) and consequently their changes in ppm on addition of NBS can be observed. However, whilst the aromatic protons in question did demonstrate significant shifting (Figure 50 and Figure 51), diagnostic of the formation of a distinct IAM (**111**)-Br^+ adduct, this provides no further insight into whether the adduct contains an I(III)-Br (**112**) or N-Br bond (**224**).

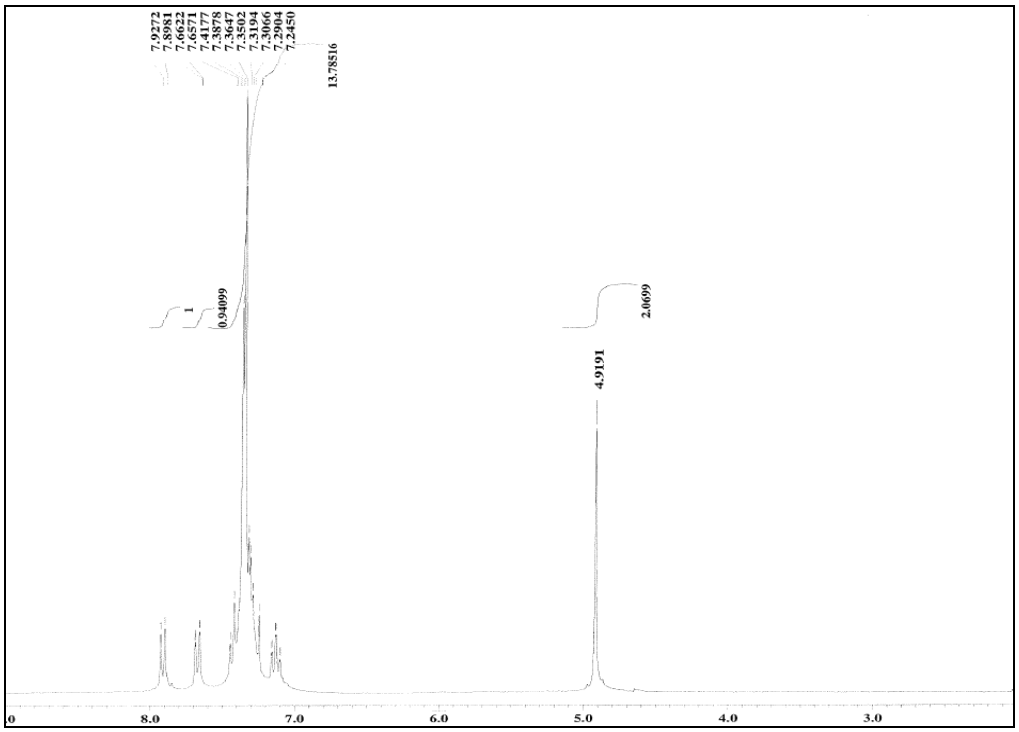

Figure 50: ^{1}H spectrum of IAM (111) in $CDCl_3$

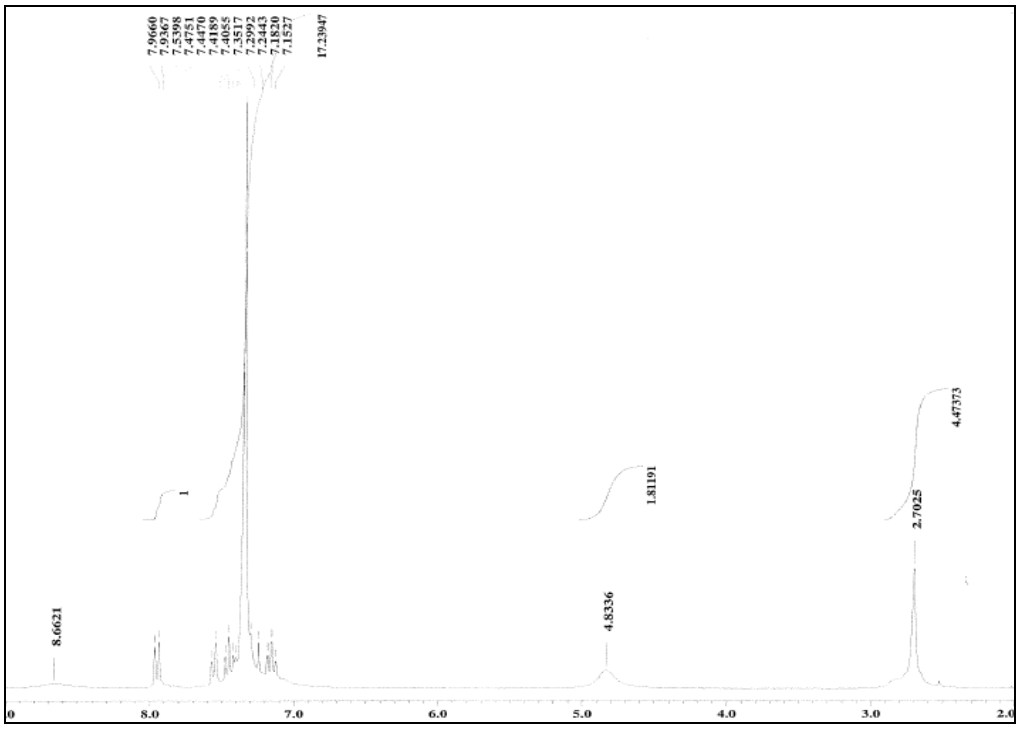

Figure 51: ^{1}H spectrum of IAM (111) 15 mins after addition of NBS in $CDCl_3$

N.B. the peak at 2.70 ppm is due to the succinimide by-product present in the reaction mixture.

The ^{13}C NMR spectrum of IAM (**111**) also demonstrated considerable changes on addition of NBS (Figure 53, Figure 54). These were generally analogous to those observed in the *iso*-amarine (**116**)/NBS system. The resonances belonging to the three carbon atoms adjacent to the amidine nitrogens (164.8 ppm and 75.8 ppm) and the quaternary carbons of the phenyl rings *C*CHN (142.8 ppm) are broadened to the extent to which all three resonances no longer appear in the spectra of the IAM (**111**)-Br^+ adduct (Figure 52).

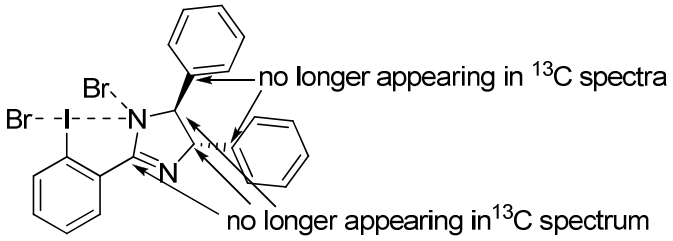

112 or **224**

Figure 52: IAM (111)-Br^+ adduct

The carbon bonded to the iodine was shifted from 94.6 ppm in IAM (**111**) to 95.8 ppm on addition of NBS. Whilst this downfield shift is consistent with the expected de-shielding of the carbon on formation of a hypervalent species, it is of considerably smaller magnitude than the shifts observed on the formation of the bromoiododinanes **103** (112.1 ppm) and **105** (109.9 ppm) from their carbinol precursors **102** (93.3 ppm) and **104** (90.6 ppm).

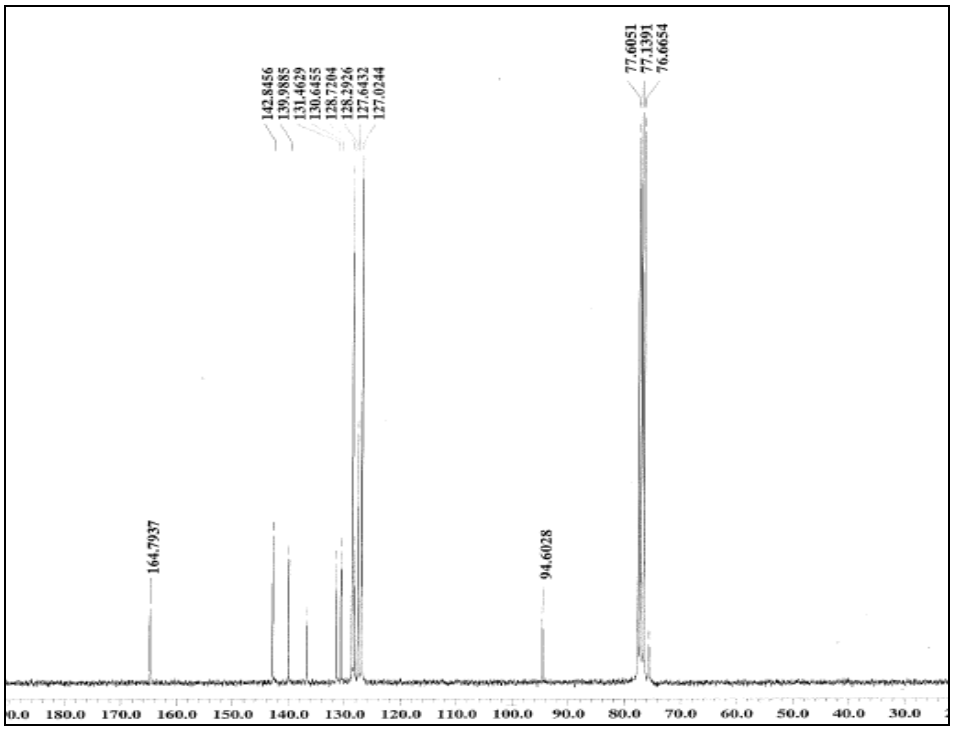

Figure 53: ^{13}C spectrum of IAM (111) in $CDCl_3$

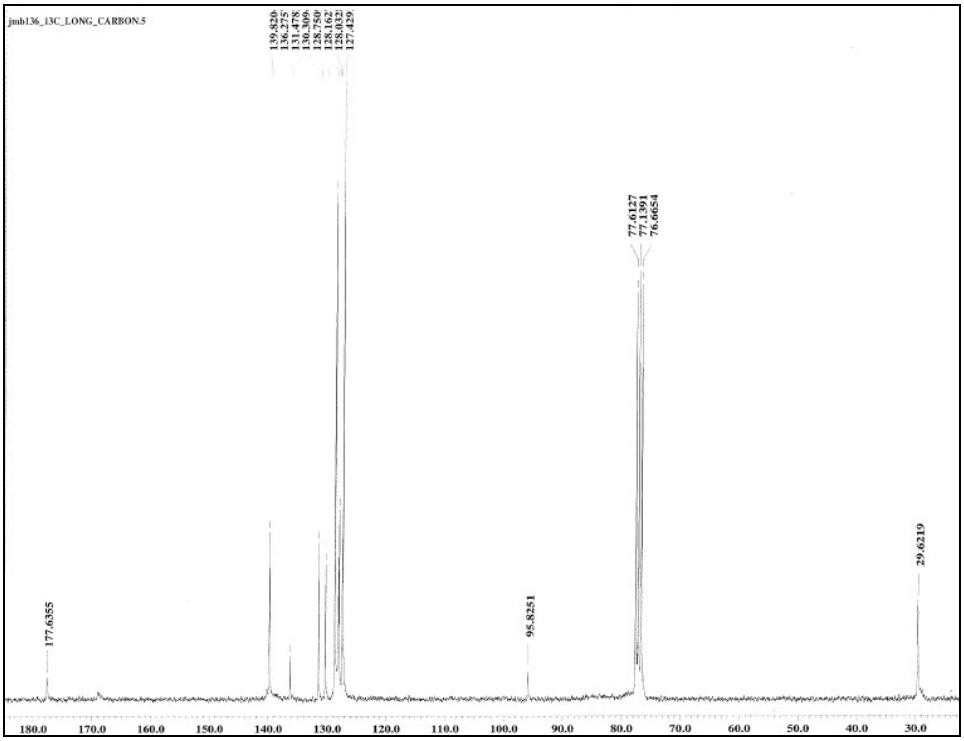

Figure 54: ^{13}C spectrum of IAM (111) 15 mins after addition of NBS in $CDCl_3$

N.B. the peaks at 177.6 ppm and 29.6 ppm are due to the succinimide by-product present in the reaction mixture.

It is hypothesised that the general line broadening and disappearance of certain peaks in the ^{13}C spectra is due to the existence of a system in which Br^+ is exchanging between catalyst molecules. It is suggested that we observe a time averaged signal over a range of species in which Br^+ is bonded to the catalyst in differing locations (i.e. either nitrogen of the amidine, or the iodine) and in differing degrees, encompassing both the distinct catalyst-Br^+ species and the intermediates of Br^+ exchange. The observations that the broadening occurs primarily at the carbon atoms in close proximity to the amidine nitrogens and that both catalyst-Br^+ adducts demonstrate similar broadening patterns suggests that a significant portion of the IAM (**111**)-Br^+ adduct is present as the N-Br species. It is noted that in concentrated solutions the amidine moiety could feasibly transfer bromine in a chain mechanism analogous to that of the Grotthus mechanism of proton transfer exchange in liquid water (Figure 55). This would facilitate a dynamically exchanging system, as implied by our observations.

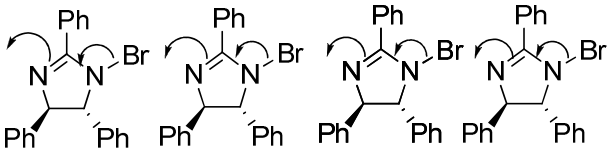

Figure 55: chain mechanism of Br^+ transfer

The addition of two equivalents of NBS to *iso*-amarine (**116**) also demonstrates full conversion of NBS to succinimide after 20 minutes. This indicates the possibility of the existence of a di-brominated *iso*-amarine species **225** (Scheme 87). Additionally, the observation that the succinimide peak is considerably broadened suggests that there may be some exchange of Br^+ back to the succinimide anion (**88**) in the absence of an available proton.

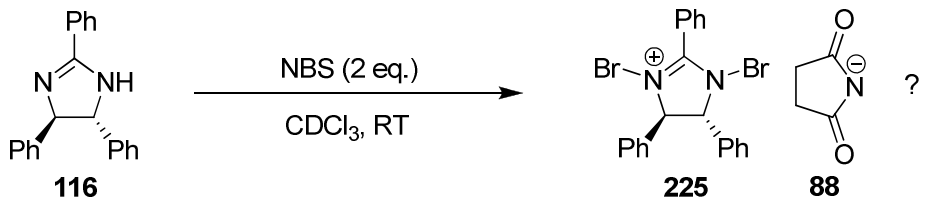

Scheme 87: formation of di-brominated *iso*-amarine (225)

3.3.3. Attempted isolation of the active brominated species

It became clear to us that although we could draw inferences from observing our stoichiometric additions by ^{1}H and ^{13}C NMR, no unambiguous conclusions could be made regarding the true structure of the catalytic intermediate using these methods. We envisaged that the only method which would give us conclusive evidence of the existence of an I(III)-Br or N-Br bond was X-ray crystallography of the catalytic intermediate. Thus, we turned our attention to the isolation of the catalyst-Br^{+} adducts with the goal of fully characterizing them.

It was originally attempted to isolate the brominated *iso*-amarine species, **117**, by removal of succinimide with an aqueous wash followed by concentration of the organic phase to yield a yellow/orange amorphous solid. However, NMR analysis and mass spectroscopy of the solid indicated extensive decomposition had occurred over the work up, resulting in a complex mixture of products.

Due to the instability of the intermediates to an aqueous work up, we investigated the use of a solvent system which would allow the precipitation of either the catalyst-Br^{+} adduct or succinimide. Stoichiometric additions were carried out in chloroform, chloroform/hexane, dichloromethane/hexane, diethyl ether, ethanol and ethanol/water, all with negative results. After a review of the current literature we identified a procedure reported by Neumer,[118] in 1972, which appeared to be suitable for our purposes. Neumer precipitated succinimide from carbon tetrachloride at 0 ºC in the preparation of an *N*-bromoimidazole. With the addition of a small amount of chloroform to aid the solubility of the catalyst species (*iso*-amarine, **116** or IAM, **111**), we were able to precipitate 92% of the theoretical mass of the succinimide (**90**) from the reaction mixture. The mixture was filtered and the filtrate concentrated to afford the catalyst-Br^{+} adduct (Scheme 88).

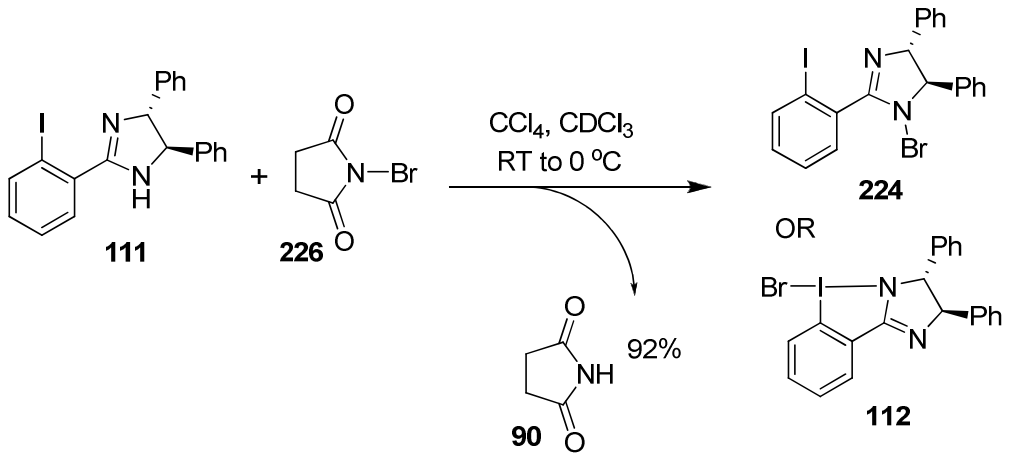

Scheme 88: isolation of the catalyst-Br$^+$ adduct

Attempted isolation of the *iso*-amarine-Br$^+$ adduct (**117**) by this procedure again produced a mixture of decomposition products, demonstrated by ^{1}H NMR analysis of the yellow/orange solid obtained. The considerable reduction of the integration of the singlet belonging to the NC*H* protons relative to the integration of the aromatic region led us to believe that a major decomposition product of the active brominated species is the analogous imidazole **228** (Scheme 89). This decomposition route requires the presence of a base to remove the proton; a function which is likely to be fulfilled by a further molecule of *iso*-amarine (**117**).

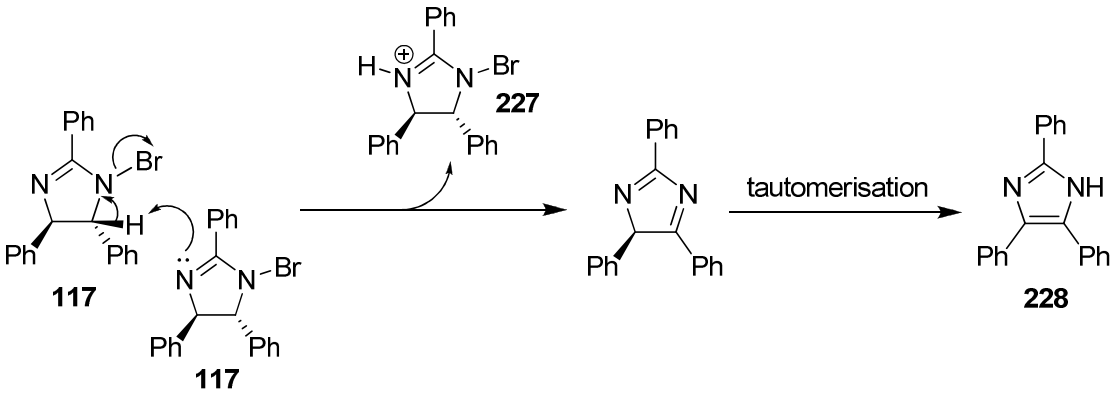

Scheme 89: decomposition of *N*-bromo*iso*-amarine 117 to imidazole 228

Indeed, if one equivalent of TFA was added to the *iso*-amarine (**116**)/NBS mixture, both the appearance of decomposition products and the loss of activity of the system as a source of electrophilic bromine were significantly slowed.

Thus, attention was briefly turned to the isolation of an *N*-bromoamidine in which elimination of HBr was not possible. There were reports in the literature[119] of the isolation of *N*-bromo amidine **229** (Figure 56) and, although there was incomplete characterisation of the isolated species, this seemed like a promising candidate for isolation.

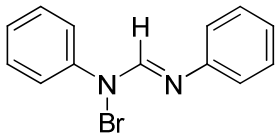

229

Figure 56: *N*-bromo-*N,N'*-diphenylformamidine

However, on addition of NBS and removal of succinimide, the major product isolated was identified by NMR and mass spectroscopy to be the result of bromination of one of the aromatic rings (**231**, Scheme 90). It seems that the conjugation of the amidine nitrogen lone pairs into the aromatic rings activate them sufficiently to electrophilic attack for self-bromination to occur in the absence of a more active substrate.

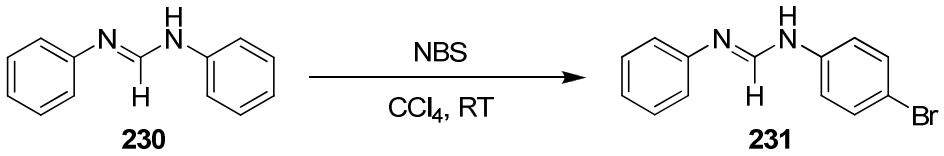

230 **231**

Scheme 90: electrophilic aromatic bromination of *N,N'*-diphenylformamidine

Our variation on Neumer's procedure was applied with considerably more success to the isolation of the IAM-Br^+ adduct (**112** or **224**). A yellow foam was isolated on removal of the solvent which, minus the succinimide peaks, had a NMR identical to that obtained on mixing IAM (**111**) with NBS directly. No decomposition of the adduct was observable by NMR. The species' IR and UV spectra were taken to gain full characterisation of the product. The IR spectrum demonstrated little change from the spectrum observed with IAM (**111**) alone other than a new peak of medium strength resonating at 909 cm^{-1}. N-Br bonds in *N*-brominated amines have previously been reported as resonating at frequencies of 670-700 cm^{-1}, however, there are no literature reports of N-Br stretching frequencies in amidines. Any I-Br stretch should appear well below the fingerprint region due to the large reduced mass of the atoms in the bond, and thus is likely not to be observable in our spectrum. UV proved more revealing, two peaks observable in the spectra of the product, one at 236 nm (IAM (**111**) gives one peak at 236 nm) and a smaller, broader peak at 283 nm. A search of literature

provided UV data for N-Br bonds (288 nm in mono-*N*-bromotaurine)[120] and for compounds containing hypervalent I-Br bonds (205 and 235 nm for iodinane **105** and 200, 235, and 332 nm for 1-bromo-1,3-dihydro-5-methyl-3,3-bis(fluoromethyl)-1,2-benziodoxole).[63] Comparison of the data does seem to suggest the formation of an N-Br over that of an I(III)-Br bond, this species giving a better match for our observed results. However, whilst such UV data confirms the formation of a new bond on addition of NBS to IAM (**111**), it does not conclusively confirm its type as no information is available for comparison for *N*-bromoamidines or nitrogen containing hypervalent iodine compounds.

Recrystallisation of the IAM-Br^+ adduct (**112** or **224**) was attempted and resulted in the isolation of a yellow solid which, as a result of its NMR spectrum, along with its solubility in polar, protic solvents such as ethanol, but extreme insolubility in chloroform, was hypothesized as being the hydrobromide salt of the active brominated catalyst (**232** or **233**).

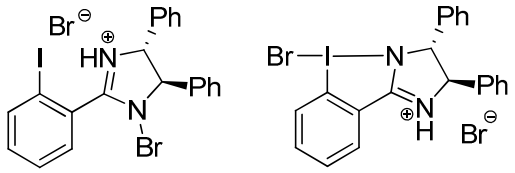

232 **233**

Figure 57: hydrobromide salts of the proposed active brominated catalytic intermediates

Frustratingly, despite screening a variety of solvent permutations, crystals suitable for X-ray crystallography could not be obtained.

3.3.4. Lifetime of the iso*-amarine and IAM-Br^+ adducts*

A series of stoichiometric additions of NBS to both the catalyst IAM (**111**) and *iso*-amarine (**116**) were undertaken to determine the relative stabilities of the catalyst-Br^+ adducts formed. NBS was added to a solution of the catalyst in deuterated chloroform and the solution was stirred in darkness at room temperature for a measured period of time, t (Table 7). After the aging of the solution, substrate was added and its conversion to bromo-lactone measured by ^{1}H NMR to determine the amount of active brominating species still present in the solution.

Table 7: determination of the lifetime of the catalytic intermediates

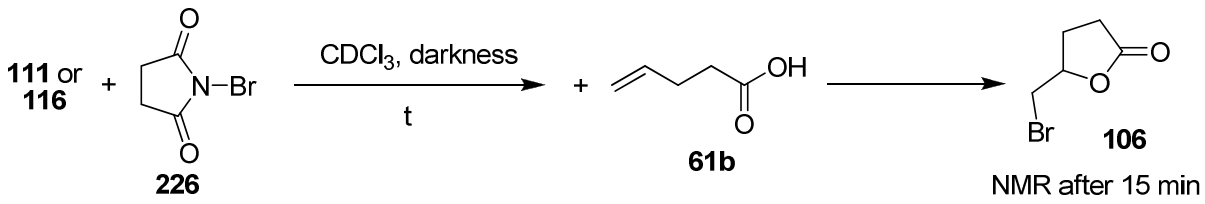

t	Conversion of substrate to bromolactone.		Decomposition products evident by NMR?	
	IAM (**111**) 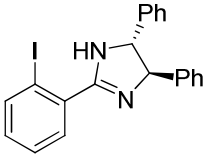	AM (**116**) 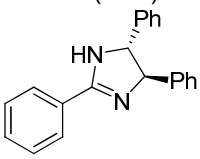	IAM (**111**) 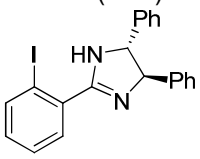	AM (**116**) 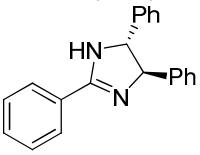
15 min	-	-	No	No
45 min	-	100%	No	No
5 h	-	67%	No	Yes
15 h	100%	55%	No	Yes
24 h	80%	52%	Trace	Yes

These results clearly show that whilst both species are reasonably stable, the iodinated compound, IAM (**111**), decomposes considerably more slowly than its iodine free analogue, **116**. This is an encouraging result; such marked differences in stability suggesting that the environment of the bromine is different in the two active species and thus implying at least some of the bromine is bonded in IAM (**111**) *via* a bond to hypervalent iodine rather than directly bonded to the amidine nitrogen.

A portion of our isolated IAM-Br^+ adduct (**112** or **224**) was used as a stoichiometric brominating agent in the bromolactonisation of cyclopenten-2-yl acetic acid (**114**) at -78 ºC in dichloromethane (Scheme 91). Bromination proceeded to give 36% yield (<5% ee) of bromolactone **115**, a result comparable to 46% yield obtained with the catalytic system.

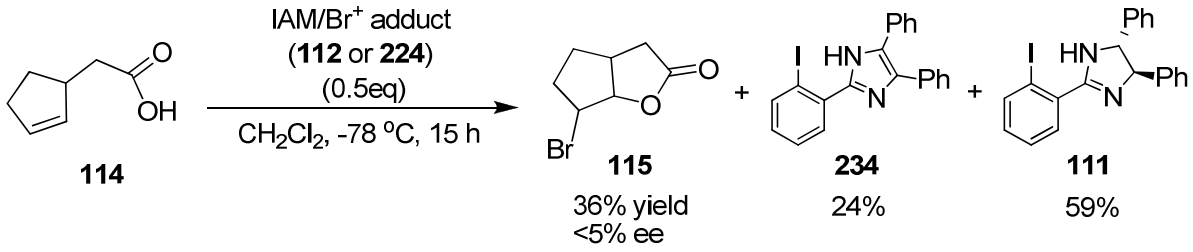

Scheme 91: stoichiometric bromolactonisation reaction with IAM-Br$^+$ adduct (112 or 224)

However, on attempted recovery of the IAM catalyst (**111**) a 2:5 ratio of imidazole (**234**) to IAM (**111**) was obtained. Whilst confirming the elimination of HBr to form the imidazole as the major decomposition route of the brominated intermediate, this raises questions as to whether such decomposition occurs over the catalysis reaction. This would lead to the loss of enantioselectivity if an achiral imidazole was responsible for the delivery of any bromine to the substrate. Screening of imidazole **234** for catalytic activity demonstrated only moderate rate acceleration. A catalytic amount (1 mol%) of imidazole **234** with stoichiometric NBS demonstrated 40% conversion of 4-phenylpent-4-enoic acid (**216**) to its bromolactone **222** in 20 min (Scheme 92), compared to 100% conversion in 20 min with IAM (**111**) as catalyst, and 30% conversion in 50 min with NBS alone.

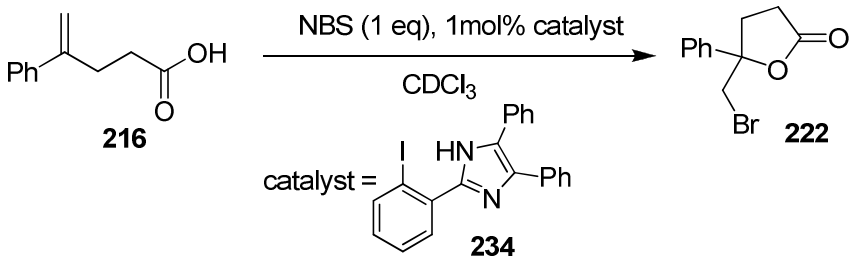

Scheme 92: screening imidazole 234 for catalytic activity

Thus, it is possible that decomposition of our brominated asymmetric catalyst, IBAM (**113**)-Br$^+$, to form an achiral bis-imidazole **235** (Scheme 93) may lead to a drop in both the observed ee and yield of our bromination reaction. This was obviously a pressing concern which was necessary to address.

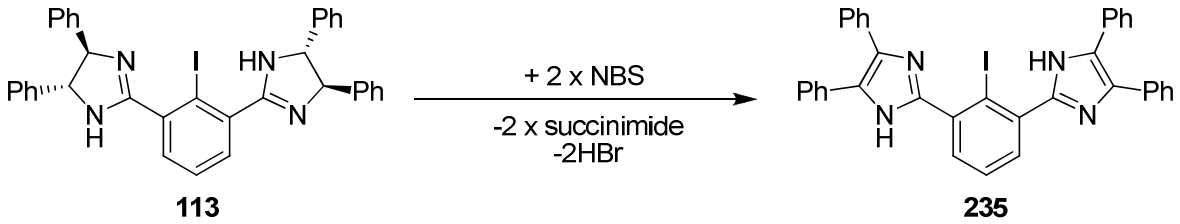

113 **235**

Scheme 93: possible route of IBAM (113) decomposition

However, we suspected that the decomposition to the imidazole occurs primarily as a result of the extended manipulation of the unstable IAM-Br^+ adduct (**112** or **224**) rather than being a process that would occur over the course of the bromination reaction itself. In order to test this theory, we conducted the low temperature bromination of lactone **114** with stoichiometric IBAM (**113**) and NBS (c.f. section *3.3.7.*). Analysis of the crude reaction mixture demonstrated the absence of any decomposition products and ^1H NMR analysis revealed the expected integration of 23:4 of the aromatic protons to the PhC*H* protons.

3.3.5. Proof of rapid Br^+ exchange between catalyst molecules

A portion of the isolated IAM-Br^+ (**112** or **224**) adduct was added to one equivalent of IAM (**111**) in deuterated chloroform (Scheme 94).

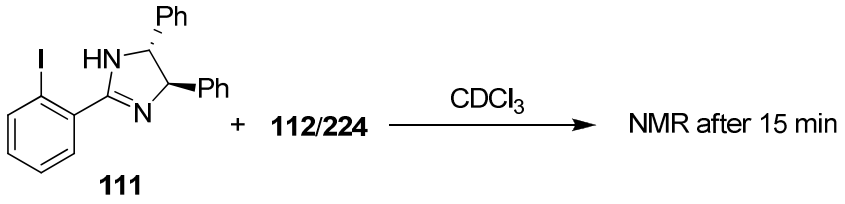

111

Scheme 94: investigation into Br^+ exchange between catalyst molecules

If exchange of Br^+ between the molecules occurs on a slower timescale than that of the ^1H NMR spectroscopy, then two distinct species should be observed in the spectra, i.e. brominated (**112** or **224**) and unbrominated IAM (**111**). However, if our theory of rapid exchange is accurate, a single species should be observable, with peaks at an intermediate chemical shift of those in the brominated and unbrominated species. As hypothesized, ^1H NMR analysis of the mixture after 15 minutes demonstrated the presence of a single component with averaged resonances between those of IAM (**111**) and IAM-Br^+ (**112** or **224**) This confirms our conception of the catalyst/Br^+ system as rapidly exchanging Br^+ between catalyst molecules.

*3.3.6. Stoichiometric additions of NBS to IBAM (**113**)*

Stoichiometric addition of NBS to IBAM (**113**) in deuterated chloroform at room temperature also resulted in the formation of a yellow/green solution from the colourless starting material. ^{1}H NMR analysis after 30 minutes demonstrated the complete conversion of NBS to succinimide. The broadening of the ^{1}H NMR spectrum of IBAM (**113**) on the addition of NBS is even more pronounced than in the *iso*-amarine (**116**) and IAM (**111**) systems. The PhC*H*N protons, which appear as a broad singlet in the spectrum of IBAM (**113**), broaden even further on addition of NBS (Figure 58 compared to Figure 59). In the IBAM-Br^{+} adduct they appear as a main peak with a pronounced shoulder, possibly indicating an inequivalence in the environments of these protons in the adduct.

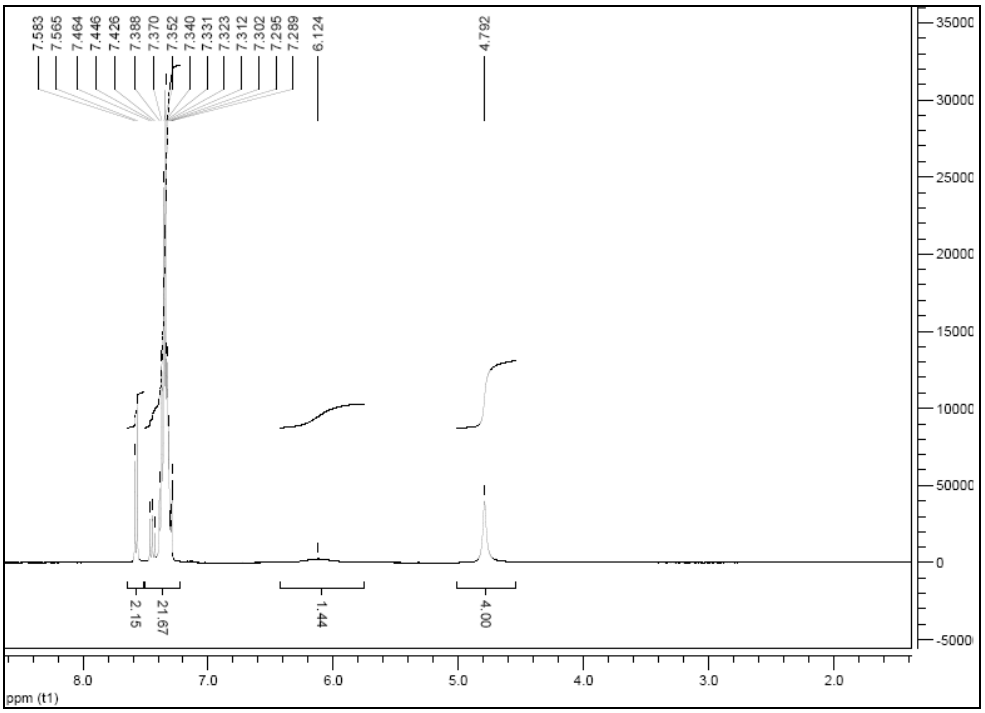

Figure 58: ^{1}H spectrum of IBAM (113) in $CDCl_3$

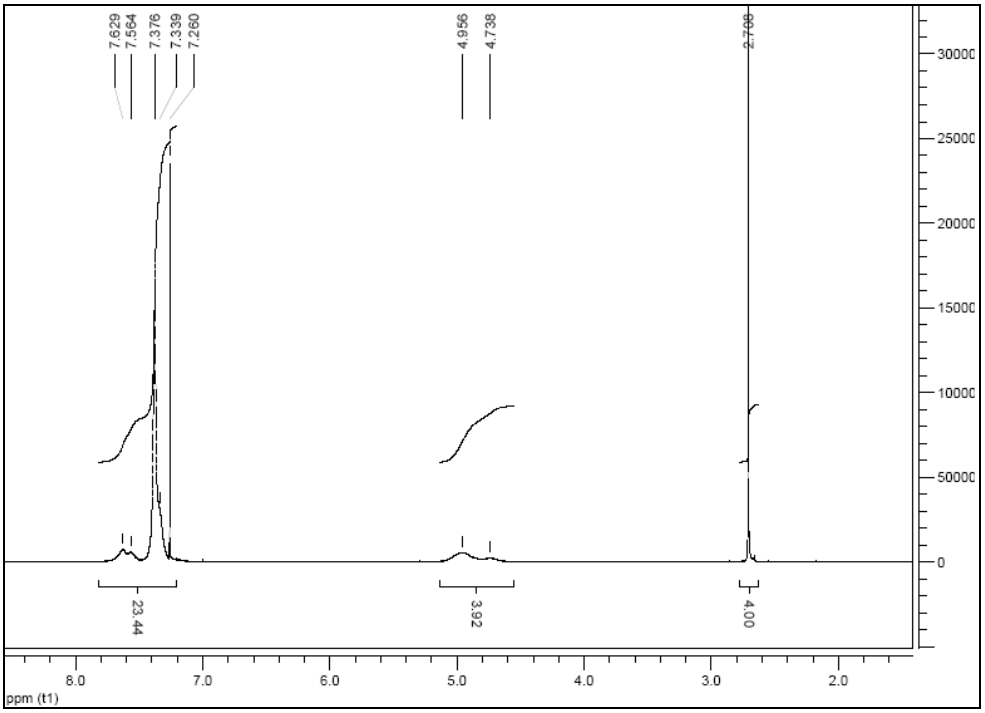

Figure 59: ^{1}H spectrum of IBAM (113) 30 mins after addition of NBS in $CDCl_3$

N.B. the peak at 2.71 ppm is due to the succinimide by-product.

The ^{13}C NMR spectrum (Figure 61 compared to Figure 60) again demonstrates the broadening of a number of the carbons (N-*C*(Ph)=N, *C*CHN, *C*-I) in a similar manner to *iso*-amarine (**116**) and IAM (**111**), suggesting a similarly dynamic system.

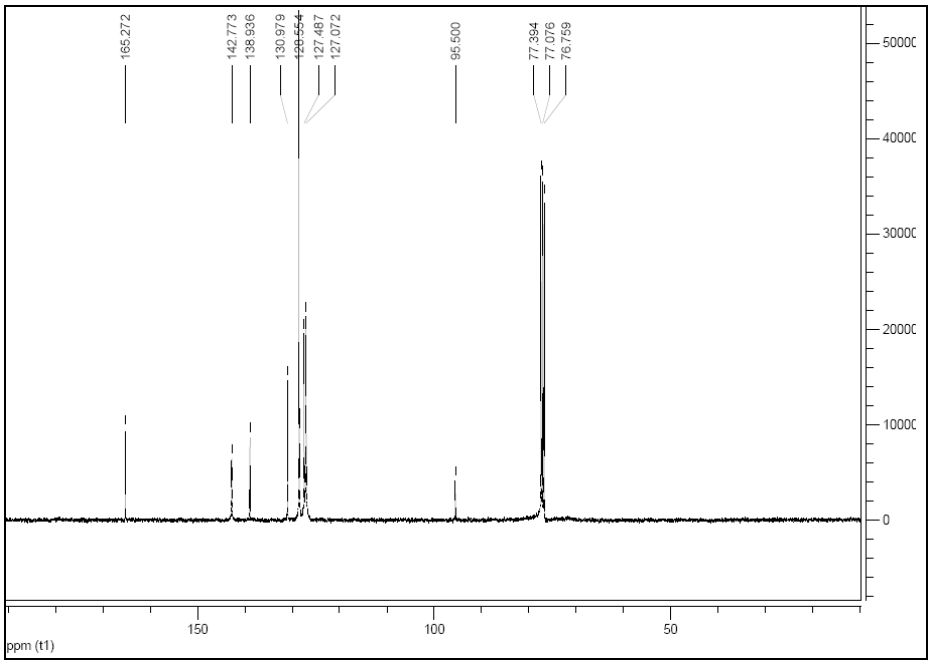

Figure 60: ^{13}C spectrum of IBAM (113) in $CDCl_3$

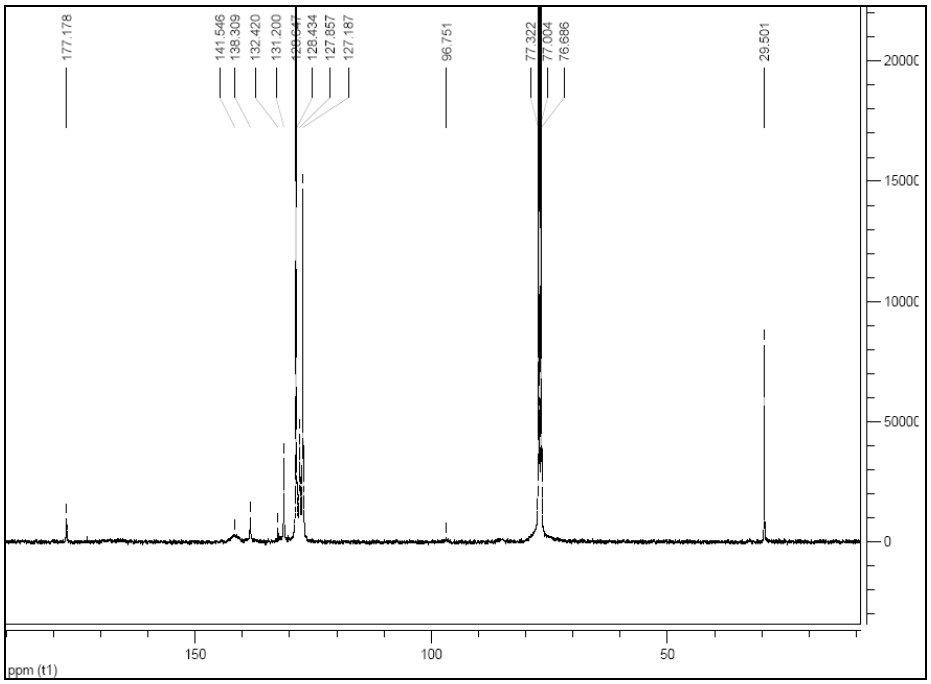

Figure 61: ^{13}C spectrum of IBAM (113) 30 mins after addition of NBS in $CDCl_3$

N.B. the peaks at 177.2 ppm and 29.5 ppm are due to the succinimide by-product.

Application of our procedure for the isolation of the catalyst-Br^+ adduct to the IBAM (**113**) catalyst proceeded with only limited success. The addition of NBS to IAM (**111**) and *iso*-amarine (**116**) had, in both cases, been easily monitored by TLC. Both IAM (**111**, R_f = 0.48, ethyl acetate) and *iso*-amarine (**116**, R_f = 0.34, 1:1 petrol:ethyl acetate) were consumed after 30 minutes and a new component was formed (R_f = 0.65, ethyl acetate, R_f = 0.68, 1:1 petrol:ethyl acetate, respectively) which were presumably the catalyst-Br^+ adducts. Addition of one equivalent of NBS to IBAM (**113**) and subsequent TLC analysis of the reaction mixture after 30 minutes also demonstrated the formation of a new component (R_f = 0.58, ethyl acetate). However, TLC also revealed incomplete consumption of the IBAM starting material (**113**, R_f = 0.15, ethyl acetate) after stirring at room temperature for two hours, despite full conversion of the NBS to succinimide. This observation can only be explained by the presence of the two amidine moieties in IBAM (**113**) facilitating the formation of an IBAM-2Br^+ adduct such as **236**, **237** or even **238**.

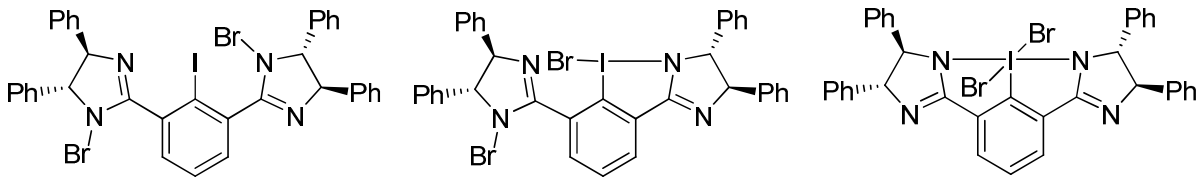

236 **237** **238**

Figure 62: di-brominated IBAM species

In such a system where only one equivalent of NBS has been added, there will necessarily be some unbrominated IBAM (**113**) in addition to mono- and di-brominated catalyst. However, the rapid exchange of Br^+ results in only one, time averaged, species being visible by ^1H and ^{13}C NMR. After precipitation of the succinimide and concentration of the filtrate, NMR analysis of the resulting adduct demonstrated a single major product which was analogous to the spectra in figures 59 and 61 with the exception of the succinimide by-product. This fascinating, but extremely frustrating system, failed to produce any crystals suitable for X-ray crystallography on attempted re-crystallisation from a range of solvents.

3.3.7. Stoichiometric Asymmetric Bromination

After our failure to isolate our IBAM-Br^+ adduct, we proceeded with investigations into the low temperature (-78 ºC) bromolactonisation of cyclopenten-2-yl acetic acid (**114**) with a pre-mixed solution of NBS and a stoichiometric amount of IBAM (**113**) (Scheme 95). The aims of

this experiment were; (i) to ensure our catalyst underwent the transfer of Br^+ in the absence of any decomposition of IBAM (**113**) to the imidazole (**235**) (ii) to ascertain if the stoichiometric reaction resulted in any improved enantioselectivity in the bromolactonisation of **114** from the observed 11% ee with a catalyst loading of 1 mol%.

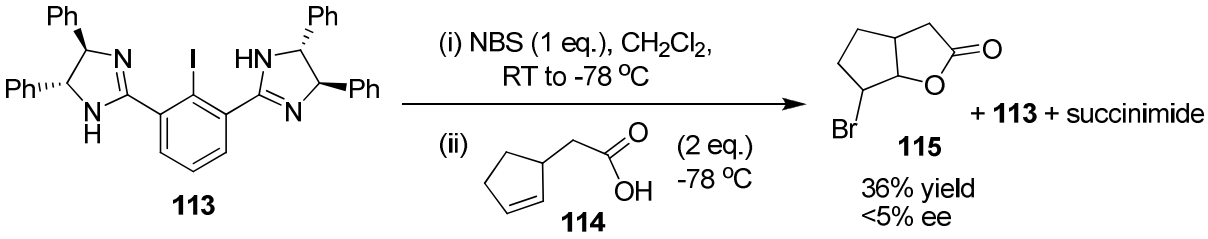

Scheme 95: use of a pre-mixed solution of 1:1 IBAM(113)/NBS as a stoichiometric brominating agent

Our first objective was achieved as detailed earlier (section *3.3.4.*). On analysis of the enantioexcess of the bromolactone product **115**, we were surprised to find an enantiomeric excess of <5%. We probed this unexpected phenomenon further, carrying out a standard asymmetric bromolactonisation reaction with the usual order of addition of reagents (i.e. NBS last, no pre-mixing of the catalyst and NBS) and a stoichiometric amount of IBAM (**113**). This also resulted in the production of racemic bromolactone. Evidently the enantioselectivity of the reaction is dependent on the stoichiometry of the catalyst.

3.4. Investigations into the relationship between catalyst loading and enantioselectivity

Consequently, we screened a range of catalyst loadings in our asymmetric bromination reaction (Table 8) and pleasingly, by raising catalyst loading to 5 mol%, we were able to achieve a small increase in enantioselectivity, isolating bromolactone **115** in 17% ee (entry 5). Intriguingly, the results demonstrate a non-linear relationship between catalyst loading and enantioexcess; a result which implies that there are at least two factors affecting enantioselectivity in our system.

Table 8: Screening the effects of catalyst loading on IBAM (113) catalysis

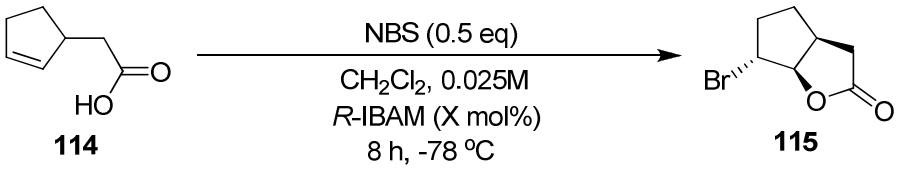

114 **115**

Entry	Catalyst loading (X mol% based on substrate)	Yield (%)	enantioexcess (%)
1	0.1 mol%	8%	< 5%
2	1 mol%	27%	11%
3	2.5 mol%	56%	13%
4[a]	2.5 mol%	45%	14%
5	5 mol%	53%	17%
6[a]	5 mol%	48%	16%
7	10 mol%	27%	9%
8	25 mol%	26%	<5%
9	50 mol%	41%	<5%
10[a]	50 mol%	43%	<5%

a – repeat reaction

We have already proposed and validated the idea that there are at least two possible catalytic intermediates; one containing an I(III)-Br bond (**120**), which delivers bromine asymmetrically to the alkene substrate, and one containing an N-Br bond (**119**), which delivers bromine in a non-asymmetric manner (Scheme 96). It is postulated that the N-Br species **119** is initially formed when bromine is transferred from NBS to IBAM (**113**) and that this subsequently undergoes an oxidative insertion reaction with the iodine to form the hypervalent I(III)-Br species **120**. The transfer of Br^+ from one catalyst molecule to another would also proceed *via* a similar mechanism with the initial formation of N-Br species **119**. The greater the concentration of IBAM (**113**), the greater the likelihood of a second molecule of IBAM (**113**) picking up Br^+ from the asymmetric hypervalent species and re-forming the non-asymmetric N-Br species. We have already demonstrated that, in a stoichiometric system at least, the transfer of Br^+ between catalyst molecules is extremely facile. When this re-capturing mechanism becomes dominant, it would be expected that the enantioexcess of

the product would decrease with increased catalyst loading due to a higher proportion of Br^+ delivered to the substrate *via* the N-Br intermediate **119**. This enantioselectivity peaks at a point where I(III)-Br to N-Br transfer is reduced, but before the catalyst loading is lowered to the point where the direct NBS bromination background reaction begins to compete with the asymmetric catalysis pathway.

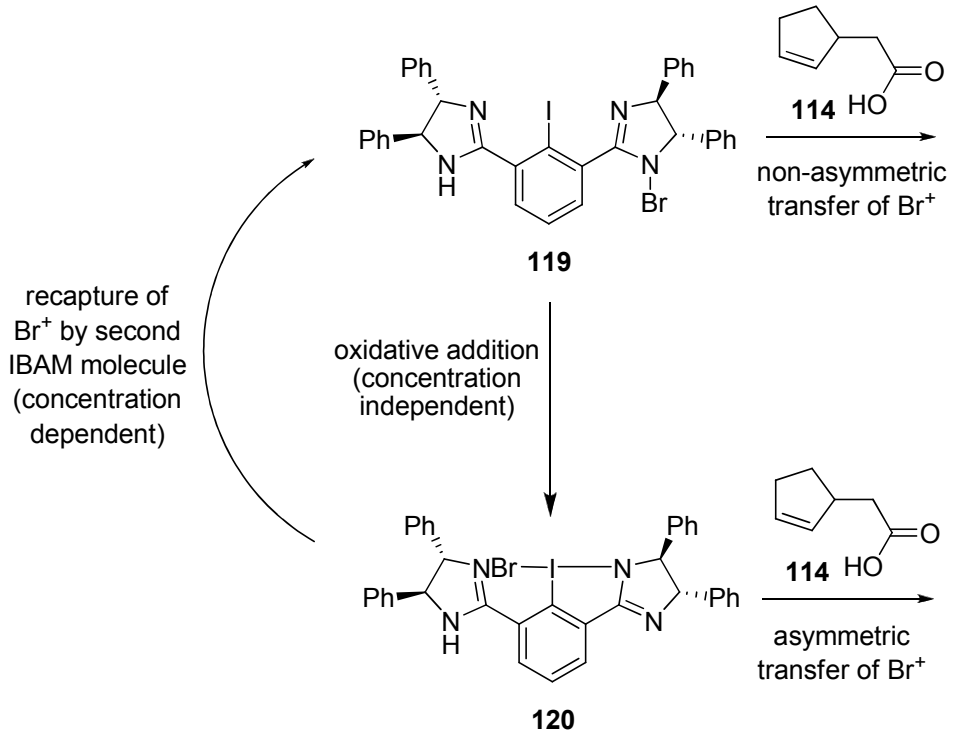

Scheme 96: I(III)-Br and N-Br IBAM intermediates and interchange between them

In order to test this hypothesis, we synthesized and screened the iodine-free analogue of IBAM (**113**), 1,3-di-(-4,5-diphenyl-4,5-dihydro-1*H*-imidazol-2-yl)benzene, or BAM (**121**, Scheme 97).

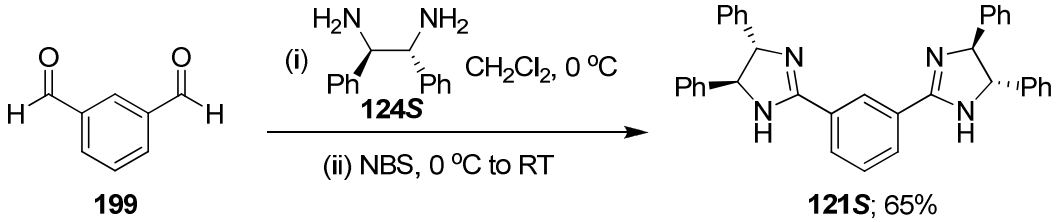

Scheme 97: synthesis of BAM (121)

As would be expected if our theory was accurate, BAM (**121**) efficiently catalysed the low temperature asymmetric bromination of **114**, but produced completely racemic bromolactone product (Scheme 98).

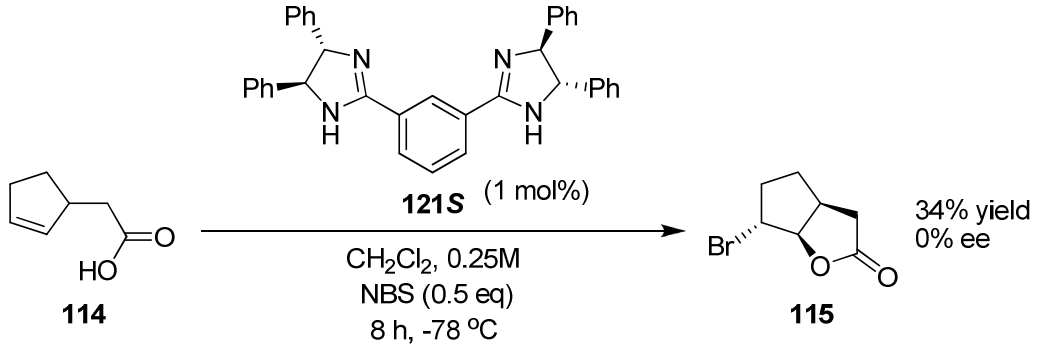

Scheme 98: BAM (121)-catalysed bromolactonisation

Thus, it is confirmed that there is a significant non-asymmetric bromination pathway competing with our asymmetric hypervalent iodine mediated bromination. It appears that the importance of this competition may be concentration dependent.

3.5. Synthesis of IBAM (113) derivatives and analogues

It was hypothesized that by modifying the catalyst structure, it may be possible to promote the asymmetric delivery of bromine *via* iodine over the non-enantioselective delivery *via* nitrogen. It was proposed that this could be achieved by placing an electron-withdrawing acyl group on one of the amidine nitrogens (**239**, Figure 63).

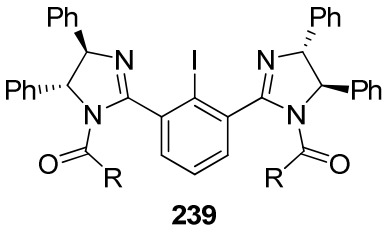

239

Figure 63: bis-acylated IBAM

This should decrease the nucleophilicity of the amidine moiety and thus reduce its capacity for nucleophilic attack on the catalyst-Br^+ hypervalent intermediate **120**. Additionally it is possible that acylation may promote the formation of a hypervalent bond to iodine due to its stabilization of the δ- placed on the nitrogen in the 4-electron, 3-centre bond (Figure 64).

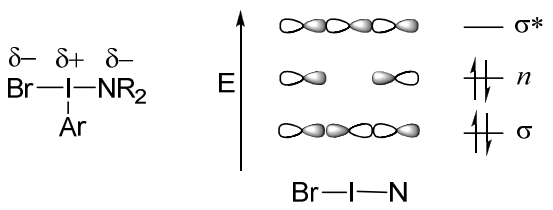

Figure 64: molecular orbitals in 4-electron, 3-centre bond in hypervalent iodine

However, such modifications raise the question of the role of a transferable proton in the apical moiety. Although ultimately a proton is lost from the substrate to replace bromine in NBS and to form succinimide, the original exchange of bromine from NBS to a catalyst lacking an acidic proton would leave a cationic catalyst species (**240**) and a succinimide anion (**88**) (Scheme 99). It is possible that "Br^{+}" transfer would not occur in these circumstances, leading to an inactive catalyst. If such bromine exchange successfully occurs in our system, rapid proton transfer from the carboxylic acid substrate to the succinimide anion (**88**) is certain to occur, leading to more stable species. However, with different substrates that do not contain acidic protons, it may be necessary to add an additional proton source to facilitate a successful catalytic cycle.

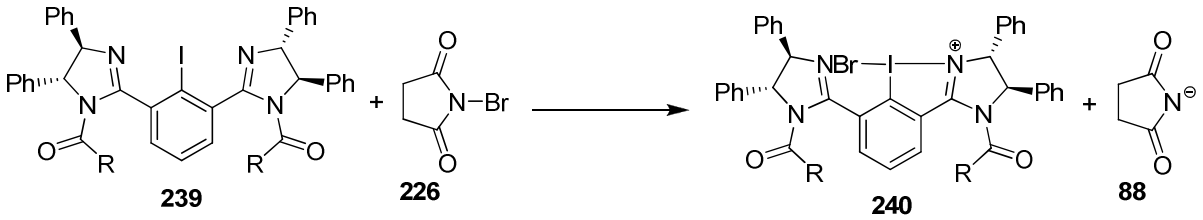

Scheme 99: transferal of Br^{+} from NBS to acylated IBAM

*3.5.1. Test of concept; benzoylated IAM (**241**) and* iso*-amarine (**169**)*

As an initial investigation into the usefulness of such proposed modifications, we synthesized benzoylated *iso*-amarine (**169**) and IAM (**241**). The racemic benzoylated *iso*-amarine (**169**) was formed as detailed earlier (c.f. Section *2.2.3.*) and benzoylated IAM (**241**) was formed in an analogous manner *via* benzoylation of IAM (**111**) with benzoyl chloride (Scheme 100).

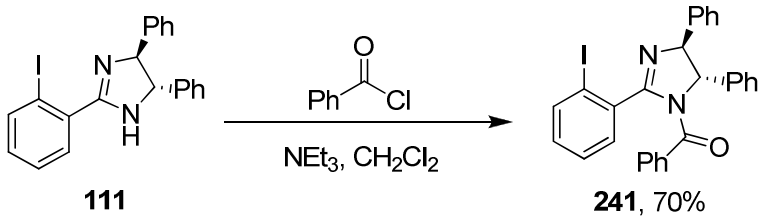

Scheme 100: benzoylation of IAM (111)

Upon screening of the catalysts (Table 9), benzoylated IAM (**241**) demonstrated no observable loss of activity relative to the unbenzoylated catalyst, IAM (**111**), whilst benzoylated *iso*-amarine (**169**) showed a considerable decrease in activity compared to its unbenzoylated analogue, *iso*-amarine (**116**). This suggests that bromine delivery *via* the amidine nitrogen is diminished with little or no negative effect on bromine delivery *via* iodine.

Table 9: catalytic activity of benzoylated *iso*-amarine (169) and IAM (241)

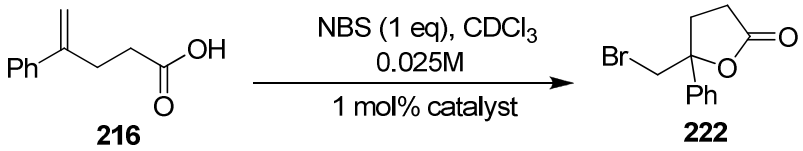

Catalyst	% conversion of substrate		
	15 min	50 min	3 h
None present (control)	____	30%	60%
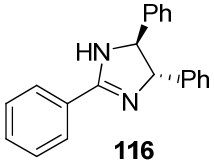 **116**	100%	____	____
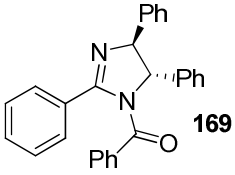 **169**	55%	100%	____
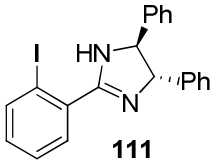 **111**	100%	____	____
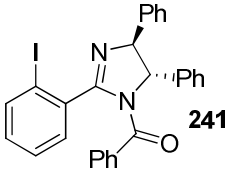 **241**	100%	____	____

Encouraged by these results, we embarked on the synthesis of a range of acylated IBAM (**113**) derivatives.

*3.5.2. Synthesis of acylated IBAM (**113**) derivatives*

We synthesised a range of acylated derivatives for screening as catalysts in our asymmetric bromination reaction (Scheme 101).

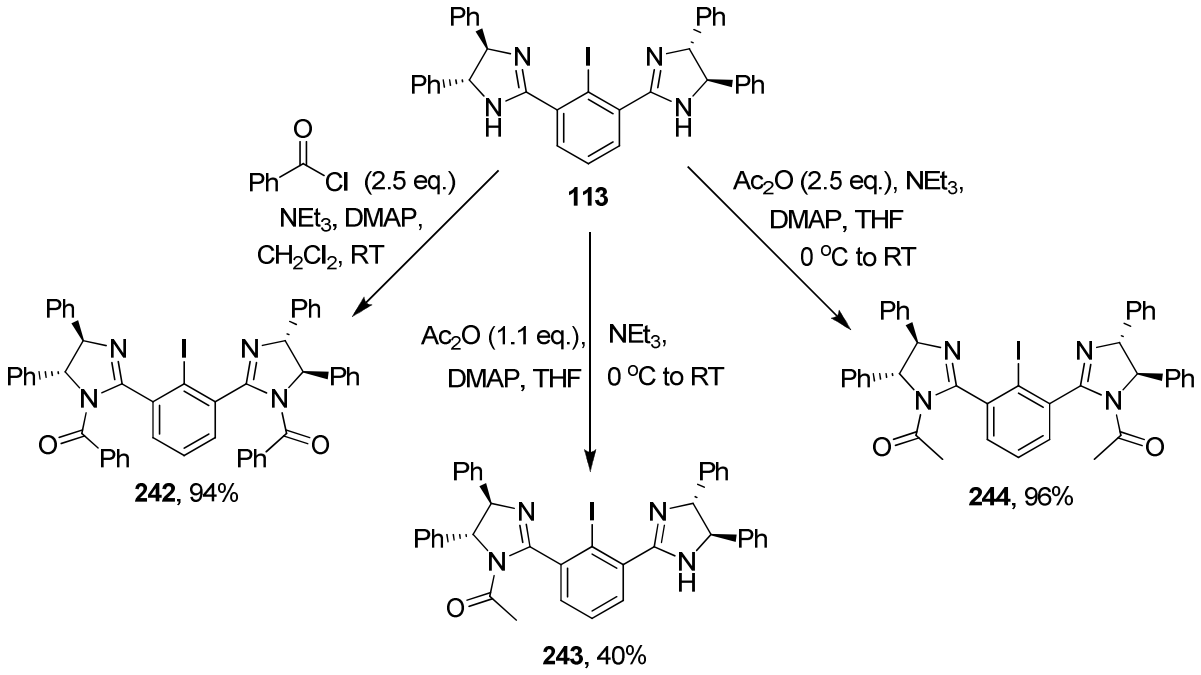

Scheme 101: synthesis of acetylated and benzoylated IBAM derivatives

Di-acetyl IBAM (**244**) and mono-acetyl IBAM (**243**) were synthesized by the addition of 2.5 or 1.1 equivalents of acetic anhydride to IBAM (**113**) in the presence of triethylamine and catalytic DMAP. Di-benzoyl IBAM (**242**) was formed under similar conditions using 2.5 equivalents of benzoyl chloride.

We also attempted the acylation of both *S*- and *R*-IBAM (**113*S*** and **113*R***) with (*R*)-acetyl mandelic acid (**173**) to form the (*S*,*S*,*R*) and (*R*,*R*,*R*) diastereomeric pair of catalysts, **245** and **246**. 2,6-Di-[(4*S*,5*S*)-1-{(*R*)-α-acetoxyphenyl acetyl}-4,5-diphenyl-4,5-dihydroimidazol-2-yl]iodobenzene (**245**) was synthesised by the DCC mediated coupling of (*R*)-acetyl mandelic acid to *S*-IBAM (**113*S***) (Scheme 102).

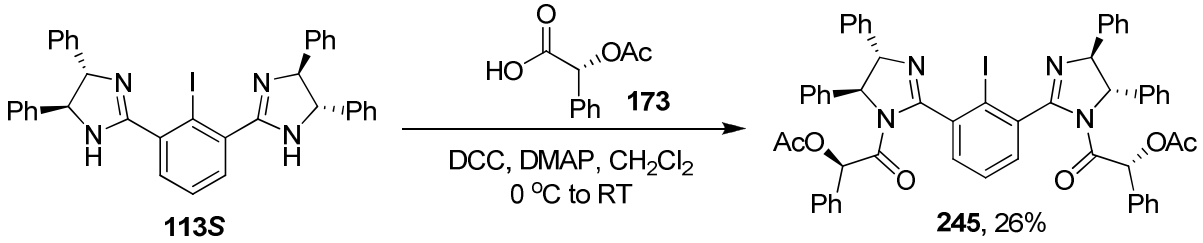

Scheme 102: synthesis of 2,6-di-[(4*S*,5*S*)-1-{(*R*)-α-acetoxyphenyl acetyl}-4,5-diphenyl-4,5-dihydroimidazol-2-yl]iodobenzene (245)

X-ray crystallography of the product confirmed the structure and diastereomeric purity of the product **245**.

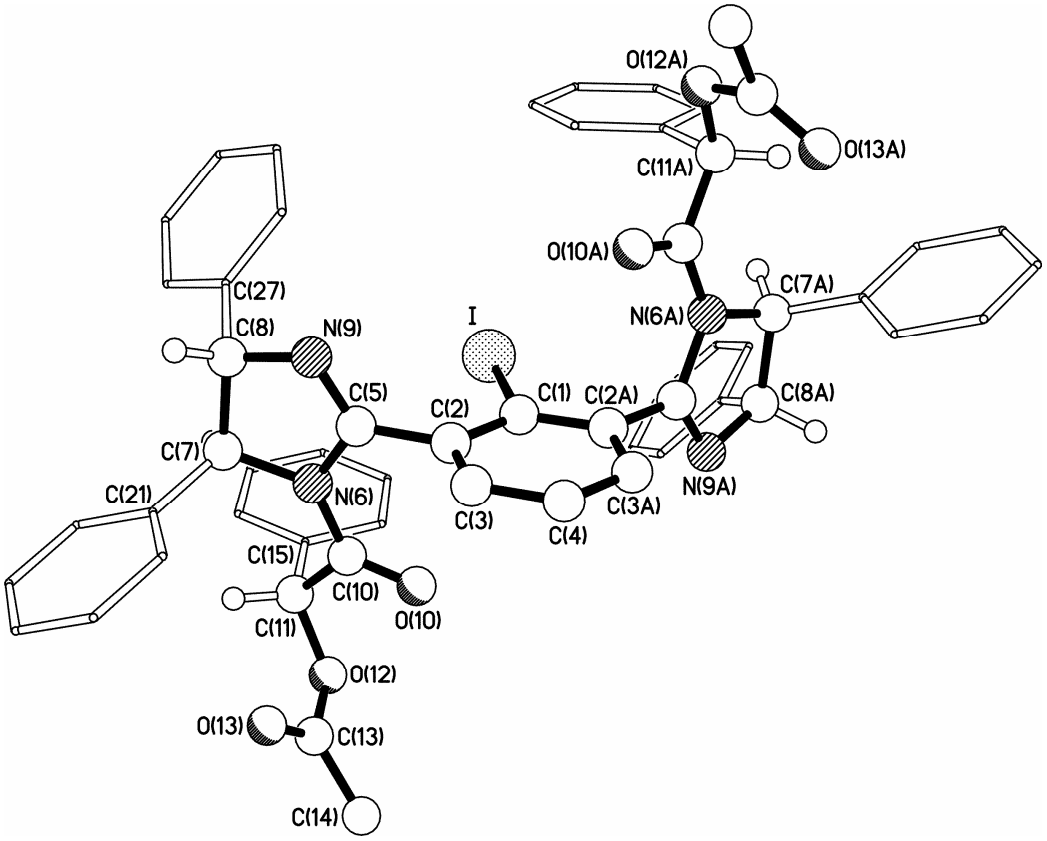

Figure 65: X-ray crystal structure of 2,6-di-[(4*S*,5*S*)-1-{(*R*)-α-acetoxyphenyl acetyl}-4,5-diphenyl-4,5-dihydroimidazol-2-yl]iodobenzene (245)

It was apparent to us on viewing the crystal structure of **245** that it may be not be a good candidate for an asymmetric bromination catalyst. If the environment of the iodine atom is considered, it is apparent that four of the phenyl rings (with quarternary carbons C(27), C(15), C(27A) and C(15A)) sit in an almost symmetrical arrangement around the iodine. As

such, a bromine atom hypervalently bonded to the iodine would, rather than lying in an asymmetric pocket, experience relatively uniform steric interactions. Thus, an approaching alkene would not be expected to exhibit a preferential approach of one of its two prochiral faces and the catalyst would not be expected to deliver bromine with any significant enantioselectivity.

We attempted to synthesise 2,6-di-[(4*R*,5*R*)-1-{(*R*)-α-acetoxyphenyl acetyl}-4,5-diphenyl-4,5-dihydroimidazol-2-yl]iodobenzene (**246**, Figure 66) *via* a similar method.

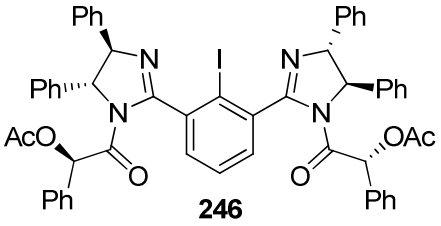

246

Figure 66: 2,6-di-[(4*R*,5*R*)-1-{(*R*)-α-acetoxyphenyl acetyl}-4,5-diphenyl-4,5-dihydroimidazol-2-yl]iodobenzene (246)

However, although the di-mandelyl derivative **246** was apparent in the crude reaction mixture, it proved extremely susceptible to decomposition on both silica and, to a lesser extent, on simply standing in solution. As a result of this instability, compounded by the solid's distinct lack of crystallinity, all attempts to purify **246** yielded mixtures of the desired catalyst and apparent decomposition products.

The mono-mandelyl IBAM derivative, **247**, proved considerably more stable. Thus we were able to isolate 2-[(4*R*,5*R*)-1-{(*R*)-α-acetoxyphenyl acetyl}-4,5-diphenyl-4,5-dihydroimidazol-2-yl]-6-[(4*R*,5*R*)-4,5-diphenyl-4,5-dihydro-1*H*-imidazol-2-yl]-iodobenzene (**247**, Scheme 103) from the reaction mixture *via* flash column chromatography.

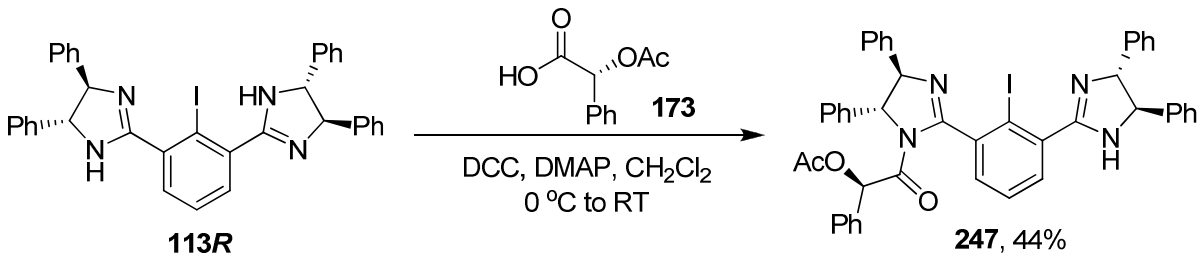

113*R*

247, 44%

Scheme 103: synthesis of 2-[(4*R*,5*R*)-1-{(*R*)-α-acetoxyphenyl acetyl}-4,5-diphenyl-4,5-dihydroimidazol-2-yl]-6-[(4*R*,5*R*)-4,5-diphenyl-4,5-dihydro-1*H*-imidazol-2-yl]-iodobenzene (247)

*3.5.3. Synthesis of alkylated IBAM (**113**) derivatives*

We additionally desired to investigate the catalytic behaviour of certain alkylated IBAM (**113**) derivatives. The anticipated undiminished nucleophilicity of the amidine moiety, combined with the absence of a proton available to protonate the succinimide anion, made such derivatives interesting to us in respect to both activity and enantioselectivity. We chose to include a carbonyl group at different positions down the alkyl chains used to functionalise IBAM (**113**). It was proposed that the hypervalent iodine may be stabilised by the donation of lone pairs from the carbonyl oxygens, thus favouring the formation of a I(III)-Br catalytic intermediate. Such stabilising interactions have been observed in the crystal structure of the bromoiodinane **105**, which demonstrated the presence of dimer pairs, linked by two I·····O interactions (Figure 67).[64]

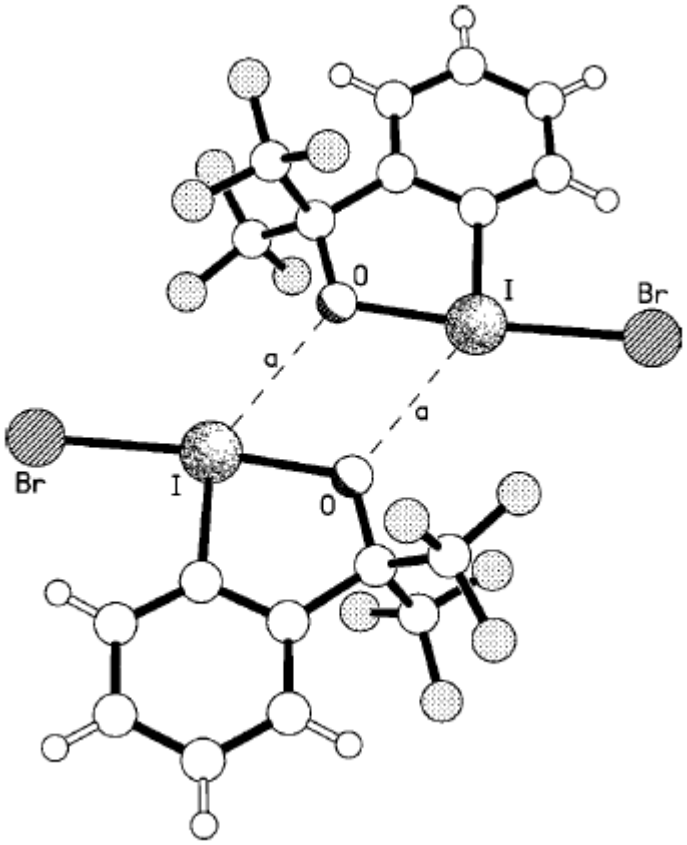

Figure 67: the linking pairs of I·····O interactions of adjacent centrosymmetrically related molecules into dimer pairs; the I·····O separation is c.a. 3.03 Å

We synthesised the di-alkyl derivative **249** *via* reaction of IBAM (**113**) with 2.2 equivalents of the corresponding α-bromoketone (**248**) in the presence of triethylamine (Scheme 104).

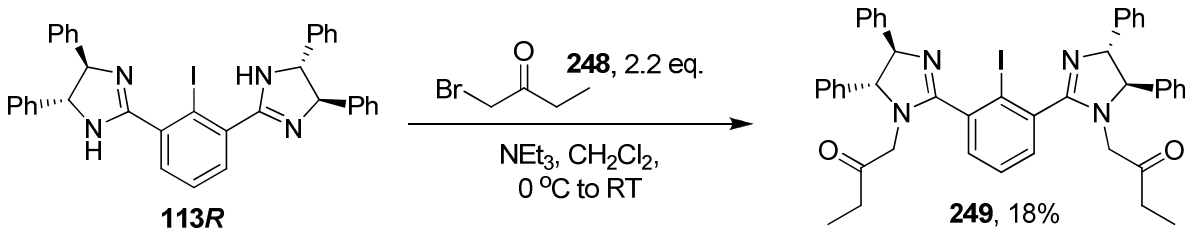

Scheme 104: synthesis of 2,6-Di-[(4*R*,5*R*)-1-(2-oxo-butan-1-yl)-4,5-diphenyl-4,5-dihydroimidazol-2-yl]iodobenzene (249)

It was noted that the reaction yielded a complex mixture of products, only one of which was the desired di-alkylated product **249**. Two of the main components of the product mixture appeared to be unreacted and mono-alkylated IBAM. Thus, when we repeated the alkylation reaction, we added 4 equivalents of the 1-bromo-2-butanone (**248**) with the goal of driving the reaction to completion. However, rather than affording the desired di-alkylated product, **249**, the major component was now the tetra-alkylated derivative, **250** (Scheme 105), isolated from the reaction mixture in 29% yield.

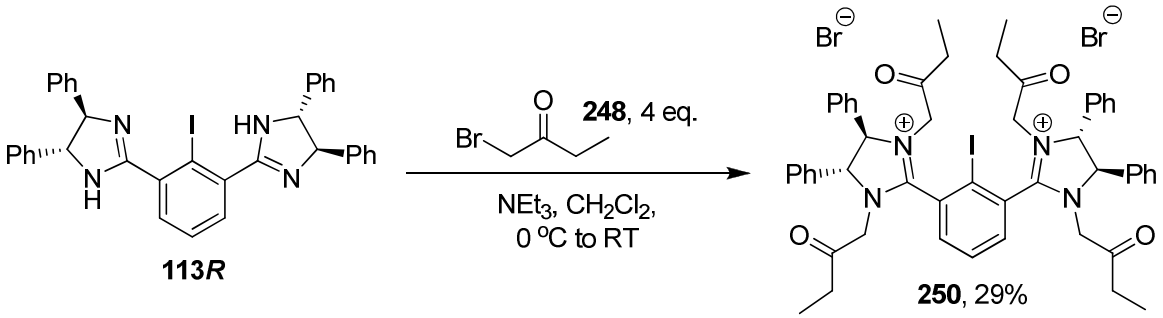

Scheme 105: formation of 2,6-Di-[(4*R*,5*R*)-1,3-di-(2-oxo-butan-1-yl)-4,5-diphenyl-4,5-dihydroimidazolium-2-yl]iodobenzene dibromide (250)

It can be concluded that, unlike the di-*N*-acylated IBAM derivatives (**242**, **244** and **245**), the reactivity of the di-*N*-alkylated IBAM **249** is of comparable or greater reactivity than the unalkylated IBAM (**113**) starting material. Presumably this difference in reactivity originates in the mesomeric electron withdrawing effect of the acyl groups on the amidine moieties (thus reducing their capacity to act as nucleophiles) compared to the inductively electron donating alkyl groups. Thus, the alkylation reaction proceeds to yield a range of mono-, di-, tri- and tetra-substituted products on addition of 2.2 equivalents of α-bromoketone **248** to IBAM (**113**). This is in contrast to the analogous acylation where the reaction halts at, and thus can be driven to, the di-acylated product. However, whilst poor yielding, the reaction afforded us adequate di-alkylated IBAM **249** for our screening purposes.

Finally, the IBAM derivative, **252** (Scheme 106), was synthesised by heating IBAM (**113**) in dioxane with 1-buten-one (**251**) and sodium acetate.

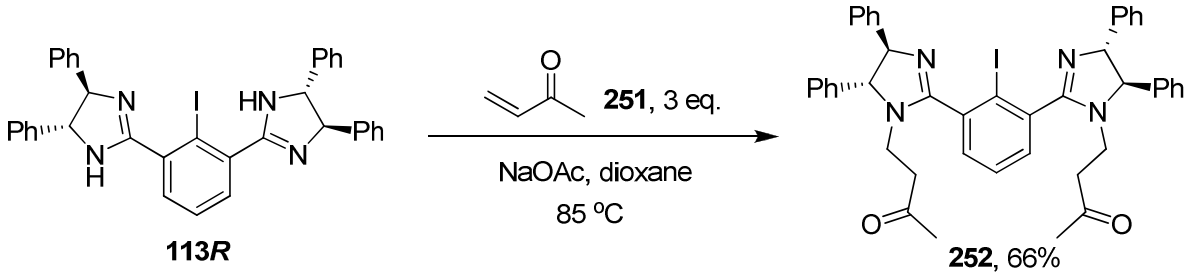

Scheme 106: synthesis of 2,6-di-[(4*R*,5*R*)-1-(3-oxo-butan-1-yl)-4,5-diphenyl-4,5-dihydroimidazol-2-yl]iodobenzene (252)

In this case, the reaction progressed no further than the di-alkylated product, **252**, presumably due to the reversible nature of the attack of the second amidine nitrogen on the 1,3-unsaturated ketone (Scheme 107).

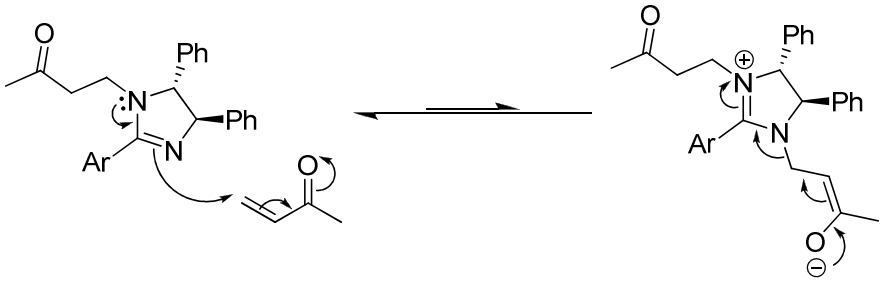

Scheme 107: reversible second alkylation of the amidine moiety

3.5.4. Synthesis of a bis-oxazoline analogue of IBAM

It was proposed that a bis-oxazoline analogue of IBAM (**253**, Figure 68) would be an attractive candidate for screening as an asymmetric electrophilic bromination catalyst. It was argued that the decreased nucleophilicity of the amide moiety compared to the amidine moiety, along with the positively charged intermediate that is necessarily formed on bromination, may again favour the hypervalent iodine route for bromine delivery over the delivery of bromine *via* one of the heteroatoms.

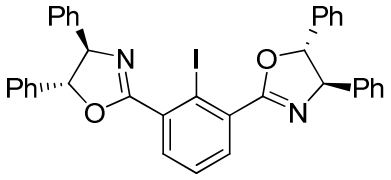

253

Figure 68: bis-oxazoline analogue of IBAM (253)

However, the identity of the bis-oxazoline analogue was somewhat limited by the chiral aminoalcohols that were available to us. As previously reported (section *3.1.3.*), attempts to form a bis-oxazoline **208** from the bis-aldehyde **199** utilizing (1*R*,2*S*)-2-amino-1,2-diphenylethanol as our chiral aminoalcohol to form the oxazoline moiety were unsuccessful. Thus, we turned our attention to alternative methods of oxazoline formation and successfully synthesised bis-oxazoline catalyst **257**, using (*S*)-phenyl alaninol **254** to form the chiral oxazolines. Diacyl chloride **187** was coupled to (*S*)-phenyl alaninol **254** to form the bis-amide **255** (Scheme 108). The alcohol moiety of amide **255** was converted to a good leaving group by formation of the mesylate with mesyl chloride. Ring closure was then achieved by deprotonation of the bis-amide **256** with sodium hydroxide and its subsequent nucleophilic substitution of the mesylate group to yield the oxazoline product, **257**.

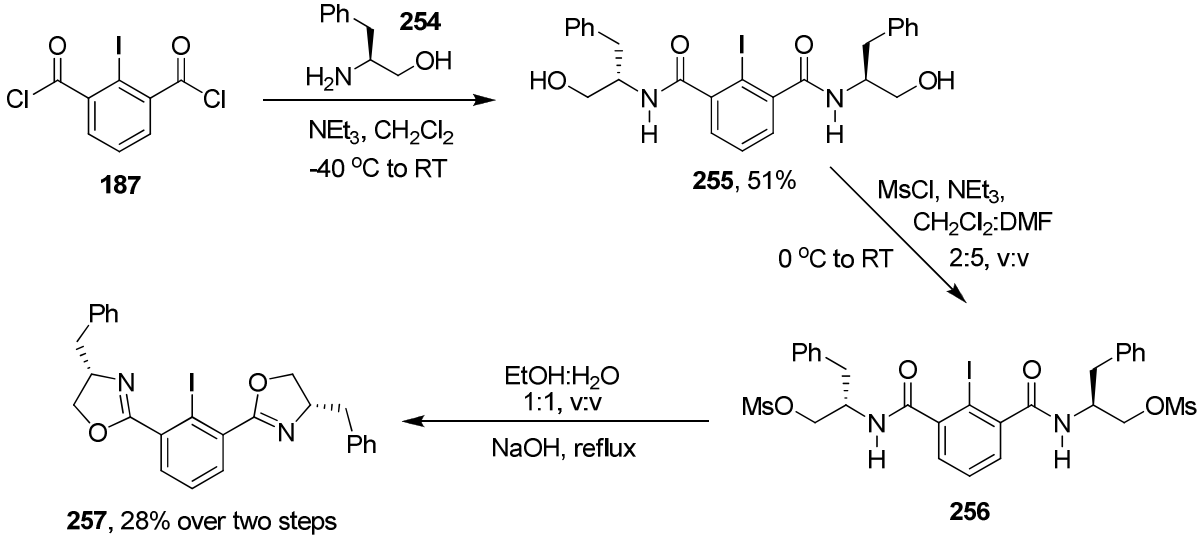

Scheme 108: synthesis of 2,6-di[(4'*R*)-4'-benzyloxazolin-2'-yl]iodobenzene (257)

*3.5.5. Screening of the IBAM (**113**) derivatives/analogues*

Following the synthesis of a range of IBAM (**113**) analogues and derivatives, we conducted a screen of their capacity to act as asymmetric bromination catalysts (Table 10). Our previously tested substrates, 2-cyclopenten-1-ylacetic acid (**114**) and (*S*)- and (*R*)-2-allyloxypropionic acid (**217*R*** and **217*S***) were utilized for our screening purposes.

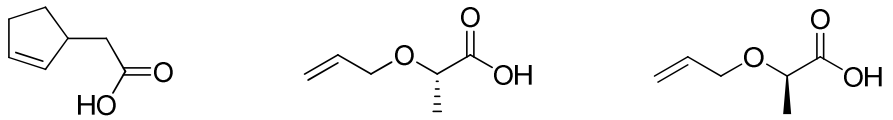

114 **217*S*** **217*R***

Figure 69: catalytic asymmetric bromolactonisation substrates

Table 10: screening of IBAM (113) analogues and derivatives

Entry	Catalyst (loading)	Substrate	Solvent	Concentration	Temperature	Time	Yield	ee or de
1	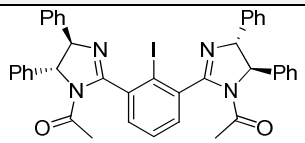 **244** (5 mol%)	**114**	CH_2Cl_2	0.25 M	-78 ºC	8 h	34%	<5% ee
2	**244** (5 mol%)	**217*S***	CH_2Cl_2	0.25 M	-78 ºC	24 h	9%	17% de
3	**244 (**5 mol%)	**217*R***	CH_2Cl_2	0.25 M	-78 ºC	24 h	-	28% de
4	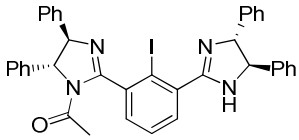 **243** (1 mol%)	**114**	CH_2Cl_2	0.025 M	-78 ºC	8 h	37%	<5% ee
5	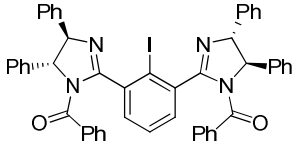 **242** (1 mol%)	**114**	CH_2Cl_2	0.25 M	-78 ºC	8 h	9%	7% ee
6	**242** (1 mol%)	**114**	acetone	0.25 M	-78 ºC	8 h	22%	<5% ee
7	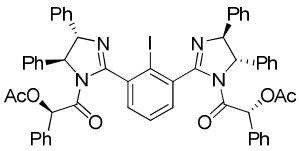 **245** (1 mol%)	**114**	CH_2Cl_2	0.25 M	-78 ºC	8 h	14%	<5% ee
8	**245** (5 mol%)	**114**	CH_2Cl_2	0.25 M	-78 ºC	8 h	34%	5% ee
9	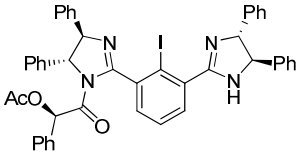 **247** (1 mol%)	**114**	CH_2Cl_2	0.025 M	-78 ºC	8 h	19%	<5% ee

Entry	Catalyst (loading)	Substrate	Solvent	Concentration	Temperature	Time	Yield	ee or de
10	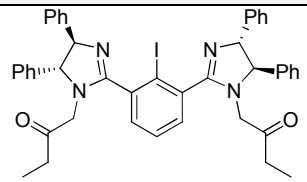 **249** (1 mol%)	**114**	CH_2Cl_2	0.25 M	-78 ºC	8 h	61%	<5% ee
11	**249** (5 mol%)	**217*S***	CH_2Cl_2	0.25 M	-78 ºC	8 h	9%	35% de
12	**249** (5 mol%)	**217*R***	CH_2Cl_2	0.25 M	-78 ºC	8 h	9%	42% de
13	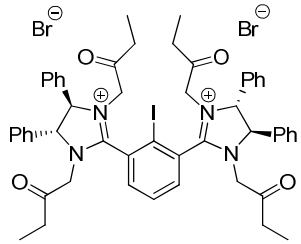 **250** (1 mol%)	**114**	CH_2Cl_2	0.25 M	-78 ºC	8 h	48%	<5% ee
14	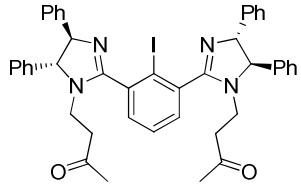 **252** (1 mol%)	**114**	CH_2Cl_2	0.025 M	-78 ºC	8 h	49%	<5% ee
15	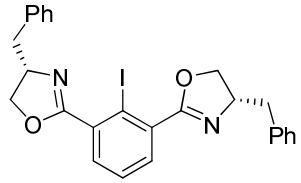 **257** (1 mol%)	**114**	CH_2Cl_2	0.25 M	-78 ºC	8 h	3%	<5% ee
16	**257** (1 mol%)	**114**	CH_2Cl_2	0.25 M	-78 ºC to RT	8 h	28%	<5% ee
17	**257** (1 mol%)	**114**	$CHCl_3$	0.25 M	-45 ºC	8 h	10%	11% ee

It is evident from our results that reducing the nucleophilicity of the groups *ortho* to iodine, *via* either acylation (entries 1-9) or substitution of an oxazoline moiety for the amidine (entries 15-17), results in a considerably diminished catalytic activity (for example, bis-oxazoline **257** compared to IBAM (**113**) catalysis under identical conditions affords 3% of

bromolactone **115** compared to 55%). Mono-acylation (entries 4 and 9) results in a similar reduction in rate, but to a lesser extent than di-acylation.

The alkylated IBAM derivatives (**249** and **252**, entries 10-12 and 14) on the other hand demonstrated no such loss of activity, both producing similar or greater yields of lactone **115** to those obtained with IBAM (**113**) under analogous conditions. Thus, it would seem that catalyst activity, at least in a system acting on a carboxylic acid substrate, is unaffected by the absence of an acidic proton on the amidine. Catalytic activity is, however, closely linked to the nucleophilicity of the groups *ortho* to the iodine.

There is also evidence of a steric effect on rate; as the size of the *N*-acyl or *N*-alkyl group increases, the rate of the catalytic bromination slows (c.f. mono-acetate **243**, entry 4, compared to mono-mandelate **247**, entry 9).

A suprising result was the observed high catalytic activity of the tetrasubstituted IBAM **250** (entry 13). This species has no lone pairs available on the amidine moieties for the attack on the electrophilic bromine of NBS and the subsequent formation of a N-Br or N-I(III)-Br bond. Thus, in this case, the catalysis is most probably occurring *via* attack of the bromine counter ion on NBS to form molecular bromine. This will then go on to rapidly brominate the alkene substrate to form the bromonium ion intermediate and regenerate bromide.

However, despite the wide range of catalysts screened, encompassing various strategies to stabilise the I(III)-Br over the N-Br intermediate, we failed to identify a candidate which facilitated an increase in the enantioselectivity of the reaction.

3.5.6. Stoichiometric additions of NBS to N-*functionalised catalysts*

Finally a number of stoichiometric addiitions of NBS to the *N*-functionalised catalysts were undertaken and the conversion of NBS to succinimide was monitored (Table 11).

Table 11: stoichiometric additions of NBS to *N*-functionalised catalysts[a]

Entry	Catalyst	Time	Conversion of NBS to Succinimide
1	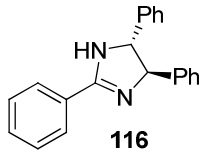 **116**	15 min	100%
2	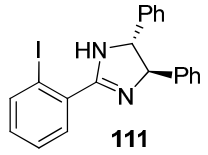 **111**	15 min	100%
3	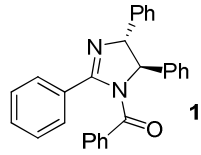 **169**	15 min	<1%
4	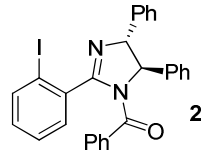 **241**	15 min	<1%
5	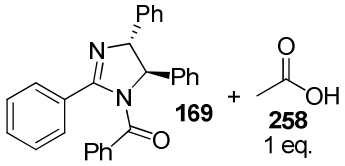 **169** + **258** 1 eq.	1 h 15 min	10%
6	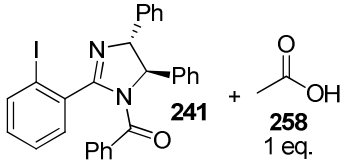 **241** + **258** 1 eq.	2 h	<1%
7	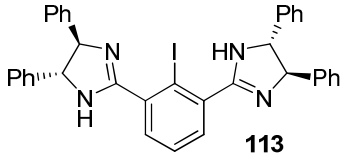 **113**	15 min	100%
8	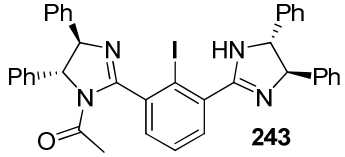 **243**	1 h 20 min	82%

Entry	Catalyst	Time	Conversion of NBS to Succinimide
9	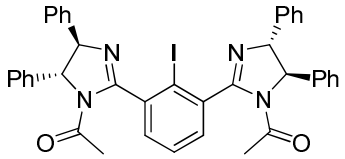 **244**	1 h 20 min	21%
10	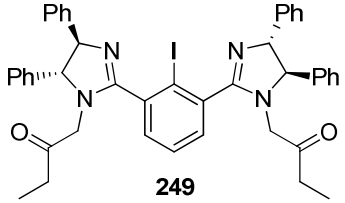 **249**	1 h 15 min	28%
11	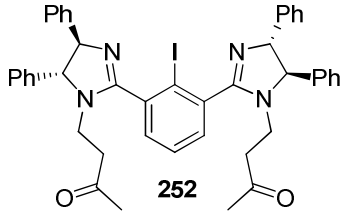 **252**	1 h 15 min	9%

a – all reactions conducted in deuterated chloroform stored over potassium carbonate and monitored by ^{1}H NMR analysis

Other than generally broadened resonances, no significant changes were initially observed in the NMR of the catalyst species. Extended stirring with NBS (20 h) resulted in the decomposition of the *N*-functionalised IBAM catalysts (**243**, **244**, **249** and **252**). The results of the stoichiometric additions demonstrated a marked difference between catalysts with an acidic proton (entries 1, 2, 7 and 8) and those without (entries 3, 4, 9-11). Although this difference was initially ascribed to the lack of an available proton to protonate the succinimide anion, addition of one equivalent of acetic acid did not facilitate improved turnover of NBS to succinimide. Therefore, the failure to form a significant amount of catalyst-Br^{+} complex must be ascribed to the inability of the brominated catalyst to lose a proton and thus form a neutral species.

3.5.7. Conclusion

A large scale preparation of our catalyst, IBAM (**113**, Figure 70), has been achieved, requiring the re-designing of the existing synthesis.

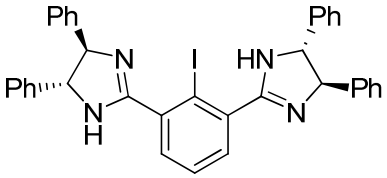

113

Figure 70: 2,6-di-[(4*R*,5*R*)-4,5-diphenyl-4,5-dihydro-1*H*-imidazol-2-yl]iodobenzene or IBAM

This represented a significant advancement in the asymmetric catalytic bromination studies, moving from catalyst preparation *via* iterative 200 mg syntheses to a single large scale preparation producing enough catalyst to facilitate three years of research. The removal of such synthetic limitations facilitated the screening of a range of catalytic asymmetric bromination reaction conditions and the stoichiometric addition of NBS to the catalyst in an attempt to elucidate the nature of the catalytic intermediate. By optimization of the concentration and catalyst loading, the enantioselectivity of the catalytic bromolactonisation of **114** was increased to produce bromolactone **115** in 17% ee.

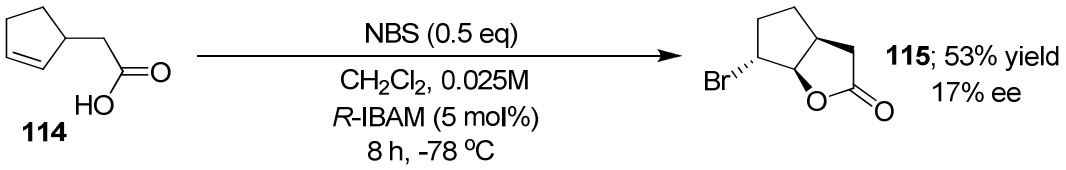

114

115; 53% yield
17% ee

Scheme 109: asymmetric bromolactonisation of 114

The competitive formation of an N-Br catalytic intermediate has been identified as a significant factor leading to a depreciation of the enantioselectivity of the reaction. A range of *N*-substituted IBAM derivatives were synthesised and screened as asymmetric bromination catalysts with a view to inhibiting this pathway. Although a number of new insights have been gained into the catalytic mechanism, disappointingly, no significant increase in the asymmetric induction of the reaction was observed.

4. Bromonium Ion - Alkene Br^+ Exchange

Our results in the field of electrophilic asymmetric bromination made it evident to us that there was still a key factor that we had overlooked with respect to rendering the reaction enantioselective. After consideration of the existing bromination literature (c.f. section *1.2.*), in conjunction with our own findings, it became apparent to us that bromonium ion-alkene Br^+ exchange may be facilitating the partial or complete racemisation of any enantioselectively formed bromonium ion (Scheme 110).

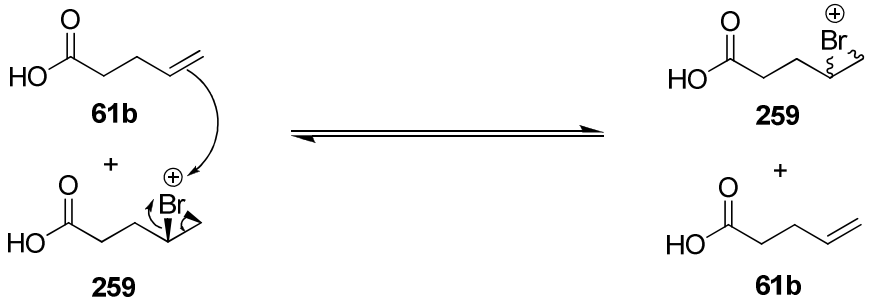

Scheme 110: racemisation of enantioenriched bromonium ion *via* bromonium ion-alkene Br^+ exchange

Thus, we were posed with three questions that required answering:

(1) Is bromonium ion – alkene Br^+ exchange occurring in our system?
(2) Does this exchange occur in a non-stereoselective manner, thus resulting in racemisation of an enantioenriched system?
(3) Can such exchange be inhibited in order to improve the enantioexcesses produced in our reaction?

4.1. Is bromonium ion – alkene Br^+ exchange occurring in our system?

In order to determine whether or not such exchange was occurring in our system, an experiment was conducted similar to that originally undertaken by Rodeburgh and Fraser-Reid in their work on the bromination of ω-alkenyl glycosides (c.f. section *1.2.2.*).[51] Two

alkenoic acids, **114** and **61b**, were selected which reacted with NBS form the corresponding bromolactones, **115** and **106**, at similar rates (Tables 11 and 12).

Table 12: bromolactonisation of 2-cyclopenten-1-ylacetic acid (114) with NBS

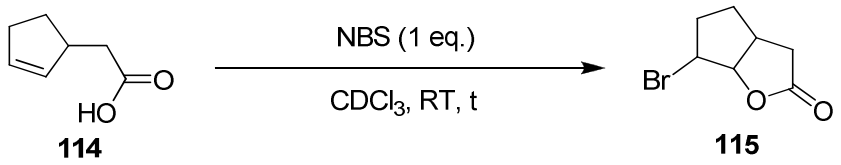

114 **115**

Time (t)	1.5 h	4.5 h	22 h	49 h
Conversion	Trace	11%	62%	100%

Table 13: bromolactonisation of 4-pentenoic acid (61b) with NBS

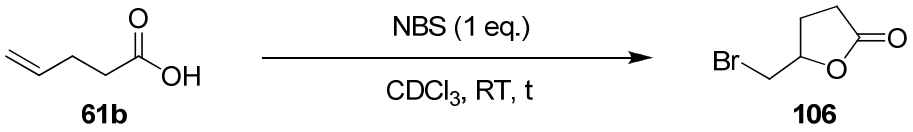

61b **106**

Time (t)	1.5 h	4.5 h	22 h	49 h
Conversion	7%	16%	65%	87%[a]

a – full consumption of NBS observed

The two alkenoic acids, **61b** and **114**, were then made to compete for insufficient NBS (Scheme 111).

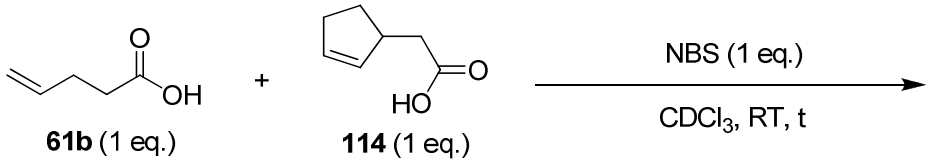

61b (1 eq.) **114** (1 eq.)

Scheme 111: competition of alkenoic acids, 61b and 114, for insufficient NBS

If the formation of a bromonium ion was irreversible, then bromonium ion formation is the rate determining step and the product distribution should reflect the relative rates of the individual bromination reactions of **61b** and **114**. Thus, an approximately 1:1 ratio of the two bromolactones (**106** and **115**) would be predicted, with a small enhancement in bromolactone **106** due to a slightly faster rate of formation. However, on stirring one

equivalent of each substrate with one equivalent of NBS, a strikingly different product distribution was obtained than that predicted by assuming irreversible bromonium ion formation (Table 14).

Table 14: competition of alkenoic acids, 61b and 114, for insufficient NBS

Time (t)	1.5 h	4.5 h	22 h	49 h
Conversion of **61b** to **106**	-	Trace	5%	10%
Conversion of **114** to **115**	Trace	6%	40%	76%
Conversion of NBS to succinimide	3%	15%	62%	100%

Thus the final product ratio obtained is 86:14 in favour of 6-bromohexahydrocyclopenta[b]furan-2-one (**115**).

This surprising result indicates a reversible step occurring within the bromolactonisation process rather than an irreversible bromonium ion formation, rapidly followed by intramolecular attack and subsequent ring closure. As Rodeburgh and Fraser-Reid pointed out, the heats of formation of succinimide (**90**) and NBS (**226**) are -109.72 kcal mol^{-1} and -80.35 kcal mol^{-1} respectively (Scheme 112) and the pKa of succinimide is 9.62. These all imply that the succinimide anion (**88**) would pick up H^+ from the carboxylic acid substrate more readily than it would remove Br^+ from a cyclic bromonium ion.

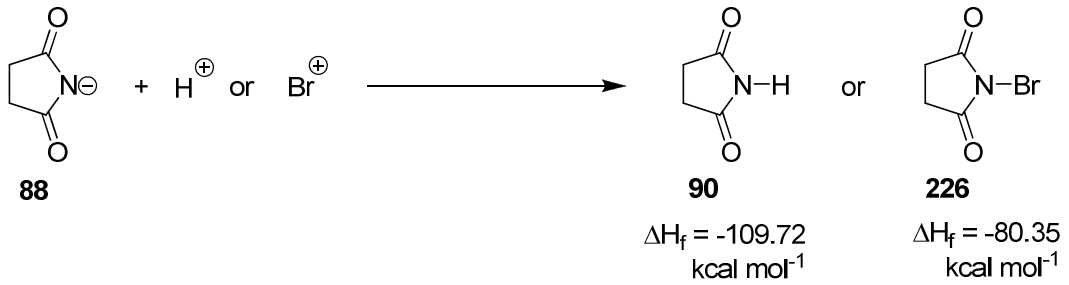

Scheme 112: heats of formation of NBS (226) and succinimide (90)

Thus, similarly to Rodeburgh's and Fraser-Reid's conclusions, the reversible reaction of an alkene with NBS can be ruled out in our system. Therefore, the transfer of Br^+ between bromonium ions and alkenes is proposed as the source of reversibility.

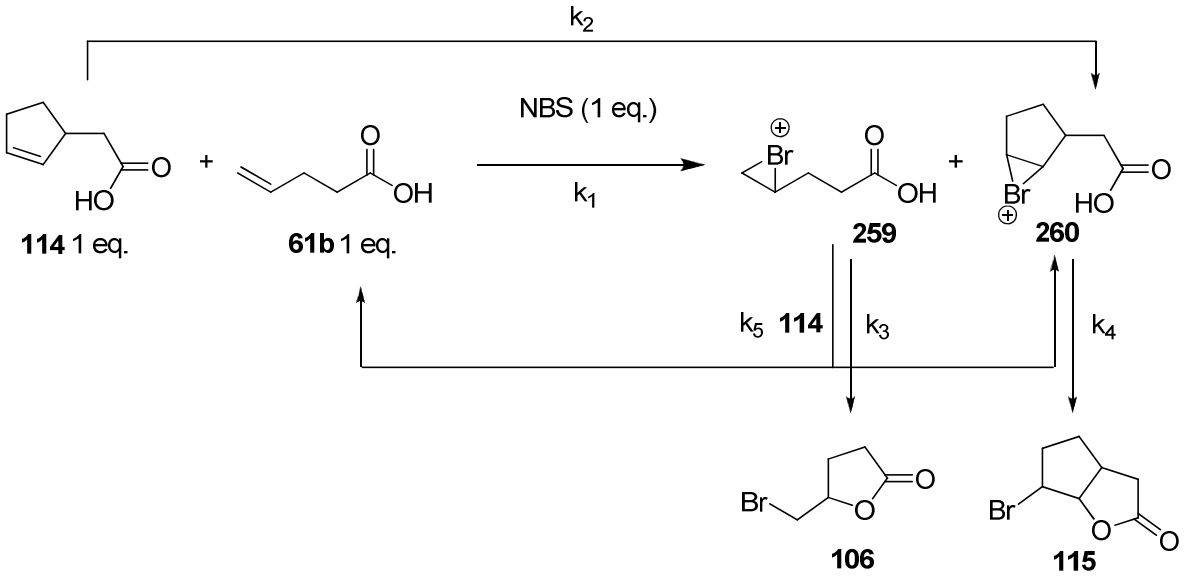

Scheme 113: Br^+ exchange in the bromolactonisation of alkenoic acids 114 and 61b

Our findings can be reasoned by proposing the relative rate constants of the bromination and cyclisation steps for each substrate (Scheme 113). The overall rates of the individual brominations will be a combination of k_1/k_3 and k_2/k_4, and we observe that $k_1/k_3 \geq k_2/k_4$. However, when the effects of exchange are apparent in the observed product distribution, we begin to be able to discriminate between the relative rates of the individual steps as Br^+ exchange becomes a competing process with the intramolecular cyclisation step. In this case, the bromolactone will dominate the product distribution which either (1) has a faster rate of cyclisation or (2) has an alkene precursor which more rapidly captures Br^+ from a bromonium ion. As there is little electronic difference between the two alkenes, **114** and **61b**, (2) seems unlikely. However, (1) seems a convincing argument as bromonium ion **260** has some degree of pre-organisation for intramolecular attack and thus a smaller entropic barrier to cyclisation. Thus, we hypothesise that $k_4 > k_3$, resulting in a product distribution enhanced in **115**.

It is also worth noting, by comparison of the rates of reaction in tables 12, 13 and 14, that the addition of excess alkene results in an overall reduction in the rate of bromination. Such

an observation is in agreement with Brown's observation that added Ad=Ad (**39**) suppressed the rate of his **39**Br^+/TfO^- -promoted bromolactonisation reactions.[48] This rate suppression can be reasoned by invoking two competing pathways for the reaction of bromonium ions; ring closure to form bromolactone product, or the transfer of Br^+ to form further bromonium ion and alkene. As the amount of alkene increases, the number of unproductive Br^+ transfers increases relative to the amount of bromolactone formation and thus the overall rate is reduced.

The same competition reaction was repeated in the presence of 1 mol% IBAM (**113**) catalyst at both room temperature and -78 ºC (Table 15).

Table 15: competition of alkenoic acids, 61b and 114, for insufficient NBS in the presence of IBAM (113)

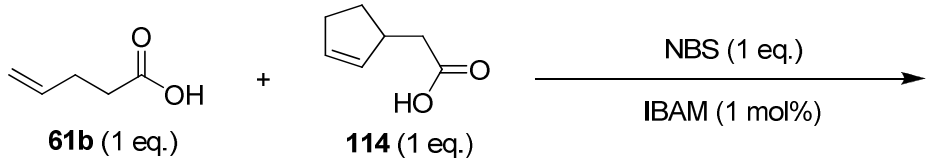

61b (1 eq.) + **114** (1 eq.)

Entry	Temperature	Catalyst loading	Solvent	Time[a]	Final product ratio, **115**:**106**
1	RT	_	$CDCl_3$	49 h	86:14
2	RT	1 mol%	$CDCl_3$	1 h	84:16
3	-78 ºC	1 mol%	CH_2Cl_2	-	94:6

a – time until NMR analysis demonstrated full conversion of NBS to succinimide.

Whilst the addition of IBAM (**113**) to the room temperature bromolactonisation appreciably shortened the reaction time, the product ratio obtained was indistinguishable from the uncatalysed reaction (taking into account the error margins of ^1H NMR). The low temperature reaction resulted in a product ratio which was still more distorted in favour of bromolactone **115**, presumably due to an increased discrimination between reaction pathways at reduced temperatures. Thus, it was concluded that under our catalytic asymmetric bromination conditions Br^+ exchange between bromonium ions and alkenes is occurring and is an important factor requiring further consideration.

4.2. Does bromonium ion – alkene Br^+ exchange result in loss of enantioexcess?

In order to determine whether bromonium ion – alkene Br^+ exchange leads to the racemisation of chiral bromonium ions, it is necessary to generate an enantiopure, or enantioenriched, chiral bromonium ion in the absence of any alkene. If this bromonium ion can be trapped by a nucleophile it should, in theory, produce enantiopure or enriched product. By the addition of alkene to this system its impact on the enantioexcess of the product obtained could then be determined (Scheme 114). The generation and study of such a system would facilitate valuable, unprecedented insights into the stereoselectivity of bromonium ion – alkene exchange and the stereochemical consequences of this in the asymmetric electrophilic bromination of alkenes.

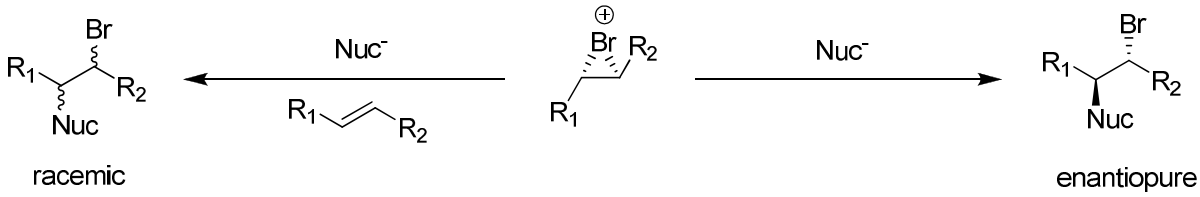

Scheme 114: determination of the stereochemical consequences of bromonium ion – alkene exchange

4.*2.1. Rearrangement of 2-bromo-2-phenylethanol (**261**)*

Previous work within the Braddock group[121] had, when attempting the synthesis of 1-bromo-2-chloro-1-phenylethane (**263**), revealed the rearrangement of 2-bromo-2-phenylethanol (**261**) on reaction with thionyl chloride to give 2-bromo-1-chloro-1-phenylethane (**262**, Scheme 115).

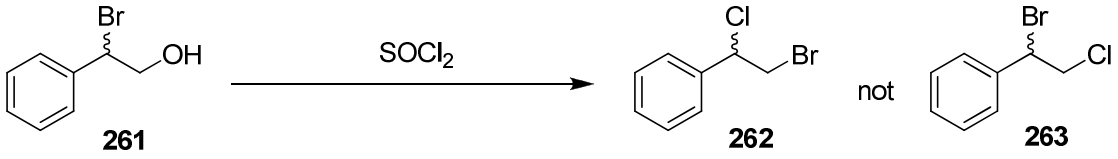

Scheme 115: rearrangement of 2-bromo-2-phenylethanol (261) on treatment with thionyl chloride

The regiochemistry of the rearranged product was confirmed by X-ray crystallography (Figure 71).

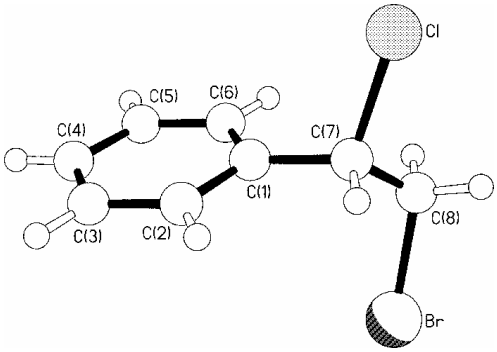

Figure 71: X-ray crystal structure of 2-bromo-1-chloro-1-phenylethane (262)[121]

The rearrangement of 2-bromo-2-phenylethanol (**261**) to afford 2-bromo-1-chloro-1-phenylethane (**262**) must necessarily proceed *via* a chiral bromonium ion intermediate, **265** (Scheme 116).

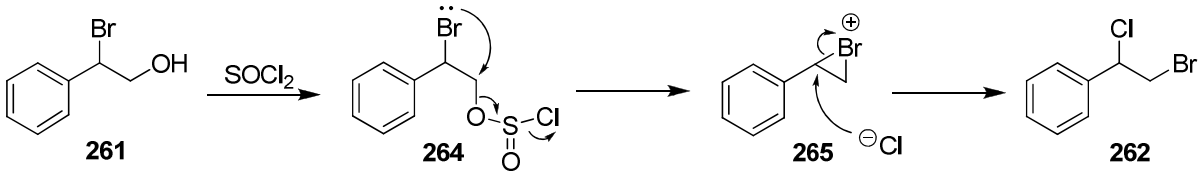

Scheme 116: rearrangement of 2-bromo-2-phenylethanol (261) on treatment with thionyl chloride

Thus, in theory, synthesis of enantiopure bromohydrin **261** should facilitate the generation of enantiopure bromonium ion **265** in the absence of any alkene.

This styrene-based substrate appeared to be suitable for our purposes not only due to the precedented rearrangement, but also due to its UV activity, thus facilitating measurement of the enantioexcess of the bromochlorinated product by a chiral HLPC method. Additionally, the enantiopure styrene oxide (**267**) can be purchased commercially and ring opening of the epoxide with hydrobromic acid should afford the desired enantiopure bromohydrin.

Our investigations were commenced with the epoxidation and subsequent ring opening of styrene (**266**) to produce the racemic bromohydrin **261** (Scheme 117).

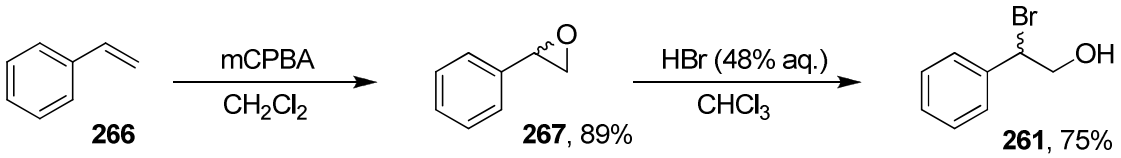

Scheme 117: synthesis of racemic 2-bromo-2-phenylethanol (261)

However, on reaction of bromohydrin **261** with thionyl chloride under the conditions previously reported to facilitate the rearrangement, the expected bromochlorinated product **262** was not observed. Instead, a product was isolated which appeared by ^{1}H and ^{13}C NMR as a complex diastereomeric mixture, suggesting dimerisation of the bromohydrin **261**. The identity of the product was eventually confirmed by X-ray crystallography as di(2-bromo-2-phenyleth-1-yl) sulfite (**268**, Figure 72).

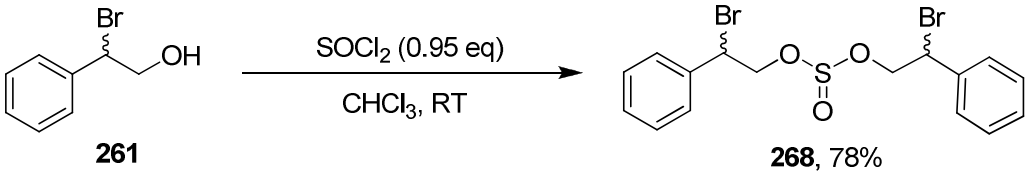

261 **268**, 78%

Scheme 118: formation of di(2-bromo-2-phenyleth-1-yl) sulfite (268)

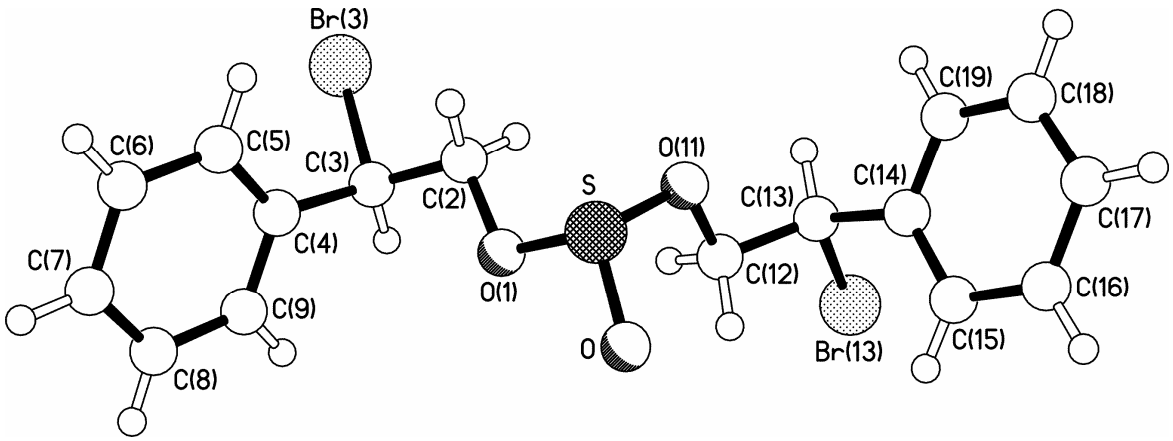

Figure 72: X-ray crystal structure of di(2-bromo-2-phenyleth-1-yl) sulfite (268)

It was hypothesised that a greater concentration of thionyl chloride and hydrochloric acid would disfavour dimer formation and promote rearrangement to the bromochloride. Indeed, after investigating a range of different reaction conditions (including addition of pyridine or TMSCl), we found that full conversion to 2-bromo-1-chloro-1-phenylethane (**262**) could be achieved by refluxing in excess neat thionyl chloride for five hours (Scheme 119). Importantly, this reaction proceeded more rapidly and cleanly if the reaction mixture was open to air rather than under an inert atmosphere if nitrogen. In the presence air thionyl chloride slowly reacts with atmospheric moisture to liberate sulphur dioxide and two equilalents of hydrochloric acid. Thus the improved conversion of the reaction when open to

air indicates the importance of a high concentration of hydrochloric acid in the reaction mixture for the collapse of the sulfite intermediate (**264** or **268**) to form the product.

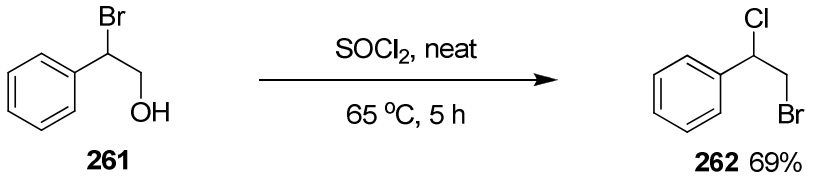

261 **262** 69%

Scheme 119: optimised conditions for the rearrangement of 2-bromo-2-phenylethanol (261)

After optimising our rearrangement conditions, we turned our attention to the synthesis and rearrangement of the enantiopure bromohydrin **261**. (*S*)-Styrene oxide (**267*S***) was opened with hydrobromic acid to afford bromohydrin **261** (Scheme 120).

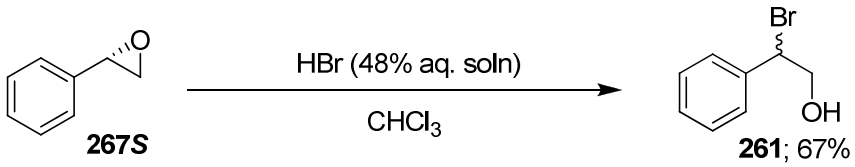

267*S* **261**; 67%

Scheme 120: opening of (*S*)-styrene oxide (267*S*) with hydrobromic acid

In order to determine the enantiopurity of the above bromohydrin product (**261**) the Mosher's esters (**270**, Scheme 121) of the bromohydrin (**261**) were formed from both the racemic and enantiopure styrene oxide (**267**). The resulting ^{1}H NMR of the ester derived from the racemic bromohydrin **261** demonstrated separation of the diastereomeric methoxy protons (3.46/3.42 ppm, Figure 73). By comparing the ^{1}H NMR of the Mosher's ester of the racemic bromohydrin, **261**, to the ^{1}H NMR of the ester formed starting from enantiopure epoxide, **267*S***, it was observed that partial racemisation of the benzylic position had occurred over the course of the ring opening, affording bromohydrin **261** in only 16% ee.

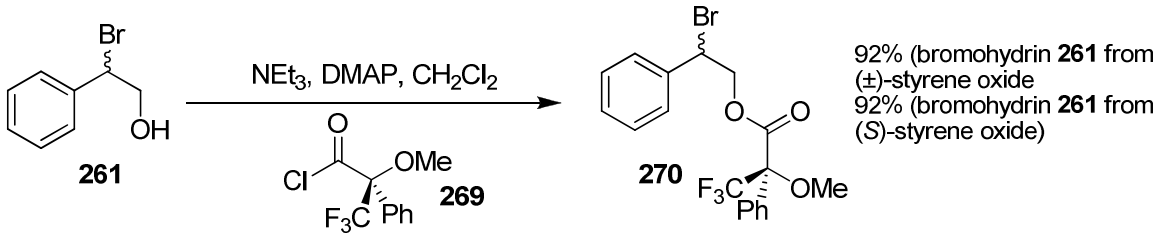

261 **269** **270**

Scheme 121: formation of Mosher's ester 279 for racemic and enantioenriched bromohydrin 261

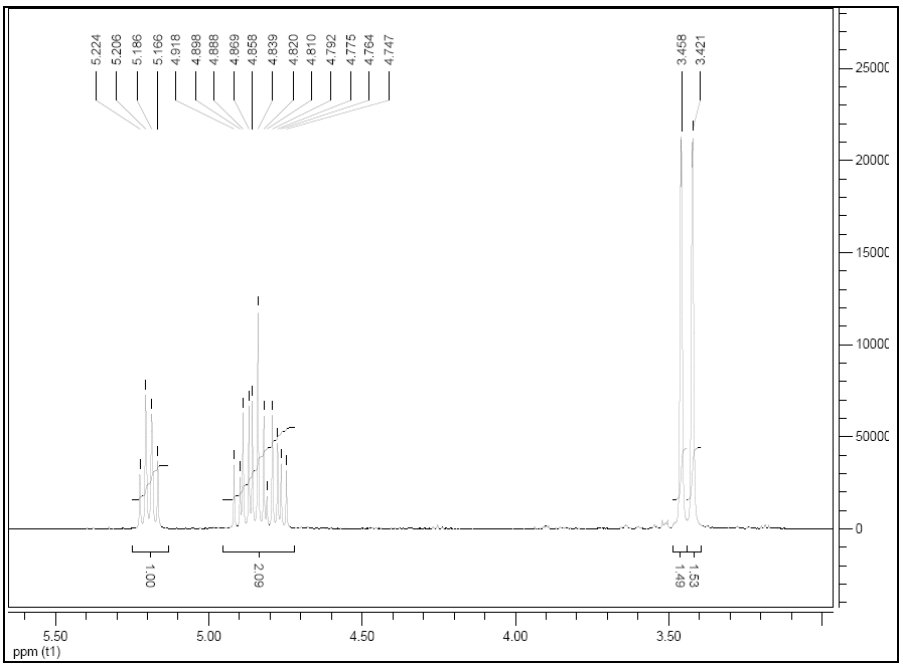

Figure 73: aliphatic portion of ^{1}H NMR spectra of Mosher's ester of racemic bromohydrin 261

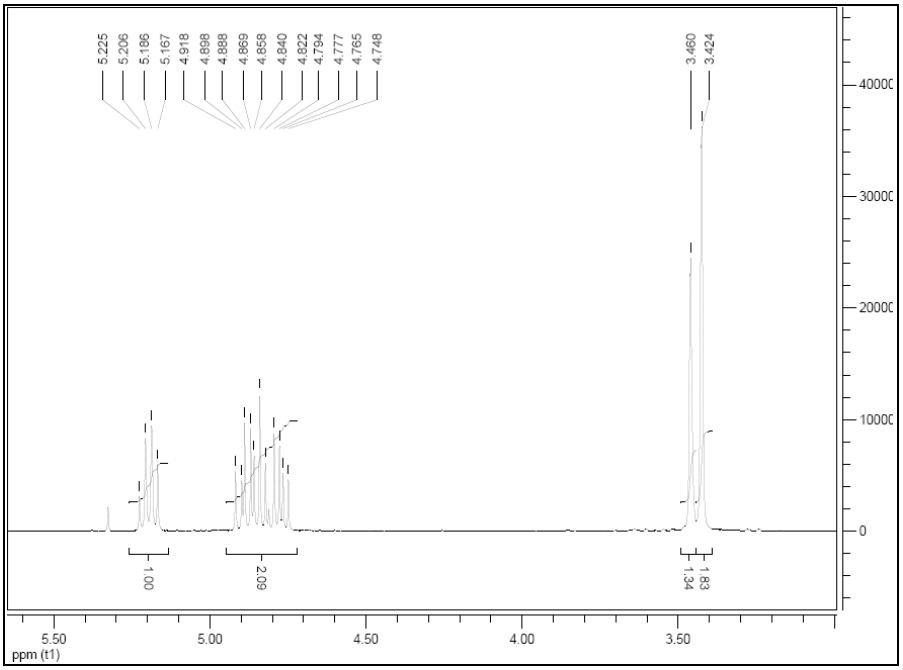

Figure 74: aliphatic portion of ^{1}H NMR spectra of Mosher's ester of bromohydrin 261 synthesised from (*S*)-styrene oxide

Presumably this loss of enantiopurity is a consequence of the participation of a benzylic carbocation (Scheme 122) in the acid-promoted opening of the epoxide **267**, resulting non-faceselective trapping of the protonated intermediate.

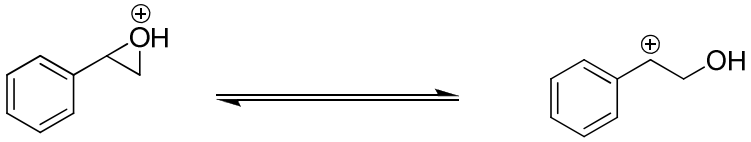

Scheme 122: participation of benzylic carbocation in ring opening of styrene oxide (267)

Presumably similar complications would also effect the rearrangement of the bromohydrin (**261**) proceeding *via* the bromonium ion intermediate (**265**). As such, it is likely the rearrangement would result in the formation of almost completely racemic bromochloride product (**262**), even without the addition of any alkene. The rearrangement was attempted on the enantioenriched bromohydrin **261** and the isolated bromochloride product (**262**) exhibited an optical rotation of zero, supporting our conclusion that bromohydrin **261** was not a viable substrate. Thus, it was decided that the substrate required re-designing to ensure we could measure the stereochemical consequences of exchange without the interference of additional factors.

4.*2.2. Rearrangement of 1-bromo-1-phenylpropan-2-ol (**271**)*

A *trans*-β-methylstyrene (**18**)-based system (Scheme 123) was proposed as a suitably modified substrate for our rearrangement and subsequent Br^+ exchange studies.

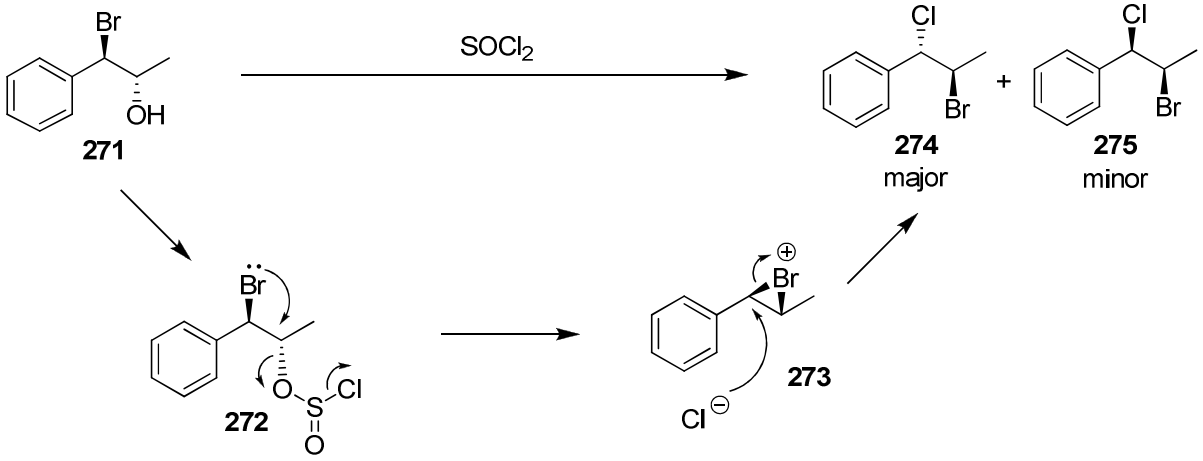

Scheme 123: rearrangement of 1-bromo-1-phenylpropan-2-ol (271)

Changing from a styrene (**266**)-based system to a *trans*-β-methylstyrene (**18**)-based system had a number of advantages, the most important of which being the introduction of a second chiral centre at C-2. Independently of the mechanism of either the epoxide opening or the

bromonium ion mediated rearrangement, this second stereocenter should remain enantiopure, thus eliminating the possibility of racemisation *via* a benzylic carbocation. Additionally, the degree of benzylic β-bromocarbonium ion versus bromonium ion character of the intermediate in the rearrangement can be easily determined *via* ^{1}H NMR by measuring the *R**,*S**(anti):*S**,*S**(syn) product ratio. Meanwhile, the UV activity of the substrate is retained, facilitating chiral HPLC analysis of the bromochlorinated product, **274**/**275**.

Therefore, racemic 1-bromo-1-phenylpropan-2-ol (**271**/**277**) was synthesised by the same strategy applied to 2-bromo-2-phenylethanol (**261**) (Scheme 124).

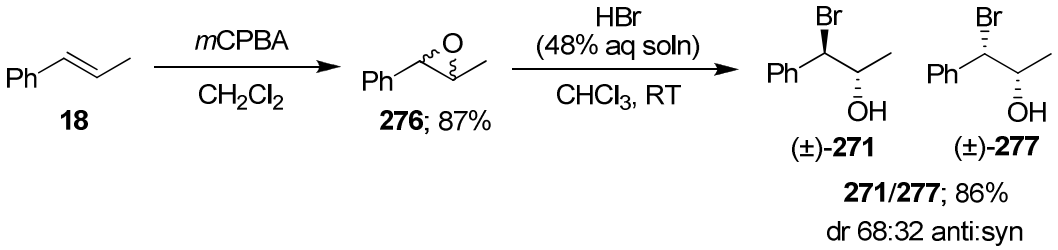

Scheme 124: synthesis of 1-bromo-1-phenylpropan-2-ol (271/277)

Table 16: variation of diastereomeric ratio with temperature

Entry	Temperature (ºC)	dr (*R**,*S**)(anti):(*S**,*S**)(syn)
1	RT	68:32
2	0	72:28
3	-10	75:25

It was found that, whilst the (*R**,*S**)(anti)**271**:(*S**,*S**)(syn)**277** ratio could be increased slightly by lowering the temperature of the reaction (Table 16), the minor diastereomer could not be completely eliminated from the product mixture. However, we proceeded with the synthesis of bromohydrin **271**/**277** from enantiopure (1*S*,2*S*)-1-phenylpropylene oxide (**276*S***, Scheme 125). On formation of the Mosher's ester and comparison with the Mosher's ester of the racemic mixture, we were pleased to observe the presence of only two epimers in the ^{1}H NMR (compared to four in the racemate, all four methoxy peaks appearing with baseline separation; Figure 75, 3.68/3.62/3.36/3.28). Thus, as predicted, the second chiral centre retains its stereochemistry in the epoxide opening.

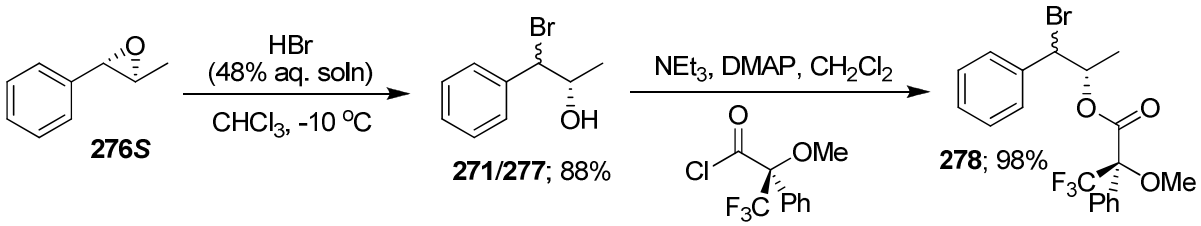

Scheme 125: synthesis of (2*S*)-1-bromo-1-phenylpropan-2-ol (271/277) and subsequent Mosher's ester formation

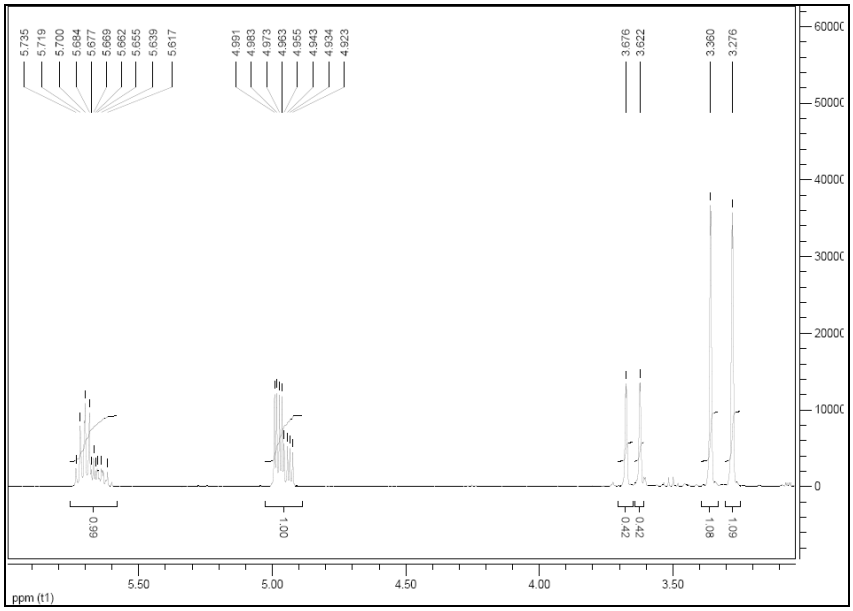

Figure 75: portion of ^{1}H NMR spectra of Mosher's ester of (±)-1-bromo-1-phenylpropan-2-ol

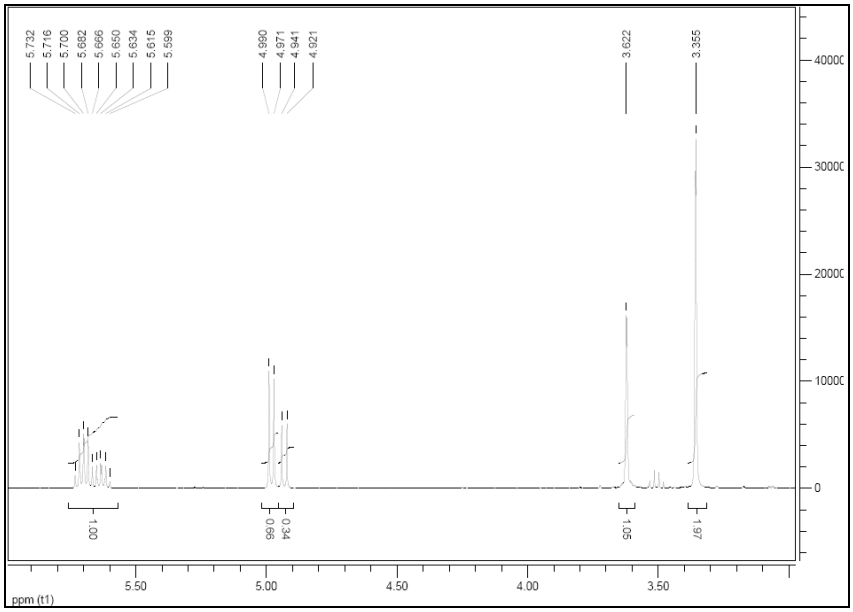

Figure 76: portion of ^{1}H NMR spectra of Mosher's ester of (2*S*)-1-bromo-1-phenylpropan-2-ol

The (*R**,*S**)- and (*S**,*S**)- diastereomers of 1-bromo-1-phenylpropan-2-ol (**271**/**277**) proved inseparable and thus it was decided to continue with the rearrangement using the diastereomeric mixture. The rearrangement of bromohydrin **271**/**277** proceeded well under our previously developed conditions and with little further decrease in the (*R**,*S**):(*S**,*S**) ratio (Scheme 126). The structure of the major diastereomer was confirmed by X-ray crystallography (Figure 77).

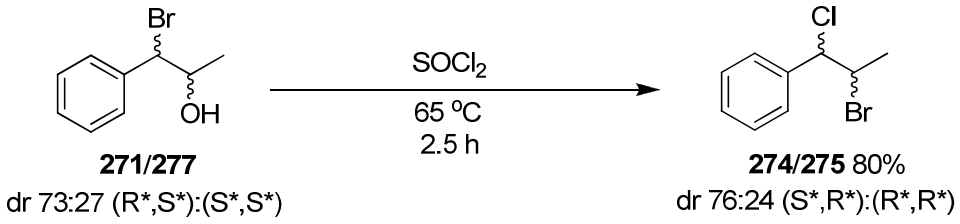

Scheme 126: thionyl chloride mediated rearrangement of (±)-1-bromo-1-phenylpropan-2-ol (271/277)

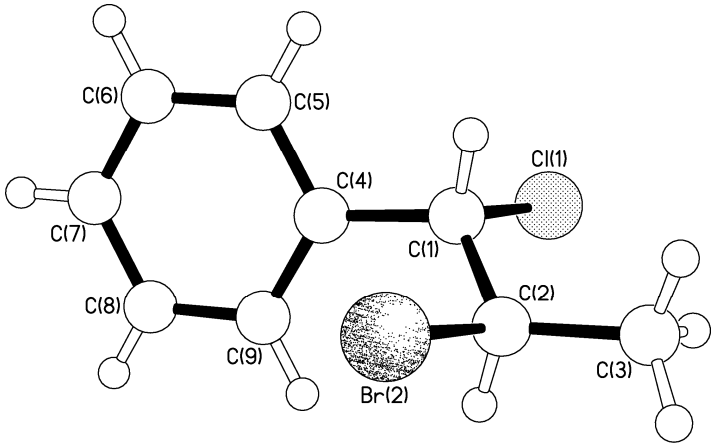

Figure 77: X-ray crystal structure of (1*S,2*R**)-2-bromo-1-chloro-1-phenylpropane (274)**

Chiral HPLC conditions were developed which facilitated some degree of separation of both the (*S**,*R**) and (*R**,*R**) diastereomers and the two enantiomers of the (*S**,*R**) major diastereomer (Figure 78). Pleasingly, on submitting the enantiopure bromohydrin **271**/**277** to our rearrangement conditions, bromochloride **274**/**275** was obtained in 97% yield and with no apparent loss of enantiopurity (Figure 78).

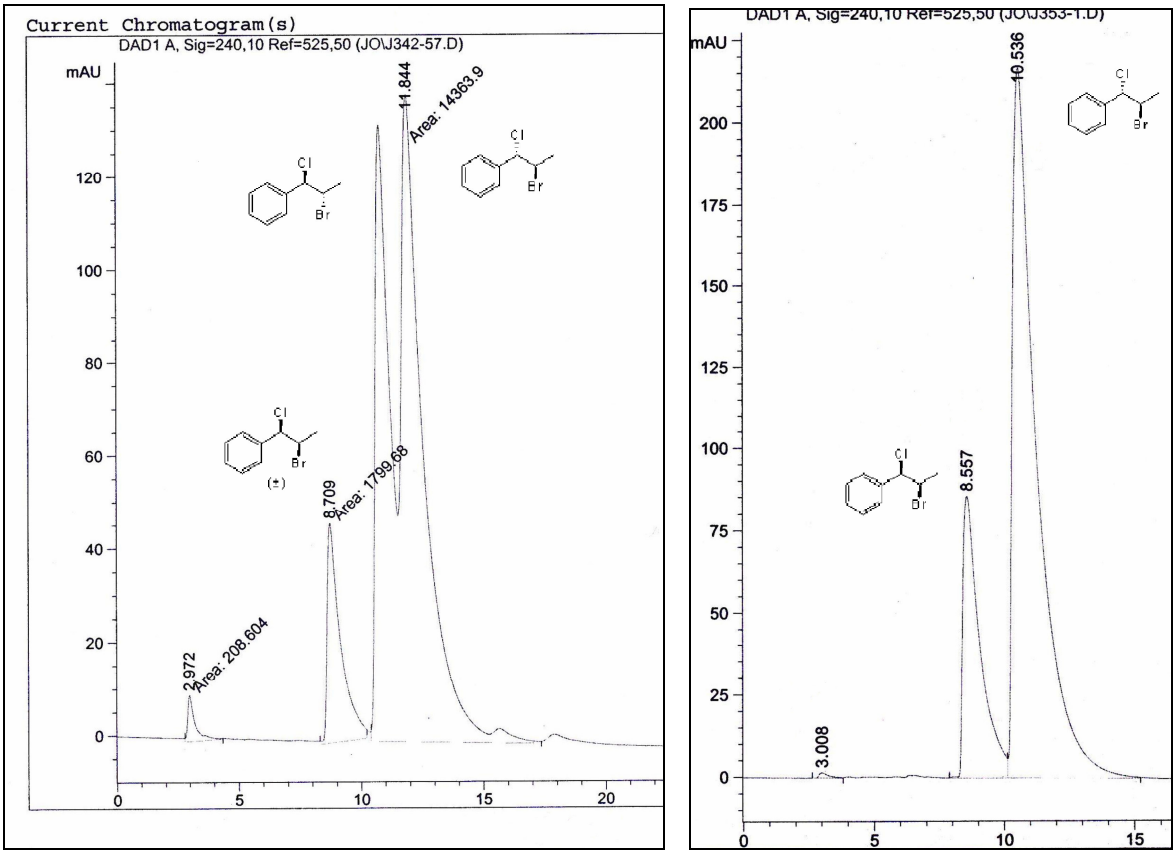

Figure 78: HPLC traces of 2-bromo-1-chloro-1-phenylpropane (274/275) formed from racemic and enantiopure bromohydrin (271/277)

Thus, not only had we achieved our goal of generating a chiral bromonium ion in the absence of alkene but also, to the best of our knowledge, we had succeeded in generating and trapping the first enantiopure or significantly enantio-enriched bromonium ion. We subsequently undertook the addition of alkene to our reaction mixture and measured the stereochemical consequences of this on the isolated product. However, to our surprise, the addition of one, or even five equivalents of *trans*-β-methylstyrene (**18**) or cyclohexene (**44**) resulted in no observable racemisation of our isolated bromochlorinated product **274**/**275** (Table 17).

Table 17: addition of alkene to rearrangement of (2*S*)-1-bromo-1-phenylpropan-2-ol (271/277)

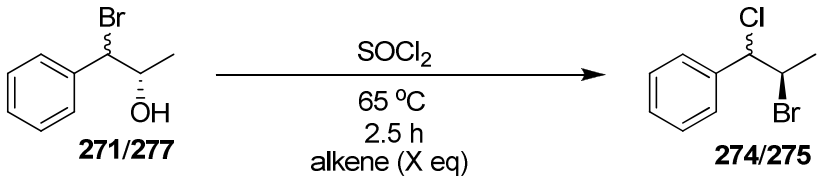

Entry	Alkene	Equivents (X eq.)	Yield	Degree of racemisation visible on HPLC trace
1	Ph **18**	1 eq	82%	None
2	Ph **18**	5 eq	57%	None
3	**44**	5 eq	56%	None

This indicated that either Br^+ exchange is occurring in a stereospecific manner or, more likely, that no exchange is occurring at all in this system. In order to probe whether any exchange is occurring over the course of the reaction, we conducted the rearrangement of bromohydrin **271**/**277** in the presence of styrene (**266**) (Scheme 127). If any transfer of Br^+ occurs from the intermediate bromonium ion (**273**) to styrene, 2-bromo-1-chloro-1-phenylethane (**262**) should be formed; a species we had previously synthesised and characterised. On carrying out this experiment and analysing the crude product mixture by ^1H NMR, no 2-bromo-1-chloro-1-phenylethane (**262**) was observed, indicating the absence of any bromonium ion – alkene Br^+ transfer.

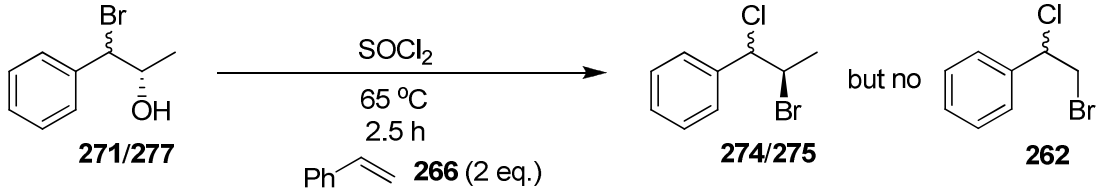

Scheme 127: addition of styrene to rearrangement of (2*S*)-1-bromo-1-phenylpropan-2-ol

At this point we paused to consider factors which may affect the extent of bromonium ion – alkene Br^+ exchange in solution. We identified a number of variables which may exert an influence:

(1) Solvent

Brown's investigations into exchange within the adamantaneadamantylidene system (c.f. section *1.2.1.*) had for the main part been conducted as dilute solutions in chlorinated solvents;[38,39,48] conditions which are far removed from the neat thionyl chloride in which our rearrangement was conducted. It is highly possible that a more polar, coordinating solvent such as thionyl chloride, with a high concentration of the chloride nucleophile, may significantly inhibit bromonium ion – alkene Br^+ exchange.

(2) Concentration

It is plausible that the concentration of the reaction mixture should influence the extent of exchange, the higher the concentration, the greater the likelihood of the bimolecular collision between a bromonium ion and alkene necessary for the transferral of Br^+.

(3) Temperature

The majority of work published in the field of Br^+ exchange has been conducted at room temperature or lower;[38,39,48,51] considerably milder conditions than our reaction conducted at 65 ºC. It is possible that raising the temperature of the reaction decreases the lifetime of the bromonium ion and thus decreases exchange.

(4) Nucleophile and leaving group

The nature of the group expelled by bromine in the first step of the rearrangement and the nucleophile used to open to the bromonium ion may affect the degree of Br^+ exchange observed. For example, it is reasonable to hypothesise that a powerful, anionic nucleophile, which both associates strongly to the bromonium ion and rapidly attacks the electrophilic carbons, will reduce the Br^+ transfer due competitive trapping of the bromonium ion.

(5) The "donor" bromohydrin and "acceptor" alkene

The electronic and steric properties of both the bromonium ion donating Br^+ ("donor" bromohydrin) and the scavenger olefin added to the reaction ("acceptor" alkene) may also influence the extent of Br^+ exchange. For example, Brown and Bellucci reported results which suggested that the reversibility of bromonium ion formation in stilbenes was dependent on the bromonium ion versus β-bromo carbonium ion character of the bromination intermediate (c.f. section *1.2.2.*).[53]

It was possible that any of these factors could be preventing exchange within our system and thus each required investigation.

4.2.3. Effects of solvent and temperature on bromonium ion – alkene Br^+ exchange

We initially decided to consider the impact of solvent and temperature on the degree of bromonium ion – alkene Br^+ exchange observed. We desired to bring our rearrangement conditions into closer agreement with both those reported in the existing work published on Br^+ exchange and with the conditions of our catalytic asymmetric bromination. Thus, substrates and reagents were investigated which would allow us to conduct our rearrangement at lower temperatures and in chlorinated solvents. It was envisaged that more variation could easily be introduced to the system by the functionalisation of the bromohydrin **271**/**277** to convert the alcohol into a good leaving group. If this intermediate could be isolated, it could be submitted to a range of rearrangement conditions with the addition of a nucleophile of our choice to open the bromonium ion.

After revisiting Brown's work on exchange, bromotriflate **279** was selected as a possible substrate, Brown having used a similar substrate, **66**, to generate bromonium ions *in situ* in exchange experiments.[50]

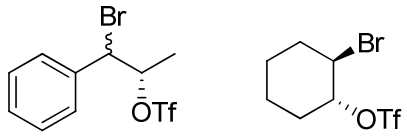

279 (±)-**66**

Figure 79: bromotriflate substrates

It was proposed that, by the use of a more labile leaving group than that generated on reaction of the bromohydrin with thionyl chloride, the rearrangement could be conducted at lower temperatures. The bromotriflate **279** was, as predicted, extremely susceptible to rearrangement to the bromonium ion, indeed the triflate leaving group of **279** proved too labile for our purposes. Whilst Brown noted the instability of bromotriflate **66** at room temperature, the triflate could be formed by the reaction of triflic anhydride and (±)-*trans*-2-bromocyclohexanol (**287**) with the temperature maintained between 0 and 5 ºC and the product subsequently stored as a solution at -78 ºC.[122] Unfortunately attempts to form bromotriflate **279** from bromohydrin **271**/**277** resulted in no reaction until the temperature was raised to room temperature. At this temperature, as soon as triflation occurred the

leaving group was immediately expelled, resulting in a complex mixture of decomposition products (Scheme 128). The major components of this mixture were various epimeric ethers, **280** (characterized by NMR and GCMS), presumably formed *via* bromonium ion formation after triflation, followed by ring opening by unreacted starting material.

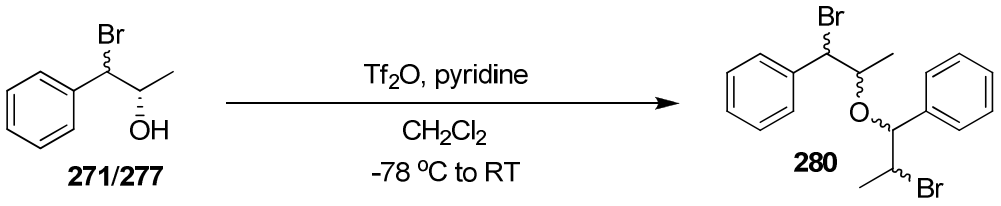

Scheme 128: attempted formation of bromotriflate 279

It would appear that the greater stability imparted to the bromonium ion of *trans*-β-methylstyrene (**273**) by the adjacent phenyl ring reduces the activation energy of the rearrangement of bromotriflate **279** relative to that of **66** to the extent where **279** cannot be isolated. The instantaneous expulsion of the triflate on its formation was confirmed by following the triflation reaction *via* a variable temperature ^{1}H NMR experiment. Whilst the formation of the ether dimer could be observed, at no point was any substantial amount of bromotriflate apparent.

The bromotosylate, **281**, was also investigated as a possible substrate for the rearrangement. However, under solvolysis conditions the tosylate leaving group proved insufficiently labile, bromotosylate **281** only undergoing reaction at high temperatures and affording a mixture of products under these conditions (Scheme 129).

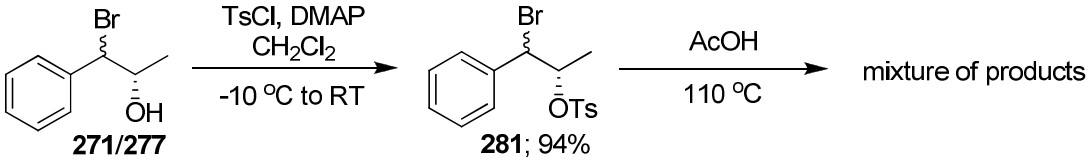

Scheme 129: formation and attempted rearrangement of (1'*S*)-2'-bromo-1'-methyl-2'-phenylethyl *p*-toluenesulfonate (281)

We therefore turned our attention to alternative methods of activating our alcohol leaving group *in situ*. It came to our attention that Mioskowski and co-workers had observed an analogous reaction of a bromohydrin to afford the rearranged bromochloride product in their racemic synthesis of halomon.[123] The reagent used in this case was Viehe's salt, **282**, which

Mioskowski reported as facilitating the rearrangement in dichloromethane between 0 ºC and room temperature. Pleasingly, when Viehe's salt (**282**) was used in our system, rearrangement was observed under similarly mild conditions (Scheme 130).

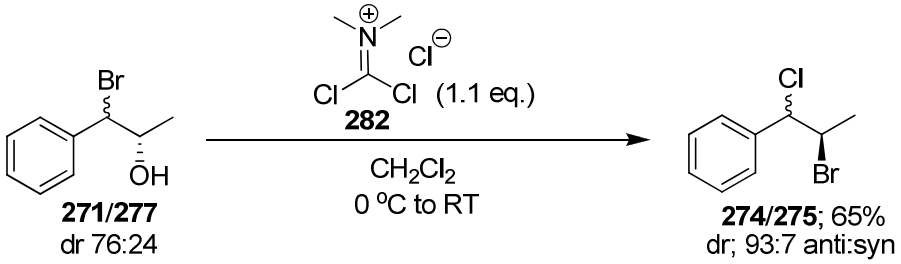

Scheme 130: Viehe's salt-mediated rearrangement of bromohydrin 271/277

The development of chiral HPLC conditions had continued coincidentally with the investigations into rearrangement conditions. It was found that by changing to a reverse phase system, much improved separation of all four diastereomers and enantiomers of the racemate could be achieved (Figure 80).[124]

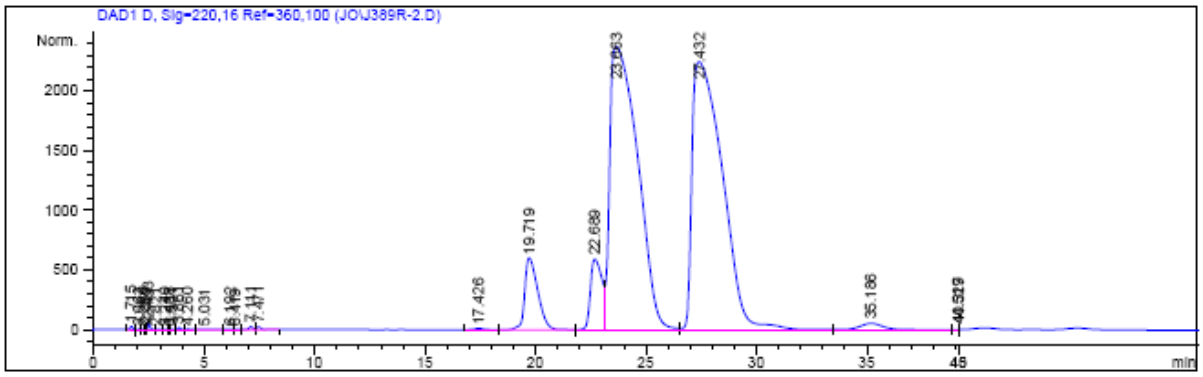

Figure 80: chiral HPLC trace demonstrating separation of diastereomers and enantiomers of (±)-2-bromo-1-chloro-1-phenylpropane (274/275)

Subsequent analysis under these conditions of the bromochloride product (**274**/**275**) from rearrangement of (2*S*)-1-bromo-1-phenylpropan-2-ol (**271**/**277**) with Viehe's salt demonstrated an enantioexcess of 94% for the major (*R**,*S**)-diastereomer.

On addition of two equivalents of styrene (**266**) to the Viehe's salt mediated rearrangement of **271**/**277**, a small amount of bromochlorinated styrene, **262**, was observed in the crude reaction mixture (Scheme 131; N.B. the control reaction, stirring styrene with Viehe's salt in deuterated chloroform, demonstrated no reaction after stirring at room temperature for four

days). The free olefin, *trans*-β-methylstyrene (**18**), was also evident in the crude ^{1}H NMR of the reaction mixture, indicating the occurrence of Br^+ exchange between the bromonium ion intermediate (**273**) and styrene (**266**, Scheme 132).

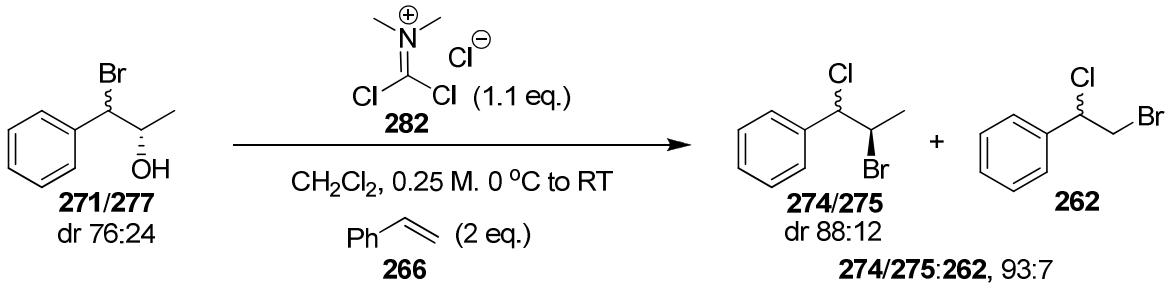

Scheme 131: evidence of bromonium ion – alkene Br^+ exchange

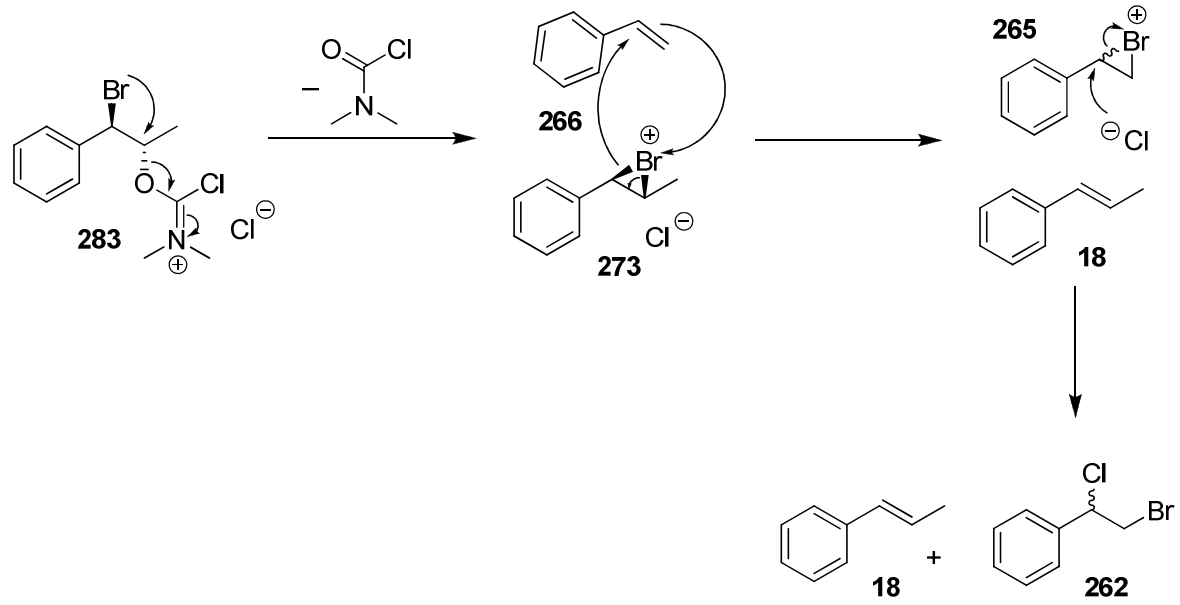

Scheme 132: proposed mechanism of formation of bromochlorinated styrene, 262

The rearrangement was also conducted in the presence of two equivalents of *trans*-β-methylstyrene (**18**, Scheme 133). In this case, although the yield was slightly reduced, no significant racemisation of the product was observable by chiral HPLC analysis.

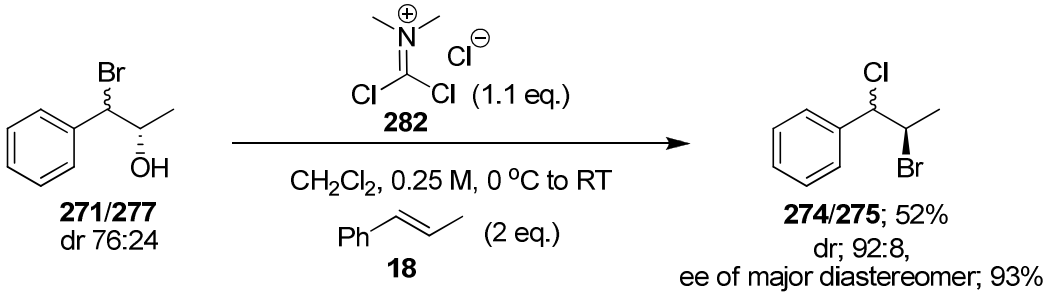

Scheme 133: addition *trans*-β-methylstyrene (18) to rearrangement of bromohydrin (271/277)

However, this result is not particularly surprising if we assume a similar degree of exchange occurs between the bromonium ion intermediate **273** and *trans*-β-methylstyrene (**18**) as between the bromonium ion **273** and styrene (**266**) (a reasonable assumption based on past bromination rate studies).[18] We will also assume that negligible transfer of Br^+ from the bromonium ion of styrene (**265**) back to *trans*-β-methylstyrene (**18**) occurs in Scheme 132; again a well-founded assumption due to the extremely low concentration of free *trans*-β-methylstyrene (**18**) in the system. In such a case, 7% of Br^+ would be transferred from the bromonium ion intermediate (**273**) to *trans*-β-methylstyrene (**18**) olefin to form supposedly racemic bromonium ion, thus generating 3.5% of the (*S*,*R*) enantiomer of 2-bromo-1-chloro-1-phenylpropane (**274**) after ring opening with chloride. This would result in an enantioexcess of 93% of the isolated (*R**,*S**)-2-bromo-1-chloro-1-phenylpropane (**274**), in keeping with our observed value.

Thus, we had demonstrated the phenomenon of bromonium ion – alkene exchange in our system, although only to a very small degree. However, the limited Br^+ exchange in our system was still at odds with the facile exchange reported in the literature and apparently occurring in our catalytic bromination reaction. Therefore, we considered further factors which may influence the extent of Br^+ exchange. It was necessary to increase the degree of exchange taking place within our system to facilitate study of the stereochemical consequences of Br^+ transfer. Additionally, it was also important to better understand the limiting factors to exchange in order to apply these to our asymmetric catalytic bromination reaction.

4.2.4. Effect of "donor" bromohydrin structure on bromonium ion – alkene Br^+ exchange

The first factor investigated was the impact of changing the structure of the "donor" bromonium ion, by modification of the bromohydrin starting material. It was hypothesized that partial benzylic carbocation character of the bromonium ion **273** (Figure 81) may result in the inhibition of Br^+ exchange.

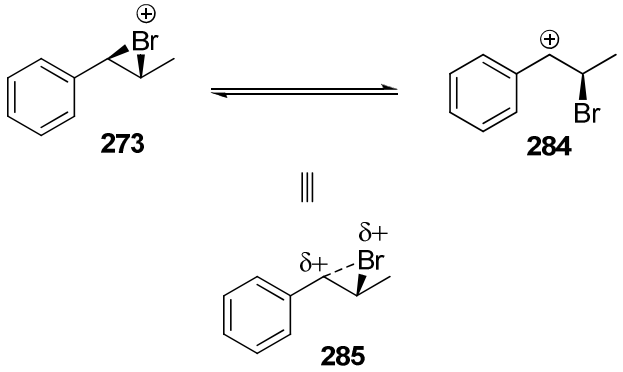

Figure 81: partial benzylic carbocation character of bromonium ion intermediate 273

A partially bridged bromonium ion, such as **285**, places significant partial positive charge on the benzylic carbon, unlike a symmetrically bridged bromonium ion, which places the majority of the charge on the bromine. Thus, nucleophilic attack at bromine by an alkene is disfavoured and the likelihood of attack at the benzylic carbon by chloride is increased. It was therefore decided to investigate bromonium ion – alkene Br^+ exchange under our rearrangement conditions from an aliphatic, symmetrical bromonium ion in order to determine if any increase in Br^+ transfer was observed. (±)-*Trans*-2-bromocyclohexanol (**287**) was selected as an easily accessible aliphatic bromohydrin substrate and it was accordingly synthesised from cyclohexene oxide (**286**, Scheme 134).

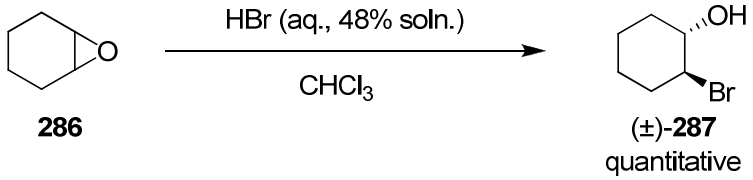

Scheme 134: synthesis of (±)-*trans*-2-bromocyclohexanol (287)

On treatment of (±)-*trans*-2-bromocyclohexanol (**287**) with Viehe's salt, the corresponding (±)-*trans*-1-chloro-2-bromocyclohexane (**288**) was obtained (Scheme 135).

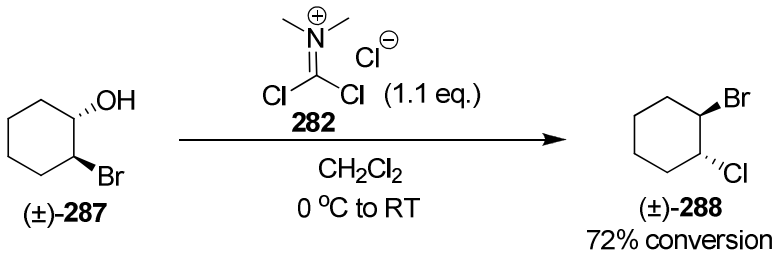

Scheme 135: conversion of (±)-*trans*-2-bromocyclohexanol (287) to (±)-*trans*-1-chloro-2-bromocyclohexane (288)

Thus, we proceeded with our exchange investigations (Table 18) and found that, on the rearrangement of **287** in the presence of either *trans*-β-methylstyrene (**18**, entry 2) or styrene (**266**, entry 3), a significantly greater degree of bromochlorinated acceptor alkene (**274**/**275** or **262**) was observed in the crude product mixture compared to that obtained on the rearrangement of (2*S*)-1-bromo-1-phenylpropan-2-ol (**271**/**277**, entry 1).

Table 18: relationship between structure of "donor" bromohydrin and degree of Br^+ transfer

Entry	"Donor" bromo-hydrin	"Acceptor" alkene	reagent	solvent	Conc.	Yield[a]	Exchange[b]
1	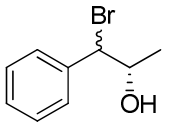 **271/277**	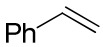 **266** (2 eq.)	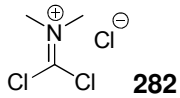 **282** (1.1 eq.)	CH_2Cl_2	0.03M	42%	3%
2	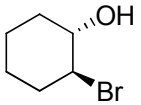 (±)-**278**	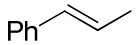 **18** (2 eq.)	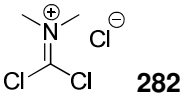 **282** (1.1 eq.)	CH_2Cl_2	0.03M	49%[c]	16%
3	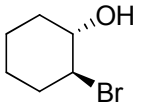 (±)-**278**	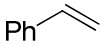 **266** (2 eq.)	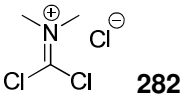 **282** (1.1 eq.)	CH_2Cl_2	0.03M	47%[c]	15%

a - combined yield of both "donor" and "acceptor" bromochlorinated products
b - % of bromochlorinated "acceptor" relative to total bromochlorinated product, c - conversion

Evidently, from these results, the degree of Br^+ transfer is significantly influenced by the degree of bromonium ion/β-bromocarbonium ion character in the Br^+ donor intermediate formed from rearrangement of the initial bromohydrin.

At this point, with two “donor” bromohydrin substrates available to us, we wished to confirm that the product distribution we were observing was kinetic rather than thermodynamic; that is, it is determined by the relative rates of exchange between bromonium ion and alkene and not by the relative stabilities of the two possible bromonium ions. Accordingly, two parallel reactions were conducted, each taking one equivalent of a donor bromonhydrin and rearranging it in the presence of one equivalent of the acceptor alkene of the other substrate (Table 19).

Table 19: proof of kinetic product distribution

Entry	“Donor” bromohydrin	“Acceptor” alkene	reagent	solvent	Conc.	Conversion[a]	Exchange[b]
1	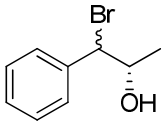 **271/277**	 **44** (1 eq.)	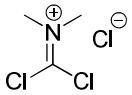 **282** (1.1 eq.)	$CDCl_3$	0.03M	34%	0%
2	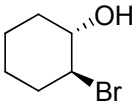 (±)-**278**	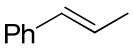 **18** (1 eq.)	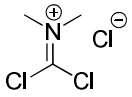 **282** (1.1 eq.)	$CDCl_3$	0.03M	38%	8%

a - combined conversion of both “donor” and “acceptor” bromochlorinated products
b - % of bromochlorinated “acceptor” relative to total bromochlorinated product

If the observed product distribution originated from thermodynamic factors, each parallel reaction should have yielded the same ratio of bromochlorinated products. The considerable difference between the two reaction products demonstrates that the exchange process in our system is determined by purely kinetic factors.

4.*2.5. Effect of “acceptor” alkene structure on bromonium ion – alkene Br^+ exchange*

Having confirmed both a kinetic product distribution and the existence of a relationship between the rate of exchange and the structure of the “donor” bromohydrin, attention was turned to the effect of structurally modifying the “acceptor” olefin. A range of alkenes were screened with regards to their capacity of accepting Br^+ from a bromonium ion (Table 20).

Table 20: relationship between structure of "acceptor" alkene and degree of Br^+ transfer

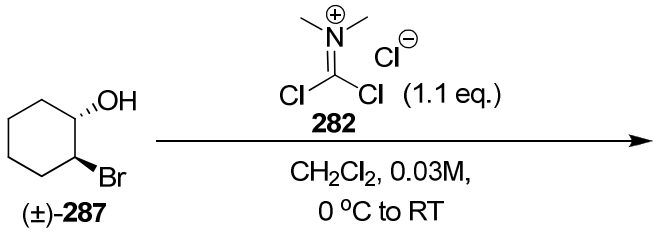

Entry	"Donor" bromohydrin	"Acceptor" alkene	Bromo-chlorinated "donor"	Bromo-chlorinated "acceptor"	Conversion[a]	Exchange[b]
1	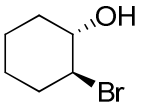 (±)-**287**	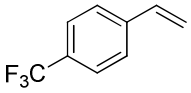 **289**	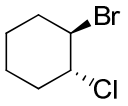 (±)-**288**	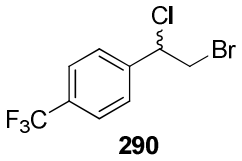 **290**	49%	0%
2	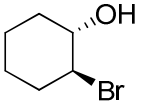 (±)-**287**	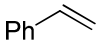 **266**	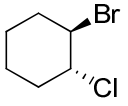 (±)-**288**	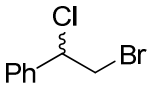 **262**	47%	15%
3	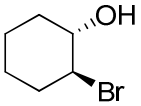 (±)-**287**	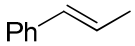 **18**	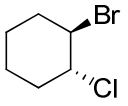 (±)-**288**	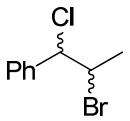 **274/275**	49%	16%
4	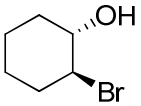 (±)-**287**	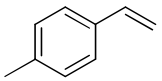 **291**	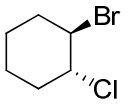 (±)-**288**	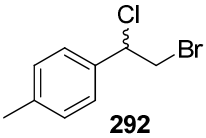 **292**	83%	40%
5	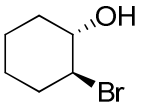 (±)-**287**	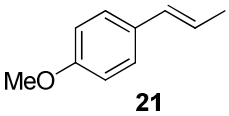 **21**	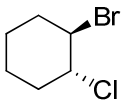 (±)-**288**	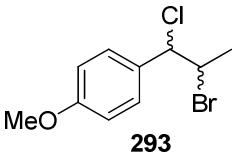 **293**	53%	43%

a - combined conversion of both "donor" and "acceptor" bromochlorinated products
b - % of bromochlorinated "acceptor" relative to total bromochlorinated product

It is apparent that there is also a strong relationship between the nucleophilicity of the acceptor alkene (and thus the stability of the resulting bromonium ion) and the degree of Br^+ transferred to it. Our results demonstrate a full spectrum of acceptor alkenes ranging from no detectable transfer of Br^+ to **289** (entry 1), through to the capture of 43% of the Br^+ by *trans*-anethole **21** (entry 5). Similarly to Rolston's and Yates' observations concerning the

relative rates of bromination of substituted styrene derivatives,[18] aromatic substitution has a much greater effect on rate than methyl substitution of the β-carbon, indicating a significant degree of stabilisation of the positive charge over the α-carbon and the aromatic ring.

4.2.6. *Effects of concentration on bromonium ion – alkene Br^+ exchange*

Attention was then turned to investigating the influence of the concentration of the reaction mixture on the degree of exchange observed (Table 21).

Table 21: effect of concentration on the degree of exchange observed

Entry	"Donor" bromohydrin	"Acceptor" alkene	reagent	solvent	Conc.	Yield[a]	Exchange[b]
1	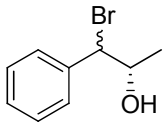 **271/277**	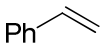 **266** (2 eq.)	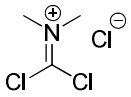 **282** (1.1 eq.)	CH_2Cl_2	0.03M	42%	3%
2	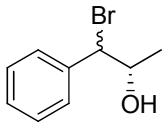 **271/277**	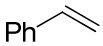 **266** (2 eq.)	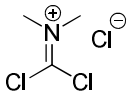 **282** (1.1 eq.)	CH_2Cl_2	0.25M	56%	7%
3	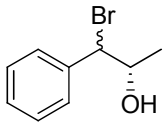 **271/277**	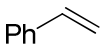 **266** (2 eq.)	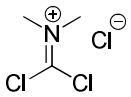 **282** (1.1 eq.)	CH_2Cl_2	1.0M	78%	6%
4	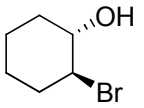 (±)-**287**	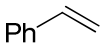 **266** (2 eq.)	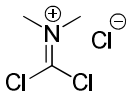 **282** (1.1 eq.)	$CDCl_3$	0.03M	33%[c]	16%
5	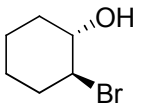 (±)-**287**	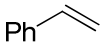 **266** (2 eq.)	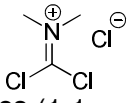 **282** (1.1 eq.)	$CDCl_3$	0.25M	51%[c]	15%
6	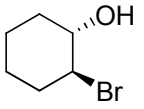 (±)-**287**	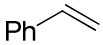 **266** (2 eq.)	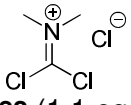 **282** (1.1 eq.)	$CDCl_3$	1.0M	74%[c]	15%

a - combined yield of both "donor" and "acceptor" bromochlorinated products
b - % of bromochlorinated "acceptor" relative to total bromochlorinated product, c - conversion

The above results (Table 21) demonstrate a negligible effect of concentration on the degree of bromonium ion – alkene Br^+ exchange from either of the bromohydrin substrates (**271**/**277** or **287**). Although initially surprising to us, these results could be reasoned by considering the two competing pathways by which the intermediate bromonium ion **273** can react, that

is, by transfer of Br^+ to an alkene molecule (**266**), or by attack and subsequent ring opening by chloride at the benzylic carbon (Scheme 136).

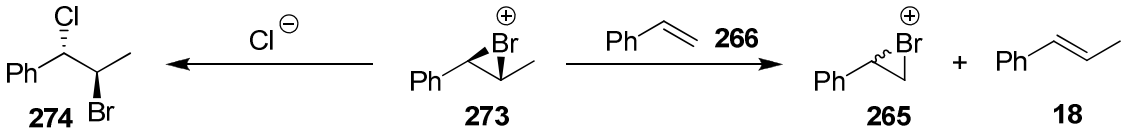

Scheme 136: competing reaction pathways of the bromonium ion

As both pathways involve bimolecular collisions, it is reasonable to propose that increasing the concentration increases both to an approximately equal extent. Therefore, no overall increase in exchange is observed on increasing the concentration of the reaction mixture.

To our knowledge, the only comparable experiments which investigated the effects of concentration on the degree of bromonium ion – alkene Br^+ exchange were undertaken by Rodebaugh and Fraser-Reid in their work on Br^+ exchange in the bromination of ω-alkenyl glycosides (c.f. section *1.2.2.*).[51] Rodebaugh and Fraser-Reid reported that the degree of Br^+ exchange observed in the system had a strong dependence on the concentration of the reaction mixture. However, in their experiments, the nucleophilic attack on the carbons of the bromonium ion was conducted by the solvent (water) which can be assumed to be at constant concentration. Thus, increasing the concentration of the reaction mixture would increase the concentration of alkene relative to the bromonium ion, but not the concentration of the nucleophile. Thus, at higher concentrations the rate of the exchange pathway would increase at the expense of the nucleophilic opening of the bromonium ion, leading to an overall increase in the degree of bromonium ion – alkene Br^+ exchange observed.

4.*2.7. Effects of alkene equivalents on bromonium ion – alkene Br^+ exchange*

The effect of the alkene equivalents added to the rearrangement reaction mixture on bromonium ion – alkene exchange was subsequently investigated (Table 22).

Table 22: effect of alkene equivalents on the degree of exchange observed

Entry	"Donor" bromohydrin	"Acceptor" alkene	reagent	solvent	Conc.	Conversion[a]	Exchange[b]
1	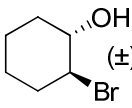 (±)-**287**	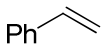 **266** (1 eq.)	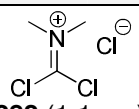 **282** (1.1 eq.)	$CDCl_3$	0.03M	27%	15%
2	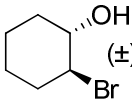 (±)-**287**	**266** (2 eq.)	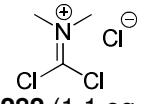 **282** (1.1 eq.)	$CDCl_3$	0.03M	33%	16%
3	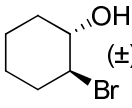 (±)-**287**	**266** (10 eq.)	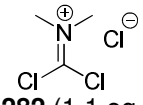 **282** (1.1 eq.)	$CDCl_3$	0.03M	38%	18%
4	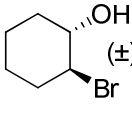 (±)-**287**	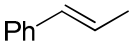 **18** (1 eq.)	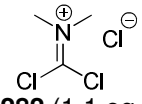 **282** (1.1 eq.)	CH_2Cl_2	0.03M	36%	17%
5	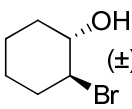 (±)-**287**	**18** (2 eq.)	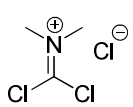 **282** (1.1 eq.)	CH_2Cl_2	0.03M	49%	16%
6	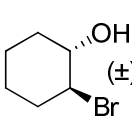 (±)-**287**	**18** (5 eq.)	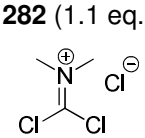 **282** (1.1 eq.)	CH_2Cl_2	0.03M	25%	21%
7	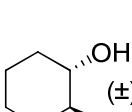 (±)-**287**	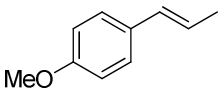 **21** (1 eq.)	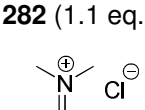 **282** (1.1 eq.)	CH_2Cl_2	0.03M	40%	43%
8	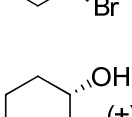 (±)-**287**	**21** (2 eq.)	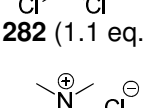 **282** (1.1 eq.)	CH_2Cl_2	0.03M	53%	43%
9	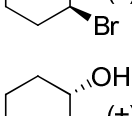 (±)-**287**	**21** (5 eq.)	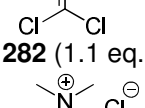 **282** (1.1 eq.)	CH_2Cl_2	0.03M	46%	44%
10	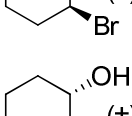 (±)-**287**	**21** (10 eq.)	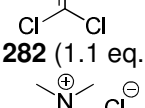 **282** (1.1 eq.)	CH_2Cl_2	0.03M	8%	48%

a - combined yield of both "donor" and "acceptor" bromochlorinated products
b - % of bromochlorinated "acceptor" relative to total bromochlorinated product

The anomalous yield obtained in entry 10 is due to a side reaction of Viehe's salt (**282**) with the electron-rich alkene **21** to give an unidentified byproduct. At ten equivalents of alkene this reaction becomes significant and results in a reduced yield of the bromochlorinated products **288** and **293**. Although small increases in exchange on increased concentration were generally observed for a particular alkene (entries 1-3, 4-6 and 7-10), the dependence of exchange on the equivalents of added alkene was also almost negligible. This result is surprising when compared to the high dependency of the rate of Br^+ transfer on the nature of the "acceptor" alkene and is not easily rationalised. However, it is obvious that the number of productive collisions between bromonium ion and alkene is vastly more dependent on the nucleophilicity of the attacking alkene than its concentration.

4.*2.8. Nucleophilic catalysis of bromonium ion – alkene Br^+ exchange*

Brown's observation that bromide could facilitate Br^+ exchange between bromonium ions and alkenes had previously been noted (section *1.2.2.*)[50]. Brown proposed that this occurred *via* attack of the bromide at the bromine of the bromonium ion and the re-formation of bromine. Thus, it was deemed necessary to consider the possibility of other nucleophiles acting in the same capacity.

Initially, consideration was given to the possibility of chloride attacking the bromide of the bromonium ion to form bromochloride, which could then go on to bromochlorinate the added acceptor alkene. However, adding 5.5 equivalents of Viehe's salt rather than 1.1 (and thus increasing the chloride concentration in the reaction mixture five-fold) led to only a small increase in observed exchange (Table 23).

Table 23: effect of chloride concentration on the degree of exchange observed

Entry	"Donor" bromohydrin	"Acceptor" alkene	reagent	solvent	Conc.	Yield[a]	Exchange[b]
1	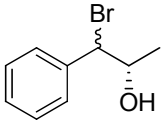 **271/277**	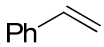 **266** (2 eq.)	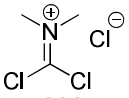 **282** (1.1 eq.)	CH_2Cl_2	0.03M	42%	3%
2	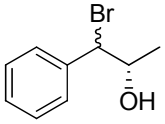 **271/277**	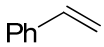 **266** (2 eq.)	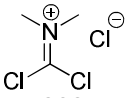 **282** (5.5 eq.)	CH_2Cl_2	0.03M	83%	6%

a - combined yield of both "donor" and "acceptor" bromochlorinated products
b - % of bromochlorinated "acceptor" relative to total bromochlorinated product

The above results demonstrate a small increase in 2-bromo-1-chloro-1-phenylethane (**262**) on increasing the chloride concentration. However, the increase is almost negligible and this, combined with the observation that no dibromide product was observed in the crude product (which would be expected, as a result of the BrCl/ Br_2 + Cl_2 equilibrium, if BrCl was present in the reaction mixture), allowed the nucleophilic attack of chloride on Br^+ to be ruled out as a significant mechanism of exchange.

We were also intrigued to determine whether our bromination catalysts could act as nucleophilic catalysts for the transfer of Br^+ between alkenes and, consequently, whether or not transfer of Br^+ from our catalyst to an alkene was reversible. Thus, a selection of exchange experiments were conducted with a catalytic amount of *iso*-amarine (**116**) and IBAM (**113**) added.

Table 24: effect of added bromination catalyst on the degree of exchange observed

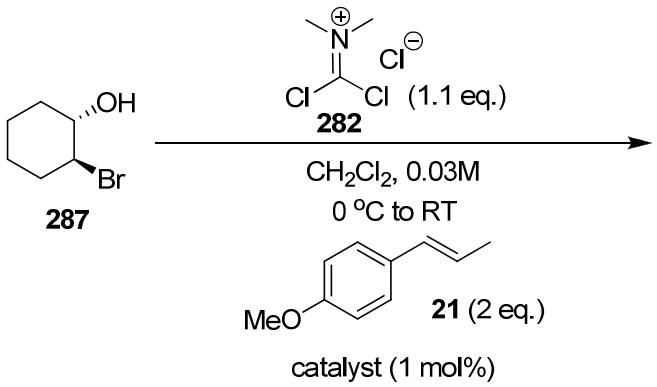

Entry	Catalyst	Conversion[a]	Exchange[b]
1	control	53%	43%
2	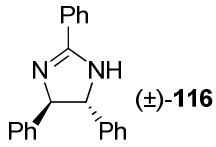 (±)-**116**	69%	45%
3	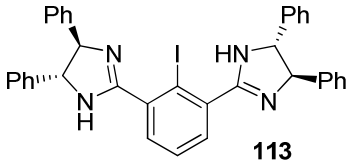 **113**	59%	42%

a - combined yield of both "donor" and "acceptor" bromochlorinated products
b - % of bromochlorinated "acceptor" relative to total bromochlorinated product

It is apparent that addition of either of the bromination catalysts, **116** or **113**, did not increase the rate of Br^+ exchange. Thus it can be concluded that, at least under these conditions, transfer of Br^+ from a bromonium ion to alkene is considerably more facile than transfer of Br^+ to our bromination catalysts. This indicates that in our catalytic system bromine transfer from catalyst to alkene may be irreversible, dispite bromonium ion to alkene bromine transfer being rapid.

4.2.9. Modifications to the leaving group; Lepore's arylsulfonate[125]

Although it had been demonstrated that exchange was considerably increased by employing a fully aliphatic bromonium ion and a more electron-rich alkene acceptor, we were still not observing the rapid Br^+ exchange that is occurring in our catalytic system. After considering

the earlier investigations into the variables of our system, it was hypothesized that the major limiting factor to exchange may be the nature of the rearrangement itself. While this is promising in terms of utilizing the rearrangement in asymmetric synthesis (the stereochemistry of the starting material being preserved in the product under the majority of conditions), this is undesirable for our purposes of studying bromonium ion – alkene Br^+ exchange.

It was proposed that two characteristics of the rearrangement may be resulting in a reduction in the observed Br^+ exchange. Firstly, the nucleophilicity of the chloride is considerably greater than that of the nucleophiles (e.g. water, alcohol, carboxylic acid, sulfonate) that have been used to trap bromonium ions in reactions where exchange has been reported to be significant. Secondly, the mechanism of the rearrangement is likely to occur *via* a tight ion pair within a solvent sphere (Scheme 137): a chloride ion will be closely associated with the positively charged Vilsmeier-type leaving group (**283**) and thus will be in close proximity to rapidly trap the newly formed bromonium ion (**273**).

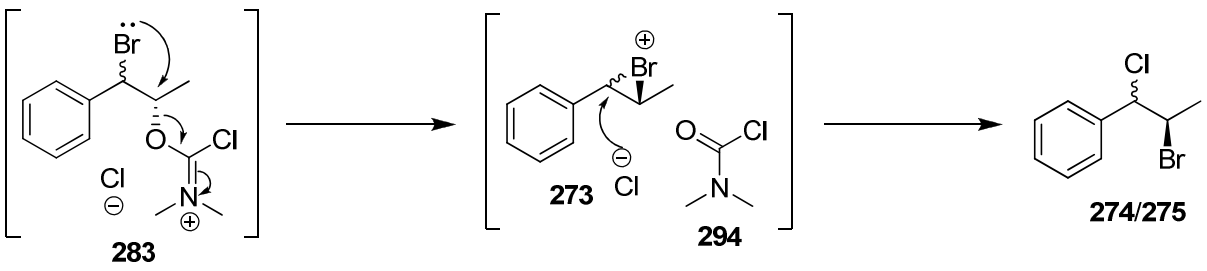

Scheme 137: rearrangement and opening of the bromonium ion 273 within a solvent sphere

Thus, attention was turned to the investigation of the effect of modifying the nature of both the leaving group and the nucleophile used to open the bromonium ion intermediate.

Lepore's work on the use of arylsulfonate leaving groups and their formation of alkyl chlorides on reaction with titanium tetrachloride[125] (Scheme 138) was attractive to us for use within our system. Lepore *et al* formulated an aryl sulfonate-based nucleophile assisted leaving group containing a polyether unit attached to the aryl ring, *ortho* to the sulfonate. It was proposed that the polyether and sulfonate oxygens strongly chelated to the titanium (IV), thus stabilizing the developing negative charge on the leaving group in the transition state. Lepore *et al* reported greatly accelerated rates for the reaction of metal halides with

such modified arylsulfonate leaving groups. Furthermore, it was also reported that the reaction of secondary arylsulphonates such as **295** with titanium tetrachloride proceeded with exclusive retention of configuration *via* a proposed S_Ni-type mechanism.

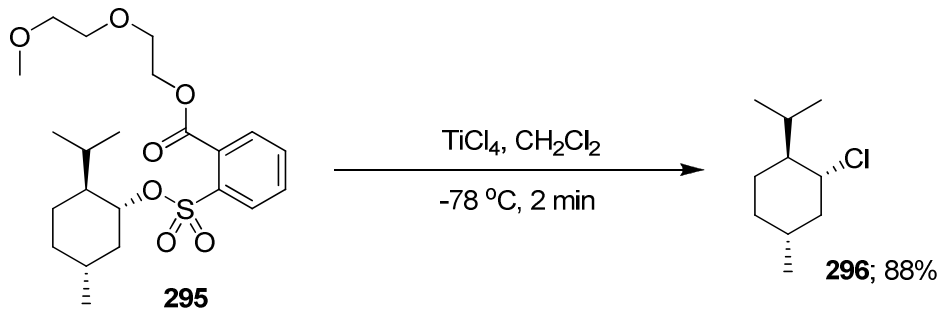

Scheme 138: representative example of S_Ni-type substitution of Lepore's arylsulphonate leaving group[125]

It was envisaged that use of Lepore's leaving group, with a chelating cation to facilitate its loss, could be an advantageous modification to our system for a number of reasons;

(1) The product distribution allows the investigation of the rate of bromonium ion formation. Lepore reports the full conversion of arylsulphonate to the corresponding chloride in less than two minutes at -78 ºC. We were curious to determine whether, when using analogous conditions with our substrate, we obtained the S_Ni-type product, **298**, or the rearranged bromochloride, **274**.

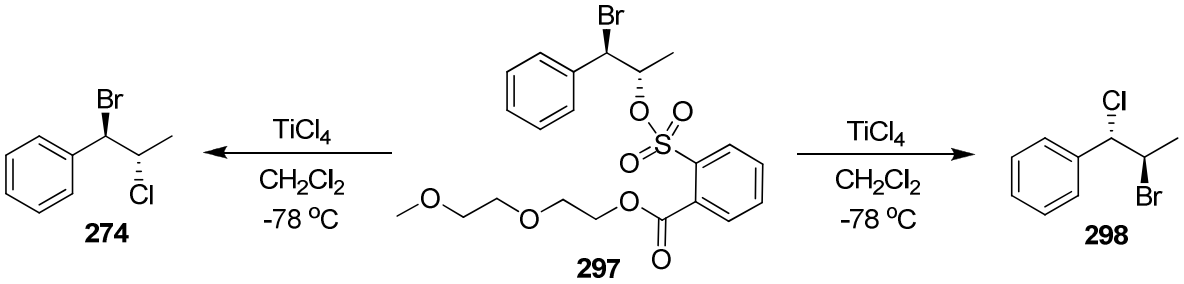

Scheme 139: possible outcomes for the reaction of arylsulphonate 297 with titanium tetrachloride

(2) The use of the arylsulfonate leaving group allows us to switch from a positively charged activated bromohydrin intermediate **283** when using Viehe's salt to a neutral reactive species **297**. The neutral species should, in theory, be less closely associated with the nucleophile anion and should lead to slower trapping of the bromonium ion. This, in turn,

may result in increased exchange of Br^+ from bromonium ion to alkene, facilitating our study of the phenomenon.

(3) All previous concerns regarding the transfer of Br^+ *via* attack of chloride to form BrCl are negated in this system; all chloride should be bound to the strongly lewis acidic titanium (IV), until released by coordination of a lone pair of the sulfonate oxygen to the titanium.

(4) The option is introduced of varying both the counterion and the nucleophile by changing the salt added to promote the loss of the leaving group. Screening of such salts would be of interest with respect to both the S_Ni (**298**) versus rearranged (**274**) product distribution and to the degree of bromonium ion – alkene Br^+ exchange.

The aryl sulfonyl chloride precursor (**300**) to Lepore's leaving group was accordingly synthesised and coupled to the chiral bromohydrin **271**/**277** (Scheme 140).

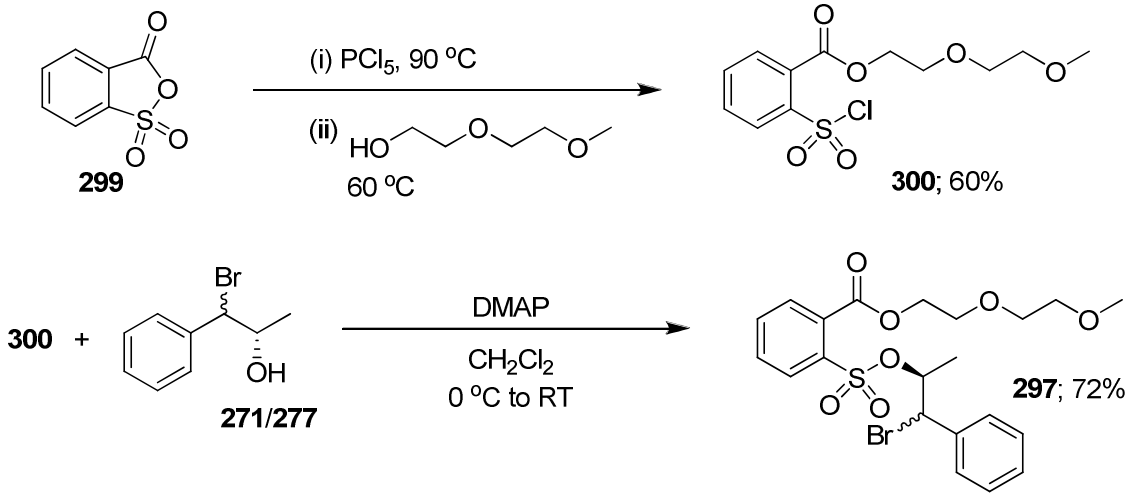

Scheme 140: synthesis of chiral bromosulphonate 297

The bromosulphonate **297** was then subjected to Lepore's S_Ni substitution conditions with surprising results (Scheme 141).

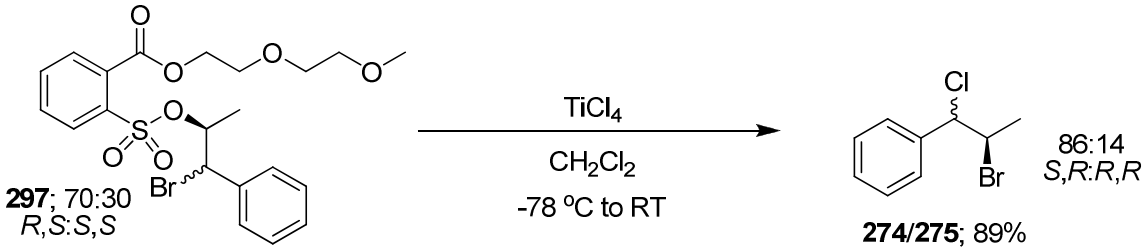

Scheme 141: reaction of bromosulphonate 297 under Lepore's conditions for S_Ni substitution

The reaction of our substrate, **297**, proceeded considerably more slowly than those reported by Lepore *et al*; TLC analysis demonstrating incomplete conversion of starting material after stirring at -78 ºC for 1.5 h. However, after allowing the reaction mixture to gradually warm to room temperature, full consumption of starting material was observed. After work up, the product mixture proved to consist entirely of the rearranged bromochloride **274**/**275**, with no evidence of any product of an S_Ni-type substitution (**298**). Furthermore, HPLC analysis revealed bromochloride **274**/**275** to be completely enantiopure (>99% ee, Figure 83)

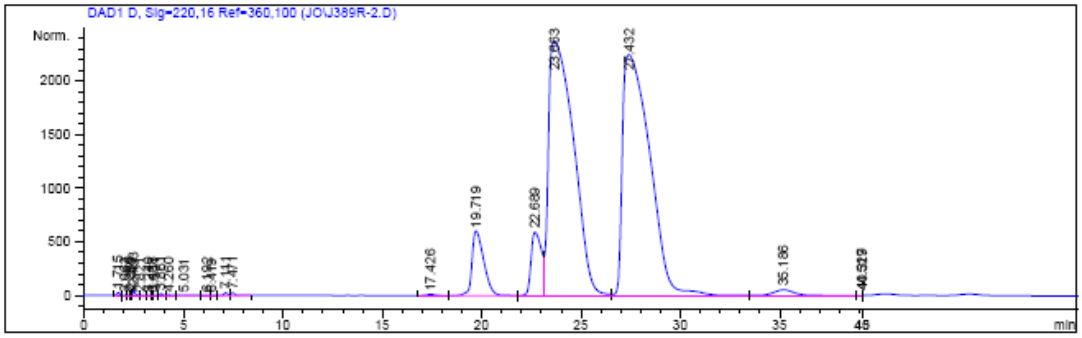

Figure 82: chiral HPLC trace demonstrating separation of diastereomers and enantiomers of (±)-2-bromo-1-chloro-1-phenylpropane (274/275)

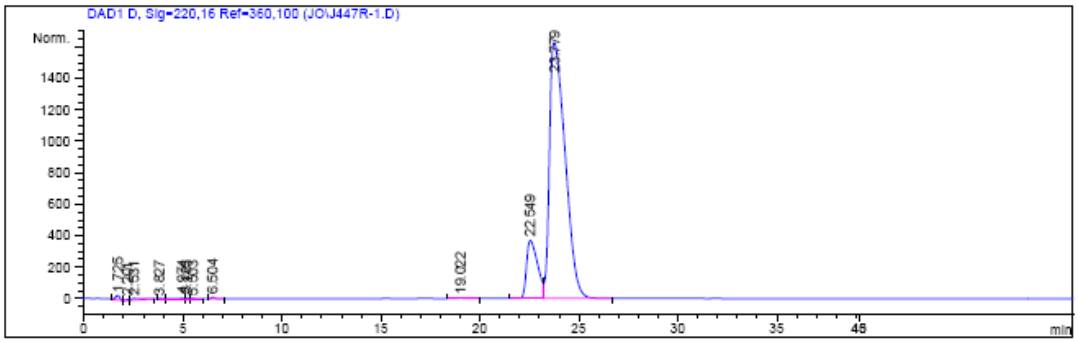

Figure 83: chiral HPLC trace of (*R*)-2-bromo-1-chloro-1-phenylpropane (274/275) product from bromosulphonate 297 under Lepore's conditions

Thus, we have demonstrated an extremely facile, efficient and, above all, enantiospecific rearrangement *via* a chiral bromonium ion. This represents an unprecedented method for generating an enantiopure bromonium ion in a controlled fashion; a potentially powerful synthetic tool.

As bromohydrin **271**/**277** represented a significant deviation from Lepore's published results, it was decided to investigate how necessary the polyether chain was to the loss of the leaving group. Due to the neighbouring group assistance of the bromine, it was hypothesized that it may be possible to conduct the rearrangement *via* the reaction of a

simple arylsulphonate substrate with titanium tetrachloride. Accordingly, the bromotosylate **281** was subjected to Lepore's conditions and quantitative conversion of **281** to the rearranged bromochloride product was observed (Scheme 142).

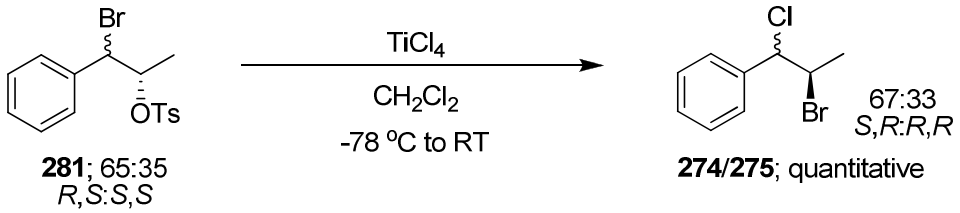

Scheme 142: reaction of bromotosylate 297 under Lepore's conditions

Although the product mixture demonstrated a few minor impurities (unlike the product of the reaction of the polyether functionalised leaving group), HPLC analysis demonstrated the bromochloride **274**/**275** to also be enantiopure.

Attention was then turned to investigation of the effects on conducting the rearrangement in the presence of alkene. On the addition of two equivalents of *trans*-β-methylstyrene (**18**) to the reaction mixture (Scheme 143) bromochloride **274**/**275** was still obtained in >99% ee.

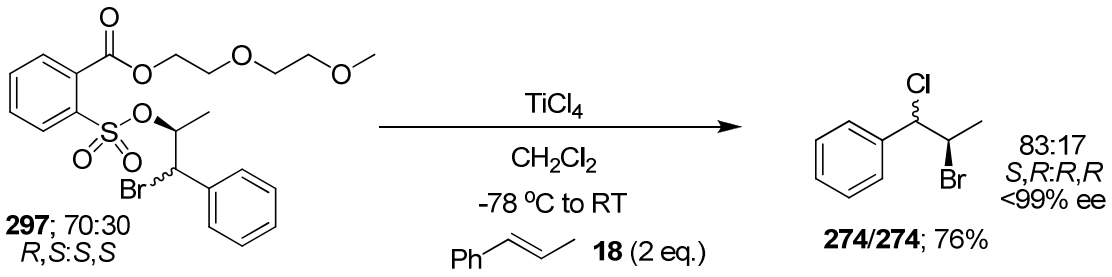

Scheme 143: rearrangement in the presence of *trans*-β-methylstyrene (18)

Subsequent rearrangement of the bromosulfonate **297** in the presence of two equivalents of styrene (**266**, Scheme 144) demonstrated the absence of any bromochlorinated styrene in the crude product mixture and thus confirmed that no Br^+ exchange was occurring in the reaction mixture.

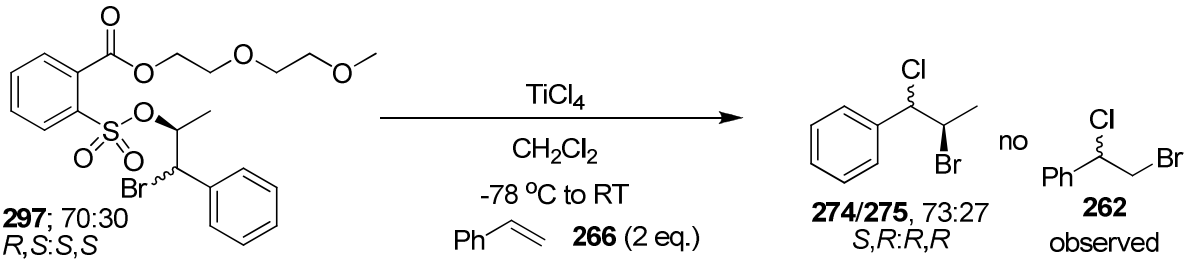

Scheme 144: rearrangement in the presence of styrene (266)

It is proposed that under Lepore's reaction conditions the delivery of chloride is equally or more rapid than in the rearrangement induced by Viehe's salt. Thus, the bromonium ion is trapped to form the bromochloride product before any transfer of Br^+ to an alkene can occur.

4.3. Can Br^+ exchange be inhibited in order to improve the enantioexcess produced in our catalytic bromination reaction?

Finally, our findings from our study of exchange were applied back to our asymmetric catalytic electrophilic bromination reaction. On considering the final question posed at the start of chapter 4; "Can Br^+ exchange be inhibited in order to improve the enantioexcess produced in our catalytic bromination reaction?", it would appear that it can be answered in the affirmative. From earlier conclusions, it is proposed that a well considered choice of alkene substrate, nucleophile and solvent would facilitate a decrease in Br^+ exchange and consequently a rise in the enantioselectivity of the reaction.

A substrate should be selected which will, when brominated, exist as a weakly bridged bromonium ion or an open β-bromocarbonium ion. It has been established that increased β-bromocarbonium ion character of a bromonium ion reduces its capacity to transfer Br^+ to an alkene molecule and, thus, choice of such a substrate will reduce exchange. However, it is imperative that chirality is not exclusively introduced at the carbocation centre, due to the reduced stereocontrol of nucleophilic attack at this position compared to that of a symmetrical bromonium ion. As such, *trans*-β-methylstyrene (**18**) is an ideal substrate for asymmetric bromination, due to the introduction of chirality at both the α- and β- carbons. The bromonium ion intermediate (**285**) has significant benzylic carbocation character

(Scheme 145), resulting in some degree of stereochemical scrambling at the α-carbon. However, the stereochemistry is fully retained at the β-carbon.

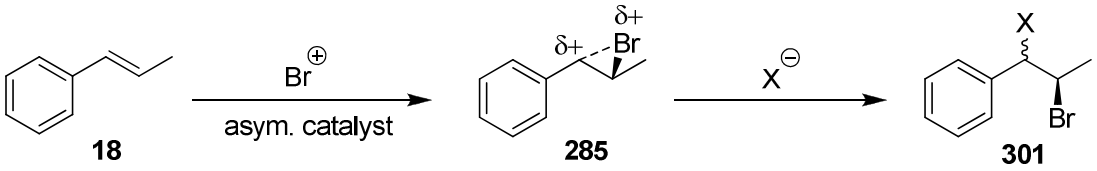

Scheme 145: proposed asymmetric bromination of *trans*-β-methylstyrene (18)

It is also hypothesized that the use of a more potent nucleophile (X^-) to open the bromonium ion than the previously employed carboxylic acid may reduce the bromonium ion's lifetime and thus the degree of Br^+ transfer observed.

A reaction had previously been developed in the Braddock group which appeared to present us with the means to fulfil both of these criteria. Kwok had reported[121] the efficient and regioselective bromochlorination of styrene using NBS, trimethylsilylchloride (TMSCl) and a catalytic amount of *iso*-amarine (**116**), IAM (**111**) or IBAM (**113**) (Scheme 146).

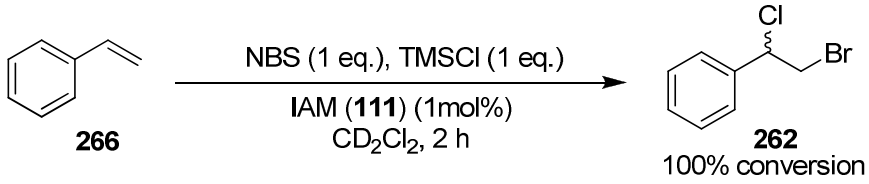

Scheme 146: catalytic bromochlorination of styrene

The reaction was proprosed to proceed *via* the nucleophilic attack of the catalyst **116** on NBS (**226**) to form the brominated catalytic intermediate **117** (Scheme 147). This then delivers bromine to the alkene (**266**) and the succinimide anion picks up a trimethylsilyl group from TMSCl. The liberated chloride subsequently attacks the bromonium ion (**265**) regiospecifically to form the bromochlorinated product **262**.

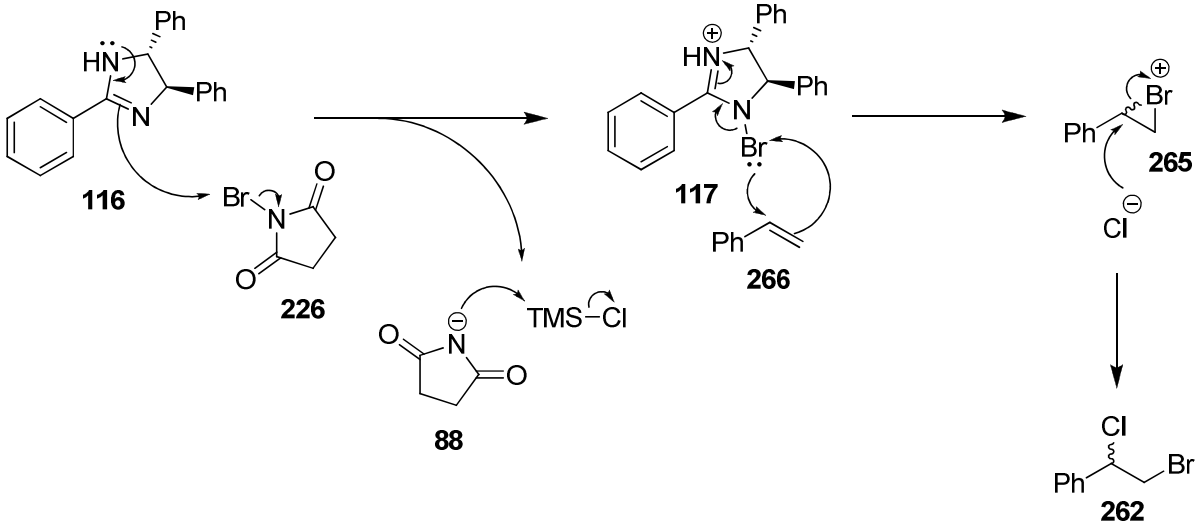

Scheme 147: original proposed mechanism for the bromochlorination of styrene (266)

We demonstrated this bromochlorination to be both repeatable and applicable to a range of alkene substrates (Table 25). The method was used routinely to prepare authentic racemic bromochlorides for NMR and HPLC analysis.

Table 25: catalylic bromochlorination of alkenes

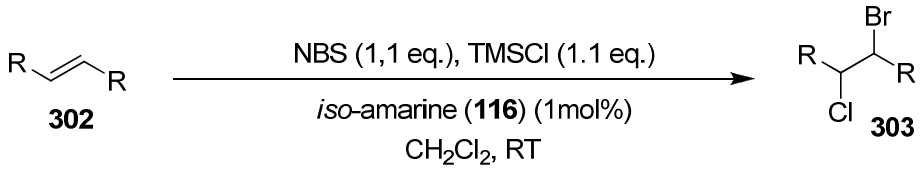

Entry	Alkene starting material (**302**)	Bromochlorinated product (**303**)	Yield
1	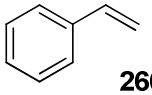 **266**	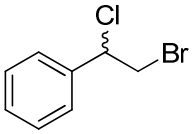 **262**	90%
2	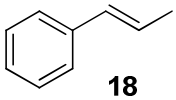 **18**	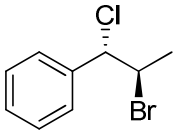 (±)-**274**	66%
3	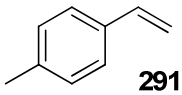 **291**	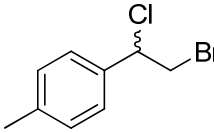 **292**	95%
4	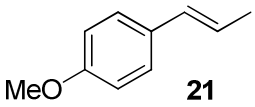 **21**	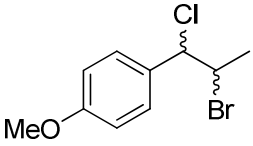 **293**	Quantitative

It was hypothesized that the IBAM (**113**) - catalysed bromochlorination of *trans*-β-methylstyrene (**18**) presented an excellent candidate for the implementation of our findings from the exchange studies. This reaction was accordingly conducted at -78 ºC and the enantiomeric excess of the bromochlorinated product **274**/**275** was analysised by chiral HPLC (Scheme 148).

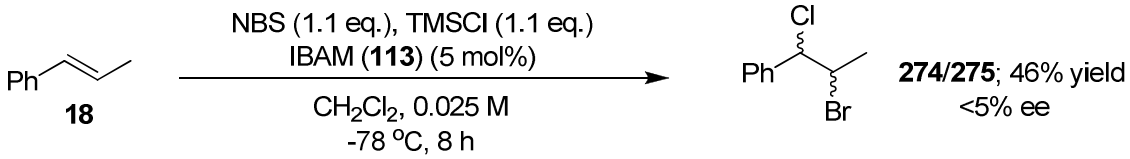

Scheme 148: attempted asymmetric bromochlorination of *trans*-β-methylstyrene (18)

Disappointingly, racemic 2-bromo-1-chloro-1-phenylpropane (**274**/**275**) was obtained, bromine transfer to the alkene occurring with no asymmetric induction.

However, studies into the uncatalysed background reaction of the bromochlorination led us to doubt the originally posed mechanism of bromination *via* an active catalyst-Br^+ intermediate (Scheme 147). The reaction of *trans*-β-methylstyrene (**18**) with NBS and TMSCl in the absence of catalyst demonstrated the slow conversion of alkene to exclusively the bromochloride product (entry 1, Table 26). This presumably occurs by bromination of the alkene directly by NBS, subsequent silylation of the succinimide anion and attack of chloride on the bromonium ion.

Table 26: Studies into the effect of catalyst and chloride source

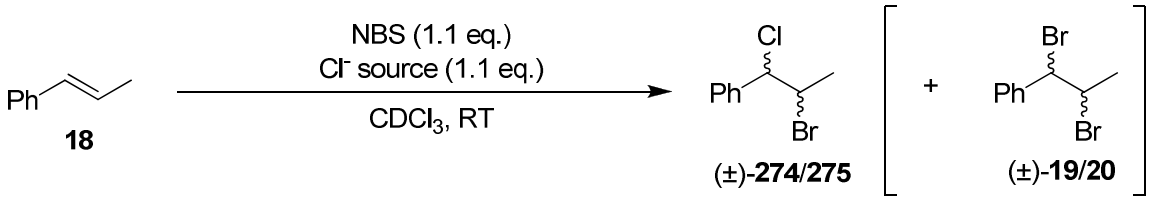

Entry	Chloride source	Catalyst	Conversion[a]	**274**/**275** : **19**/**20** ratio
1	TMSCl	–	25 min: 3%	100 : 0
			2h 25 min: 15%	100 : 0
2	TMSCl	*R*-IBAM (**113**) (5 mol%)	25 min: 43%	80 : 20
			2h 25 min: 71%	83 : 17
3	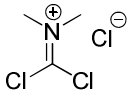 **282**	–	20 min: 87%	85 : 15
4	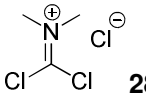 **282**	*R*-IBAM (**113**) (5 mol%)	20 min: 93%	90 : 10

a – conversion of *trans*-β-methylstyrene (**18**) to bromochloride (**274**/**275**) and dibromide (**19**/**20**)

However, all catalysed bromochlorinations demonstrated a considerable amount of dibromide **19**/**20** in the crude product mixture (up to 17%; entries 2 and 4, Table 26). On investigating the use of free, anionic sources of chlorine in the absence of catalyst (entry 3, Table 26), not only a similar rate of bromochlorination was observed to that obtained in the NBS/TMSCl/catalyst system, but also a similar product distribution.

Thus, an alternative mechanism for Kwok's catalytic bromochlorination of alkenes is proposed, involving the release of free chloride by IBAM (**113**) *via* the nucleophilic attack of the amidine on TMSCl (Scheme 149). This then goes on to attack the electrophilic bromine of NBS, forming BrCl, and this is the reactive species which then goes on to brominate the alkene.

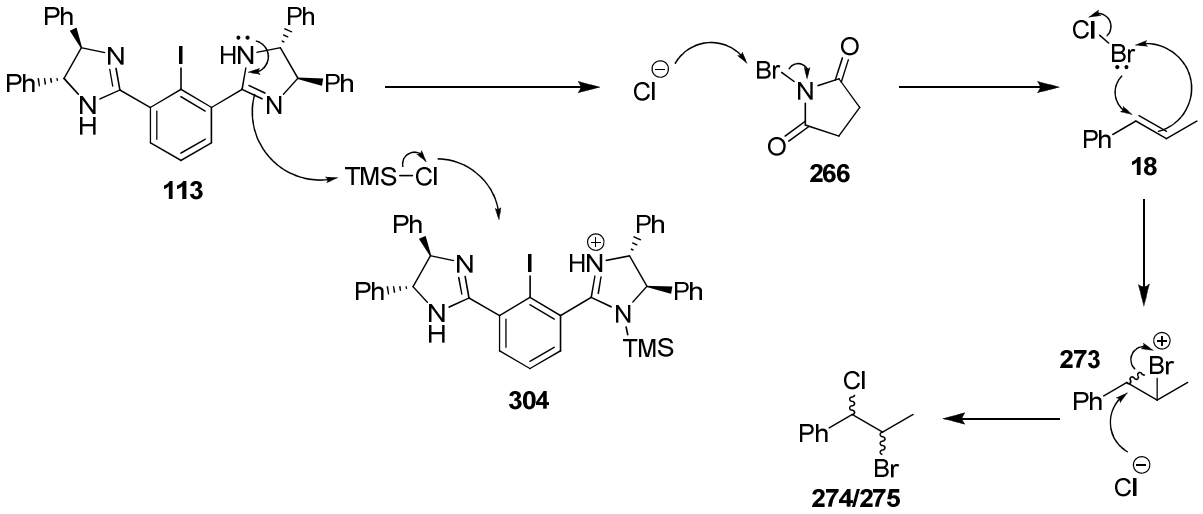

Scheme 149: revised mechanism for the catalytic bromochlorination of alkenes

The dibromide **19**/**20** formation originates from the generation of molecular bromine *via* the equilibrium;

$$2BrCl \rightleftharpoons Br_2 + Cl_2$$

This proposed mechanism is also in agreement with Kwok's observation that the rate of reaction decreases on transition from the use of TMSCl to TESCl and finally to TIPSCl as the chloride source. As the bulk of the alkyl groups around the silicon atom increases, the attack of the catalyst on the silicon becomes more sterically encumbered and thus slower, reducing the rate of reaction.

Thus, in this instance, it is proposed that IBAM (**113**) is acting as a nucleophilic catalyst to release chloride rather than catalytically delivering Br^+ to the alkene. Therefore, it is not surprising that bromine is delivered with no enantioselectivity in our catalytic reaction, as the active brominating species (BrCl) is achiral.

4.4. Conclusion

Bromonium ion – alkene exchange has been identified as a dominant and important factor in our catalytic asymmetric bromination reaction of alkenes. In order to study such a phenomenon in an asymmetric context, a method for the controlled generation and subsequent trapping of the first example of an enantiopure bromonium ion has been developed *via* the rearrangement of enantiopure bromohydrin **271**/**277**. Subsequent investigations into bromonium ion – alkene exchange have demonstrated that whilst concentration and alkene equivalents have little impact on the degree of Br^+ exchange occurring in our system, the structure of the "donor" bromonium ion and the "acceptor" alkene exert a profound effect. The solvent and the leaving group employed for the rearrangement have also been demonstrated to have some impact on the degree of exchange observed.

From our findings, it can be concluded that the generation of an enantiopure, aliphatic bromonium ion will best facilitate our study of the stereochemical consequences of exchange. An enantiopure, aliphatic bromonium ion should demonstrate a considerably greater propensity for Br^+ transfer to added alkene than our enantiopure bromonium ion generated from (2*S*)-1-bromo-1-phenylpropan-2-ol (**271**/**277**). Thus, any racemisation resulting from bromonium ion – alkene exchange should be observed in the rearranged product and be detectable by chiral HPLC. Conversely, the most appropriate choice of substrate for an asymmetric catalytic bromination reaction is an alkene which generates a highly asymmetric bromonium ion; a high degree of β-bromocarbonium ion character having been shown to decrease the degree of exchange observed.

4.5. Further work

4.4.1. Bromonium ion –alkene Br^+ exchange

Lepore's leaving group has, to date, only been applied to our (2*S*)-1-bromo-1-phenylpropan-2-ol (**271**/**277**) substrate; a substrate which only demonstrated a small degree of exchange on reaction with Viehe's salt due to the high β-bromocarbonium ion character of the intermediate bromonium ion. Further work will apply Lepore's method to an aliphatic

bromosulphonate **305** and investigate Br^+ exchange from the bromonium ion generated in its rearrangement.

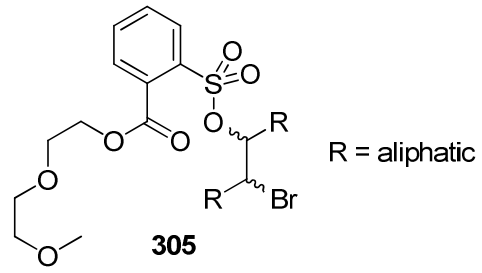

Figure 84: aliphatic bromosulphonate (305)

The synthesis of a chiral, enantiopure, aliphatic bromohydrin **306** will also be undertaken. From our findings, it is proposed that this substrate and its rearrangement using either Lepore's conditions or Viehe's salt (**282**) should allow a definitive study of the stereochemical consequences of bromonium ion – alkene Br^+ exchange.

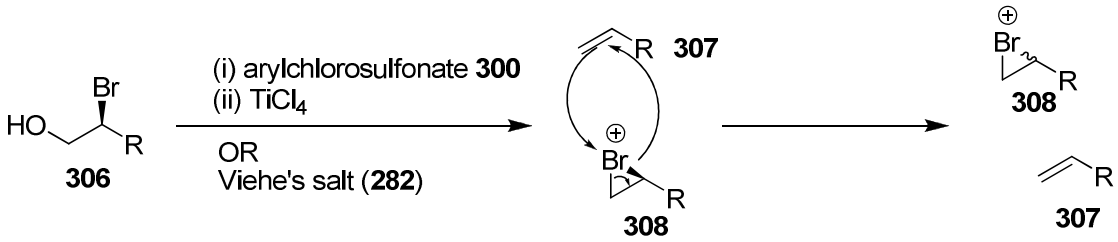

Scheme 150: Br^+ exchange in a chiral, aliphatic system

Further work may also be undertaken to fully realise the potential of the stereoselective rearrangement of bromohydrins using Lepore's arylsulphonate leaving group. This method of generating and trapping an enantiopure bromonium ion could, in theory, be utilized to form a wider selection of enantiopure brominated products *via* trapping the bromonium ion with other nucleophiles. This is easily achieved by simply varying the metal salt added to promote the explusion of the leaving group to include additives with different anionic components. Furthermore, if the metal salt has a non-coordinating anion (e.g. triflate) the bromonium ion could be opened by an internal nucleophile in an intramolecular cyclisation. Lepore had already demonstrated that lithium cations are excellent chelators of the polyethylene side chain of Lepore's sulphonate.[125] Thus, lithium triflate should be an appropriate choice of metal salt for leaving group activation when attack of an internal nucleophile is desired. An example of the application of such methodology is the formation of the enantiopure bromonium ion **310** *via* the action of lithium triflate on the sulphonate

leaving group in **309** (Scheme 151).[126] The bromonium ion would then promote diastereoselective polyene cyclisation to give enantiomerically pure product **311**.

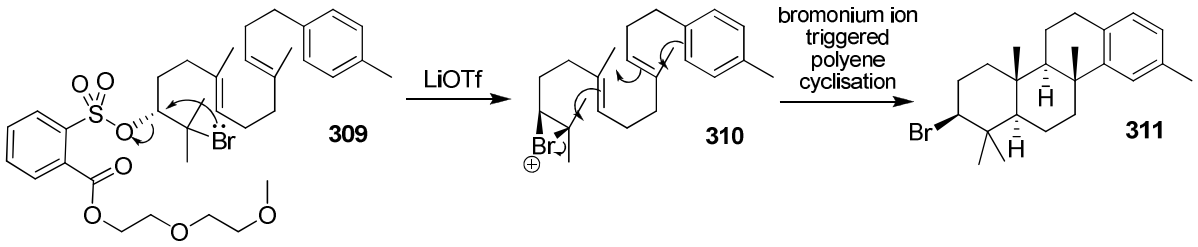

Scheme 151: enantiopure bromonium ion triggered polyene cyclisation

This would not only test the wider applicability of our generation of an enantiopure pure bromonium ion in a controlled fashion, but it would also form the basis of an asymmetric approach to a range of natural products (**312**-**315**, Figure 85).

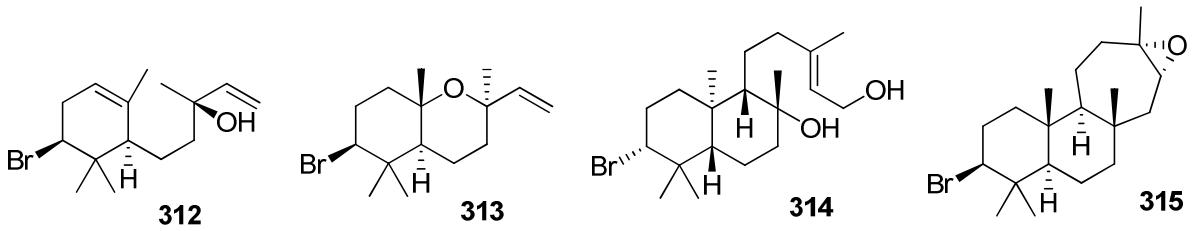

Figure 85: examples of natural products possessing the α,α-dimethylcyclohexyl bromide moiety

4.4.2. Catalytic Asymmetric Electrophilic Bromination of Alkenes

Whilst initial attempts to make an educated modification of the substrate and nucleophile in our catalytic asymmetric bromination failed (section 4.3), the theory behind such a strategy is still sound. Based on our previous findings, possible attractive substrates include alkenoic acids such as **316** (Scheme 152), which should display a considerably lower rate of Br^+ exchange due to a high degree of β-bromocarbonium ion character in the intermediate bromonium ion **317**.

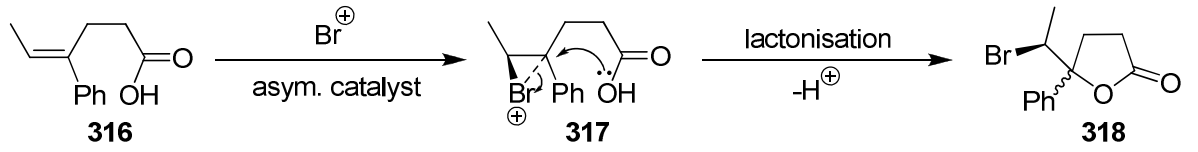

Scheme 152: favourable substrate for catalytic asymmetric bromolactonisation

Another possible modification of the substrate is to make the transition from alkenoic acids (**61b**) to alkenols (**60b**). The more nucleophilic alcohol moiety should attack the bromonium ion intermediate more rapidly and thus ring closure will compete more effectively with Br^+ transfer.

Figure 86: representative alkenoic acid (61b) and alkenol (60b)

The possibility of the addition of a nucleophile to open the bromonium ion can also be explored in more detail. It would seem favourable in the light of our findings in our exchange studies to include a powerful nucleophile to rapidly trap the bromonium ion as it is formed. However, our initial experiments in implementing this proposal revealed competition between the attack of the added nucleophile with the attack of the asymmetric catalyst on the electrophilic bromine of NBS. This was identified as a problem in our catalytic bromochlorination system, where the active electrophilic brominating species was the achiral BrCl, resulting in no enantioselectivity in the bromination. Thus, it appears imperative to strike a balance in the potency of the nucleophile to facilitate the rapid opening of the bromonium ion but to minimise its attack on the electrophilic bromine of NBS or the catalyst-Br^+ species (Figure 87).

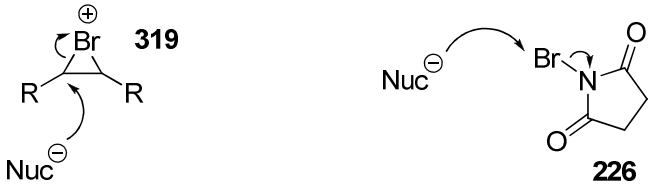

Figure 87: possible modes of nucleophilic attack with our catalytic bromination reaction

It is possible that the selection of a “hard” nucleophile may favour attack at the carbon center of a bromonium ion rather than at “softer” electrophilic bromine. Thus, a good selection of nucleophile in further investigations may include anionic oxygen nucleophiles such as acetate or tosylate.

The association of the nucleophile with the catalyst itself is also hypothesized as being a favourable modification. This, in theory, should facilitate the rapid delivery of the nucleophile to open of the bromonium ion immediately after its formation. Therefore, the mono- and bis-

salts of IBAM (**320** and **321**, Figure 88) will be investigated as potential catalysts, incorporating such catalyst – nucleophile association.

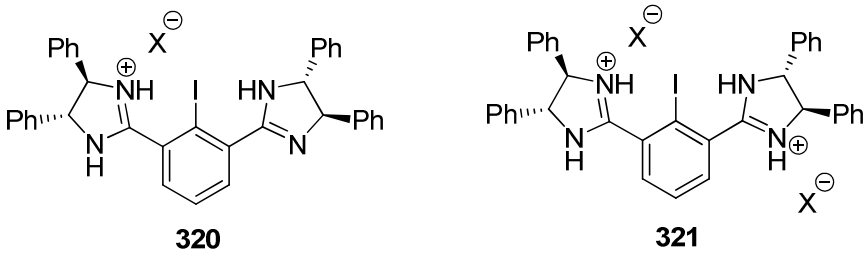

Figure 88: mono- and bis- salts of IBAM

Although *N*-functionalisation of the catalyst has been attempted and failed to produce any increase in the enantioselectivity of the reaction, other modifications to IBAM (**113**) are also possible to promote I(III)-Br over N-Br bond formation. The introduction of electron donating groups, such as methoxy, *para* to the iodine on the benzene ring core of the catalyst should increase the iodine's nucleophilicity (Figure 89). Consequently, the iodine's capacity to attack bromine on the amidine nitrogen in the oxidative addition to form the N-I(III)-Br bond should also be increased. Additionally, the hypervalent N-I(III)-Br intermediate should be stabilised due to the additional electron density placed on the electron deficient hypervalent iodine.

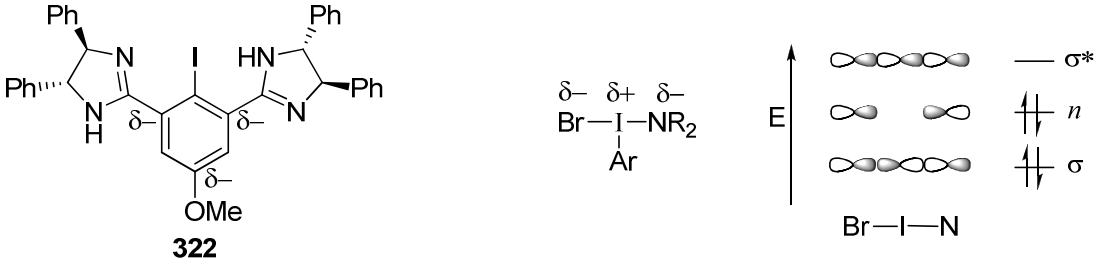

Figure 89: stabilisation of hypervalent iodine by increasing electron density on iodine

5. Conclusion

Over the course of our research, the competitive non-asymmetric delivery of bromine to the substrate *via* an N-Br catalytic intermediate has been identified as a significant factor leading to a depreciation of the enantioselectivity of the asymmetric bromination reaction. This phenomenon is dependent on the catalyst loading; an optimum in the asymmetric induction of the bromination being reached at a loading of 5 mol%.

The exchange of Br^+ between asymmetrically formed chiral bromonium ions and unreacted alkene starting material has also been proposed and investigated as a mechanism by which the enantioexcess of the isolated product is reduced. Investigations into this phenomenon have demonstrated the extent of such exchange to be dependent on the structure of both the “donor” bromonium ion and the “acceptor” alkene. The proximity of the nucleophile to the bromonium ion upon its generation is also proposed to have a significant impact on the degree to which exchange is observed. Any further modifications made to our asymmetric catalytic bromination system should be made with consideration of these factors.

6. Experimental Section

6.1. General Information

Analytical Methods: Melting points were recorded on a Reichart Thermovar melting point apparatus and are uncorrected. Optical rotations were recorded on a Perkin-Elmer 241 polarimeter with a path length of 1 dm using the 589.3 D-line of sodium. Solutions were prepared using spectroscopic grade solvents and concentrations (*c*) are quoted in g/100 mL. Fourier transform infra-red (IR) spectra were recorded as thin films on NaCl plates using a Mattson 500 FT IR spectrometer. ^{1}H NMR were recorded at 270 MHz on a Jeol GSX-270 spectrometer, 300 MHz on a Bruker DRX-300 spectrometer, 400 MHz on either a Bruker DRX-400 spectrometer or a Bruker AV-400 spectrometer and 500 MHz on a Bruker AV-500 spectrometer. ^{13}C NMR were recorded at 68 MHz on a Jeol GSX-270 spectrometer, 75 MHz on a Bruker DRX-300 spectrometer, 100 MHz on either a Bruker DRX-400 spectrometer or a Bruker AV-400 spectrometer and 125 MHz on a Bruker AV-500 spectrometer. Spectra recorded at 500 MHz (^{1}H NMR) and 125 MHz (^{13}C NMR) were performed by the Imperial College Department of Chemistry NMR Service. NMR samples were run in the indicated solvents ane were referenced internally. All chemical shift values are quoted in parts per million (ppm) and coupling constants quoted in Hz. The following abbreviations are used for the multiplicity of NMR signals: br = broad, s = singlet, d = doublet, dd = doublet of doublets, t = triplet, dt = doublet of triplets, m = multiplet. Low Resolution Mass Spectra (MS) [EI, CI, ES and FAB] and High Resolution Mass Spectra (HRMS) were recorded by the Imperial College Department of Chemistry Mass Spectroscopy Service. GC-MS spectra were recorded on a HP 5890 Series II gas chromatograph and HP 5972 MS detector with a HP 5 MS column (30 m, i.d. 0.25 mm, film µm). HPLC was performed on a HP-1100 liquid chromatograph. All elution times are stated in minutes. X-ray crystal structure was obtained at Imperial College Crystallographic Service using an OD Xcalibur 3 diffractometer or an OD Xcalibur PX Ultra diffractometer. Microanalyses were performed by Mr. S. Boyer at London Metropolitan University, UK.

Experimental Procedures: Analytical thin-layer chromatography (TLC) was carried out on silica gel $F_{254/366}$ 60 Å plates with visualisation using UV light (254 nm) or potassium permanganate as appropriate. Chromatography was performed using BDH 33-70 µm grade silica gel. Air and moisture sensitive reagents were transferred *via* syringe or cannular and

reactions involving these materials were carried out in oven dried flasks under a positive pressure of nitrogen.

Solvents: Dichloromethane was distilled from calcium hydride. Diethylether was distilled from sodium/benzophenone. THF was distilled from potassium/benzophenone. Ethanol was distilled from and stored over 4 Å molecular sieves. Chloroform and deuterated chloroform were stored over potassium carbonate. All other solvents were used as received. Petrol refers to BDH Anal® petroleum spirit 40-60 °C. Water refers to distilled water.

Materials: *N*-Bromosuccinimide was purified by re-crystallisation according to standard procedures.[127] Triethylamine was distilled under nitrogen and stored over sodium hydroxide pellets. Benzoyl chloride and benzaldehyde were distilled under nitrogen before use. (*R*)- and (*S*)-mandelic acid was recrystalised from chloroform. All other reagents were used as received. 4-Phenylpent-4-enoic acid (**216**) was prepared in house by Gemma Cansell.

6.2. Synthesis and Resolution of 1,2-Diphenylethylenediamine

cis-4,5-Dihydro-2,4,5-triphenyl-1*H*-imidazole (amarine) (161)

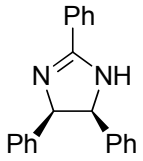

Benzaldehyde (96 mL, 950 mmol) and hexamethyldisilazane (240 mL, 1.15 mol) were stirred at 120 °C under an inert atmosphere of nitrogen with a catalytic amount of benzoic acid (575 mg, 4.7 mmol). After 24 h, crude ^{1}H NMR analysis of a sample removed from the reaction mixture indicated the reaction had gone to completion, with only trace amounts of benzaldehyde and the imine intermediate remaining. On cooling to RT an amorphous yellow solid formed and the entire mixture was taken up in toluene (500 mL). The organic phase was washed with saturated aqueous sodium hydrogen carbonate (2 × 250 mL), water (250 mL), brine (250 mL), dried ($MgSO_4$), filtered and concentrated *in vacuo*. The resulting residue was purified by re-crystallisation from toluene/diethyl ether to yield *cis*-4,5-dihydro-

2,4,5-triphenyl-1*H*-imidazole (**161**) (57 g, 61%) as a white crystalline solid with spectral data consistent with literature:[128] m.p. 124-127 °C [lit.[128] 127-128 °C]; FT IR (NaCl) ν_{max} 3383 (br), 3175 (br), 3061, 3028, 2920, 2953, 1952 (w), 1895 (w),1808 (w), 1615, 1599, 1570, 1503 cm^{-1}; ^1H NMR (270 MHz, $CDCl_3$) δ 7.97 (d, J = 6.9 Hz, 2H, Ar-*H*), 7.49-7.47 (m, 3H, Ar-*H*), 7.00-6.95 (m, 10H, Ar-*H*), 5.45 (s, 2H, NC*H*), 4.75 (br s, 1H, N*H*) ppm; ^{13}C NMR (68 MHz, $CDCl_3$) δ 164.6, 138.9, 131.2, 129.9, 128.8, 127.7, 127.6, 127.4, 126.9, 70.8 ppm; MS (CI^+) 299 ($M+H^+$); HRMS calcd for ($M+H^+$) $C_{21}H_{19}N_2$ 299.1548, found 299.1543.

(±)-*trans*-4,5-Dihydro-2,4,5-triphenyl-1*H*-imidazole (*iso*-amarine) (116)[92]

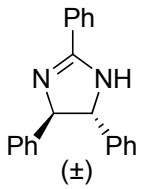

A stirred mixture of amidine **161** (42 g, 141 mmol), water (6 mL), diethylene glycol (35 mL) and sodium hydroxide (9.0 g, 225 mmol) was boiled in an open beaker until the temperature reached 155 °C. This was maintained for 45 min, during which time the sodium salt of the *iso*-amarine had precipitated and the solution became a thick slurry. After cooling to RT, the slurry was treated with glacial acetic acid (25 mL), diluted with ethanol (125 mL) and heated to boiling (105 °C) until all remaining solid had dissolved. After cooling, the solution was basified with concentrated aqueous ammonia. The resulting tan precipitate was filtered, washed with cold ethanol, and dried *in vacuo*. The crude product was re-crystallised from toluene to yield racemic *trans*-4,5-dihydro-2,4,5-triphenyl-1*H*-imidazole (*iso*-amarine) (**116**) (29 g, 70%) as colourless fine needles with spectral data consistent with literature:[128] m.p. 199-204 °C [lit.[92] 198-201 °C]; R_f = 0.33 (1:19, methanol/dichloromethane); FT IR (NaCl, nujol®) ν_{max} 3145 (br), 3027, 1953 (w), 1889 (w), 1810 (w), 1594, 1565, 1509 cm^{-1}; ^1H NMR (270 MHz, $CDCl_3$) δ 7.94 (dd, J^3 = 8.3 Hz, J^4 = 1.9 Hz, 2H, Ar-*H*), 7.51-7.25 (m, 13H, Ar-*H*), 5.42 (br s, 1H, N*H*) 4.90 (s, 2H, NC*H*) ppm; ^{13}C NMR (68 MHz, $CDCl_3$) δ 163.1, 143.6, 131.1, 130.2, 128.8, 128.7, 127.6, 127.5, 126.9, 71.8 ppm; MS (CI^+) 299 ($M+H^+$); HRMS calcd for ($M+H^+$) $C_{21}H_{19}N_2$ 299.1548, found 299.1554.

(*R*)-(–)-α-Acetoxyphenyl acetic acid (173)[107]

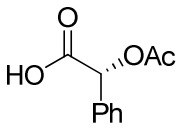

(*R*)-(–)-Mandelic acid (**172**) (25.5 g, 168 mmol) was added in three portions to a stirred flask containing acetyl chloride (60 mL) at 0 °C. The resulting solution was allowed to warm to RT and stirred for a further 15 h under an inert atmosphere of nitrogen. The solvent was removed *in vacuo* and the resulting crude product was re-crystallised from hot toluene to yield (*R*)-(–)-α-acetoxyphenyl acetic acid (**173**) (26.4 g, 81%) as a colourless crystalline solid with spectral data consistent with literature:[129] m.p. 96-98 °C [lit.[107] 96-98 °C]; R_f = 0.60 (ethyl acetate) $[\alpha]^{25}_D$ = -146.0 (c = 12.1, $CHCl_3$) [lit.[129] $[\alpha]^{25}_D$ = -154 (c = 1.01, $CHCl_3$)]; FT IR (NaCl) ν_{max} 3500-2500 (br), 1702 cm^{-1}; ^1H NMR (300 MHz, $CDCl_3$) δ 10.76 (br s, 1H, COO*H*), 7.51-7.41 (m, 5H, Ar-*H*), 5.95 (s, 1H, PhC*H*), 2.22 (s, 3H, COOCH_3) ppm; MS (CI^+) 212 ($M+NH_4^+$); HRMS calcd for ($M+NH_4^+$) $C_{10}H_{14}NO_4$ 212.0923, found 212.0926.

(*R*)-α-Acetoxybenzeneacetyl chloride (174)

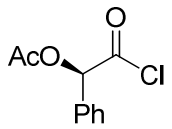

Two drops of DMF were added to a solution of (*R*)-acetylmandelic acid (**173**) (250 mg, 1.29 mmol) and oxalyl chloride (133 µL, 1.55 mmol) in dichloromethane. After stirring at RT for 1 h the effervescence had stopped, and the solution was concentrated *in vacuo* to yield (*R*)-α-acetoxybenzeneacetyl chloride (**174**) (274 mg, quantative) as a yellow oil with spectral data consistent with literature:[130] R_f 0.36 (ethyl acetate); $[\alpha]^{25}_D$ = -148.6 (*c*, 10.7, CH_2Cl_2), [lit.[130] $[\alpha]_D^{20}$ = -173.6 (*c*, 1.2, CH_2Cl_2)]; IR (NaCl) ν_{max} 3067, 3036, 2943, 1963 (w), 1785, 1754 cm^{-1}; ^1H NMR (270 MHz, $CDCl_3$) δ 7.48-7.39 (m, 5H, Ar-*H*), 6.07 (s, 1H, C*H*), 2.19 (s, 3H, COOCH_3).

(–)-(4*R*,5*R*)-1-[(*R*)-α-Acetoxybenzeneacetyl]-4,5-dihydro-2,4,5-triphenylimidazole (175) and (+)-(4*S*,5*S*)-1-[(*R*)-α-acetoxybenzeneacetyl]-4,5-dihydro-2,4,5-triphenylimidazole (176)

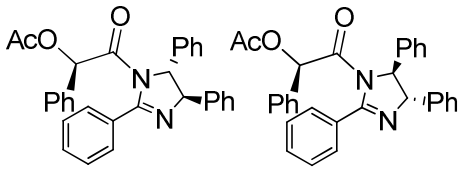

Racemic *trans*-4,5-dihydro-2,4,5-triphenyl-1*H*-imidazole (**116**) (32 g, 107 mg) and (*R*)-α-acetoxyphenyl acetic acid (**173**) (25 g, 129 mmol) were stirred in dichloromethane (350 mL) at -20 ºC under an inert atmosphere of nitrogen. DCC (27 g, 129 mmol) was added and the reaction mixture was allowed to slowly warm to RT. After 5 h a voluminous white precipitate had formed. The reaction mixture was filtered and the filtrate was concentrated *in vacuo* to yield the crude product as a mixture of diastereoisomers **175** and **176** (58.8 g, quantitative). The crude mixture of diastereomers **175** and **176** was taken up in refluxing diisopropyl ether (1050 mL). The solution was then allowed to slowly cool to RT and after 15 h was cooled to 0 ºC for a further 5 h. The resulting crystals were filtered, washed with a small amount of cold diisopropyl ether and dried under reduced pressure to yield pure (–)-(4*S*,5*S*)-1-[(*R*)-α-acetoxybenzeneacetyl]-4,5-dihydro-2,4,5-triphenylimidazole (**176**) (17.2 g, 68%) as colourless crystals: m.p. 170-171 ºC; R_f = 0.33 (2:1, petrol/ethyl acetate); $[\alpha]^{25}_D$ = –107.5 (c = 9.1, $CHCl_3$); FT IR (NaCl) ν_{max} 3063, 3029, 2979, 2936, 1956 (w), 1892 (w), 1807 (w), 1738, 1707, 1626 cm^{-1}; ^1H NMR (270 MHz, $CDCl_3$) δ 7.83 (d, *J* = 6.5 Hz, 2H, Ar-*H*), 7.51-7.12 (m, 16H, Ar-*H*), 6.97-6.92 (m, 2H, Ar-*H*), 5.55 (s, 1H, NC(=O)C*H*), 5.04 (d, *J* = 2.5 Hz, 1H, NC*H*Ph), 4.99 (d, *J* = 2.5 Hz, 1H, NC*H*Ph), 2.03 (s, 3H, COOCH_3) ppm; ^{13}C NMR (68 MHz, $CDCl_3$) δ 170.4, 166.2, 159.8, 140.3, 140.3, 131.8, 131.1, 130.9, 129.9, 129.5, 129.2, 128.9, 128.9, 128.6, 128.2, 127.9, 126.0, 125.3, 78.6, 75.1, 68.1, 20.7 ppm; MS (Cl^+) 475 ($M+H^+$); HRMS calcd for ($M+H^+$) $C_{31}H_{27}N_2O_3$ 475.2022, found 475.2030; Anal. calcd for $C_{31}H_{26}N_2O_3$: C, 78.46; H, 5.52; N, 5.90; found: C, 78.53; H, 5.47; N, 5.94; *Crystal data for* **176**: $C_{31}H_{26}N_2O_3$, *M* = 474.54, orthorhombic, $P2_12_12_1$, (no. 19), *a* = 10.1710(7), *b* = 14.6196(9) *c* = 17.2572(11) Å, *V* = 2566.1(3) $Å^3$, *Z* = 4, D_c = 1.228 g cm^{-3}, μ(Cu-Kα) = 0.633 mm^{-1}, *T* = 173 K, colourless blocks, Oxford Diffraction Xcalibur PX Ultra diffractometer; 4696 independent measured reflections, F^2 refinement, R_1 = 0.039, wR_2 = 0.101, 4638 independent observed absorption-corrected reflections [$|F_o| > 4\sigma(|F_o|)$, $2\theta_{max}$ = 137°], 329

parameters. The absolute structure of **176** could not be unambiguously determined by either an *R*-factor test [$R_1^+ = 0.0390$, $R_1^- = 0.0392$] or by use of the Flack parameter [$x^+ = 0.0(2)$, $x^- = 1.1(2)$] and so was assigned by internal reference. The combined filtrates were concentrated *in vacuo* to give an amorphous solid (37.5 g, 79.1 mmol) containing (*R*,*R*,*R*) diastereomer **175** in a 4:1 excess over (*R*,*S*,*S*) diastereomer **176**. A portion of this mixture could be purified by column chromatography (4:1→3:1, petrol/ethyl acetate) to produce analytically pure (*R*,*R*,*R*) diastereomer **175**: m.p. 67-73 ºC; R_f = 0.39 (2:1, petrol/ethyl acetate); $[\alpha]^{25}_D = -38.8$ (c = 2.3, $CHCl_3$); FT IR (NaCl) ν_{max} 3062, 3029, 2927, 2854, 1957 (w), 1889 (w), 1808 (w), 1737, 1704, 1693 cm^{-1}; ^1H NMR (270 MHz, $CDCl_3$) δ 7.70-6.86 (m, 20H, Ar-*H*), 5.83 (br s, 1H, NC*H*Ph), 5.45 (br s, 1H, NC*H*Ph*),* 5.06 (s, 1H, NC(=O)C*H*), 1.98 (s, 3H, COOCH_3) ppm; ^{13}C NMR (68 MHz, $CDCl_3$) δ 170.7, 142.3, 140.4, 132.2, 131.3, 131.1, 129.6, 129.5, 129.0, 128.8, 128.5, 128.3, 128.0, 126.4, 125.6, 78.5, 75.6, 70.7, 20.5 ppm; MS (CI^+) 475 ($M+H^+$); HRMS calcd for ($M+H^+$) $C_{31}H_{27}N_2O_3$ 475.2022, found 475.2018.

(+)-*N*-(*R*)-Acetoxyphenylacetyl-*N'*-benzoyl-(1*S*,2*S*)-1,2-diphenylethylene diamine (177)

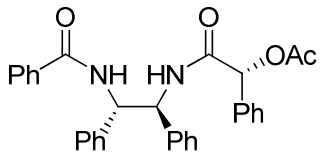

(–)-(4*S*,5*S*)-1-[(*R*)-α-Acetoxybenzeneacetyl]-4,5-dihydro-2,4,5-triphenylimidazole (**176**) (16.8 g, 35.4 mmol) was suspended in a mixture of THF (50 mL), water (100 mL) and concentrated hydrochloric acid (10 mL). The mixture was heated to reflux for 2 h, after which it was allowed to cool to RT and concentrated to 2/3 of its original volume *in vacuo*. After standing at RT for 1 h, the white precipitate was filtered, washed with cold water and dried by dry stirring at 60 ºC under vacuum to yield diamide **177** (16.1 g, 92%) as a fine colourless solid: m.p. >230 ºC; $[\alpha]^{25}_D = +7.3$ (c = 4.3 , 10:1, $CHCl_3$/MeOH); FT IR (NaCl) ν_{max} 3308, 3065, 3035, 3015, 1964 (w), 1731, 1668, 1641, 1578, 1539 cm^{-1}; ^1H NMR (270 MHz, DMSO-d_6) δ 9.05 (d, *J* = 7.6 Hz, 1H, N*H*), 8.98 (d, *J* = 7.4 Hz, 1H, N*H*), 7.78 (d, *J* = 6.9 Hz, 2H, Ar-*H*), 7.54-7.44 (m, 3H, Ar-*H*), 7.26-7.10 (m, 15H, Ar-*H*), 5.88 (s, 1H, NC(=O)C*H*), 5.50 (t, *J* = 7.5 Hz, 1H, NC*H*Ph), 5.45 (t, *J* = 7.5 Hz, 1H, NC*H*Ph) 2.11 (s, 3H, COOCH_3) ppm; ^{13}C NMR (68 MHz, DMSO-d_6) δ 170.0, 168.1, 166.9, 140.9, 140.6, 136.0, 135.1, 131.8, 128.8, 128.4, 128.3, 128.0, 128.0, 127.8, 127.4, 75.7, 58.2, 57.3, 21.3 ppm; MS (CI^+) 493 ($M+H^+$);

HRMS calcd for (M+H$^+$) $C_{31}H_{29}N_2O_4$ 493.2127, found 493.2123; Anal. calcd for $C_{31}H_{28}N_2O_4$: C, 75.59; H, 5.73; N, 5.69; found: C, 75.52; H, 5.80; N, 5.71.

(–)-*N*-(*R*)-Acetoxyphenylacetyl-*N'*-benzoyl-(1*R*,2*R*)-1,2-diphenylethylene diamine (179)

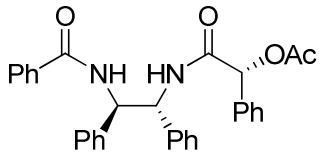

The combined filtrates from the re-crystallization of diastereomer **176** were suspended in a mixture of THF (120 mL), water (240 mL) and concentrated hydrochloric acid (24 mL), and the reaction proceeded as outlined above in the formation of pure diamide **177** to yield the diamide product as a 4:1, (*R*,*R*,*R*):(*R*,*S*,*S*) mixture of diastereomers (30.8 g, 79%). The crude solid was dissolved in refluxing chloroform (1.9 L) and the hot solution was allowed to cool slowly to RT. On cooling the pure (*R*,*R*,*R*) diamide precipitated, and was collected by filtration. Removal of a further 600 mL of solvent *in vacuo* and cooling to 0 ºC resulted in the precipitation on a second crop of diastereomerically pure *R*,*R*,*R* diamide, which was again collected by filtration. The two crops were combined and dried in vacuo to yield pure diamide **179** (13.6 g, 58%) as a colourless solid: m.p. >230 ºC; $[\alpha]^{25}_D$ = –69.5 (c = 2.3, 10:1, $CHCl_3$/MeOH); FT IR (NaCl, nujol®) ν_{max} 3305, 1739, 1667, 1633, 1602, 1579, 1520 cm^{-1}; ^{1}H NMR (270 MHz, DMSO-d_6) δ 9.08 (d, *J* = 8.1 Hz, 1H, N*H*), 8.81 (d, *J* = 8.8 Hz, 1H, N*H*), 7.66 (d, *J* = 7.4 Hz, 2H, Ar-*H*), 7.56-7.41 (m, 3H, Ar-*H*), 7.31-7.10 (m, 15H, Ar-*H*), 5.88 (s, 1H, NC(=O)C*H*), 5.45 (t, *J* = 8.6 Hz, 1H, NC*H*Ph), 5.32 (t, *J* = 8.4 Hz, 1H, NC*H*Ph), 2.01 (s, 3H, COOCH_3) ppm; ^{13}C NMR (68 MHz, DMSO-d_6) δ 170.0, 168.0, 166.6, 140.9, 140.9, 136.0, 135.0, 131.7, 128.7, 128.3, 127.9, 127.8, 127.6, 127.4, 127.3, 75.6, 57.9, 57.6, 21.1 ppm; MS (CI$^+$) 493 (M+H$^+$); HRMS calcd for (M+H$^+$) $C_{31}H_{29}N_2O_4$ 493.2127, found 493.2148; Anal. calcd for $C_{31}H_{28}N_2O_4$: C, 75.59; H, 5.73; N, 5.69; found: C, 75.64; H, 5.77; N, 5.61.

(–)-(1*S*,2*S*)-1,2-Diphenylethylene diamine (124*S*)

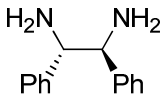

A mixture of (+)-*N*-(*R*)-acetoxyphenylacetyl-*N'*-benzoyl-(1*S*,*2S*)-1,2-diphenylethylene diamine (**177**) (12.8 g, 25.9 mmol), glacial acetic acid (33 mL) and 48% aqueous hydrobromic acid (65 mL) were refluxed for 6 h. At this point, further portions of aqueous hydrobromic acid (15 mL) and acetic acid (8 mL) were added, and the reaction was refluxed for a further 20 h. The solution was concentrated to 1/3 its original volume, cooled to 5 ºC, and allowed to stand for 15 h at RT. The resulting precipitate was filtered, washed with cold diethyl ether and dissolved in 30 mL of water. The aqueous solution was filtered to remove insoluble by-products, and the residue was washed with a further 10 mL of water. Aqueous sodium hydroxide solution (40%, *ca*. 4.5 mL) was added slowly to the filtrate such that the temperature did not exceed 25 °C. The mixture was cooled to 5 ºC for 15 min and the resulting precipitate from the aqueous phase was extracted with ether (3 × 80 mL). The organic layers were combined, dried over solid sodium hydroxide, filtered and concentrated *in vacuo*. The crude product was re-crystallised from petrol/diethyl ether (10 mL : 20 mL) to yield diamine **124*S*** (1.9 g, 34%) as a colourless, crystalline solid with spectral data consistent with literature:[102] m.p. 81-84 ºC [lit.[131] 83-85 ºC]; $[\alpha]^{25}_{D}$ = –91.0 (*c* = 4.6, EtOH) [lit.[132] $[\alpha]^{25}_{D}$ = –87.1 (c = 2.3, EtOH)]; FT IR (NaCl) ν_{max} 3360 (br), 3295 (br), 3060, 3028, 2908, 2857, 1952 (w), 1884 (w), 1811 (w) 1647, 1601 cm^{-1}; ^{1}H NMR (270 MHz, $CDCl_3$) δ 7.27-7.25 (m, 10H, Ar-*H*), 4.09 (s, 2H, NC*H*), 1.62 (br s, 4H, NH_2) ppm; ^{13}C NMR (68 MHz, $CDCl_3$) δ 143.5, 128.3, 127.1, 127.0, 62.0 ppm; MS (CI^+) 213 ($M+H^+$); HRMS calcd for ($M+H^+$) $C_{14}H_{16}N_2$ 213.1392, found 213.1390. The optical purity was assessed by the Synder's method employing the use of mandelic acid as a chiral solvating agent in ^{1}H NMR analysis of the chiral amines.[109]

(+)-(1*R*,2*R*)-1,2-Diphenylethylene diamine (124*R*)

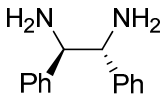

Following the above procedure starting from diamide **179** (12.5 g, 25.5 mmol) gave diamine **124*R*** (2.46 g, 46%) as a colourless, crystalline solid with spectral data consistent with literature:[102] m.p. 78-82 °C [lit.[133] 79-83 °C]; $[\alpha]^{25}_{D}$ = +90.7 (c = 3.4, EtOH) [lit.[134] $[\alpha]^{25}_{D}$ = +90.4 (c = 1.9, EtOH)]. The other spectral data is identical to that for its enantiomer.

(+)-(4*R*,5*R*)-4,5-Dihydro-2,4,5-triphenyl-1*H*-imidazole (116*R*)

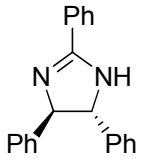

Racemic *iso*-amarine **116** (5.00 g, 16.8 mmol) and (*S*)-(+)-mandelic acid (**172**) (2.55 g, 16.8 mmol) were dissolved in refluxing isopropanol (28 mL). After refluxing for 1 h, heating was stopped and the flask was left in the oil bath to cool slowly to RT with gentle stirring. After 16 h, the solution was cooled to 0 °C and left to stir for a further 4 h. The resulting white crystals were collected by filtration through a cold scinter and dried *in vacuo*. The salt was re-crystallised to optical purity from further isopropanol and the crystals dried *in vacuo* to yield the 1:1 mandelic acid: *iso*-amarine diastereomeric salt **182** (2.99 g, 87%): m.p. 181-185 ºC; $[\alpha]^{25}_{D}$ = +128.0 (*c* = 2.3, EtOH); FT IR (NaCl, nujol®) ν_{max} 3430, 3065, 3025, 3100-2000 (br), 1969 (w), 1882 (w), 1807 (w), 1589, 1555 cm^{-1}; ^{1}H NMR (270 MHz, DMSO-d_6) δ 8.05 (d, *J* = 6.7 Hz, 2H, Ar-*H*), 7.62-7.52 (m, 3H, Ar-*H*), 7.41-7.20 (m, 15H, Ar-*H*), 4.95 (s, 2H, NC*H*Ph), 4.82 (s, 1H, PhC*H*(OH)CO_2) ppm; ^{13}C NMR (68 MHz, DMSO-d_6) δ 174.7, 163.3, 143.1, 142.0, 132.5, 129.3, 129.3, 129.1, 128.5, 128.4, 127.6, 127.2, 127.1, 101.8, 73.3 ppm; MS (FAB^+) 299 (cation) 452 (cation+anion+$2H^+$); MS (FAB^-) 151 (anion); Anal. calcd for $C_{29}H_{26}N_2O_4$: C, 77.31; H, 5.82; N, 6.22; found: C, 77.42; H, 5.91; N, 6.15. *Crystal data for* **182**: $C_{29}H_{26}N_2O_3$, *M* = 450.52, orthorhombic, $P2_12_12_1$, (no. 19), *a* = 8.6149(5), *b* = 16.0588(8) *c* = 17.2764(8) Å, *V* = 2390.1(2) $Å^3$, *Z* = 4, D_c = 1.252 g cm^{-3}, μ(Cu-Kα) = 0.650 mm^{-1}, *T* = 293 K, colourless prisms, Oxford Diffraction Xcalibur PX Ultra diffractometer; 4365 independent measured reflections, F^2 refinement, R_1 = 0.047, wR_2 = 0.107, 3623 independent observed absorption-corrected reflections [$|F_o| > 4\sigma(|F_o|)$, $2\theta_{max}$ = 137°], 317 parameters. The absolute structure of **182** could not be unambiguously determined by either an *R*-factor test [R_1^+ = 0.0472, R_1^- = 0.0472] or by use of the Flack parameter [x^+ = 0.1(3), x^-

= 0.9(3)] and so was assigned by internal reference. The diastereomeric salt (2.77 g, 6.16 mmol) was suspended in dichloromethane (150 mL) and 1M aqueous sodium hydroxide (100 mL) was added. The biphasic mixture was rapidly stirred until all the solid had dissolved and the organic layer was separated. The aqueous layer was re-extracted with dichloromethane (100 mL) and the combined organic layers were washed with water (100 mL), dried ($MgSO_4$) and concentrated *in vacuo* to give (*R*,*R*)-amidine **116*R*** (1.83 g, quantitative) as colourless needles with spectral data consistent with literature:[128] m.p. 175-178 °C [lit.[111] 180 °C]; $[\alpha]^{25}_D$ = +46.0 (c = 2.0, EtOH) [lit.[111] $[\alpha]_D$ = +46.3 (c = 1.1, EtOH)]. Other spectral data are identical to that of the racemate (±)-**116**.

(+)-(4*S*,5*S*)-4,5-Dihydro-2,4,5-triphenyl-1*H*-imidazole (116*S*)

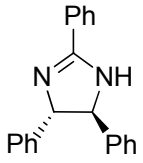

Racemic *iso*-amarine **116** (14.0 g, 47 mmol) and (*R*)-(+)-mandelic acid (7.14 g, 47 mmol) were dissolved in refluxing isopropanol (78 mL). After refluxing for 1 h, heating was stopped and the flask was left in the oil bath to cool slowly to RT with gentle stirring. After 21 h, the solution was cooled to 0 °C and left to stir for a further 4 h. The resulting precipitate was collected by filtration through a cold scinter and the residue dried *in vacuo*. The salt was re-crystallised to optical purity from further *iso*propanol and the crystals dried *in vacuo* to yield the 1:1 mandelic acid: *iso*-amarine diastereomeric salt **182** (8.55 g, 82%): m.p. 189-191.5 ºC; $[\alpha]^{25}_D$ = -128.0 (*c* = 2.07, EtOH); all other spectral data is identical to the other enantiomer. The diastereomeric salt (8.5 g, 18.9 mmol) was suspended in dichloromethane (50 mL) and 1M aqueous sodium hydroxide solution (50 mL) was added. The biphasic mixture was rapidly stirred until all the solid had dissolved and the organic layer was separated. The aqueous layer was re-extracted with dichloromethane (50 mL) and the combined organic layers were washed with water (50 mL), dried ($MgSO_4$) and concentrated *in vacuo* to give (*S*,*S*)-amidine **116*S*** (5.53 g, 98%) as colourless needles with spectral data consistent with literature:[128] m.p. 174-177 °C [lit.[98] 177-180 °C]; $[\alpha]^{25}_D$ = -46.2 (c = 1.9, EtOH) [lit.[111] $[\alpha]_D$ = -46.9 (c = 1.0, EtOH)]. Other spectral data are identical to that of the racemate (±)-**116**.

(+)-(1*S*,2*S*)-*N*-benzoyl-*N'*-acetyl-1,2-diamino-1,2-diphenylethane (163*S*) [101]

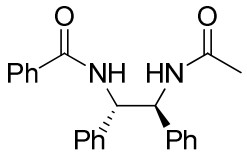

A mixture of (*S*,*S*)-*iso*-amarine (**116*S***) (5.0 g, 16.8 mmol), sodium acetate (200 mg, 2.4 mmol) and acetic anhydride (9 mL) were heated to 150 °C for 3.5 h. Water (20 mL) and concentrated hydrochloric acid (1.3 mL) were added and the reaction mixture was heated to 100 °C. After 2 h, the reaction mixture was filtered whilst still hot and the residue washed with water (30 mL) and dried *in vacuo* to give diamide **163*S*** (5.7 g, 15.9 mmol, 95 %) as a colourless fluffy solid: m.p. >230 °C; $[\alpha]^{25}_{D}$ = +64.9 (*c* 1.0 , 9:1, $CHCl_3$/MeOH); FT IR (NaCl, nujol®) ν_{max} 3314, 1651, 1633 cm^{-1}; ^1H NMR (400 MHz, DMSO-d_6) δ 8.89 (d, *J* = 8.8 Hz, 1H, N*H*), 8.70 (d, *J* = 8.8 Hz, 1H, N*H*), 7.76 (d, *J* = 6.8 Hz, 2H, Ar-*H*), 7.55-7.45 (m, 3H, Ar-*H*), 7.32-7.12 (m, 10H, Ar-*H*), 5.46 (t, *J* = 8.4 Hz, 1H, NC*H*Ph), 5.38 (t, *J* = 8.4 Hz, 1H, NC*H*Ph) 1.80 (s, 3H, COOCH_3) ppm; ^{13}C NMR (100 MHz, DMSO-d_6) δ 169.8, 166.9, 141.0, 141.0, 134.9, 131.8 128.8, 128.4, 127.8, 127.7, 127.4, 58.2, 57.3, 23.1 ppm; MS (CI^+) 359 ($M+H^+$); HRMS calcd for ($M+H^+$) $C_{23}H_{22}N_2O_2$ 359.1760, found 359.1771.

(-)-(1*S*,2*S*)-1,2-diamino-1,2-diphenylethane (124*S*)

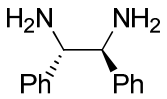

Starting from diamide **163*S*** (5.0 g, 14.0 mmol) and following the procedure previously described for the hydrolysis of (+)-*N*-(R)-acetoxyphenylacetyl-*N'*-benzoyl-(1*S*,*2S*)-1,2-diphenylethylene diamine (**177**) gave diamine **124*S*** (1.44 g, 49%) as colourless needles after re-crystallisation (diethyl ether/petrol), with spectral data consistent with literature:[102] m.p. 78-81 °C [lit.[135] 83-85 °C]; $[\alpha]^{25}_{D}$ = –106.0 (c = 1, EtOH); [lit.[136] $[\alpha]^{20}_{D}$ = –102 (c = 1.0, EtOH)]; other data identical to that previously reported.

6.3. Catalyst Synthesis

2-Iodobenzamide (108)

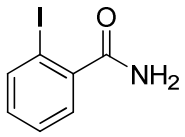

2-Iodobenzoic acid (2.00 g, 8.1 mmol) was added portion-wise to thionyl chloride (30 mL). The solution was heated to reflux for 3.5 h, after which time the solution was allowed to cool to RT and was concentrated *in vacuo* to give a beige solid. The solid was dissolved in dry dichloromethane (12 mL) and cooled to 0 ºC. Aqueous ammonia solution (12 mL) was added drop-wise to the reaction mixture and the biphasic mixture was stirred at RT for 20 h. The resulting white precipitate was collected by filtration, washed with water (2 × 25 mL) and dried under vacuum at 40ºC to yield 2-iodo-benzamide (**108**) (1.46 g, 65%) with spectral data consistent with literature:[55] m.p. 177-179 °C [lit.[137] 183-185 °C]; FT IR (NaCl) ν_{max} 3361, 3181, 1643 cm^{-1}; ^{1}H NMR (300 MHz, DMSO-d_6) δ 7.88-7.84 (m, 2H, Ar-*H*, N*H*), 7.53 (br s, 1H, N*H*), 7.43 (t, J = 7.4 Hz, 1H, Ar-*H*), 7.34 (d, J = 7.3 Hz, 1H, Ar-*H*), 7.15 (t, J = 6.9 Hz, 1H, Ar-*H*) ppm; ^{13}C NMR (68 MHz, DMSO-d_6) δ 171.3, 143.7, 139.7, 131.1, 128.5, 128.3, 93.7 ppm; MS (CI^+) 248 ($M+H^+$); HRMS calcd for ($M+H^+$) C_7H_6NOI 247.9572, found 247.9578.

(4*R*,5*R*)-2-(2-Iodophenyl)-4,5-diphenyl-4,5-dihydro-1H-imidazole (*R*-IAM) (111*R*)

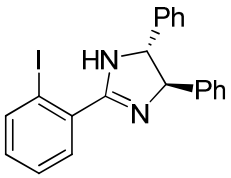

Dichloromethane (5.5 mL) was added to a mixture of 2-iodobenzamide (**108**) (600 mg, 2.4 mmol) and trimethyloxonium tetrafluoroborate (468 mg, 3.2 mmol) and the resulting white suspension was allowed to stir under nitrogen for 22 h. The mixture was concentrated *in vacuo* and the residue was washed with dry ether (2 × 1 mL) to yield the crude imidate

(844 mg, quantitative) as a colourless solid: ^{1}H NMR (270 MHz, DMSO-d_6) δ 8.07 (d, J = 7.9 Hz, 1H, Ar-*H*), 7.71-7.61 (m, 2H, Ar-*H*), 7.43 (dt, ^{3}J = 7.4 Hz, ^{4}J = 1.8 Hz, 1H, Ar-*H*), 4.24 (s, 3H, OC*H*$_3$) ppm; ^{13}C NMR (68 MHz, DMSO-d_6) δ 175.8, 140.9, 134.7, 134.0, 130.7, 129.0, 94.7, 60.9 ppm. The crude imidate (820 mg, 2.4 mmol) was dissolved in dry ethanol (8 mL), and (+)-(1*R*,2*R*)-1,2-diphenylethylene diamine (**124*R***) (598 mg, 2.8 mmol) was added to the solution. The reaction was left to stir at RT under nitrogen for 1.5 h, followed by a further 3 h at reflux. The reaction mixture was allowed to cool to RT and concentrated *in vacuo*. The residue was partitioned between 5% aqueous sodium hydroxide solution (30 mL) and dichloromethane (30 mL). The organic layer was separated and the aqueous layer was washed with dichloromethane (30 mL). The combined organic layers were dried ($MgSO_4$), filtered and concentrated *in vacuo* to give a pale green oil. This was purified by flash column chromatography (ethyl acetate) to give the product as a colourless oil. After trituration with petrol, **111*R*** was obtained (1.81 g, 77%) as a colourless solid with spectral data consistent with literature:[82] m.p. 113-114 °C [lit.[82] 114-117 °C]; R_f = 0.38 (ethyl acetate); $[\alpha]^{25}_{D}$ = +62.6 (c = 1.8, CH_2Cl_2) [lit.[1] $[\alpha]^{25}_{D}$ = +71 (c = 0.24, CH_2Cl_2)]; FT IR (NaCl) ν_{max} 3383 (br), 3132 (br), 3059, 3028, 2923, 2856, 1949 (w), 1886 (w), 1807 (w), 1668, 1611, 1578 cm^{-1}; ^{1}H NMR (270 MHz, $CDCl_3$) δ 7.91 (dd, J^{4} = 1.1 Hz, J^{3} = 7.9 Hz, 1H, Ar-*H*), 7.67 (dd, J^{4} = 1.7 Hz, J^{3} = 7.6 Hz, 1H, Ar-*H*), 7.42 (dt, J^{4} = 1.1 Hz, J^{3} = 7.6 Hz, 1H, Ar-*H*), 7.37-7.29 (m, 10H, Ar-*H*), 7.13 (dt, J^{4} = 1.7 Hz, J^{3} = 7.9 Hz, 1H, Ar-*H*), 4.92 (s, 2H, NC*H*Ph) ppm; ^{13}C NMR (68 MHz, $CDCl_3$) δ 164.7, 142.9, 140.0, 136.9, 131.4, 130.7, 128.7, 128.3, 127.6, 127.0, 94.6, 75.5 ppm; MS (CI^+) 425 ($M+H^+$); HRMS calcd for ($M+H^+$) $C_{21}H_{18}N_2I$ 425.0515, found 425.0515.

(4*S*,5*S*)-2-(2-Iodophenyl)-4,5-diphenyl-4,5-dihydro-1H-imidazole (111*S*)

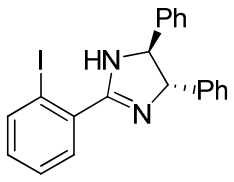

Following the above procedure for the preparation of the chiral amidine **111*R*** using (*S*,*S*)-diamine **124*S*** gave the corresponding (*S*,*S*) enantiomer **111*S*** (793 mg, 77%) as white crystals: m.p.116-118 °C; $[\alpha]^{25}_{D}$ = -60.9 (c = 2.5, CH_2Cl_2). The other spectral data is identical to that for its enantiomer.

(±)-1-Benzoyl-*trans*-4,5-dihydro-2,4,5-triphenylimidazole (169)

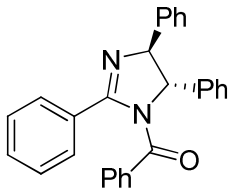

Racemic *trans*-4,5-dihydro-2,4,5-triphenyl-1*H*-imidazole (**116**) (150 mg, 0.50 mmol), was stirred in deuterated chloroform (1.5 mL) with triethylamine (140 µL, 1.00 mmol) at RT under an inert atmosphere of nitrogen. Distilled benzoyl chloride (88 µL, 0.78 mmol) was added and the reaction mixture was stirred for 35 min after which time NMR analysis showed 100% conversion of starting material. The reaction mixture was diluted with dichloromethane (20 ml) and washed with 0.5M aqueous hydrochloric acid (20 mL). The aqueous phase was re-extracted with dichloromethane (20 mL) and the combined organic phases were washed with water (20 mL) and brine (20 mL), dried ($MgSO_4$), filtered and concentrated *in vacuo*. The resulting residue was purified by flash column chromatography (0.5% methanol, 95.5% dichloromethane) to yield benzoylated amidine **169** (136 mg, 68%) as a white crystalline solid with spectral data consistent with literature:[128] m.p. 173-176 °C [lit.[128] 179 °C]; R_f = 0.38 (0.5% methanol, 95.5% dichloromethane); FT IR (NaCl) ν_{max} 3064, 3017, 2967, 1957 (w), 1898 (w), 1806 (w), 1710, 1669 cm^{-1}; ^1H NMR (270 MHz, $CDCl_3$) δ 7.75 (d, J = 6.9 Hz, 2H, Ar-*H*), 7.42-7.08 (m, 18H, Ar-*H*), 5.15, 5.20 (ABq, J_{AB} = 3.2 Hz, 2H, NC*H*Ph) ppm; ^{13}C NMR (75 MHz, $CDCl_3$) δ 170.4 161.5, 142.0, 140.6, 134.7, 131.7, 131.2, 130.7, 129.3, 129.1, 128.6, 128.6, 128.3, 128.2, 128.0, 126.4, 125.7, 78.2, 72.5 ppm; MS (CI^+) 403 ($M+H^+$); HRMS calcd for ($M+H^+$) $C_{28}H_{22}N_2O$ 403.1810, found 403.1797.

(4*R*,5*R*)-1-Benzoyl-2-(2-iodophenyl)-4,5-diphenyl-4,5-dihydroimidazole (241)

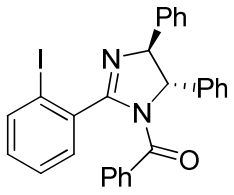

(4*R*,5*R*)-2-(2-Iodophenyl)-4,5-diphenyl-4,5-dihydro-1*H*-imidazole (**111**) (97 mg, 0.24 mmol), was stirred in deuterated chloroform (1.0 mL) with triethylamine (66 µL, 0.47 mmol) at RT under an inert atmosphere of nitrogen. Distilled benzoyl chloride (41 µL, 0.35 mmol) was added and the reaction mixture was stirred for 50 min after which time NMR analysis showed 100% conversion of starting material. The reaction mixture was diluted with dichloromethane (20 mL), and washed with 0.5M aqueous hydrochloric acid (20 mL). The aqueous phase was then re-extracted with dichloromethane (20 mL) and the combined organic phases were washed with water (20 mL) and brine (20 mL), then dried ($MgSO_4$), filtered and concentrated *in vacuo*. The resulting residue was purified by flash column chromatography (0.5% methanol, 95.5% dichloromethane) to yield (4*R*,5*R*)-1-benzoyl-2-(2-iodophenyl)-4,5-diphenyl-4,5-dihydroimidazole (**241**) (86.5 mg, 70%) as an amorphous colourless solid: m.p. 67-71 °C; R_f = 0.39 (0.5% methanol, 95.5% dichloromethane); $[\alpha]^{25}_D$ = +83.1 (c = 2.0, $CHCl_3$); FT IR (NaCl) ν_{max} 3062, 3030, 1671, 1625 cm^{-1}; ^1H NMR (270 MHz, $CDCl_3$) δ 7.62 (d, *J* = 7.9 Hz, 1H, Ar-*H*), 7.47-7.06 (m, 18H, Ar-*H*), 6.91 (t, *J* = 7.5 Hz, 1H, Ar-*H*), 5.27, 5.27 (ABq, J_{AB} = 7.8 Hz, 2H, NC*H*) ppm; ^{13}C NMR (75 MHz, $CDCl_3$) δ 169.0, 160.2, 141.4, 140.8, 139.1, 137.5, 135.0, 131.2, 130.7, 129.0, 128.9, 128.3, 128.1, 127.9, 127.8, 127.7, 127.1, 126.9, 96.4, 78.4, 72.7 ppm; MS (CI^+) 529 ($M+H^+$); HRMS calcd for ($M+H^+$) $C_{28}H_{22}N_2OI$ 529.0777, found 529.0761.

2-Iodoisophthalic acid (186)

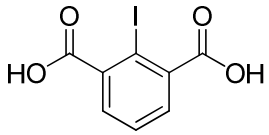

Potassium permanganate (13.6 g, 86.1 mmol) was added to a suspension of 2,6-dimethyliodobenzene (**185**) (10.0 g, 43.1 mmol) in *tert*-butanol (40 mL) and water (40 mL). The suspension was heated at reflux for 1 h and then allowed to cool to RT. A further portion of potassium permanganate (13.6 g, 86.1 mmol) was added and the suspension was heated at reflux for a further 17 h. The reaction mixture was filtered whilst still warm, allowed to cool, concentrated to one half of its original volume, and acidified to pH 1 using concentrated hydrochloric acid. After leaving to cool the precipitate was filtered, washed with water, and dried in a dessicator over silica to yield the diacid **186** (6.0 g, 48 %) as a fine

colourless powder with spectral data consistent with literature:[55] m.p. >230 °C [lit.[138] 244-246 °C]; FT IR (NaCl) ν_{max} 3703-3101 (br), 1699, 1679 cm^{-1}; ^1H NMR (300 MHz, DMSO-d_6) δ 7.62-7.48 (m, 3H, Ar-*H*), 3.37 (br s, 2H, O*H*) ppm; ^{13}C NMR (75 MHz, DMSO-d_6) δ 169.8, 141.7, 130.1, 128.8, 91.7 ppm; MS (CI^+) 310 ($M+NH_4^+$); HRMS calcd for ($M+NH_4^+$) $C_8H_9IO_4N$ 309.9576, found 309.9570.

2-Iodo-1,3-benzenedicarbonyl chloride (187)

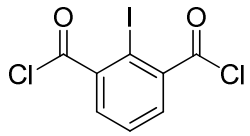

Diacid **186** (307 mg, 1.1 mmol) was heated at reflux for 2.5 h in thionyl chloride (9 mL). The reaction mixture was allowed to cool and was concentrated *in vacuo* to yield 2-iodo-1,3-benzenedicarbonyl chloride (**187**) (324 mg, 94%) as a beige crystalline solid with spectral data consistant with that previously reported:[55] ^1H NMR (270 MHz, $CDCl_3$) δ 7.88 (d, J = 7.8 Hz, 2H, Ar-*H*), 7.62 (t, J = 7.8 Hz, 1H, Ar-*H*) ppm; ^{13}C NMR (75 MHz, $CDCl_3$) δ 167.8, 143.3, 133.0, 128.8, 88.5 ppm.

2-Iodoisophthalamide (122)

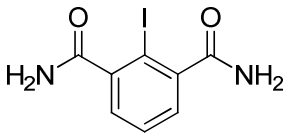

Aqueous ammonia (35%, 50 mL) was added drop-wise over 1 h to a stirred suspension of diacyl chloride **187** (3.3 g, 9.9 mmol) in dichloromethane (50 mL) at 0 °C. The reaction mixture was allowed to slowly warm to RT and stirred for a further 15 h. The resulting white precipitate was filtered, washed with water (20 mL) and dried *in vacuo* over silica gel for 48 h to yield diamide **122** (1.6 g, 64%) as a white powder with spectral data consistant with that previously reported:[55] m.p. >230 °C; FT IR (NaCl) ν_{max} 3294, 3131, 1657, 1611, 1580 cm^{-1}; ^1H NMR (270 MHz, DMSO-d_6) δ 7.83 (br s, 2H, N*H*), 7.54 (br s, 2H, N*H*), 7.41 (t, J = 7.5 Hz,

1H, Ar-*H*), 7.26 (d, *J* = 7.5 Hz, 2H, Ar-*H*) ppm; ^{13}C NMR (68 MHz, DMSO-d_6) δ 171.6, 145.4, 128.4, 127.7, 91.7 ppm; MS (EI$^{+\cdot}$) 290 ($M^{+\cdot}$); HRMS calcd for ($M+H^+$) $C_8H_7N_2O_2I$ 289.9552, found 289.9553.

2,6-Di-[(4*R*,5*R*)-4,5-diphenyl-4,5-dihydro-1*H*-imidazol-2-yl]iodobenzene (IBAM) (113*R*); *preparation from the diamide*

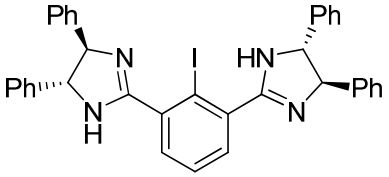

Dichloromethane (5 mL) was added to a mixture of diamide **122** (200 mg, 0.7 mmol) and trimethyloxonium tetrafluoroborate (285 mg, 1.9 mmol) and the resulting white suspension was refluxed under nitrogen for 48 h. The mixture was concentrated *in vacuo* and the residue was washed with dry ether (2 × 1.5 mL) to yield the crude imidate (379 mg, quantitative) as a grey-white solid. A portion of the crude imidate (348 mg, 0.6 mmol) was dissolved in dry ethanol (2 mL), and a solution of (+)-(1*R*,2*R*)-1,2-diphenylethylene diamine (**124*R***) (300 mg, 1.4 mmol) in dry ethanol (3 mL) was transferred to the reaction flask *via* cannular. The reaction was left to stir at RT under nitrogen for 1.5 h, followed by a further 4 h at reflux. The reaction mixture was allowed to cool to RT and concentrated *in vacuo*. The residue was partitioned between 5% aqueous sodium hydroxide solution (15 mL) and dichloromethane (20 mL) and the organic layer was separated. The aqueous layer was washed with dichloromethane (20 mL) and the combined organic layers were dried ($MgSO_4$), filtered and concentrated *in vacuo* to give a pale green solid. This was purified by flash column chromatography (1:9, methanol/ethyl acetate) to give the product as a colourless oil. After trituration with petrol **113*R*** (250 mg, 66%) was obtained as a colourless solid with spectral data consistant with that previously reported:[55] m.p. 123-128 °C [lit.[55] 154-156 °C]; R_f = 0.20 (1:9, methanol/ethyl acetate); $[\alpha]^{25}_D$ = + 88.2 (c = 2.1, CH_2Cl_2) [lit.[55] $[\alpha]^{25}_D$ = + 100.0 (c = 0.24 , CH_2Cl_2)]; FT IR (NaCl) ν_{max} 3442, 3156, 3061, 3029, 2922, 1618 cm^{-1}; ^{1}H NMR (270 MHz, $CDCl_3$) δ 7.56-7.23 (m, 23H, Ar-*H*), 5.37 (s, 2H, N*H*), 4.69 (s, 4H, NC*H*Ph) ppm; ^{13}C NMR (68 MHz, $CDCl_3$) δ 165.4, 142.3, 138.1, 131.1, 128.7, 127.7, 127.0,

95.5, 75.0 ppm; MS (FAB$^+$) 645 (M+H$^+$); HRMS calcd for (M+H$^+$) $C_{36}H_{30}N_4I$ 645.1515, found 645.1519.

2,6-Di-[(4*S*,5*S*)-4,5-diphenyl-4,5-dihydro-1*H*-imidazol-2-yl]iodobenzene (*S*-IBAM) (113*S*)

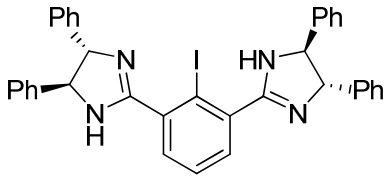

Following the above procedure for the preparation of the chiral diamidine **113*R*** using (*S*,*S*)-diamine **124*S*** gave the corresponding (*S*,*S*) enantiomer **113*S*** (191 mg, 68%) as white crystals with spectral data consistent with that previously reported:[55] m.p.127-130 ºC [lit.[55] 152-153 ºC]; $[\alpha]^{25}_D$ = -97.7 (c = 4.8 , CH_2Cl_2) [lit.[55] $[\alpha]^{25}_D$ = -103.8 (c = 0.24, CH_2Cl_2)]; The other spectral data is identical to that for its enantiomer.

2,6-Dicyano-1-iodobenzene (192)

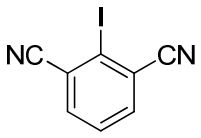

A cooled (-20 ºC) solution of lithium diisopropylamide (LDA) (296 mL, 1.8 M in THF/heptane/ethylbenzene, 533 mmol) was added drop-wise over 30 min to a stirred solution of 1,3-dicyanobenzene (**189**) (65 g, 508 mmol) in 2-methyltetrahydrofuran (mTHF) (2.5 L) at -90 ºC under an inert atmosphere of nitrogen. After stirring for an additional 15 mins, a cooled (-20 ºC) solution of iodine (135 g, 533 mmol) in mTHF (250 mL) was added over 100 min and the reaction mixture was allowed to slowly warm to RT. After 16 h, the resulting deep orange-red solution was quenched with 20% aqueous sodium sulphite solution (1 L) and biphasic mixture was transferred to a controlled laboratory reactor (CRL) and stirred to facilitate thorough mixing. The organic phase was separated, washed with water (1 L), brine (1 L) and divided into two portions. Each portion was filtered through a

500 mL silica plug and washed through with a further mTHF (2 × 350 mL). The portions were recombined along with the washings and concentrated to a volume of 400 mL to yield a brown slurry. After standing for 2 d the slurry was filtered and the residue washed with industrial methylated spirit (100 mL) and dried in a vacuum oven to yield 2,6-dicyano-1-iodobenzene **192** (82 g, 64%) as a pale beige solid with spectral data consistent with literature:[113] m.p. 205-209 ºC; [lit.[113] 208-209 ºC]; R_f = 0.32 (4:3, petrol/ethyl acetate); FT IR (NaCl) ν_{max} 3090, 3060, 3054, 2230 cm^{-1}; ^1H NMR (400 MHz, $CDCl_3$) δ 7.81 (d, J = 7.6 Hz, 2H, Ar-*H*), 7.64 (t, J = 7.6 Hz, 1H, Ar-*H*) ppm; ^{13}C NMR (100 MHz, $CDCl_3$) δ 137.2, 129.1, 123.3, 118.2, 103.7 ppm; MS (EI$^+$) 254 ($M^{+\cdot}$); HRMS calcd for ($M^{+\cdot}$) $C_8H_3IN_2$ 253.9341, found 253.9329.

2-Iodoisophalaldehyde (199)

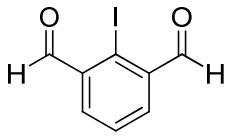

A solution of iodonitrile **192** (10 g, 39.4 mmol) in dichloromethane (150 mL) was cooled to -78 ºC under an inert atmosphere of nitrogen. A solution of DIBAL-H (80 mL, 1.5M in toluene) was added over a period of 10 min *via* a cooled (-10 ºC) dropping funnel. The reaction mixture was stirred with the temperature maintained between -70 ºC to -78 ºC for 2 h, after which time the temperature was allowed to gradually rise to 0 ºC. Over this time the reaction mixture changed from colourless to deep orange-red. After stirring for a further 3 h the reaction mixture was cooled to -10 ºC prior to the drop-wise addition of an ice-cold 3 M aqueous hydrochloric acid (150 mL). The resulting slurry was stirred at 0ºC for 1.5 h, after which time it was allowed to gradually warm to room temperature. After stirring at room temperature for a further 20 h, the biphasic mixture was separated and the aqueous phase was extracted with dichloromethane (150 mL). The combined organic phases were washed with water (150 mL), brine (150 mL), dried ($MgSO_4$), filtered and concentrated *in vacuo*. The crude product was dissolved in a solution of ethyl acetate (75 mL), ethanol (22 mL) and water (9 mL) at 40 ºC under an inert atmosphere of nitrogen. Sodium bisulfite (5.94 g, 57.1 mmol) was added and after stirring for 2 h the resulting precipitate was separated by filtration. The residue was washed with ethanol (15 mL), ethyl acetate (15 mL) and dried overnight in a vacuum oven (40 ºC) to yield the bis-bisulfite salt of dialdehyde **199** (16.0 g,

34.2 mmol) as a colourless powder: m.p. 335 ºC (decomp.); ^{1}H NMR (400 MHz, $CDCl_3$) δ 7.59 (d, J = 7.6 Hz, 2H, Ar-H), 7.18 (t, J = 7.6 Hz, 1H, Ar-H), 6.04 (d, J = 5.6 Hz, 2H), 5.50 (d, J = 5.6 Hz, 2H) ppm. The bisulfite salt (15.5 g, 33 mmol) was dissolved in water (260 mL) and the aqueous phase was overlain with ethyl acetate (260 mL). The biphasic mixture was stirred in an ice-bath and 10M aqueous sodium hydroxide solution (18 mL) was added. After stirring for 15 mins the organic phase was separated and the aqueous phase re-extracted with ethyl acetate (250 mL). The combined organic phases were washed with water (250 mL), brine (250 mL), dried ($MgSO_4$), filtered and concentrated *in vacuo* to afford dialdehyde **199** (7.2 g, 70% over three steps) as pale yellow needles: m.p. 131-134 ºC; R_f = 0.30 (4:1, petrol/ethyl acetate); FT IR (NaCl) ν_{max} 3051, 1679 cm^{-1}; ^{1}H NMR (400 MHz, $CDCl_3$) δ 10.2 (s, 2H, C(=O)*H*), 8.09 (d, J = 7.6 Hz, 2H, Ar-*H*), 7.56 (t, J = 7.6 Hz, 1H, Ar-*H*) ppm; ^{13}C NMR (100 MHz, $CDCl_3$) δ 195.0, 136.0, 135.7, 129.0, 106.2 ppm; MS (EI$^+$) 260 ($M^{+\cdot}$); HRMS calcd for ($M^{+\cdot}$) $C_8H_5IO_2$ 259.9334, found 259.9325; Anal. calcd for $C_8H_5O_2I$: C, 36.95; H, 1.94; found: C, 37.00; H, 1.87.

2,6-Di-[(4*R*,5*R*)-4,5-diphenyl-4,5-dihydro-1*H*-imidazol-2-yl]iodobenzene (*R*-IBAM) (113*R*); *preparation from the dialdehyde*

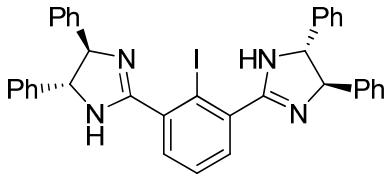

(1*R*,2*R*)-(+)-1,2-Diphenylethylenediamine (**124*R***) (20.1 g, 94.6 mmol) was added to a stirred solution of bis-aldehyde **199** (12 g, 46.2 mmol) at 0 ºC in toluene (600 mL). The reaction vessel was flushed with nitrogen and left to stir at 0 ºC. After 3 h the volatiles were removed *in vacuo* and the residue was taken up in dry dichloromethane (600 mL) under an inert atmosphere of nitrogen. The solution was cooled to 0ºC, NBS (16.8 g, 94.6 mmol) added and the reaction mixture allowed to warm slowly to RT with stirring. After 16 h the reaction mixture was diluted with dichloromethane (500 mL), washed with a 10% aqueous solution of sodium hydroxide (600 mL), water (500 mL), brine (500 mL), dried (Na_2SO_4), filtered and concentrated *in vacuo*. The crude product was re-crystalised from hot ethanol (660 mL) to afford 2,6-di-[(4*R*,5*R*)-4,5-diphenyl-4,5-dihydro-1*H*-imidazol-2-yl]iodobenzene **113*R*** (24.3 g,

82%) as a white powder with spectral data consistent with that previously reported:[55] m.p. 131-133 °C [lit.[55] 154-156 °C]; $[\alpha]^{26}_{D}$ = + 90.0 (c = 0.96, CH_2Cl_2) [lit.[55] $[\alpha]^{25}_{D}$ = + 100.0 (c = 0.24 , CH_2Cl_2)]. All other data is identical to that reported above.

1,3-Di-[(4*S*,5*S*)-4,5-diphenyl-4,5-dihydro-1*H*-imidazol-2-yl]benzene (*S*-BAM) (121*S*)

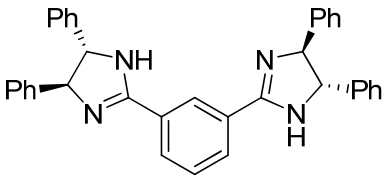

A solution of (1*S*,2*S*)-(-)-1,2-diphenylethylenediamine **124*S*** (332 mg, 1.56 mmol) in dichloromethane (5 mL) at 0°C was added *via* cannular to a stirred solution of isophthaldehyde (100 mg, 14.9 mmol) in dichloromethane (5 mL) at 0°C under an inert atmosphere of nitrogen. After stirring at 0°C for 5 h, NBS was added and the reaction mixture was allowed to slowly warm to RT. After 22 h, the reaction mixture was diluted with dichloromethane (20 mL), washed with a 10% solution of aqueous sodium hydroxide (20 mL), water (20 mL), brine (20 mL), dried (Na_2SO_4), filtered and concentrated *in vacuo*. The crude product was purified by re-crystallisation from hot ethanol (2 mL) with water, added drop-wise until the solution clouded slightly. On cooling with slow stirring, a precipitate was observed and was isolated by filtration. The residue was washed with water/ ethanol (1:3) and dried in a vacuum oven to afford the pure 1,3-di-[(4*S*,5*S*)-4,5-diphenyl-4,5-dihydro-1*H*-imidazol-2-yl]benzene (*S*-BAM, **121*S***) (251 mg, 65%) as a white powder: m.p. 129-135°C; R_f = 0.11 (dichloromethane, 4% methanol); $[\alpha]^{20}_{D}$ = -16.1 (c = 2.05 , CH_2Cl_2); FT IR (NaCl) ν_{max} 3400-3100 (br), 3060, 3028, 2903, 1950 (w), 1886 (w), 1807 (w), 1620, 1573 cm^{-1}; ^1H NMR (400 MHz, $CDCl_3$) δ 8.50 (s, 1H, Ar-*H*), 8.09 (d, *J* = 7.2 Hz, 2H, Ar-*H*), 7.53 (t, *J* = 7.2 Hz, 1H, Ar-*H*), 7.36-7.26 (m, 20H, Ar-*H*), 4.90 (br s, 4H, NC*H*) ppm; ^{13}C NMR (100 MHz, $CDCl_3$) δ 162.4, 143.2, 130.4, 129.9, 128.9, 128.7, 127.6, 126.6, 126.3, 77.2 ppm; MS (FAB$^+$) 519 (M+H$^+$); HRMS calcd for (M+H$^+$) $C_{36}H_{31}N_4$ 519.2549, found 519.2554; Anal. calcd for $C_{36}H_{30}N_4$: C, 83.37; H, 5.83; N, 10.80; found: C, 83.31; H, 5.78; N, 10.72.

2,6-Di-[(4*R*,5*R*)-1-acetyl-4,5-diphenyl-4,5-dihydroimidazol-2-yl]iodobenzene (244)

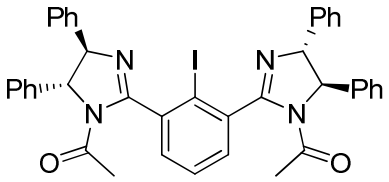

Acetic anhydride (70 µL, 0.75 mmol) was added to a solution of 2,6-di-[(4*R*,5*R*)-4,5-diphenyl-4,5-dihydro-1*H*-imidazol-2-yl]iodobenzene (*R*-IBAM, **113*R***) (200 mg, 0.31 mmol), triethylamine (95 µL, 0.68 mmol) and DMAP (8 mg, 0.06 mmol) in THF (6 mL) stirred at 0 ℃ under an inert atmosphere of nitrogen. The mixture was allowed to gradually warm to RT and stirred for 17 h. The reaction mixture was concentrated *in vacuo* and the resulting residue purified by flash column chromatography (2:1, ethyl acetate/petrol) to afford **244** as a colourless amorphous solid (218 mg, 96%): m.p. 135-140 ℃; R_f = 0.36 (2:1, ethyl acetate/petrol); $[\alpha]^{20}_D$ = + 80.0 (c = 1.15, CH_2Cl_2); FT IR (NaCl) ν_{max} 3060, 3030, 2966, 1952 (w), 1883 (w), 1812 (w), 1691, 1632 cm^{-1}; ^1H NMR (400 MHz, $CDCl_3$) δ 7.70-7.38 (m, 23H, Ar-*H*), 5.29 (br s, 4H, NC*H*Ph), 1.87 (s, 6H, C(O)CH_3) ppm; ^{13}C NMR (100 MHz, $CDCl_3$) δ 168.0, 159.3, 141.7, 140.2, 130.5, 130.0, 129.3, 128.9, 128.7, 128.3, 128.0, 127.0, 98.5, 78.4, 70.9, 24.8 ppm; MS (FAB^+) 729 ($M+H^+$); HRMS calcd for ($M+H^+$) $C_{40}H_{34}N_4O_2I$ 729.1727, found 729.1726; Anal. calcd for $C_{40}H_{33}N_4O_2I$; C, 65.94; H, 4.57; N, 7.69; found: C, 65.86; H, 4.48; N, 7.62.

2,6-Di-[(4*R*,5*R*)-1-(2-oxo-butan-1-yl)-4,5-diphenyl-4,5-dihydroimidazol-2-yl]iodobenzene (249)

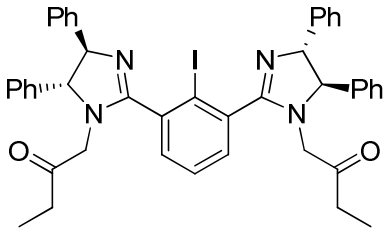

2,6-Di-[(4*R*,5*R*)-4,5-diphenyl-4,5-dihydro-1*H*-imidazol-2-yl]iodobenzene (*R*-IBAM, **113*R***) (200 mg, 0.31 mmol) was stirred with triethylamine (95 µL, 0.68 mmol) in dichloromethane (6 mL) at 0 ℃ under an inert atmosphere of nitrogen. 1-bromo-2-butanone (70 µL,

0.68 mmol) was added *via* syringe and the solution was allowed to slowly warm to RT. After 24 h the reaction mixture was diluted with dichloromethane (25 mL), washed with saturated aqueous sodium hydrogen carbonate solution (25 mL), water (25 mL), brine (25 mL), dried (Na_2SO_4), filtered and concentrated *in vacuo* to afford an orange solid. The crude product was purified by flash column chromatography (1:1, dichloromethane/ethyl acetate) to yield **249** (44 mg, 18%) as a colourless amorphous solid: m.p. 91-94°C; R_f = 0.30 (1:1, dichloromethane/ethyl acetate); $[\alpha]^{20}_D$ = + 57.6 (c = 0.92, CH_2Cl_2); FT IR (NaCl) ν_{max} 3060, 3028, 2959, 2925, 2854, 1953 (w), 1885 (w), 1809 (w), 1723, 1616 cm^{-1}; ^1H NMR (400 MHz, $CDCl_3$) δ 7.59 (d, *J* = 7.2 Hz, 2H, Ar-*H*), 7.49-7.30 (m, 21H, Ar-*H*), 5.09 (d, *J* = 10.8 Hz, 2H, NC*H*Ph), 4.79 (d, *J* = 10.8 Hz, 2H, NC*H*Ph), 3.72 (d, J^2 = 19.2 Hz, 2H, NC*H*H'C(=O)), 3.63 (d, J^2 = 19.2 Hz, 2H, NCH*H'*C(=O)), 2.06 (q, *J* = 7.2 Hz, 4H, C(=O)CH_2CH$_3$), 0.90 (t, *J* = 7.2 Hz, 6H, C(=O)CH$_2$CH_3) ppm; ^{13}C NMR (100 MHz, $CDCl_3$) δ 207.5, 166.0, 143.2, 140.7, 138.1, 132.3, 129.0, 128.6, 128.4, 128.1, 127.8, 127.6, 127.3, 96.3, 79.3, 74.7, 52.8, 32.9, 7.3 ppm; MS (FAB^+) 785 ($M+H^+$); HRMS calcd for ($M+H^+$) $C_{44}H_{42}N_4O_2I$ 785.2353, found 785.2341.

2,6-Di-[(4*R*,5*R*)-1,3-di-(2-oxo-butan-1-yl)-4,5-diphenyl-4,5-dihydroimidazolium-2-yl]iodobenzene dibromide (250)

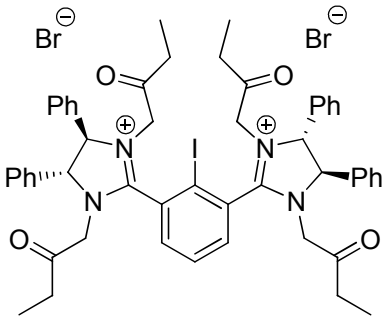

2,6-Di-[(4*R*,5*R*)-4,5-diphenyl-4,5-dihydro-1*H*-imidazol-2-yl]iodobenzene (*R*-IBAM, **113*R***) (200 mg, 0.31 mmol) was stirred with triethylamine (173 µL, 1.24 mmol) in dichloromethane (6 mL) at 0 °C under an inert atmosphere of nitrogen. 1-Bromo-2-butanone (127 µL, 1.24 mmol) was added *via* syringe and the solution was allowed to slowly warm to RT. After 44 h the reaction mixture was diluted with dichloromethane (25 mL), washed with saturated aqueous sodium hydrogen carbonate solution (25 mL), water (25 mL), brine (25 mL), dried

(Na_2SO_4), filtered and concentrated *in vacuo* to afford an orange solid. The crude product was purified by flash column chromatography (1:1, dichloromethane/ethyl acetate→ 92:8 dichloromethane/methanol) to yield **250** (99 mg, 29%) as a colourless amorphous solid: m.p. 175-185°C (decomp.); R_f = 0.08 (92:8, dichloromethane/methanol); $[\alpha]^{20}_D$ = + 254.1 (c = 1.5, CH_2Cl_2); FT IR (NaCl) ν_{max} 3388 (br), 3060, 3036, 2976, 2937, 2905, 1968 (w), 1898 (w), 1816 (w), 1723, 1579 cm^{-1}; ^1H NMR (400 MHz, $CDCl_3$) δ 7.92 (t, *J* = 7.9 Hz, 1H, Ar-*H*), 7.72 (d, *J* = 7.9 Hz, 2H, Ar-*H*), 7.55-7.28 (m, 20H, Ar-*H*), 5.89 (d, J^2 = 18.8 Hz, 2H, NC*H*H'C(=O)), 5.88 (d, J^2 = 18.8 Hz, 2H, NC*H*H'C(=O)), 5.55 (d, *J* = 9.8 Hz, 2H, NC*H*Ph), 5.17 (d, *J* = 9.8 Hz, 2H, NC*H*Ph), 4.18 (d, J^2 = 18.8 Hz, 2H, NCH*H'*C(=O)), 3.86 (d, J^2 = 18.8 Hz, 2H, NCH*H'*C(=O)), 3.11 (dq, J^2 = 18.8 Hz, J^3 = 7.2 Hz, 2H, C(=O)C*H*H'CH_3), 2.73 (dq, J^2 = 18.0 Hz, J^3 = 7.2 Hz, 2H, C(=O)C*H*H'CH_3), 2.35-2.22 (m, 4H, 2 x C(=O)CH*H'*CH_3), 0.99 (t, *J* = 7.2 Hz, 6H, C(O)CH_2C*H*$_3$), 0.86 (t, *J* = 7.2 Hz, 6H, C(O)CH_2C*H*$_3$) ppm; ^{13}C NMR (100 MHz, $CDCl_3$) δ 205.8, 205.2, 167.0, 135.3, 134.5, 134.0, 132.4, 130.8, 130.6, 130.0, 129.7, 128.5, 128.4, 94.2, 73.2, 72.8, 54.8, 54.6, 34.3, 34.2, 7.3, 7.2 ppm; MS (FAB^+) 925 (dication-H^+); HRMS calcd for (dication-H^+) $C_{52}H_{54}N_4O_4I$ 925.3190, found 925.3155; Anal. calcd for $C_{52}H_{55}N_4O_4I$: C, 57.47; H, 5.10; N, 5.16; found: C, 57.49; H, 5.04; N, 5.12.

2,6-Di-[(4*R*,5*R*)-1-(3-oxo-butan-1-yl)-4,5-diphenyl-4,5-dihydroimidazol-2-yl]iodobenzene (252)

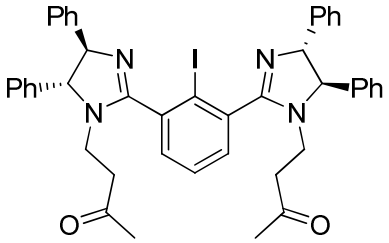

2,6-Di-[(4*R*,5*R*)-4,5-diphenyl-4,5-dihydro-1*H*-imidazol-2-yl]iodobenzene (*R*-IBAM, **113*R***) (200 mg, 0.31 mmol), 1-buten-3-one (83 µL, 0.99 mmol) and sodium acetate (25 mg, 0.31 mmol) were heated at 85 °C in dioxane (2 mL) under an inert atmosphere of nitrogen. After 24 h the reaction mixture was concentrated *in vacuo* and the resulting residue was partitioned between dichloromethane (25 mL) and water (25 mL). The organic layer was separated and the aqueous layer extracted with a further portion of dichloromethane (25 mL). The organic layers were combined, washed with brine (25 mL), dried ($MgSO_4$), filtered

and concentrated *in vacuo*. The crude product was purified by flash column chromatography (ethyl acetate, 4% methanol, 0.5% triethylamine) to yield **252** (161 mg, 66%) as a colourless amorphous solid: m.p. 91-95 °C; R_f = 0.24 (ethyl acetate, 4% methanol, 0.5% triethylamine); $[\alpha]^{20}_D$ = + 21.2 (c = 0.99, CH_2Cl_2); FT IR (NaCl) ν_{max} 3061, 3029, 2964, 2921, 2859, 1954 (w), 1885 (w), 1812 (w), 1712, 1612 cm^{-1}; ^1H NMR (400 MHz, $CDCl_3$) δ 7.69-7.30 (m, 23H, Ar-*H*), 5.17-5.11 (m, 2H, NC*H*Ph), 4.55-4.49 (m, 2H, NC*H*Ph), 3.40-3.24 (m, 4H, NCH_2CH_2), 2.38-2.29 (m, 4H, NCH_2CH_2C(O)), 1.86-1.76 (m, 6H, C(O)CH_3) ppm; ^{13}C NMR (100 MHz, $CDCl_3$) δ 206.2, 206.0, 166.6, 165.9, 143.5, 142.1, 141.4, 138.9, 131.8, 131.0, 129.0, 128.7, 128.6, 128.5, 128.1, 128.0, 127.4, 127.3, 126.8, 99.2, 97.5, 79.7, 78.9, 75.8, 74.5, 42.0, 41.5, 41.1, 40.4, 30.0 ppm; MS (ES^+) 785 ($M+H^+$); HRMS calcd for ($M+H^+$) $C_{44}H_{42}N_4O_2I$ 785.2353, found 785.2319.

2,6-Di-[(4*R*,5*R*)-1-(benzoyl)-4,5-diphenyl-4,5-dihydroimidazol-2-yl]iodobenzene (242)

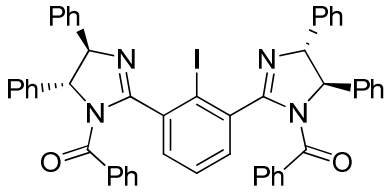

2,6-Di-[(4*R*,5*R*)-4,5-diphenyl-4,5-dihydro-1*H*-imidazol-2-yl]iodobenzene (*R*-IBAM, **113*R***) (200 mg, 0.31 mmol) was stirred with triethylamine (108 µL, 0.78 mmol) and DMAP (8 mg, 0.06 mmol) in dichloromethane (4 mL) under an inert atmosphere of nitrogen. Benzoyl chloride (90 µL, 0.78 mmol) was added *via* syringe and the reaction mixture was stirred at RT for 18 h. The reaction mixture was diluted with dichloromethane (20 mL) and washed with 0.5 M aqueous hydrochloric acid (20 mL). The aqueous phase was re-extracted with a further portion of dichloromethane (20 mL) and the combined organic phases were washed with saturated aqueous sodium hydrogen carbonate solution (20 mL), water (20 mL), dried ($MgSO_4$), filtered and concentrated *in vacuo* to afford a colourless foam. The crude product was purified by flash column chromatography (2:1, ethyl acetate/petrol) to yield **242** (250 mg, 94%) as a colourless amorphous solid: m.p. 137-141 °C; R_f = 0.50 (2:1, ethyl acetate/petrol); $[\alpha]^{20}_D$ = + 20.0 (c = 1.6, CH_2Cl_2); FT IR (NaCl) ν_{max} 3060, 3030, 2979, 2901, 1953, 1886, 1809, 1668, 1631 cm^{-1}; ^1H NMR (400 MHz, $CDCl_3$) δ 7.45-7.07 (m, 29H, Ar-*H*), 7.09 (t, *J* = 7.6 Hz, 4H, Ar-*H*), 5.35 (d, *J* = 8.0 Hz, 2H, NC*H*Ph), 5.31 (d, *J* = 8.0 Hz, 2H,

NC*H*Ph) ppm; ^{13}C NMR (100 MHz, $CDCl_3$) δ 170.0, 159.9, 141.6, 140.6, 138.7, 134.8, 131.4, 130.9, 129.0, 128.8, 128.2, 128.0, 127.9, 127.0, 126.8, 98.5, 78.5, 72.7 ppm; MS (ES^+) 853 ($M+H^+$); HRMS calcd for ($M+H^+$) $C_{50}H_{38}N_4O_2I$ 853.2040, found 853.2059; Anal. calcd for $C_{50}H_{37}N_4O_2I$: C, 70.42; H, 4.37; N, 6.57; found: C, 70.39; H, 4.28; N, 6.48.

2,6-Di-[(4*S*,5*S*)-1-{(*R*)-α-acetoxyphenyl acetyl}-4,5-diphenyl-4,5-dihydroimidazol-2-yl]iodobenzene (245)

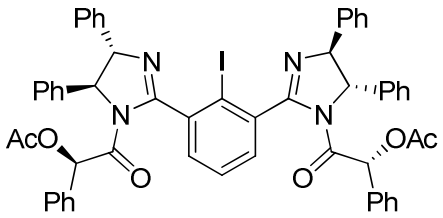

2,6-Di-[(4*S*,5*S*)-4,5-diphenyl-4,5-dihydro-1*H*-imidazol-2-yl]iodobenzene (*S*-IBAM, **113*S***) (105 mg, 0.16 mmol), (*R*)-(–)-α-acetoxyphenyl acetic acid (**173**) (76 mg, 0.39 mmol) and DMAP (5 mg, 0.04 mmol) were stirred in dichloromethane (4 mL) at 0 °C under an inert atmosphere of nitrogen. DCC (81 mg, 0.39 mmol) was added and the solution was allowed to slowly warm to RT with stirring. After 20 h the reaction mixture was filtered, the residue washed with ethyl acetate (5 mL) and the combined filtrate and washings were concentrated *in vacuo*. The resulting crude product was purified by flash column chromatography (1:1, ethyl acetate/petrol), followed by re-crystallisation from ethyl acetate/di*iso*propyl ether to yield **245** (42 mg, 26%) as colourless cubic crystals: m.p. 125-135 °C; R_f = 0.16 (1:1, ethyl acetate/petrol); $[\alpha]^{22}_D$ = + 136.2 (c = 1.8, CH_2Cl_2); FT IR (NaCl) ν_{max} 3062, 3034, 1959(w), 1883(w), 1745, 1708, 1638 cm^{-1}; ^{1}H NMR (400 MHz, $CDCl_3$) δ 7.47-7.13 (m, 33H, Ar-*H*), 5.64 (br s, 2H, NC(=O)C*H*), 5.15 (br s, 4H, NC*H*Ph), 1.98 (s, 6H, CO_2CH_3) ppm; ^{13}C NMR (100 MHz, $CDCl_3$) δ 170.0, 165.2, 158.6, 140.7, 140.3, 139.5, 131.9, 129.8, 129.6, 129.3, 129.1, 128.7, 127.8, 126.8, 126.3, 97.7, 80.0, 74.7, 68.3, 20.5 ppm; MS (FAB^+) 997 ($M+H^+$); HRMS calcd for ($M+H^+$) $C_{56}H_{46}N_4O_6I$ 997.2462, found 997.2461; Anal. calcd for $C_{56}H_{45}N_4O_6I$: C, 67.47; H, 4.55; N, 5.62; found: C, 67.40; H, 4.49; N, 5.62; *Crystal data for* **245**: $C_{56}H_{45}IN_4O_6$, *M* = 996.86, monoclinic, *P*2 (no. 3), *a* = 10.1088(17), *b* = 8.9540(15), *c* = 13.6000(8) Å, β = 90.045(8)°, *V* = 1231.0(3) Å^3, *Z* = 1 (C_2 symmetry), D_c = 1.345 g cm^{-3}, μ(Mo-Kα) = 0.705 mm^{-1}, *T* = 173 K, colourless blocks, Oxford Diffraction Xcalibur 3

diffractometer; 7620 independent measured reflections, F^2 refinement, R_1 = 0.022, wR_2 = 0.056, 7199 independent observed absorption-corrected reflections [$|F_o| > 4\sigma(|F_o|)$, $2\theta_{max}$ = 64°], 306 parameters. The absolute structure of **245** was determined by a combination of *R*-factor tests [R_1^+ = 0.0223, R_1^- = 0.0389] and by use of the Flack parameter [x^+ = +0.000(7), x^- = +1.003(7)].

2-[(4*R*,5*R*)-1-acetyl-4,5-diphenyl-4,5-dihydroimidazol-2-yl]-6-[(4*R*,5*R*)-4,5-diphenyl-4,5-dihydro-1*H*-imidazol-2-yl]-iodobenzene (243)

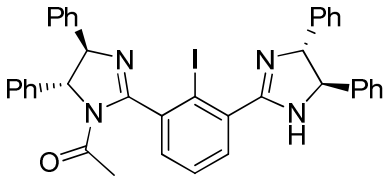

Acetic anhydride (64 µL, 0.68 mmol) was added to a solution of 2,6-di-[(4*R*,5*R*)-4,5-diphenyl-4,5-dihydro-1*H*-imidazol-2-yl]iodobenzene (*R*-IBAM, **113*R***) (400 mg, 0.62 mmol), triethylamine (85 µL, 0.62 mmol) and DMAP (8 mg, 0.06 mmol) in THF (10 mL) stirred at 0 °C under an inert atmosphere of nitrogen. The mixture was allowed to gradually warm to RT and, after stirring for 23 h, TLC analysis (ethyl acetate) indicated the formation of two new products (R_f = 0.36 and R_f = 0.59) which were identified as the mono- and bis-acetylated products respectively. The reaction mixture was concentrated *in vacuo* and the resulting residue purified by flash column chromatography (2:1, ethyl acetate/petrol→ethyl acetate) to afford the mono-acetylated product **243** as a colourless amorphous solid (169 mg, 40%): m.p. 129-135 °C; R_f = 0.36 (ethyl acetate); $[\alpha]^{20}_D$ = + 72.3 (c = 1.3, CH_2Cl_2); FT IR (NaCl) ν_{max} 3391(br), 3061, 3029, 2924, 1951 (w), 1885 (w), 1808 (w), 1687, 1629 cm^{-1}; ^1H NMR (400 MHz, $CDCl_3$) δ 7.76-7.73 (m, 1H, Ar-*H*), 7.60-7.59 (m, 2H, Ar-*H*), 7.50-7.34 (m, 20H, Ar-*H*), 5.57 (br s, 1H, N*H*), 5.31 (br s, 1H, NC*H*Ph), 5.24 (br s, 1H, NC*H*Ph), 4.99 (br s, 2H, NC*H*Ph), 1.81 (s, 3H, C(=O)C*H*$_3$) ppm; ^{13}C NMR (100 MHz, $CDCl_3$) δ 168.0, 164.8, 159.8, 143.0, 142.0, 141.5, 140.6, 139.0, 131.3, 130.6, 129.6, 129.1, 128.9, 128.5, 128.2, 127.8, 127.3, 126.2, 97.1, 78.6, 71.5, 70.7, 25.0 ppm; MS (ES^+) 687 ($M+H^+$); HRMS calcd for ($M+H^+$) $C_{38}H_{32}N_4OI$ 687.1621, found 687.1611; Anal. calcd for $C_{38}H_{31}N_4OI$: C, 66.48; H, 4.55; N, 8.16; found: C, 66.72; H, 4.62; N, 8.03.

.

2-[(4*R*,5*R*)-1-{(*R*)-α-Acetoxyphenyl acetyl}-4,5-diphenyl-4,5-dihydroimidazol-2-yl]-6-[(4*R*,5*R*)-4,5-diphenyl-4,5-dihydro-1*H*-imidazol-2-yl]-iodobenzene (247)

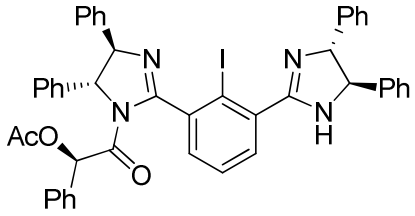

2,6-Di-[(4*R*,5*R*)-4,5-diphenyl-4,5-dihydro-1*H*-imidazol-2-yl]iodobenzene (*R*-IBAM, **113*R***) (250 mg, 0.39 mmol), (*R*)-(–)-α-acetoxyphenyl acetic acid (**173**) (158 mg, 0.82 mmol) and DMAP (9 mg, 0.08 mmol) were stirred in dichloromethane (10 mL) at 0 °C under an inert atmosphere of nitrogen. DCC (160 mg, 0.78 mmol) was added and the solution was allowed to slowly warm to RT with stirring. After 3 d the reaction mixture was filtered, the residue washed with ethyl acetate (10 mL) and the combined filtrate and washings were concentrated *in vacuo*. The resulting crude product was purified by flash column chromatography (1:2→2:3→1:1→1:0, ethyl acetate/petrol) to afford **247** (139 mg, 44%) as a colourless amorphous solid: m.p. 126-130 °C; R_f = 0.46 (ethyl acetate); $[\alpha]^{23}_D$ = + 2.2 (c = 0.89, CH_2Cl_2); FT IR (NaCl) ν_{max} 3379 (br), 3167, 3061, 3031, 2965, 2930, 1953(w), 1884(w), 1810(w), 1737, 1701, 1636, 1575 cm^{-1}; ^1H NMR (400 MHz, $CDCl_3$) δ 7.74 (d, *J* = 7.6 Hz, 1H, Ar-*H*), 7.54-7.13 (m, 25H, Ar-*H*), 6.74 (br d, *J* = 6.4 Hz, 2H, Ar-*H*), 5.74 (s, 1H, NC(=O)C*H*), 5.66 (br s, 1H, C(=O)NC*H*Ph), 5.25 (br s, 1H, NC*H*Ph), 4.98 (br s, 2H, NC*H*Ph), 2.05 (s, 3H, CO_2CH_3) ppm; ^{13}C NMR (125 MHz, $CDCl_3$) δ 171.0, 167.0, 165.0, 159.4, 142.6, 141.6, 140.7, 138.7, 132.4, 131.9, 131.0, 129.4, 129.2, 128.9, 128.8, 128.6, 128.5, 128.4, 128.3, 128.1, 127.5, 127.0, 126.3, 96.3, 80.3, 74.3, 70.4, 68.1, 20.5 ppm; MS (ES^+) 821 ($M+H^+$); HRMS calcd for ($M+H^+$) $C_{46}H_{38}N_4O_3I$ 821.1989, found 821.1964; Anal. calcd for $C_{46}H_{37}N_4O_3I$: C, 67.32; H, 4.54; N, 6.83; found: C, 67.35; H, 4.40; N, 6.79.

2,6-Di[*N*-(1'*R*)-(1'-benzyl-2'-hydroxyethyl)amino]iodobenzene (255)

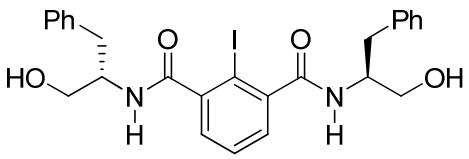

Diacyl chloride **187** (277 mg, 0.84 mmol) was dissolved in distilled dichloromethane (3 mL) and the solution was cooled to -40 °C under an inert atmosphere of nitrogen. In a separate flask (*S*)-phenyl alaninol (280 mg, 1.85 mmol) and triethylamine (351 µL, 2.53 mmol) were stirred in distilled dichloromethane (5 mL) at -40 °C under nitrogen. The diacyl chloride solution was then transferred to the reaction flask by cannular under nitrogen, and the reaction mixture was allowed to slowly warm to RT. After 16 h, the reaction mixture was cooled to -20 °C in order to maximise precipitation of the solid product. The precipitate was filtered, washed with water (8 mL), ethanol (8 mL) and dried in a dessicator over silica to yield diamide **255** (240 mg, 51%) as a white crystalline solid: m.p. 185-189 °C; R_f = 0.09 (1:99, methanol/ethyl acetate); $[\alpha]_D$ = -35.8 (c = 1.1, 1:9, MeOH:$CHCl_3$); FT IR (NaCl, nujol®) ν_{max} 3265 (br), 1941 (w), 1875 (w), 1803 (w), 1742 (w), 1649 cm^{-1}; ^1H NMR (270 MHz, $CDCl_3$) δ 8.27 (d, *J* = 8.5 Hz, 2H, N*H*), 7.49-7.19 (m, 11H, Ar*H*), 6.97 (d, *J* = 7.4 Hz, 2H, Ar*H*) 4.84 (br s, 2H, O*H*), 4.06 (br m, 2H, C*H*), 3.56 (m, 2H, 2 × C*H*H'OH), 3.35 (m, 2H, 2 ×CH*H*'OH), 2.98 (dd, J^{β} = 13.6 Hz, J^{β} = 4.5 Hz, 2H, 2 ×C*H*H'Ph), 2.69 (dd, J^{β} = 13.6 Hz, J^{β} = 9.1 Hz, 2H, 2 ×CH*H*'Ph) ppm; ^{13}C NMR (68 MHz, $CDCl_3$) δ 169.2, 145.1, 139.8, 129.8, 129.7, 128.7, 127.8, 126.5, 92.4, 63.3, 53.3, 36.8 ppm; MS (Cl^+) 576 ($M+NH_4^+$), 559 ($M+H^+$).

2,6-Di[(4'*R*)-4'-benzyloxazolin-2'-yl]iodobenzene (257)

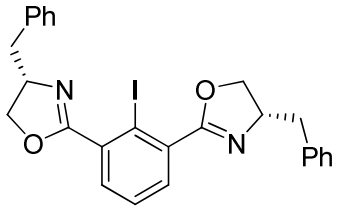

A solution of diamide **255** (200 mg, 0.35 mmol) and triethylamine (237 µL, 1.70 mmol) in DMF (2 mL) and dichloromethane (5 mL) was stirred at 0 °C under an inert atmosphere of nitrogen. Mesyl chloride (90 mg, 0.78 mmol) was added *via* syringe, and the solution was stirred for 24 h. The reaction mixture was diluted with dichloromethane (20 mL) and poured into water (20 mL). The organic layer was separated and the aqueous layer was re-extracted with dichloromethane (20 mL). The combined organic extracts were washed with brine (20 mL), dried ($MgSO_4$), filtered and concentrated *in vacuo*. The crude mesylate was taken straight on to the oxazoline; the residue was dissolved in ethanol (4 mL) and to this a solution of sodium hydroxide (100 mg) in water (4 mL) was added. The reaction mixture was

heated at reflux for 2.5 h, after which time the ethanol was evaporated *in vacuo* and the remaining suspension was extracted with dichloromethane (20 mL). The organic layer was washed with 0.5M aqueous hydrochloric acid (20 mL) and the aqueous layer was re-extracted with dichloromethane (20 mL). The combined organic layers were washed with saturated aqueous sodium hydrogen carbonate (20 mL), water (20 mL), brine (20 mL), dried ($MgSO_4$), filtered and concentrated *in vacuo*. The crude product was purified by flash column chromatography (1:6, petrol/ethyl acetate) to yield bis-oxazoline **257** (53 mg, 28%) as an amorphous colourless solid: R_f = 0.36 (1:6, petrol/ethyl acetate); ^{1}H NMR (300 MHz, $CDCl_3$) δ 7.54-7.20 (m, 13H, Ar*H*), 4.66 (quintet, *J* = 7.6 Hz, 2H, NC*H*), 4.44 (t, *J* = 8.9 Hz, 2H, 2 × OC*H*H'), 4.24 (t, *J* = 7.9 Hz, 2H, 2 × OCH*H*'), 3.27 (dd, J^2 = 13.8 Hz, J^3 = 5.4 Hz, 2H, 2 ×C*H*H'Ph), 2.87 (dd, J^2 = 13.8 Hz, J^3 = 8.2 Hz, 2H, 2 ×CH*H*'Ph) ppm; ^{13}C NMR (75 MHz, $CDCl_3$) δ 165.1, 137.7, 136.4, 131.7, 129.4, 128.6, 127.9, 126.6, 96.0, 72.3, 68.2, 41.5 ppm; MS (Cl^+) 523 ($M+H^+$); HRMS calcd for ($M+H^+$) $C_{26}H_{24}N_2O_2I$ 523.0883, found 523.0883.

6.4. Substrate Synthesis

(*S*)-2-Allyloxypropionic Acid Ethyl Ester (219*S*)[139]

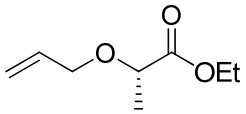

To a solution of (*S*)-ethyl lactate (**218*S***) (4.9 mL, 42 mmol) in diethyl ether (100 mL) was added silver oxide (19.6 g, 85 mmol) and allyl bromide (7.7 mL, 89 mmol). The mixture was stirred for 4 days under an inert atmosphere of nitrogen, at RT, in the dark, until TLC (1:1, petrol/ethyl acetate) indicated the full consumption of the starting material (R_f = 0.40). The solids were filtered off through Celite® and washed with a further portion of diethyl ether (100 mL). The combined filtrates were concentrated *in vacuo* to afford the crude product. This was purified by flash column chromatography (6:1, petrol/diethyl ether) to afford the pure (*S*)-2-allyloxypropionic acid ethyl ester (**219*S***) (4.4 g, 66%) as a colourless oil with spectral data consistent with literature:[139] R_f = 0.28 (6:1, petrol/diethyl ether); $[\alpha]^{25}_D$ = -71.5 (c = 3.83 , EtOH) [lit.[117] $[\alpha]^{23}_D$ = -73.6 (EtOH)]; FT IR (NaCl) ν_{max} 3082, 2983, 2937, 1747 cm^{-1}; ^{1}H NMR

(400 MHz, $CDCl_3$) δ 5.93 (ddt, J^{β}_{trans} = 17.2 Hz, J^{β}_{cis} = 10.4 Hz, J^{β} = 5.8 Hz, 1H, CH_2=C*H*), 5.29 (d, J^{β}_{trans} = 17.2 Hz, 1H, CH_{trans}H$_{cis}$=CH), 5.20 (d, J^{β}_{cis} = 10.4 Hz, 1H, CH$_{trans}H_{cis}$=CH), 4.22 (m, 2H, OCH_2CH$_3$), 4.15 (dd, J^{2} = 12.4 Hz, J^{β} = 5.6 Hz, CH_2=CHC*H*H'), 4.01 (q, J^{β} = 6.8 Hz, 1H, OC*H*(CH_3)CO_2), 3.95 (dd, J^{2} = 12.4 Hz, J^{β} = 6.0 Hz, 1H, CH_2=CHCH*H'*), 1.42 (d, J^{β} = 6.8 Hz, 3H, OCH(CH_3)CO_2), 1.29 (t, J^{β} = 7.2 Hz, 3H, OCH_2CH_3) ppm; ^{13}C NMR (100 MHz, $CDCl_3$) δ 173.4, 133.8, 117.4, 73.7, 70.7, 60.5, 18.3, 13.9 ppm; MS (CI^+) 176 ($M+NH_4^+$); HRMS calcd for ($M+NH_4^+$) $C_8H_{18}NO_3$ 176.1287, found 176.1293.

(*S*)-2-Allyloxypropionic acid (**217*S***) (200 mg, 1.54 mmol), ethanol (108 µL, 1.85 mmol) and DMAP (38 mg, 0.31 mmol) were stirred in dichloromethane (15 mL) at 0°C under an inert atmosphere of nitrogen. DCC (381 mg, 1.85 mmol) was added and the solution was allowed to slowly warm to RT with stirring. After 18 h the reaction mixture was filtered, the residue washed with ethyl acetate (5 mL) and the combined filtrate and washings were concentrated *in vacuo*. The resulting crude product was purified by flash column chromatography (6:1, petrol/diethyl ether) to afford pure (*S*)-2-allyloxypropionic acid ethyl ester (**219*S***) (171 mg, 65%) as a colourless oil: $[\alpha]^{24}_D$ = -74.4 (c = 0.86 , EtOH) [lit.[117] $[\alpha]^{23}_D$ = -73.6 (EtOH)]; all other data identical to that previously reported.

(*R*)-2-Allyloxypropionic Acid Ethyl Ester (219*R*)[139]

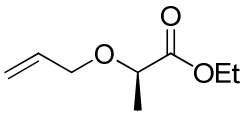

To a solution of (*R*)-ethyl lactate (**128*R***) (3.8 mL, 33 mmol) in diethyl ether (80 mL) was added silver oxide (15.2 g, 66 mmol) and allyl bromide (5.6 mL, 66 mmol). The mixture was stirred for 3 days under an inert atmosphere of nitrogen, at RT, in the dark, until TLC (1:1, petrol/ethyl acetate) indicated the full consumption of the starting material (R_f = 0.40). The solids were filtered off through Harbourlite® and washed with a further portion of ether (100 mL). The combined filtrates were concentrated *in vacuo* to afford the crude product. This was purified by flash column chromatography (6:1, petrol/diethyl ether) to afford the pure (*R*)-2-allyloxypropionic acid ethyl ester (**219*R***) (4.1 g, 97%) as a colourless oil: $[\alpha]^{27}_D$ = +76.5 (c = 2.7, EtOH). The other spectral data is identical to that for its enantiomer.

(*S*)-2-Allyloxypropionic Acid (217*S*)

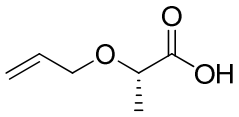

A solution of ester **219*S*** (200 mg, 1.27 mmol), lithium hydroxide monohydrate (266 mg, 6.33 mmol), methanol (15 mL) and water (3 mL) was stirred at RT for 18 h. The reaction mixture was partitioned between water (40 mL) and diethyl ether (40 mL). The aqueous layer was separated, acidified to pH1 with 2M aqueous hydrochloric acid and extracted with ethyl acetate (3 × 40 mL). The combined organic extracts were washed with brine (40 mL), dried ($MgSO_4$), filtered and concentrated *in vacuo* to afford (*S*)-2-allyloxypropionic acid (**217*S***) (169 mg, quantitative) as a pale yellow oil: R_f = 0.28 (1:1, petrol/diethyl ether); $[\alpha]^{24}_D$ = -13.9 (c = 1.44 , CH_2Cl_2); FT IR (NaCl) ν_{max} 3600-2300 (br), 2984, 1726 cm^{-1}; ^1H NMR (400 MHz, $CDCl_3$) δ 5.84 (ddt, J^{β}_{trans} = 17.2 Hz, J^{β}_{cis} = 10.0 Hz, J^{β} = 5.6 Hz, 1H, CH_2=C*H*), 5.32 (d, J^{β}_{trans} = 17.2 Hz, 1H, C$H_{trans}H_{cis}$=CH), 5.23 (d, J^{β}_{cis} = 10.0 Hz, 1H, $CH_{trans}H_{cis}$=CH), 4.18 (dd, J^{2} = 12.4 Hz, J^{β} = 5.6 Hz, CH_2=CHC*H*H'), 4.08 (q, J^{β} = 6.8 Hz, 1H, OC*H*(CH_3)CO_2H), 4.01 (dd, J^{2} = 12.4 Hz, J^{β} = 6.0 Hz, 1H, CH_2=CHCH*H'*), 1.48 (d, J^{β} = 6.8 Hz, 3H, OCH(C*H*$_3$)CO_2H) ppm; ^{13}C NMR (100 MHz, $CDCl_3$) δ 178.8, 133.7, 118.2, 73.4, 71.2, 18.4 ppm; MS (CI^+) 148 ($M+NH_4^+$); HRMS calcd for ($M+NH_4^+$) $C_6H_{14}NO_3$ 148.0974, found 148.0975.

(*R*)-2-Allyloxypropionic Acid (217*R*)

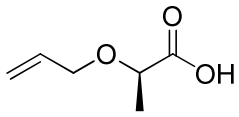

A solution of ester **219*R*** (2.0 g, 12.7 mmol), lithium hydroxide monohydrate (2.6 g, 63.3 mmol), methanol (150 mL) and water (30 mL) was stirred at RT for 20 h. The reaction mixture was partitioned between water (400 mL) and diethyl ether (400 mL). The aqueous layer was separated, acidified to pH1 with a 2M aqueous solution of hydrochloric acid and extracted with ethyl acetate (3 × 300 mL). The combined organic extracts were washed with brine (200 mL), dried ($MgSO_4$), filtered and concentrated *in vacuo* to afford (*R*)-2-

allyloxypropionic acid (**217*R***) (1.6 g, 98%) as a pale colourless oil: $[\alpha]^{27}_{D}$ = +8.0 (c = 1.7, CH_2Cl_2). The other spectral data is identical to that for its enantiomer.

6.5. Catalytic Electrophilic Bromination of Alkenes

A General Procedure for NBS/Amidine-Catalyst Bromolactonisation[140]

NBS (1 eq.) was added to a stirred solution of substrate (1 eq.) and (±)-*iso*-amarine **116** (0.01 eq.) in dichloromethane or deuterated chloroform (0.25M) at RT. The reaction mixture was stirred for 1-2 h, quenched with 20% aqueous sodium sulphite solution, and extracted with dichloromethane. The organic layer was washed with water, brine, dried ($MgSO_4$), filtered and concentrated *in vacuo*.

Bromolactones

(±)-5-Bromomethyl-γ-butyrolactone (106)

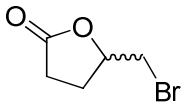

Starting from 4-pentenoic acid (**61b**) (100 µL, 1.0 mmol) and following the general procedure afforded the crude bromolactone. The crude product was purified by flash column chromatography (1:2, petrol/diethyl ether) to yield 5-bromomethyl-γ-butyrolactone (**106**) (161 mg, 90%) as a colourless oil with spectral data consistant with that previously reported[55]: R_f = 0.27 (1:2, petrol/diethyl ether); FT IR (NaCl) ν_{max} 2962, 1776 cm^{-1}; ^1H NMR (270 MHz, $CDCl_3$) δ 4.71 (m, 1H, OC*H*), 3.51 (d, *J* = 5.3 Hz, 2H, CH_2Br), 2.69-2.33 (m, 3H, CH_2C*H*H'), 2.14-2.00 (m, 1H, CH*H'*) ppm; ^{13}C NMR (68 MHz, $CDCl_3$) δ 176.3, 77.9, 34.3, 28.5, 26.2 ppm; MS (CI^+) 196/198 ($M+NH_4^+$); HRMS calcd for ($M+NH_4^+$) $C_5H_{11}NO_2{}^{79}Br$ 197.9953 and $C_5H_{11}NO_2{}^{81}Br$ 195.9973, found 197.9950 and 195.9971; HPLC (3:7, ethanol/hexane); Chiralpak AD: 0.5 mL/min; 225 nm, t_R(*R*) 17.12 min, t_R(*S*) 19.74 min.

(±)-5-Bromomethyl-5-phenyldihydrofuran-2-one (222)

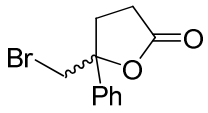

Starting from 4-phenylpent-4-enoic acid (**216**) (176 mg, 1.0 mmol) and following the general procedure afforded the crude bromolactone. The crude product was purified by flash column chromatography (2:3, petrol/dichloromethane) to yield (±)-5-bromomethyl-5-phenyldihydrofuran-2-one (**222**) (219 mg, 86%) as a colourless oil with spectral data consistant with that previously reported:[55] R_f = 0.33 (2:3, petrol/dichloromethane); FT IR (NaCl) ν_{max} 3060, 3028, 2961, 1959 (w), 1788 cm^{-1}; ^1H NMR (270 MHz, $CDCl_3$) δ 7.40-7.34 (m, 5H, Ar*H*), 3.73, 3.67 (ABq, J_{AB} = 11.3 Hz, 2H, 2 × H_2CBr), 2.85-2.73 (m, 2H, CH_2), 2.60-2.44 (m, 2H, CH_2) ppm; ^{13}C NMR (68 MHz, $CDCl_3$) δ 175.6, 140.8, 128.9, 128.8, 125.0, 86.5, 41.1, 32.5, 29.1 ppm; MS (CI^+) 272/274 ($M+NH_4^+$); HRMS calcd for ($M+NH_4^+$) $C_{11}H_{15}NO_2{}^{79}Br$ 274.0266 and $C_{11}H_{15}NO_2{}^{81}Br$ 272.0286, found 274.0263 and 272.0279; HPLC (1:9, ethanol/hexane); Chiralpak AD: 0.5 mL/min; 225 nm, t_R 32.59 and 35.31 min, the absolute configuration was not determined.

(±)-6-Bromohexahydrocyclopenta[b]furan-2-one (115)

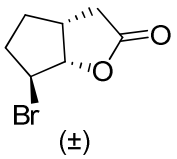

(±)

Starting from 2-cyclopenten-1-ylacetic acid (**114**) (240 µL, 2.0 mmol) and following the general procedure afforded the crude bromolactone. The crude product was purified by flash column chromatography (dichloromethane) to yield (±)-6-bromohexahydrocyclopenta[b]furan-2-one (**115**) (352 mg, 86%) as a colourless oil with spectral data consistant with that previously reported:[55] R_f = 0.31 (dichloromethane); FT IR (NaCl) ν_{max} 2969, 2881, 1776 cm^{-1}; ^1H NMR (270 MHz, $CDCl_3$) δ 5.05 (d, J = 6.2 Hz, 1H, C(=O)OC*H*), 4.43 (d, J = 4.2 Hz, 1H, C*H*Br), 3.20-3.10 (m, 1H, C*H*), 2.86 (dd, J = 18.5, 10.4 Hz, 1H, C*H*H'), 2.49-2.19 (m, 4H, CH_2), 1.58-1.63 (m, 1H, CH*H'*) ppm; ^{13}C NMR

(68 MHz, $CDCl_3$) δ 176.5, 90.5, 52.9, 36.0, 36.0, 33.1, 31.4 ppm; MS (CI^+) 222/224 ($M+NH_4^+$); HRMS calcd for ($M+NH_4^+$) $C_7H_{13}NO_2{}^{79}Br$ 222.0130 and $C_7H_{13}NO_2{}^{81}Br$ 224.0109, found 222.0129 and 224.0112; HPLC (3:7, ethanol/hexane); Chiralpak AD: 0.5 mL/min; 225 nm, t_R 19.52 and 25.19 min, the absolute configuration was not determined.

(2*S*)-5-Bromomethyl-3-oxa-2-methyl-δ-pentano-5-lactone (220*S*/221*S*)

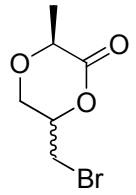

Starting from (*S*)-2-allyloxypropionic acid (**217*S***) (100 mg, 0.77 mmol) and following the general procedure afforded the crude bromolactone. The crude product was purified by flash column chromatography (5:1, dichloromethane/petrol) to afford **220*S*/221*S*** (92 mg, 57%) as a colourless oil in a 63:37 mixture of the (2*S*,5*S*) and (2*S*,5*R*) diastereomers: R_f = 0.30 (5:1, dichloromethane/petrol); $[\alpha]^{23}_D$ = -4.0 (c = 1.3 , CH_2Cl_2); FT IR (NaCl) ν_{max} 2987, 2941, 2871, 1748 cm^{-1}; ^1H NMR (400 MHz, $CDCl_3$) (2*S*,5*S*) diastereomer δ 4.84-4.78 (m, 1H, $CH_2CH(CH_2Br)O$), 4.30 (q, J = 6.9 Hz, 1H, $OCH(CH_3)C(=O)$), 4.19 (dd, J^2 = 12.8 Hz, J^3 = 3.6 Hz,1H, $OCHH'CH(CH_2Br)O$), 3.70 (dd, J^2 = 12.8 Hz, J^3 = 9.6 Hz, $OCHH'CH(CH_2Br)O$), 3.51 (dd, J^2 = 11.0 Hz, J^3 = 4.4 Hz, 1H, $CHH'Br$), 3.46 (dd, J^2 = 11.0 Hz, J^3 = 6.8 Hz, 1H, $CHH'Br$), 1.55 (d, J = 6.9 Hz, 3H, CH_3) ppm; (2*S*,5*R*) diastereomer δ 4.69-4.64 (m, 1H, $CH_2CH(CH_2Br)O$), 4.38 (q, J = 6.9 Hz, 1H, $OCH(CH_3)C(=O)$), 4.16 (dd, J^2 = 12.8 Hz, J^3 = 2.8 Hz, 1H, $OCHH'CH(CH_2Br)O$), 3.93 (dd, J^2 = 12.8 Hz, J^3 = 3.0 Hz, $OCHH'CH(CH_2Br)O$), 3.65-3.56 (m, 2H, CH_2Br), 1.54 (d, J = 6.9 Hz, 3H, CH_3) ppm; ^{13}C NMR (100 MHz, $CDCl_3$) (2*S*,5*S*) diastereomer δ 168.9, 77.1, 72.7, 65.6, 28.9, 17.7 ppm; (2*S*,5*R*) diastereomer δ 168.8, 77.3, 72.9, 62.5, 28.9, 17.7 ppm; MS (EI^+) 208/210 (M^+); HRMS calcd for (M^+) $C_6H_9O_3{}^{79}Br$ 207.9735 and $C_6H_9O_3{}^{81}Br$ 209.9715, found 207.9734 and 209.9719; Anal. calcd for $C_6H_9O_3Br$; C, 34.47; H, 4.34; found: C, 34.53; H, 4.24.

(2*R*)-5-Bromomethyl-3-oxa-2-methyl-δ-pentano-5-lactone (220*R*/221*R*)

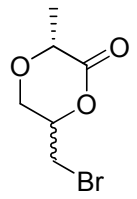

Starting from (*R*)-2-allyloxypropionic acid (**217*R***) (100 mg, 0.77 mmol) and following the general procedure afforded the crude bromolactone. The crude product was purified by flash column chromatography (5:1, dichloromethane/petrol) to afford **220*R*/221*R*** (90 mg, 56%) as a colourless oil in a in a 63:37 mixture of the (2*R*,5*R*) and (2*R*,5*S*) diastereomers: $[\alpha]^{24}_{D}$ = +4.3 (c = 1.2, CH_2Cl_2). The other spectral data is identical to that for its enantiomer. On standing in at 5 ºC for 2 weeks a number of fine colourless needles formed within the product colourless oil. On separation and analysis these proved to consist of exclusively the major (2*R*,5*R*) diastereoisomer: *Crystal data for* **220*R***: $C_6H_9BrO_3$, M = 209.04, orthorhombic, $P2_12_12_1$ (no. 19), a = 6.94127(12), b = 8.74587(16), c = 12.6315(2) Å, V = 766.83(3) Å^3, Z = 4, D_c = 1.811 g cm^{-3}, μ(Mo-Kα) = 5.306 mm^{-1}, T = 173 K, colourless needles, Oxford Diffraction Xcalibur 3 diffractometer; 2658 independent measured reflections, F^2 refinement, R_1 = 0.032, wR_2 = 0.064, 1876 independent observed absorption-corrected reflections [$|F_o| > 4\sigma(|F_o|)$, $2\theta_{max}$ = 65°], 91 parameters. The absolute structure of **220*R*** was determined by a combination of *R*-factor tests [R_1^+ = 0.0315, R_1^- = 0.0596] and by use of the Flack parameter [x^+ = +0.000(10)].

A General Procedure for NBS/Catalyst Asymmetric Bromolactonisation

NBS (1 eq.) was added to a stirred solution of substrate (1 eq.) and catalyst (0.05 eq.) in dichloromethane (0.025M) at -78 ºC under an inert atmosphere of nitrogen. The reaction mixture was stirred for 8 h, quenched with 20% aqueous sodium sulphite solution and extracted with dichloromethane. The organic layer was washed with water, brine, dried ($MgSO_4$), filtered and concentrated *in vacuo*. Where necessary, the brominated product was purified by flash column chromatography. Where applicable, diastereo-excess of the bromolactone product was determined by ^{1}H NMR ($CDCl_3$) analysis and enantio-excess by chiral HPLC analysis. The effects of the variation of catalyst structure and stoichiometry,

solvent, temperature, concentration and time on the yield and the enantioselectivity of the reaction are all detailed in the main text (chapter 3).

Attempted NBS/Catalyst/TMSCl Asymmetric Bromochlorination

(1*R,2*S**)-2-Bromo-1-chloro-1-phenylpropane (274)**

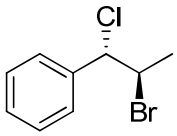

R-IBAM (**113**) (32 mg, 0.05 mmol), trimethylsilylchloride (140 µL, 1.1 mmol) and *trans*-β-methylstyrene (**18**) (130 µL, 1.1 mmol) were stirred at -78 ºC in dichloromethane (40 mL). NBS (196 mg, 1.1 mmol) was added and the reaction mixture stirred at -78 ºC for 8 h under an inert atmosphere of nitrogen. The reaction was quenched with 20% aqueous sodium sulfite solution (40 mL) and the organic phase separated. The aqueous phase was extracted with a further portion of dichloromethane (40 mL) and the combined organic phases were washed with water (40 mL), dried ($MgSO_4$), filtered and concentrated *in vacuo*. The crude product was purified by flash column chromatography (petrol) to afford (1*S**,2*R**)- **274** (108 mg, 46%) as a single diastereomer as colourless needles with spectral data consistent with literature:[141] m.p. 35-37 ºC; [lit.[142] 35-36.5 ºC]; R_f = 0.33 (petrol); FT IR (NaCl) ν_{max} 3064, 3033, 2983, 2932, 2868, 1951(w) cm^{-1}; ^1H NMR (400 MHz, $CDCl_3$) δ 7.44-7.37 (m, 5H, Ar-*H*), 5.02 (d, *J* = 8.4 Hz, 1H, PhC*H*Cl), 4.50 (dq, *J* = 6.8, 8.4 Hz, 1H, C*H*BrCH$_3$), 1.96 (d, *J* = 6.8 Hz, 3H, C*H*$_3$) ppm; ^{13}C NMR (100MHz, $CDCl_3$) δ 139.5, 128.9, 128.6, 127.6, 51.7, 23.6; MS (EI^+) 232/234/236 ($M^{+\cdot}$); HRMS calcd for (M^+) $C_9H_{10}{}^{35}Cl^{79}Br$ 231.9654, $C_9H_{10}{}^{37}Cl^{79}Br$ 233.9625, $C_9H_{10}{}^{35}Cl^{81}Br$ 233.9634 and $C_9H_{10}{}^{37}Cl^{81}Br$ 235.9604, found 231.9657, 231.9630 and 235.9642; HPLC (1:1, water/acetonitrile+0.05% TFA); Chiralcel OJ-RH: 1 mL/min; 240 nm, R_f(*S*,*R*) 23.65 min, R_f(*R*,*S*) 27.39 min; *Crystal data for* **274**: $C_9H_{10}BrCl$, *M* = 233.53, monoclinic, *I*2/*a* (no. 15), *a* = 18.7196(5), *b* = 5.4883(1), *c* = 19.2225(5) Å, β = 104.159(3)°, *V* = 1914.90(8) Å^3, *Z* = 8, D_c = 1.620 g cm^{-3}, µ(Cu-Kα) = 7.877 mm^{-1}, *T* = 173 K, colourless needles, Oxford Diffraction Xcalibur PX Ultra diffractometer; 1508 independent measured

reflections, F^2 refinement, $R_1 = 0.028$, $wR_2 = 0.075$, 1270 independent observed absorption-corrected reflections [$|F_o| > 4\sigma(|F_o|)$, $2\theta_{max} = 126°$], 131 parameters.

A General Procedure for stoichiometric addition of NBS to catalyst

NBS (1-5 mmol) was added to a stirred solution of catalyst (1-5 mmol) in carbon tetrachloride/chloroform (5.5-30 mL; carbon tetrachloride/chloroform ratio dependent on particular catalyst's solubility). The reaction was stirred at RT for 45 min to 1 h, until TLC demonstrated the complete consumption of starting material. A further portion of carbon tetrachloride (5 mL) was then added, and then reaction mixture cooled to 0°C. After standing for 30 min a fine white precipitate of succinimide (84-92%) had formed, and was removed by filtration through a cold scinter. The filtrate was concentrated *in vacuo* to afford the bromination product as an amorphous solid (quantitative).

2-(2-Iodophenyl)-4,5-diphenyl-1H-imidazole (234)

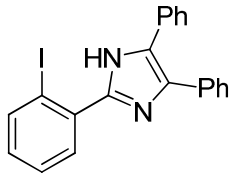

Following the above procedure, NBS (178 mg, 1 mmol) was added to *R*-IAM (**111*R***) (425 mg, 1 mmol) and the resulting brominated intermediate was isolated as a yellow foam (543 mg, quantitative). A portion of this (252 mg, 0.5 mmol) was then dissolved in dichloromethane (4 mL) and cooled to -78 °C. 2-Cyclopentene-1-acetic acid (**114**) (120 µL, 1 mmol) was added and then solution was stirred for 15 h. The reaction mixture was quenched with 20% aqueous sodium sulphite solution (25 mL), and extracted with dichloromethane (20 mL). The organic layer was washed with water (20 mL) and brine (20 mL), dried ($MgSO_4$), filtered and concentrated *in vacuo*. The resulting mixture of products was separated by flash column chromatography (dichloromethane → methanol/dichloromethane, 1:24) to yield bromolactone **115** (36.6 mg, 36%): as previously characterized; recovered *R*-IAM (**111*R***) (127 mg, 59% based on active catalytic species

added): as previously characterized; and a small amount of 2-(2-iodophenyl)-4,5-diphenyl-1H-imidazole (**234**) (52 mg, 24% based on active catalytic species added): R_f = 0.17 (dichloromethane); m.p. >230°C; FT IR (NaCl) ν_{max} 1600, 1503 cm^{-1}; ^1H NMR (270 MHz, $CDCl_3$) δ 9.92 (sbr, 1H, N*H*), 8.10 (dd, J^3 = 7.8 Hz, J^4 = 1.6 Hz, 1H, Ar*H*), 7.94 (dd, J^3 = 8.1 Hz, J^4 = 1.2 Hz, 1H, Ar*H*), 7.59 (m, 4H, Ar*H*), 7.43 (dt, J^3 = 7.8 Hz, J^4 = 1.2 Hz, 1H, Ar*H*), 7.38-7.29 (m, 6H, Ar*H*), 7.06 (dt, J^3 = 7.9 Hz, J^4 = 1.6 Hz, 1H, Ar*H*) ppm; MS (Cl^+) 423 ($M+H^+$); HRMS calcd for ($M+H^+$) $C_{21}H_{16}N_2I$ 423.0358, found 423.0370.

6.6. Bromonium ion - Alkene Br^+ exchange

(±)-Styrene oxide (267)

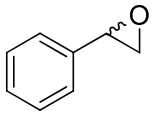

*m*CPBA (1.66 g, 9.65 mmol) was added to a stirred solution of styrene (**266**) (550 µL, 4.80 mmol) in dichloromethane (8 mL) at 15 °C. The reaction was allowed to slowly warm to RT and stirred for 20 h. The reaction mixture was quenched with 20% aqueous sodium sulfite solution (10 mL) and partitioned between dichloromethane (40 mL) and water (40 mL). The organic phase was separated and the aqueous phase re-extracted with a further portion of dichloromethane (40 mL). The combined organic layers were washed with saturated aqueous sodium hydrogen carbonate (40 mL), water (40 mL), dried ($MgSO_4$), filtered and concentrated *in vacuo*. The crude product was purified by flash column chromatography (2:3, dichloromethane /petrol) to afford racemic styrene oxide (**267**) (511 mg, 89%) as a colourless oil with spectral data consistent with literature:[143] R_f = 0.35 (2:3, dichloromethane /petrol); FT IR (NaCl) ν_{max} 2962, 2898, 1261 cm^{-1}; ^1H NMR (400 MHz, $CDCl_3$) δ 7.40-7.28 (m, 5H, Ar-*H*), 3.89 (dd, *J* = 4.2, 2.7 Hz, 1H, PhC*H*), 3.18 (dd, *J* = 5.5, 4.2 Hz, 1H, C*H*H'), 2.83 (dd, *J* = 5.5, 2.7 Hz, 1H, CH*H*') ppm; ^{13}C NMR (100 MHz, $CDCl_3$) δ 137.6, 128.5, 128.2, 125.5, 52.4, 51.3 ppm; MS (ES^+) 120 ($M^{+\cdot}$).

(±)-2-Bromo-2-phenylethanol, (261)

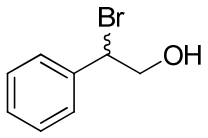

A 48% aqueous solution of hydrobromic acid (33 mL) was added to racemic styrene oxide (**267**) (1.54 mg, 12.8 mmol) stirred at RT in chloroform (33 mL). The biphasic mixture was stirred for 30 mins, following which it was diluted with water (400 mL) and extracted with dichloromethane (2 x 200 mL). The combined organic extracts were dried ($MgSO_4$), filtered and concentrated *in vacuo*. The crude product was purified by flash column chromatography (4:1, dichloromethane/petrol) to afford racemic 2-bromo-2-phenylethanol (**261**) (1.93 g, 75%) as colourless needles with spectral data consistent with literature:[144] m.p. 37-38 °C; [lit.[144] 35-36.5 °C]; R_f = 0.26 (4:1, dichloromethane/petrol); FT IR (NaCl) ν_{max} 3383 (br), 3032, 2929 cm^{-1}; ^1H NMR (400 MHz, $CDCl_3$) δ 7.46-7.34 (m, 5H, Ar-*H*), 5.09 (dd, *J* = 7.8, 5.8 Hz, 1H, PhC*H*), 4.10 (dd, J^{β} = 7.8 Hz, J^{ρ} = 12.2 Hz, 1H, C*H*H'OH), 3.98 (dd, J^{β} = 5.8 Hz, J^{ρ} = 12.2 Hz 1H, CH*H'*OH), 2.20 (s (br), 1H, O*H*) ppm; ^{13}C NMR (100 MHz, $CDCl_3$) δ 138.3, 129.0, 128.9, 128.0, 67.5, 57.0 ppm; MS (CI^+) 218/220 ($M+NH_4^+$); HRMS calcd for ($M+NH_4^+$) $C_8H_{13}NO^{79}Br$ 218.0181 and $C_8H_{13}NO^{81}Br$ 220.0160, found 218.0186 and 220.0166.

(*S*)-Mosher's acyl chloride, (269)

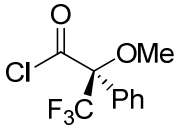

Oxallyl chloride (126 µL, 1.44 mmol), followed by a drop of DMF, was added to a solution of (*R*)-Mosher's acid (187 mg, 0.80 mmol) stirred in hexane at RT under an inert atmosphere of nitrogen. The resulting reaction mixture was stirred at RT for 3 h until it ceased to effervesce. The hexane layer was decanted off from the oily residue which remained at the bottom of the flask. The residue was washed with a further portion of hexane (2 mL) and the decanted liquid, plus washings, was concentrated *in vacuo* to afford (*S*)-Mosher's acyl chloride (**269**) (0.83 mmol, quantative) as a colourless oil with spectral data consistent with literature:[145] ^1H NMR (400 MHz, $CDCl_3$) δ 7.57 (d, *J* = 7.6 Hz, 2H, Ar-*H*), 7.50-7.45 (m, 3H,

Ar-*H*), 3.79 (q, *J* = 1.9 Hz, 3H, OC*H*$_3$) ppm; ^{13}C NMR (100 MHz, $CDCl_3$) δ 171.0, 130.7, 130.4, 128.7, 126.9, 122.6 (q, *J* = 289 Hz), 89.2 (q, *J* = 27 Hz), 56.7 ppm.

(2*R*)-2'-Bromo-2'-phenylethyl 2-methoxy-2-trifluoromethylphenylacetate (270)

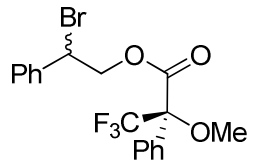

Racemic 2-bromo-2-phenylethanol (**261**) (50 mg, 0.26 mmol), triethylamine (90 µL, 0.65 mmol) and DMAP (64 mg, 0.52 mmol) were stirred in dichloromethane (2 mL) at RT under an inert atmosphere of nitrogen. (*S*)-Mosher's acyl chloride (**269**) (132 mg, 0.52 mmol) was added as a 0.55M solution in deuterated chloroform and the reaction mixture was allowed to stir for 3.5 h. The reaction mixture was quenched with 0.1M aqueous hydrochloric acid (40 mL) and extracted with diethylether (40 mL). The organic layer was washed with a saturated aqueous solution of sodium hydrogen carbonate (40 mL), brine (40 mL), dried ($MgSO_4$), filtered and concentrated *in vacuo* to yield (**270**) (100 mg, 92%), in a 1:1 mixture of diastereomers, as a viscous colourless oil: R_f = 0.84 (4:1, dichloromethane/petrol); ^{1}H NMR (400 MHz, $CDCl_3$) (2'*S*,2*R*) δ 7.45-7.23 (m, 10H, Ar-*H*), 5.22-5.17 (m, 1H, PhC*H*Br), 4.92-4.75 (m, 2H, BrCC*H*$_2$O), 3.45 (s, 3H, OC*H*$_3$) ppm; (2'*R*,2*R*) δ (m, 10H, Ar-*H*), 5.22-5.17 (m, 1H, PhC*H*Br), 4.92-4.75 (m, 2H, BrCC*H*$_2$O), 3.42 (s, 3H, OC*H*$_3$) ppm.

Di(2-bromo-2-phenyleth-1-yl) sulfite (268)

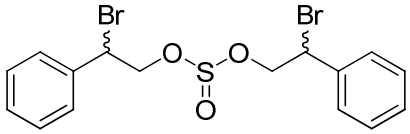

A solution of thionyl chloride (61 µL, 0.83 mmol) in dichloromethane (0.2 mL) was added to a solution of racemic 2-bromo-1-phenyl-ethanol (**261**) (150 mg, 0.75 mmol) stirred at RT in

dichloromethane (0.8 mL). The reaction mixture was stirred for 26 h before quenching with saturated aqueous solution of sodium hydrogen carbonate (10 mL). The mixture was extracted with dichloromethane (2 × 15 mL) and the combined organic phases were washed with water (15 mL), brine (15 mL), dried ($MgSO_4$), filtered and concentrated *in vacuo*. The crude product mixture was purified by flash column chromatography (1:1, dichloromethane/petrol) to afford di(2-bromo-2-phenyleth-1-yl) sulfite (**268**) (135 mg, 78%) in a complex mixture of epimers as colourless low melting needles: R_f = 0.51 (4:1, dichloromethane/petrol); FT IR (NaCl) ν_{max} 3033, 1494, 1455, 1266, 1205 cm^{-1}; ^1H NMR (400 MHz, $CDCl_3$) δ 7.42-7.34 (m, 10H, Ar-*H*), 5.06-5.01 (m, 2H, PhC*H*Br), 4.52-4.27 (m, 4H, PhCHBrC*H*$_2$) ppm; ^{13}C NMR (100 MHz, $CDCl_3$) δ 137.6, 137.4, 129.3, 129.0, 127.9, 65.2, 50.0, 49.7 ppm; MS (CI^+) 464/466/468 ($M+NH_4^+$); HRMS calcd for ($M+NH_4^+$) $C_{16}H_{20}NO_3S^{79}Br_2$ 463.9531, $C_{16}H_{20}NO_3S^{79}Br^{81}Br$ 465.9510 and $C_{16}H_{20}NO_3S^{81}Br_2$ 467.9490, found 463.9539, 465.9519 and 467.9497; Anal. calcd for $C_{16}H_{16}O_3SBr_2$: C, 42.88; H, 3.60; found: C, 43.00; H, 3.67; *Crystal data for* **268**: $C_{16}H_{16}Br_2O_3S$, M = 448.17, monoclinic, *I*2/*a* (no. 15), a = 23.8581(2), b = 5.52906(5), c = 26.0239(3) Å, β = 102.5258(9)°, V = 3351.19(11) $Å^3$, Z = 8, D_c = 1.777 g cm^{-3}, μ(Cu-Kα) = 7.384 mm^{-1}, T = 173 K, colourless platy needles, Oxford Diffraction Xcalibur PX Ultra diffractometer; 3214 independent measured reflections, F^2 refinement, R_1 = 0.055, wR_2 = 0.139, 3080 independent observed absorption-corrected reflections [$|F_o| > 4\sigma(|F_o|)$, $2\theta_{max}$ = 142°], 199 parameters.

(±)-1-Phenylpropylene oxide (276)

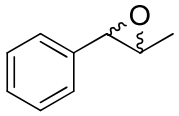

*m*CPBA (6.45 g, 37.4 mmol) was added to a stirred solution of *trans*-β-methylstyrene (**18**) (2.0 mL, 18.7 mmol) in dichloromethane (30 mL) at 15 °C. The reaction was allowed to slowly warm to RT and stirred for 18 h. The reaction mixture was quenched with 20% aqueous sodium sulfite solution (40 mL) and partitioned between dichloromethane (200 mL) and water (200 mL). The organic phase was separated and the aqueous phase re-extracted with a further portion of dichloromethane (200 mL). The combined organic layers were washed with saturated aqueous sodium hydrogen carbonate (200 mL), water (200 mL),

dried ($MgSO_4$), filtered and concentrated *in vacuo* to afford (±)-1-phenylpropylene oxide (**276**) (2.17 g, 87%) as a pale yellow oil with spectral data consistent with literature:[146] R_f = 0.36 (2:3, dichloromethane/petrol); FT IR (NaCl) ν_{max} 3088, 3865, 3033, 2987, 2928, 1954 (w), 1883 (w), 1770 (w) cm^{-1}; ^1H NMR (400 MHz, $CDCl_3$) δ 7.38-7.31 (m, 5H, Ar-*H*), 3.61 (d, *J* = 2.1 Hz, 1H, PhC*H*), 3.08 (dq, *J* = 5.2, 2.1 Hz, 1H, CH(O)C*H*CH_3), 1.49 (d, *J* = 5.2 Hz, 3H, C*H*$_3$) ppm; ^{13}C NMR (100 MHz, $CDCl_3$) δ 137.8, 128.5, 128.1, 125.6, 59.6, 59.1, 17.9 ppm; MS (ES^+) 134 (M^+).

(±)-1-Bromo-1-phenylpropan-2-ol (271/277)

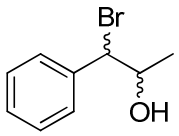

A cooled (-10 °C) 48% aqueous solution of hydrobromic acid (10 mL) was added to racemic 1-phenylpropylene oxide (**276**) (500 mg, 3.72 mmol) stirred at -10 °C in chloroform (10 mL). The biphasic mixture was stirred for 2 h, following which it was diluted with water (200 mL) and extracted with dichloromethane (2 x 100 mL). The combined organic extracts were washed with water (100 mL), dried ($MgSO_4$), filtered and concentrated *in vacuo*. The crude product was purified by flash column chromatography (4:1, dichloromethane/petrol) to afford racemic 1-bromo-1-phenylpropan-2-ol (**271**/**277**) (581 mg, 73%) as a colourless oil in a 73:27 inseparable mixture of the (1*R**,2*S**) and (1*S**,2*S**) diastereomers with spectral data consistent with literature:[147] R_f = 0.36 (4:1, dichloromethane/petrol); FT IR (NaCl) ν_{max} 3409 (br), 3092, 3030, 2978, 2932, 2897, 1953(w), 1882(w), 1807(w), 1710(w) cm^{-1}; ^1H NMR (400 MHz, $CDCl_3$) (1*R**,2*S**) δ 7.50-7.48 (m, 2H, Ar-*H*), 7.43-7.33 (m, 3H, Ar-*H*), 4.90 (d, *J* = 6.4 Hz, 1H, PhC*H*), 4.29-4.19 (m, 1H, C*H*(OH)CH_3), 2.04 (s (br), 1H, O*H*), 1.38 (d, *J* = 6.0 Hz, 3H, C*H*$_3$) ppm; (1*S**,2*S**) δ 7.43-7.33 (m, 5H, Ar-H), 4.89 (d, *J* = 8.4 Hz, 1H, PhC*H*), 4.29-4.19 (m, 1H, C*H*(OH)CH_3), 2.04 (s (br), 1H, O*H*), 1.13 (d, *J* = 6.4 Hz, 3H, C*H*$_3$) ppm; ^{13}C NMR (100MHz, $CDCl_3$) (1*R**,2*S**) δ 138.2, 128.8, 128.8, 128.7, 71.6, 60.8, 20.1 ppm; (1*S**,2*S**) δ 139.1, 128.8, 128.8, 128.0, 71.6, 65.1, 19.7 ppm; GCMS (EI^+) 12.98 min; (1*S**,2*S**)-diastereomer, 170/172 ($PhCHBr+H^+$), 214/216 (M^+), 13.38 min; (1*R**,2*S**)-diastereomer, 170/172 ($PhCHBr+H^+$), 214/216 (M^+); HRMS calcd for (M^+) $C_9H_{11}O^{79}Br$ 213.9993 and $C_9H_{11}O^{81}Br$ 215.9973, found 213.9989 and 215.9971.

(2*R*)-2'-Bromo-1'-methyl-2'-phenylethyl 2-methoxy-2-trifluoromethylphenylacetate (278)

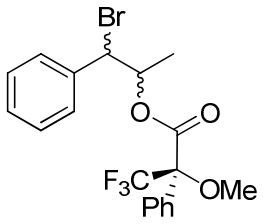

Racemic 1-bromo-1-phenylpropan-2-ol (**271**/**277**) (50 mg, 0.23 mmol) as a 27:73, (1*S**,2*S**):(1*R**,2*S**) mixture of diastereomers, triethylamine (81 µL, 0.58 mmol) and DMAP (57 mg, 0.46 mmol) were stirred in dichloromethane (2 mL) at RT under an inert atmosphere of nitrogen. (*S*)-Mosher's acyl chloride (**269**) (117 mg, 0.46 mmol) was added as a 0.55M solution in deuterated chloroform and the reaction mixture was allowed to stir for 2.5 h. The reaction mixture was quenched with 0.1M aqueous hydrochloric acid (40 mL) and extracted with diethylether (40 mL). The organic layer was washed with a saturated aqueous solution of sodium hydrogen carbonate (40 mL), brine (40 mL), dried ($MgSO_4$), filtered and concentrated *in vacuo* to yield Mosher's ester (**278**) (99 mg, 98%) as a colourless amorphous solid in a mixture of the four epimers (2'*R*,1'*S*,2*R*):(2'*S*,1'*R*,2*R*):(2'*S*,1'*S*,2*R*):(2'*R*,1'*R*,2*R*), 36:36:14:14: ^{1}H NMR (400 MHz, $CDCl_3$) (2'*R*,1'*S*,2*R*) δ 7.44-7.24 (m, 10H, Ar-*H*), 5.74-5.60 (m, 1H, PhCHBrC*H*O), 4.98 (d, *J* = 7.2 Hz, 1H, PhC*H*Br), 3.36 (s, 3H, OCH_3), 1.58 (d, *J* = 6.4 Hz, 3H, CH_3) ppm; (2'*S*,1'*R*,2*R*) δ 7.44-7.24 (m, 10H, Ar-*H*), 5.74-5.60 (m, 1H, PhCHBrC*H*O), 4.97 (d, *J* = 8.0 Hz, 1H, PhC*H*Br), 3.28 (s, 3H, OCH_3), 1.51 (d, *J* = 6.0 Hz, 3H, CH_3) ppm; (2'*S*,1'*S*,2*R*) δ 7.63-7.61 (m, 2H, Ar-H), 7.44-7.24 (m, 8H, Ar-*H*), 5.74-5.60 (m, 1H, PhCHBrC*H*O), 4.93 (d, *J* = 8.0 Hz, 1H, PhC*H*Br), 3.62 (s, 3H, OCH_3), 1.28 (d, *J* = 6.4 Hz, 3H, CH_3) ppm; (2'*R*,1'*R*,2*R*) δ 7.63-7.61 (m, 2H, Ar-H), 7.44-7.24 (m, 8H, Ar-*H*), 5.74-5.60 (m, 1H, PhCHBrC*H*O), 4.94 (d, *J* = 8.4 Hz, 1H, PhC*H*Br), 3.67 (s, 3H, OCH_3), 1.14 (d, *J* = 6.4 Hz, 3H, CH_3) ppm.

(2*S*)-1-Bromo-1-phenylpropan-2-ol (271/277)

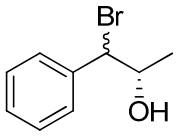

A cooled (-10 °C) 48% aqueous solution of hydrobromic acid (20 mL) was added to (1*S*,2*S*)-1-phenylpropylene oxide (**276**) (1.05 mL, 7.75 mmol) stirred at -10 °C in chloroform (20 mL). The biphasic mixture was stirred for 35 mins following which it was diluted with water (300 mL) and extracted with dichloromethane (2 x 150 mL). The combined organic extracts were washed with water (200 mL), dried ($MgSO_4$), filtered and concentrated *in vacuo*. The crude product was purified by flash column chromatography (4:1, dichloromethane/petrol) to afford (2*S*)-1-bromo-1-phenylpropan-2-ol (**271**/**277**) (1.47 g, 88%) as a colourless oil in a 75:25 inseparable mixture of the (1*R*,2*S*) and (1*S*,2*S*) diastereomers: $[\alpha]^{27}_{D}$ = -43.4 (c = 2.2, CH_2Cl_2). All other spectral data is identical to that reported above for the racemic mixture.

(1'*S*,2*R*)-2'-Bromo-1'-methyl-2'-phenylethyl 2-methoxy-2-trifluoromethylphenylacetate (278)

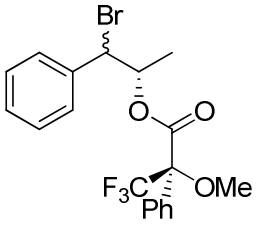

(2*S*)-1-Bromo-1-phenylpropan-2-ol (**271**/**277**) (50 mg, 0.23 mmol) as a 32:68, (1*S*,2*S*):(1*R*,2*S*) mixture of diastereomers, triethylamine (81 µL, 0.58 mmol) and DMAP (57 mg, 0.46 mmol) were stirred in dichloromethane (2 mL) at RT under an inert atmosphere of nitrogen. (*S*)-Mosher's acyl chloride (**269**) (117 mg, 0.46 mmol) was added as a 0.55M solution in deuterated chloroform and the reaction mixture was allowed to stir for 2.5 h. The reaction mixture was quenched with 0.1M aqueous hydrochloric acid (40 mL) and extracted with diethylether (40 mL). The organic layer was washed with a saturated aqueous solution of sodium hydrogen carbonate (40 mL), brine (40 mL), dried ($MgSO_4$), filtered and concentrated *in vacuo* to yield Mosher's ester (**278**) (99 mg, 98%) as a colourless

amorphous solid in a mixture of two epimers (2'*R*,1'*S*,2*R*):(2'*S*,1'*S*,2*R*), 65:35: ^{1}H NMR (400 MHz, $CDCl_3$) (2'*R*,1'*S*,2*R*) δ 7.44-7.28 (m, 10H, Ar-*H*), 5.57 (dq, *J* = 6.0 and 7.6 Hz, 1H, PhCHBrC*H*O), 4.98 (d, *J* = 7.6 Hz, 1H, PhC*H*Br), 3.36 (s, 3H, OCH_3), 1.58 (d, *J* = 6.0 Hz, 3H, CH_3) ppm; (2'*S*,1'*S*,2*R*) δ 7.63-7.61 (m, 2H, Ar-*H*), 7.44-7.28 (m, 8H, Ar-*H*), 5.63 (dq, *J* = 6.4 and 8.0 Hz, 1H, PhCHBrC*H*O), 4.93 (d, *J* = 8.0 Hz, 1H, PhC*H*Br), 3.62 (s, 3H, OCH_3), 1.28 (d, *J* = 6.4 Hz, 3H, CH_3) ppm.

(±)-*trans*-2-Bromocyclohexanol (287)

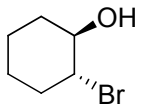

(±)

A 48% aqueous solution of hydrobromic acid (13 mL) was added to cyclohexene oxide (**286**) (515 µL, 5.1 mmol) stirred at RT in chloroform (13 mL). The biphasic mixture was stirred for 1 h, following which it was diluted with water (120 mL) and extracted with dichloromethane (2 x 60 mL). The combined organic extracts were washed with water (60 mL), dried ($MgSO_4$), filtered and concentrated *in vacuo*. The crude product was purified by flash column chromatography (dichloromethane) to afford racemic *trans*-2-bromocyclohexanol (**287**) (938 mg, quantitative) as a colourless oil with spectral data consistent with literature:[148] R_f = 0.27 (dichloromethane); FT IR (NaCl) ν_{max} 3396 (br), 2939, 2861 cm^{-1}; ^{1}H NMR (400 MHz, $CDCl_3$) δ 3.92 (ddd, *J* = 11.8, 9.4, 4.4 Hz, 1H, C*H*Br), 3.66-3.59 (m, 1H, C*H*OH), 2.59 (d, *J* = 2.4 Hz, 1H, O*H*), 2.40-2.34 (m, 1H, C*H*H), 2.19-2.13 (m, 1H, C*H*H), 1.91-1.69 (m, 3H, CH_2), 1.45-1.25 (m, 3H, CH_2) ppm; ^{13}C NMR (100 MHz, $CDCl_3$) δ 75.4, 61.9, 36.2, 33.5, 26.7, 24.1 ppm; MS (EI$^+$) 178/180 (M$^+$).

A General Procedure for Rearrangement of Bromohydrins (*via *intervention of a bromonium ion) to form the Bromochloride;

(i) with Thionyl Chloride

The bromohydrin (1 eq.) was stirred at 65 °C in neat thionyl chloride (25-30 eq.) for 1.5-5.5 h. The reaction mixture was allowed to cool and concentrated *in vacuo*. The residue was taken up in dichloromethane and washed with a saturated aqueous solution of sodium hydrogen carbonate. The aqueous phase was re-extracted with dichloromethane and the combined organic phases were washed with water, dried ($MgSO_4$), filtered and concentrated *in vacuo*. The crude product was subjected to flash column chromatography (petrol) to afford the pure bromochloride.

(ii) with Viehe's Salt

A 0.33M solution of the bromohydrin (1 eq.) in dichloromethane was stirred at 0 °C under an inert atmosphere of nitrogen. Viehe's salt (1.1 eq.) was added and the reaction mixture was allowed to gradually warm to RT. After stirring for 18-24 h, the reaction mixture was concentrated *in vacuo* and the crude residue was subjected to flash column chromatography (petrol) to afford the pure bromochloride.

Bromochlorides formed* via *Rearrangement of the Bromohydrin

(±)-2-Bromo-1-chloro-1-phenylethane (262)

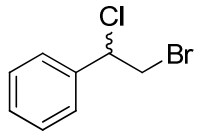

Starting from (±)-2-bromo-2-phenylethanol (**261**) (50 mg, 0.25 mmol) and following procedure (i) afforded (±)-2-bromo-1-chloro-1-phenylethane (**262**) (38 mg, 69%) as colourless low melting needles with spectral data consistent with literature:[121] m.p. 21-22.5 °C; [lit.[149] 26-27 °C]; R_f = 0.25 (petrol); FT IR (NaCl) ν_{max} 3065, 3034, 2960, 1953

(w), 1884 (w), 1805 (w) cm^{-1}; ^1H NMR (400 MHz, $CDCl_3$) δ 7.45-7.39 (m, 5H, Ar-*H*), 5.09 (dd, *J* = 8.8, 6.4 Hz, 1H, PhC*H*Cl), 3.94 (dd, J^{β} = 6.4 Hz, J^{β} = 10.4 Hz, 1H, C*H*H'Br), 3.86 (dd, J^{β} = 8.8 Hz, J^{β} = 10.4 Hz, 1H, CH*H'*Br) ppm; ^{13}C NMR (100 MHz, $CDCl_3$) δ 138.4, 129.2, 128.8, 127.4, 61.3, 36.0 ppm; MS (EI^+) 218/220/222 ($M^{+\cdot}$), 125/127 ($PhCHCl^{+\cdot}$); HRMS calcd for ($M^{+\cdot}$) $C_8H_8{}^{35}Cl\ {}^{79}Br$ 217.9498, $C_8H_8{}^{35}Cl{}^{81}Br$ 219.9477, $C_8H_8{}^{37}Cl{}^{79}Br$ 219.9468 and $C_8H_8{}^{37}Cl{}^{81}Br$ 221.9448, found 217.9494, 219.9474 and 221.9444.

(±)-2-Bromo-1-chloro-1-phenylpropane (274/275)

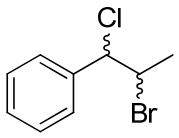

Starting from (±)-1-bromo-1-phenylpropan-2-ol (**271**/**274**) (50 mg, 0.23 mmol) in a 73:27 mixture of (1*R**,2*S**) and (1*S**,2*S**) diastereomers and following procedure (i) afforded (±)-2-bromo-1-chloro-1-phenylpropane (**271**/**277**) (43 mg, 80%) as a colourless oil as a 77:23 inseparable mixture of the (1*S**,2*R**) and (1*R**,2*R**) diastereomers with spectral data consistent with literature:[141] R_f = 0.33 (petrol); FT IR (NaCl) ν_{max} 3064, 3033, 2982, 2932, 2868, 1952 (w) cm^{-1}; ^1H NMR (400 MHz, $CDCl_3$) (1*S**,2*R**) δ 7.47-7.36 (m, 5H, Ar-*H*), 5.02 (d, *J* = 8.4 Hz, 1H, PhC*H*Cl), 4.57-4.46 (m, 1H, C*H*BrCH$_3$), 1.96 (d, *J* = 6.4 Hz, 1H, C*H*$_3$) ppm; (1*R**,2*R**) δ 7.47-7.36 (m, 5H, Ar-*H*), 5.12 (d, *J* = 6.0 Hz, 1H, PhC*H*Cl), 4.57-4.46 (m, 1H, C*H*BrCH$_3$), 1.69 (d, *J* = 6.8 Hz, 1H, C*H*$_3$) ppm; ^{13}C NMR (100 MHz, $CDCl_3$) (1*S**,2*R**) δ 139.5, 128.9, 128.6, 127.6, 51.7, 23.6 ppm; (1*R**,2*R**) δ 137.2, 128.4, 128.2, 127.6, 67.5, 53.0, 22.4 ppm; GCMS (EI^+) 13.67 min; (1*S**,2*R**)-diastereomer, 125/127 ($PhCHCl^{+\cdot}$), 232/234/236 ($M^{+\cdot}$), 14.17 min; (1*R**,2*R**)-diastereomer, 125/127 ($PhCHCl^{+\cdot}$), 232/234/236 ($M^{+\cdot}$); HRMS calcd for (M^+) $C_9H_{10}{}^{35}Cl{}^{79}Br$ 231.9654, $C_9H_{10}{}^{37}Cl{}^{79}Br$ 233.9625, $C_9H_{10}{}^{35}Cl{}^{81}Br$ 233.9634 and $C_9H_{10}{}^{37}Cl{}^{81}Br$ 235.9604, found 231.9650, 233.9629 and 235.9612; HPLC (1:1, water/acetonitrile+0.05% TFA); Chiralcel OJ-RH: 1 mL/min; 240 nm, t_R(*S*,*S*) 19.71 min, t_R(*R*,*R*) 22.68 min, t_R(*S*,*R*) 23.65 min, t_R(*R*,*S*) 27.39 min.

Starting from (±)-1-bromo-1-phenylpropan-2-ol (**271**/**277**) (300 mg, 1.4 mmol) in a 73:27 mixture of (1*R**,2*S**) and (1*S**,2*S**) diastereomers and following procedure (ii) afforded (±)-2-bromo-1-chloro-1-phenylpropane (**274**/**275**) (280 mg, 86%) as a colourless oil as a 90:10

inseparable mixture of the (1*S**,2*R**) and (1*R**,2*R**): all data is identical to that previously reported.

(2*R*)-2-Bromo-1-chloro-1-phenylpropane (274/275)

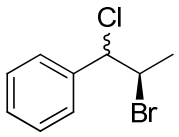

Starting from (2*S*)-1-bromo-1-phenylpropan-2-ol (**271**/**277**) (50 mg, 0.23 mmol) in a 68:32 mixture of (1*R*,2*S*) and (1*S*,2*S*) diastereomers and following procedure (i) afforded (*R*)-2-bromo-1-chloro-1-phenylpropane (**274**/**275**) (59 mg, 97%) as a colourless oil in a 60:40 inseparable mixture of the (1*S*,2*R*) and (1*R*,2*R*) diastereomers. All spectral data is identical to that previously reported for the racemic mixture.

Starting from (2*S*)-1-bromo-1-phenylpropan-2-ol (**271**/**277**) (50 mg, 0.23 mmol) in a 76:24 mixture of (1*R*,2*S*) and (1*S*,2*S*) diastereomers and following procedure (ii) afforded (*R*)-2-bromo-1-chloro-1-phenylpropane (**274**/**275**) (36 mg, 65%) as a colourless oil in a 93:7 inseparable mixture of the (1*S*,2*R*) and (1*R*,2*R*) diastereomers. All spectral data is identical to that previously reported for the racemic mixture.

(±)-*trans*-1-Chloro-2-bromocyclohexane (288)

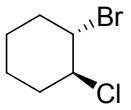

(±)

Starting from (±)-*trans*-2-bromocyclohexanol (**287**) (100 mg, 0.56 mmol) and following procedure (i) afforded (±)-*trans*-1-chloro-2-bromocyclohexane (**288**) (133 mg, quantitative) as a colourless oil with spectral data consistent with literature:[150] FT IR (NaCl) ν_{max} 2941, 2863 cm^{-1}; ^1H NMR (400 MHz, $CDCl_3$) δ 4.27-4.20 (m, 2H, C*H*Br and C*H*Cl), 2.46-2.39 (m, 2H, CH_2), 1.95-1.75 (m, 2H, CH_2), 1.53-1.44 (m, 2H, CH_2) ppm; ^{13}C NMR (100 MHz, $CDCl_3$)

δ 62.9, 55.5, 33.4, 32.8, 23.4, 22.6 ppm; MS (EI^+) 196/198/200 (M^+); HRMS calcd for (M^+) $C_6H_{10}{}^{35}Cl^{79}Br$ 195.9654, found 195.9645.

A General Procedure for the Bromochlorination of Alkenes

(±)-*Iso*-amarine (0.01 eq.), trimethylsilylchloride (1.1 eq.) and the alkene (1 eq.) were stirred at RT in dichloromethane (0.25M solution). NBS (1.1 eq.) was added and the reaction mixture stirred for 2 h. The reaction was quenched with 20% aqueous sodium sulfite solution and extracted with two portions of dichloromethane. The combined organic phases were washed with water, dried ($MgSO_4$), filtered and concentrated *in vacuo* to afford the crude bromochlorinated products.

Bromochlorides formed* via *Bromochlorination of the Alkenes

(±)-2-Bromo-1-chloro-1-phenylethane (262)

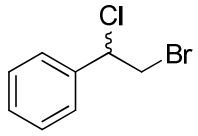

Starting from styrene (**266**) (573 µL, 5 mmol) and following the general procedure afforded the crude bromochloride. The crude product was purified by flash column chromatography (petrol) to yield racemic 2-bromo-1-chloro-1-phenylethane (**262**) (983 mg, 90%). All data is identical to that previously reported.

(1*R,2*S**)-2-Bromo-1-chloro-1-phenylpropane (274)**

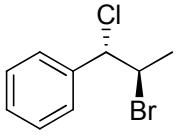

(±)

Starting from *trans*-β-methylstyrene (**18**) (130 µL, 1 mmol) and following the general procedure afforded the crude bromochloride. The crude product was purified by flash column chromatography (petrol) to yield (1*R**,2*S**)-2-bromo-1-chloro-1-phenylpropane (**274**) (154 mg, 66%) as a single diastereomer as colourless needles. All spectral data is identical to that previously reported.

(±)-2-Bromo-1-chloro-1-(4-methoxyphenyl)propane (293)

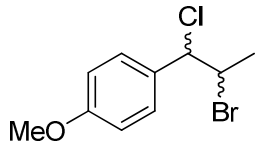

(±)

Starting from *trans*-anethole (**21**) (148.5 µL, 1 mmol) and following the general procedure afforded the crude bromochloride. The product mixture was triturated with dichloromethane/petrol and the resulting white ppt was removed by filtration. The filtrate was concentrated *in vacuo* to yield **293** as a colourless oil (287 mg, quantative), obtained as a 87:13 mixture of the (1*S**,2*R**) and (1*R**,2*R**) diastereomers: FT IR (NaCl) ν_{max} 3037, 2968, 2993, 2837, 2057 (w), 1889 (w), 1720 (w) cm^{-1}; ^{1}H NMR (400 MHz, $CDCl_3$) (1*S**,2*R**) δ 7.35 (d, *J* = 8.8 Hz, 2H, Ar-*H*), 6.93 (d, *J* = 8.8 Hz 2H, Ar-*H*), 5.00 (d, *J* = 8.8 Hz, 1H, PhC*H*Cl), 4.55-4.45 (m, 1H, C*H*BrCH$_3$), 3.85 (s, 3H, OC*H*$_3$), 1.96 (d, *J* = 6.4 Hz, 3H, CHBrC*H*$_3$) ppm; (1*R**,2*R**) δ 7.38 (d, *J* = 8.8 Hz, 2H, Ar-*H*), 6.93 (d, *J* = 8.8 Hz, 2H, Ar-*H*), 5.10 (d, *J* = 5.6 Hz, 1H, PhC*H*Cl), 4.55-4.45 (m, 1H, C*H*BrCH$_3$), 3.85 (s, 3H, OC*H*$_3$), 1.68 (d, *J* = 6.8 Hz, 3H, CHBrC*H*$_3$) ppm; ^{13}C NMR (100MHz, $CDCl_3$) (1*S**,2*R**) δ 159.8, 131.7, 128.8, 113.8, 67.5, 55.3, 52.1, 23.7 ppm; (1*R**,2*R**) δ 159.8, 313.7, 129.4, 113.6, 67.3, 55.3, 53.3, 22.2 ppm; GCMS (EI$^+$) 17.37 min; (1*S**,2*R**)-diastereomer, 155/157 (PhCHCl+H$^+$), 262/264/266 (M$^+$), 17.66 min; (1*R**,2*R**)-diastereomer, 155/157 (PhCHCl+H$^+$), 262/264/266 (M$^+$); HRMS calcd for (M$^+$) $C_{10}H_{12}O^{35}Cl^{79}Br$ 261.9760, found 261.9760.

(±)-2-Bromo-1-chloro-1-(4-methylphenyl)ethane (292)

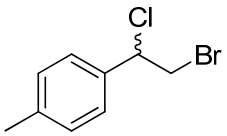

Starting from 4-methylstyrene (**291**) (132 µL, 5 mmol) and following the general procedure afforded the crude bromochloride. The crude product was purified by flash column chromatography (petrol) to yield **292** (223 mg, 95%) as a colourless oil: R_f = 0.25 (petrol); FT IR (NaCl) ν_{max} 3027, 2956, 2922, 2862, 1904 (w), 1794 (w) cm^{-1}; ^1H NMR (400 MHz, $CDCl_3$) δ 7.34 (d, *J* = 8.2 Hz, 2H, Ar-*H*), 7.24 (d, *J* = 8.2 Hz, 2H, Ar-*H*), 5.07 (dd, *J* = 6.1, 8.9 Hz, 1H, PhC*H*Cl), 3.94 (dd, J^{β} = 6.1 Hz, J^{β} = 10.4 Hz, 1H, C*H*H'Br), 3.86 (dd, J^{β} = 8.9 Hz, J^{β} = 10.4 Hz, 1H, CH*H*'Br), 2.41 (s, 3H, Ar-C*H*$_3$) ppm; ^{13}C NMR (100 MHz, $CDCl_3$) δ 139.2, 135.5, 129.5, 127.2, 61.3, 36.0, 21.3 ppm; MS (EI^+) 232/234/236 ($M^{+\cdot}$), 139/141 ($ArCHCl^{+\cdot}$); HRMS calcd for ($M^{+\cdot}$) $C_9H_{10}{}^{35}Cl^{79}Br$ 231.9653, found 231.9654.

A General Procedure for Investigating Br$^+$ Exchange between Bromonium Ions and Alkenes;

(i) with Thionyl Chloride

The bromohydrin was stirred with the alkene (1-5 eq.) at 65 °C in neat thionyl chloride (25-30 eq.) for 2.5 h. The reaction mixture was allowed to cool and concentrated *in vacuo*. The residue was taken up in dichloromethane and washed with a saturated aqueous solution of sodium hydrogen carbonate. The aqueous phase was re-extracted with dichloromethane and the combined organic phases were washed with water, dried ($MgSO_4$), filtered and concentrated *in vacuo*. The composition of the crude product mixture was analysed by ^1H NMR ($CDCl_3$) analysis. Where applicable, the product was purified by flash column chromatography (petrol) and analysed by chiral HPLC.

(ii) with Viehe's Salt

A 0.33M solution of the bromohydrin and alkene (1-10 eq.) in dichloromethane was stirred at 0℃ under an inert atmosphere of nitrogen. Viehe's salt (1.1 eq.) was added and the reaction mixture was allowed to gradually warm to RT. After stirring for between 18 and 24 h, the reaction mixture was concentrated *in vacuo* and the composition of the crude product mixture was analysed by ^{1}H NMR ($CDCl_3$) analysis. Where applicable, the product was purified by flash column chromatography (petrol) and analysed by chiral HPLC.

Bromosulfonates: Synthesis and Rearrangement to form the Bromochloride

(1'*S*)-2'-Bromo-1'-methyl-2'-phenylethyl *p*-toluenesulfonate (281)

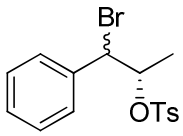

(2*S*)-1-Bromo-1-phenylpropan-2-ol (**271**/**277**) (100 mg, 0.47 mmol), as a 73:27 mixture of the (1*R*,2*S*) and (1*S*,2*S*) diastereomers, was stirred with DMAP (114 mg, 0.93 mmol) in dichloromethane (4 mL) under an inert atmosphere of nitrogen. The solution was cooled to 0 ºC and tosyl chloride (133 mg, 0.70 mmol) was added. The reaction mixture was allowed to gradually warm to RT and stirred for 19 h. The mixture was diluted with dichloromethane (20 mL), washed with brine (20 mL), dried (Na_2SO_4), filtered and concentrated *in vacuo*. The crude product was purified by flash column chromatography (1:1, dichloromethane/petrol) to afford **281** (161 mg, 94%) as a colourless amorphous solid in a 72:28 inseparable mixture of the (1*R*,2*S*) and (1*S*,2*S*) diastereomers: R_f = 0.29 (1:1, dichloromethane/petrol); $[\alpha]^{23}_D$ = -15.5 (c = 1.0, CH_2Cl_2); FT IR (NaCl) ν_{max} 3064, 3032, 2990, 2938, 2873, 1920 (w), 1809 (w), 1362, 1177 cm^{-1}; ^{1}H NMR (400 MHz, $CDCl_3$) (1*R**,2*S**) δ 7.58 (d, *J* = 8.4 Hz, 2H, Ar-*H*), 7.36-7.24 (m, 7H, Ar-*H*), 4.94-4.89 (m, 2H, PhC*H*Br and C*H*(OSO_2Ar)CH_3), 2.45 (s, 3H, Ar-C*H*$_3$), 1.55 (d, *J* = 5.6 Hz, 3H, CH(OSO_2Ar)C*H*$_3$) ppm; (1*S**,2*S**) δ 7.83 (d, *J* = 8.0 Hz, 2H, Ar-*H*), 7.36-7.24 (m, 7H, Ar-*H*), 5.02 (pseudo quintet, *J* = 6.4 Hz, 1H, C*H*(OSO_2Ar)CH_3), 4.94-4.89 (m, 1H, PhC*H*Br), 2.47 (s, 3H, Ar-C*H*$_3$), 1.29 (d, *J* = 6.4 Hz, 3H, CH(OSO_2Ar)C*H*$_3$) ppm; ^{13}C NMR (100MHz, $CDCl_3$) (1*R**,2*S**); δ 144.7, 137.2, 133.7, 129.7, 128.7, 128.6,

128.5, 127.7, 80.8, 56.0, 21.7, 18.9 ppm; (1*S**,2*S**); δ 144.9, 136.8, 133.8, 129.8, 128.9, 128.6, 128.6, 128.0, 81.1, 55.1, 21.7, 18.6 ppm; MS (CI^+) 386/388 ($M+NH_4^+$); HRMS calcd for ($M+NH_4^+$) $C_{16}H_{21}NO_3{}^{79}BrS$ 386.0426 and $C_{16}H_{21}NO_3{}^{81}BrS$ 388.0405, found 386.0428 and 388.0407; Anal. calcd for $C_{16}H_{17}O_3BrS$: C, 52.04; H, 4.64; found: C, 52.13; H, 4.62.

2,5-Dioxoheptyl 2-(chlorosulfonyl)benzoate (300)[125]

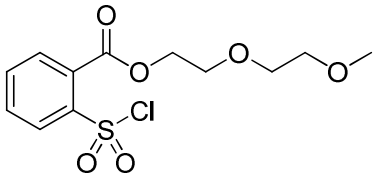

A mixture of *o*-sulfobenzoic acid anhydride (**299**) (1.23 g, 6.6 mmol) and phosphorus pentachloride (3.68g, 13.2 mmol) was heated at 90 ºC under an inert atmosphere of nitrogen for 6 h. The resulting oil was allowed to cool, dissolved in diethyl ether (50 mL), and rinsed with ice-water (50 mL). The organic phase was dried ($MgSO_4$), filtered and concentrated *in vacuo* to afford 1.71 g of crude oil. The crude oil was then dissolved in excess methoxyethoxyethanol (2.4 mL, 20 mmol) and heated to 60 ºC under an inert atmosphere of nitrogen for 20 h. The reaction mixture was purified by flash column chromatography (9:1, ethyl acetate/petrol) to afford 2,5-dioxoheptyl 2-(chlorosulfonyl)benzoate (**300**) (1.3 g, 60%) as a colourless oil with spectral data consistent with literature:[125] R_f = 0.47 (9:1, ethyl acetate/petrol); FT IR (NaCl) ν_{max} 3098, 2882, 1964(w), 1738, 1376 (SO_2), 1184 (SO_2) cm^{-1}; ^1H NMR (400 MHz, $CDCl_3$) δ 8.17 (d, J = 8.0 Hz, 1H, Ar-*H*), 7.83-7.72 (m, 3H, Ar-*H*), 4.59-4.57 (m, 2H, C(O)OC*H*$_2$), 3.88-3.86 (m, 2H, C*H*$_2$O), 3.69-3.67 (m, 2H, C*H*$_2$O), 3.57-3.55 (m, 2H, C*H*$_2$O), 3.38 (s, 3H, OC*H*$_3$) ppm; ^{13}C NMR (100 MHz, $CDCl_3$) δ 165.8, 141.5, 135.2, 132.3, 131.5, 130.3, 129.0, 71.8, 70.5, 68.9, 65.7, 59.1 ppm; MS (ES^+) 323/325 ($M+H^+$), 345/347 ($M+Na^+$); HRMS calcd for ($M+H^+$) $C_{12}H_{16}O_6S^{35}Cl$ 323.0356 and $C_{12}H_{16}O_6S^{37}Cl$ 325.0327, found 323.0352 and 325.0332; calcd for ($M+Na^+$) $C_{12}H_{16}O_6S^{35}ClNa$ 345.0176 and $C_{12}H_{16}O_6S^{37}ClNa$ 347.0146, found 345.0174 and 347.0147.

(1'*S*)-2'-Bromo-1'-methyl-2'-phenylethyl 2-(2,5-dioxoheptylcarboxy)-1-benzosulfonate (297)

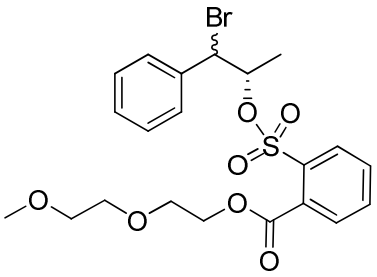

(2*S*)-1-Bromo-1-phenylpropan-2-ol (**271**/**277**) (100 mg, 0.47 mmol), as a 75:25 mixture of the (1*R*,2*S*) and (1*S*,2*S*) diastereomers, was stirred with DMAP (85 mg, 0.70 mmol) in dichloromethane (3 mL) under an inert atmosphere of nitrogen. The solution was cooled to 0 ºC and a solution of sulfonyl chloride **300** (180 mg, 0.56 mmol) in dichloromethane (2 mL) was added. The reaction mixture was allowed to gradually warm to RT and stirred for 20 h. The mixture was concentrated *in vacuo* and the resulting crude oil was purified by flash column chromatography (3:2, ethyl acetate/petrol) to yield 1-bromo-1-phenylpropyl 2-(2,5-dioxoheptylcarboxy)-1-benzosulfonate (**297**) (167 mg, 72%) as a colourless gummy material in a 70:30 inseparable mixture of the (1*R*,2*S*) and (1*S*,2*S*) diastereomers: R_f = 0.48 (3:2, ethyl acetate/petrol); $[\alpha]^{24}_D$ = -7.3 (c = 2.6, CH_2Cl_2); FT IR (NaCl) ν_{max} 3065, 3032, 2880, 1959(w), 1736, 1367 (SO_2), 1185 (SO_2) cm^{-1}; ^1H NMR (400 MHz, $CDCl_3$) (1*R**,2*S**) δ 7.78 (d, *J* = 8.0 Hz, 1H, Ar-*H*), 7.70-7.21 (m, 8H, Ar-*H*), 5.15 (pseudo quintet, *J* = 6.2 Hz, 1H, C*H*(OSO_2Ar)CH_3), 5.06 (d, *J* = 6.0 Hz, 1H, PhC*H*Br), 4.58-4.54 (m, 2H, C(O)OC*H*$_2$), 3.87-3.85 (m, 2H, C*H*$_2$O), 3.71-3.67 (m, 2H, C*H*$_2$O), 3.59-3.56 (m, 2H, C*H*$_2$O), 3.40 (s, 3H, OC*H*$_3$) 1.58 (d, *J* = 6.4 Hz, 3H, C*H*$_3$) ppm; (1*S**,2*S**) δ 8.04 (d, *J* = 8.0 Hz, 1H, Ar-*H*), 7.70-7.21 (m, 8H, Ar-*H*), 5.26 (pseudo quintet, *J* = 6.5 Hz, 1H, C*H*(OSO_2Ar)CH_3), 5.02 (d, *J* = 6.8 Hz, 1H, PhC*H*Br), 4.58-4.54 (m, 2H, C(O)OC*H*$_2$), 3.87-3.85 (m, 2H, C*H*$_2$O), 3.71-3.67 (m, 2H, C*H*$_2$O), 3.59-3.56 (m, 2H, C*H*$_2$O), 3.40 (s, 3H, OC*H*$_3$) 1.31 (d, *J* = 6.4 Hz, 3H, C*H*$_3$) ppm; ^{13}C NMR (100MHz, $CDCl_3$) (1*R**,2*S**); δ 166.2, 137.1, 134.8, 133.3, 132.9, 130.7, 129.3, 128.6, 128.5 128.4, 82.1, 71.9, 70.5, 68.7, 65.3, 59.0, 56.1, 18.8 ppm; (1*S**,2*S**); δ 166.8, 136.8, 134.8, 133.5, 133.2, 130.7, 129.7, 129.5, 129.3, 128.9, 82.3, 71.9, 70.4, 68.7, 65.3, 59.0, 54.9, 18.5 ppm; MS (ES^+) 523/525 ($M+Na^+$); HRMS calcd for ($M+Na^+$) $C_{21}H_{25}O_7S^{79}BrNa$ 523.0402 and $C_{21}H_{25}O_7S^{81}BrNa$ 525.0382, found 523.0381 and 525.0365; Anal. calcd for $C_{21}H_{25}O_7SBr$: C, 50.31; H, 5.03; found: C, 50.43; H, 5.09.

Procedure for Rearrangement of Bromosulfonate 297 with $TiCl_4$[125]

(2*R*)-2-Bromo-1-chloro-1-phenylpropane (274/275)

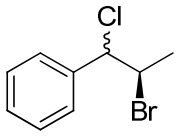

To a dichloromethane solution of 1-bromo-1-phenylpropyl 2-(2,5-dioxoheptylcarboxy)-1-benzosulfonate (**297**) (50 mg, 0.1 mmol), cooled to -78 ºC, was added $TiCl_4$ (22 µL, 0.2 mmol). The resulting bright yellow mixture was allowed to gradually warm to RT and stirred for 24 h. The reaction was quenched with water (10 mL) and extracted with dichloromethane (10 mL). The organic phase was passed through a silica gel plug and concentrated *in vacuo* to give pure (2*R*)-2-bromo-1-chloro-1-phenylpropane (**274**/**275**) (21 mg, 89%) as a colourless oil in a mixture of the (1*S*,2*R*) and (1*R*,2*R*) diastereomers in a 86:14 ratio: $[\alpha]^{27}_{D}$ = +41.8 (c = 3.4, CH_2Cl_2). All other spectral data is identical to that previously reported for the racemic mixture.

A Typical Procedure for Investigating Br^+ Exchange between Bromonium Ions and Alkenes with Bromosulfonate 297 and $TiCl_4$

To a dichloromethane solution of 1-bromo-1-phenylpropyl 2-(2,5-dioxoheptylcarboxy)-1-benzosulfonate (**297**) and alkene (2 eq.), cooled to -78 ºC, was added $TiCl_4$ (2 eq.). The resulting bright yellow mixture was allowed to gradually warm to RT and stirred for 24 h. The reaction was quenched with water and extracted with dichloromethane. The organic phase was passed through a silica gel plug and concentrated *in vacuo*. The crude product mixture was analysed by ^{1}H NMR analysis ($CDCl_3$) and, where appropriate, HPLC analysis.

7. References

1. Roberts, I.; Kimball, G. E. *J. Am. Chem. Soc.* **1937**, *59*, 947-948.
2. (a) Barlett, P. D.; Tarbell, D. S. *J. Am. Chem. Soc.* **1936**, *58*, 466-474; (b) Tarbell, D. S.; Barlett, P. D. *J. Am. Chem. Soc.* **1937**, *59*, 407-410.
3. (a) Terry, E. M.; Eichelberger, L. *J. Am. Chem. Soc.* **1925**, *47*, 1067-1078; (b) McKenzie, A. *J. Chem. Soc.* **1912**, *101*, 1196-1205; (c) Frankland, P. F. *J. Chem. Soc., Trans.* **1912**, 654-687.
4. Winstein, S.; Lucas, H. J. *J. Am. Chem. Soc.* **1939**, *61*, 1576-1581.
5. Winstein, S.; Lucas, H. J. *J. Am. Chem. Soc.* **1939**, *61*, 2845-2848.
6. Winstein, S.; Lucas, H. J. *J. Am. Chem. Soc.* **1936**, *58*, 2396-2402.
7. Winstein, S.; Lucas, H. J. *J. Am. Chem. Soc.* **1939**, *61*, 1581-1584.
8. Benjamin, B. M.; Schaeffer, H. J.; Collins, C. J. *J. Am. Chem. Soc.* **1957**, *79*, 6160-6164..
9. Traynham, J. G. *J. Chem. Educ.* **1963**, *40*, *8*, 392-395, and the references stated therein.
10. Winstein, S.; Buckles, R. E. *J. Am. Chem. Soc.* **1942**, *64*, 2780-2786.
11. Winstein, S.; Grunwald, E.; Ingraham, L. L. *J. Am. Chem. Soc.* **1948**, *70*, 821-828.
12. Grunwald, E. *J. Am. Chem. Soc.* **1951**, *73*, 5458-5459.
13. Buckles, R. E.; Long, J. W. *J. Am. Chem. Soc.* **1951**, *73*, 998-1000.
14. Henbest, H. B.; Wilson, R. A. L. *J. Chem. Soc.* **1959**, *837*, 4136-4138.
15. Fahey, R. C.; Schneider, H-J *J. Am. Chem. Soc.* **1968**, *90*, 4429-4434.
16. Rolston, J. H.; Yates, K. *J. Am. Chem. Soc.* **1969**, *91*, 1469-1476.
17. (a) Yates, K.; Wright, W. V. *Tetrahedron Lett.* **1965**, *24*, 1927-1933; (b) Yates, K.; Wright, W. V. *Can. J. Chem.* **1967**, *45*, 167-173.
18. Rolston, J. H.; Yates, K. *J. Am. Chem. Soc.* **1969**, *91*, 1483-1491.
19. Dubois, J. E.; Schwarcz, A. *Tetrahedron Lett.* **1964**, *32*, 2167-2173.
20. Barlett, P. D.; Tarbell, D. S. *J. Am. Chem. Soc.* **1936**, *58*, 466-474.
21. Yates, K.; McDonald, R. S. *J. Am. Chem. Soc.* **1971**, *93*, 6297-6299.
22. Yates, K.; McDonald, R. S. *J. Org. Chem.* **1973**, *38*, *7*, 2465-2478.
23. (a) Heasley, G. E.; Bower, T. R.; Dougharty, K. W.; Easdon, J. C. *J. Org. Chem.* **1980**, *45*, 5150-5155; (b) Cadogan, J. I. G.; Cameron, D. K.; Gosney, I.; Highcock, R. M.; Newlands, S. F. *J. Chem. Soc., Chem. Commun.* **1985**, 1751-1752.
24. (a) Hamman, S.; Beguin, C. G. *Journal of Fluorine Chemistry* **1979**, *13*, 163-174; (b) Angelini, G; Speranza, M. *J. Am. Chem. Soc.* **1981**, *103*, 3792-3799.
25. (a) Hassner, A.; Boerwinkle, F. P.; Levy, A. B. *J. Am. Chem. Soc.* **1970**, *92*, 4879-4883; (b) De Young, S.; Berliner, E. *J. Org. Chem.* **1979**, *44*, 1088-1092; (c) Negoro, T.; Ikeda, Y *Bull. Chem. Soc. Jpn.* **1986**, *59*, 3519-3522; (d) Chrétien, J. R.; Coudert, J.-D.; Ruasse, M.-F. *J. Org. Chem.* **1993**, *58*, 1917-1921.

26. Ruasse, M.-F. *Acc. Chem. Res.* **1990**, *23*, *3*, 87-93, and the references therein.
27. (a) McManus, S. P.; Peterson, P. E. *Tetrahedron Lett.* **1975**, *32*, 2753-2756; (b) McManus, S. P.; Ware, D. W. *Tetrahedron Lett.* **1974**, *48*, 4271-4274.
28. Modro, A.; Schmid, G. H.; Yates, K. *J. Org. Chem.* **1977**, *42*, 3673-3676.
29. Rolston, J. H.; Yates, K. *J. Am. Chem. Soc.* **1969**, *91*, 1477-1483.
30. Hamilton, T. P.; Schaefer, H. F. *J. Am. Chem. Soc.* **1990**, *112*, 8260-8265.
31. Galland, B.; Evieth, E. M.; Ruasse, M.-F. *J. Chem. Soc., Chem. Commun.* **1990**, 898-900.
32. Klobukowaki, M.; Brown, R. S. *J. Org. Chem.* **1994**, *59*, 7156-7160.
33. (a) Olah, G. A.; Bollinger, J. M.; Brinich, J. *J. Am. Chem. Soc.* **1968**, *90*, 2587-2594; (b) Olah, G. A.; Bollinger, J. M. *J. Am. Chem. Soc.* **1968**, *90*, 6082-6086.
34. Servis, K. L.; Domenick, R. L. *J. Am. Chem. Soc.* **1985**, *107*, 7186-7187.
35. Ohta, B. K.; Hough, R. E.; Schubert, J. W. *Org. Lett.* **2007**, *9*, *12*, 2317-2320.
36. Strating, J.; Wieringa, J. H.; Wynberg, H. *J. Chem. Soc., Chem. Commun.* **1969**, 907-908.
37. Slebocka-Tilk, H.; Ball, R. G.; Brown, R. S. *J. Am. Chem. Soc.* **1985**, *107*, 4504-4508.
38. Bennet, A. J.; Brown, R. S.; McClung, R. E. D.; Klobukowski, M.; Aarts, G. H. M.; Santarsiero, B. D.; Bellucci, G.; Bianchini, R. *J. Am. Chem. Soc.* **1991**, *113*, 8532-8535.
39. Brown, R. S.; Nagorski, R. W.; Bennet, A. J.; McClung, R. E. D.; Aarts, G. H. M.; Klobukowski, M.; McDonald, R.; Santarsiero, B. D. *J. Am. Chem. Soc.* **1994**, *116*, 2448-2456.
40. Lenoir, D.; Chiappe, C. *Chem. Eur. J.* **2003**, *9*, 1036-1044, and the references therein.
41. Sperka, J.; Liotta, D. C. *Hetereocycles* **1993**, *35*, *2*, 701-706.
42. Brown, R. S. *Acc. Chem. Res.* **1997**, *30*, 131-137, and the references therein.
43. Bellucci, G.; Bianchini, R.; Chiappe, C.; Marioni, F.; Ambrosetti, R.; Brown, R. S.; Slebocka-Tilk, H. *J. Am. Chem. Soc.* **1989**, *111*, 2640-2647.
44. Brown, R. S.; Gedye, R.; Slebocka-Tilk, H.; Buschek, J. M.; Kopecky, K. R. *J. Am. Chem. Soc.* **1984**, *106*, 4515-4521.
45. Bellucci, G.; Bianchini, R.; Chiappe, C.; Marioni, F.; Spagna, R. *J. Am. Chem. Soc.* **1988**, *110*, 546-552.
46. Brown, R. S.; Slebocka-Tilk, H.; Bennet, A. J.; Bellucci, G.; Bianchini, R.; Ambrosetti, R. *J. Am. Chem. Soc.* **1990**, *112*, 6310-6316.
47. Blanco, F. H.; Braddock, D. C.; Martín-Santamaría, S.; Rzepa, H. S. *The Internet J. Chem.* **2001**, *4*, 10-16.
48. Neverov, A. A.; Brown, R. S. *Can. J. Chem.* **1994**, *72*, 2540-2543; Neverov, A. A.; Brown, R. S. *J. Org. Chem.* **1996**, *61*, 962-968.
49. Ruasse, M.-F.; Motallebi, S.; Galland, B. *J. Am. Chem. Soc.* **1991**, *113*, 3440-3446.
50. Zheng, C. Y.; Slebocka-Tilk, H.; Nagorski, R. W.; Alvarado, L.; Brown, R. S. *J. Org. Chem.* **1993**, *58*, 2122-2127.

51. (a) Rodebaugh, R.; Fraser-Reid, B *J. Am. Chem. Soc.* **1994**, *116*, 3155-3156; (b) Rodebaugh, R.; Fraser-Reid, B *Tetrahedron* **1996**, *52*, *22*, 7663-7678.
52. Merrigan, S. R.; Singleton, D. A. *Org. Lett.* **1999**, *1*, *2*, 327-329.
53. Bellucci, G.; Bianchini, R.; Chiappe, C.; Brown, R. S.; Slebocka-Tilk, H. *J. Am. Chem. Soc.* **1991**, *113*, 8012-8016.
54. Cossi, M.; Persico, M.; Tomasi, J. *J. Am. Chem. Soc.* **1994**, *116*, 5373-5378.
55. Cansell, G. *PhD Thesis, University of London* **2005**.
56. Sakakura, A.; Ukai, A.; Ishihara, K. *Nature* **2007**, *445*, 900-903.
57. El-Qisairi, A. K.; Qaseer, H. A.; Katsigras, G.; Lorenzi, P.; Trivedi, U.; Tracz, S.; Hartman, A.; Miller, J.A.; Henry, P. M. *Org. Lett.* **2003**, *5*, 439-441.
58. (a) Marigo, M.; Jørgensen, K. A. *Chem. Commun.* **2006**, 2001-2011, and the references therein; (b) Dogo-Isonagie, C.; Bekele, T,; France, S.; Wolfer J.; Weatherwax, A.; Taggi, A. E.; Lectka, T. *J. Org. Chem.* **2006**, *71*, 8946-8949; (c) Bartoli, G.; Bosco, M.; Carlone, A.; Locatelli, M.; Melchiorre, P.; Sambri, L. *Angew. Chem. Int. Ed.* **2005**, *44*, 6219-6222.
59. Kalsuki, T.; Sharpless, K. B. *J. Am. Chem. Soc.* **1980**, 5974-5976.
60. (a) Noyori, R.; *Angew. Chem. Int. Ed.* **2002**, *41*, 2008-2022; (b) Burk, M. J.; Hems, W.; Herzberg, D.; Malan, C.; Zanotti-Gerosa, A. *Org. Lett.* **2000**, *2*, 4173-4176.
61. (a) Rho, H. S.; Ko, B.-S. *Synth. Commun.* **2001**, *31*, 2101-2106; (b) Rho, H. S.; Ko, B.-S.; Kim, H. K.; Ju, Y.-S. *Synth. Commun.* **2002**, *32*, 1303-1310; (c) Evans, P. A.; Nelson, J. D.; Manangan, T. *Synlett* **1997**, 986-970; (d) Evans, P. A.; Brandt, T. A. *Tetrahedron Lett.* **1996**, 6443-6446; (e) Evans, P. A.; Brandt, T. A. *J. Org. Chem.* **1997**, *62*, 5321-5326; (f) Hasham, M. A. J., A.; Ries, M.; Kirsching, A. *Synlett* **1998**, 195-198.
62. Braddock, D. C.; Cansell, G.; Hermitage, S. A. *Synlett* **2004**, *3*, 461-464.
63. Amey, R. L.; Martin, J. C. *J. Org. Chem.* **1979**, *44*, 1779-1784.
64. Braddock, D. C.; Cansell, G.; Hermitage, S. A.; White, A. J. P. *Chem. Commun.,* **2006**, 1442-1444.
65. Corey, E. J.; Jardine, P. DS.; Virgil, S.; Yuen, P.-W.; Connell, R. D. *J. Am. Chem. Soc.* **1989**, *111*, 9243-9244.
66. Corey, E. J.; Yu, C.-M.; Lee, D.-H. *J. Am. Chem. Soc.* **1990**, *112*, 878-879.
67. Corey, E. J.; Yu, C.-M.; Kim, S. S. *J. Am. Chem. Soc.* **1989**, *111*, 5495-5496.
68. Corey, E. J.; Kim, S. S. *J. Am. Chem. Soc.* **1990**, *112*, 4976-4977.
69. Corey, E. J.; Imwinkelried, R.; Pikul, S.; Xiang, Y. B. *J. Am. Chem. Soc.* **1989**, *111*, 5493-5495.
70. Noyori, R.; Yamakawa, M.; Hashiguchi, S. *J. Org. Chem.* **2001**, *66*, 7931-7944.
71. Ngo, H. L.; Lin, W. *J. Org. Chem.* **2005**, *70*, 1177-1187.
72. Xu, Y.; Clarkson, G. C.; Docherty, G.; North, C. L.; Woodward, G.; Wills, M. *J. Org. Chem.* **2005**, *70*, 8079-8087.

73. (a) Mikami, K.; Wakabayashi, K.; Aikawa, K. *Org. Lett.* **2006**, *8*, *8*, 1517-1519; (b) Jing, Q.; Sandoval, C. A.; Wang, Z.; Ding, K. *Eur. J. Org. Chem.* **2006**, 3606-3616.
74. Xie, J.-H.; Zhou, Z.-T.; Kong, W.-L.; Zhou, Q.-L. *J. Am. Chem. Soc.* **2007**, *129*, *7*, 1868-1869.
75. Xue, D.; Chen, Y.-C.; Cui, X.; Wang, Q.-W.; Zhu, J,; Deng, J.-G. *J. Org. Chem.* **2005**, *70*, 3584-3591.
76. (a) Zhang, W.; Loebach, J. L.; Wilson, S. R.; Jacobsen, E. R. *J. Am. Chem. Soc.* **1990**, *112*, 2801-2803; (b) Zhang, W.; Jacobsen, E. R. *J. Org. Chem.* **1991**, *56*, 2296-2298; (c) Amato, M. E.; Francesco, P. B.; Pappalardo, A.; Tomaselli, G. A.; Toscano, R. M.; Williams, D. J. *Eur. J. Org. Chem.* **2005**, 3562-3570.
77. Martinez, A.; Hemmert, C.; Loup, C.; Barré, G.; Meunier, B. *J. Org. Chem.* **2006**, *71*, 1449-1457.
78. Gao, J.; Woolley, F. R.; Zingaro, R. A. *Org. Biomol. Chem.* **2005**, *3*, 2126-2128.
79. Kim, S. S.; Lee, S. H. *Synth. Commun.* **2005**, *35*, 751-759.
80. Evans, D. A.; Nelson, S. G. *J. Am. Chem. Soc.* **1997**, *119*, 6452-6453.
81. (a) Weiss, M. E.; Fischer, D. F.; Xin, Z.; Jautze, S.; Schweiser, W. B.; Peters, R. *Angew. Chem. Int.* Ed. **2006**, *45*, 5694-5698; (b) Jautze, S.; Seiler, P.; Peters, R. *Angew. Chem. Int.* Ed. **2007**, *46*, 1260-1264.
82. Busacca, C. A.; Grossbach, D.; So, R. C.; O'Brien, E. M.; Spinelli, E. M. *Org. Lett.* **2003**, *5*, *4*, 595-598.
83. Bhor, S.; Anikumar, G.; Tse, M. K.; Klawonn, M.; Döbler, C.; Bitterlich, B.; Grotevendt, A.; Beller, M. *Org. Lett.* **2005**, *7*, *16*, 3393-3396.
84. Funk, T. W.; Berlin, J. M.; Grubbs, R. H. *J. Am. Chem. Soc* **2006**, *128*, *6*, 1840-1846.
85. Berlin, J. M.; Goldberg, S. D.; Grubbs, R. H. *Angew. Chem. Int. Ed.* **2006**, *45*, 7591-7595.
86. Van Veldhuizen, J. J.; Campbell, J. E.; Giudici, R. E.; Hoveyda, A. H. *J. Am. Chem. Soc.* **2005**, *127*, *18*, 6877-6882.
87. Brown, M. K.; May, T. L.; Baxter, C. A.; Hoveyda, A. H. *Angew. Chem. Int. Ed.* **2007**, *46*, 1097-1100.
88. Faller, J. W.; Fontaine, P. P. *Organometallics* **2006**, *25*, 5887-5893.
89. Xiong, Y.; Huang, X.; Gou, S.; Huang, J.; Wen, Y.; Feng, X. *Adv. Synth. Cat.* **2006**, *348*, 538-544.
90. Tsogoeva, S. B.; Wei, S. *Chem. Comm.* **2006**, 1451-1453.
91. Lalonde, M. P.; Chen, Y.; Jacobsen, E. N. *Angew. Chem. Int. Ed.* **2006**, *45*, 6366-6370.
92. Williams, O. F.; Bailar, J. C. *J. Am. Chem. Soc.* **1959**, *81*, 4464-4469.
93. Pikul, S.; Corey, E. J. *Org. Synth*. **1993**, *71*, 22-29.
94. Fenton, R. R.; Vagg, R. S.; Williams, P. A. *Inorg. Chim. Acta* **1988**, *148*, 37-44.
95. Saigo, K.; Kubota, N.; Takebayashi, S.; Hasegawa, M. *Bull. Chem. Soc. Jpn.* **1986**, *59*, 931-932.
96. Shimizu, M.; Kamel, M; Fujisawa, T. *Tetrahedron Lett.* **1995**, *36*, 8607-8610.
97. Pini, D.; Iuliano, A; Rosini, P.; Salvadori, P. *Synthesis* **1990**, 1023-1024.
98. Oi, R.; Sharpless, K. B. *Tetrahedron Lett*. **1991**, *32*, 999-1002.

99. Sun, X.; Wang, S.; Sun, S.; Zhu, J.; Deng, J. *Synlett* **2005**, *18*, 2776-2780.
100. Liao, J.; Sun, X.; Cui, X.; Yu, K.; Zhu, J.; Deng, J. *Chem. Eur. J.* **2003**, *9*, 2611-2615.
101. Lifshitz, I.; Bos, J. G. *Rec. Trav. Chim.* **1940**, *59*, 173-183.
102. Corey, E. J.; Kühnle, N. M. *Tetrahedron Lett*. **1997**, *38*, 50.
103. Braddock, D. C.; Redmond, J. M.; Hermitage, S. A.; White, A. J. P. *Adv. Synth. Catal.* **2006**, *348*, 911-916.
104. Uchida, H.; Shimizu, T.; Reddy, P. Y.; Nakamura, S.; Toru, T. *Synthesis* **2003**, *8*, 1236-1240.
105. Laurent, M. A. *Liebigs Ann. Chem.* **1837**, *21*, 130.
106. Ahmad, S. M.; Braddock, D. C.; Cansell, G.; Hermitage, S. A. *Tetrahedron Lett.* **2007**, *48*, 915-918.
107. Saravanan, P.; Bisai, A.; Baktharaman, S.; Chandrasekhar, M.; Singh, V. K. *Tetrahedron* **2002**, *58*, 4693-4706.
108. (a) Sheehan, J. C.; Hess, G. P. *J. Am. Chem. Soc.* **1955**, *77*, 1067-1068; (b) Sheehan, J. C.; Goodman, M.; Hess, G. P. *J. Am. Chem. Soc.* **1956**, *78*, 1367-1369.
109. Benson, S. C.; Cai, P.; Colon, M.; Haiza, M. A.; Tokles, M.; Snyder, J. K. *J. Org. Chem.* **1988**, *53*, 5335-5341.
110. Braddock, D. C.; Hermitage, S. A.; Redmond, J. M.; White, A. J. P. *Tetrahedron: Asymm.* **2006**, *17*, 2935-2937.
111. Lifschitz, I.; Bos, J. G. *Recl. Trav. Chim.* **1939**, *58*, 638-642.
112. Field, J. E.; Hill, T. J.; Venkatarman, D. *J. Org. Chem.* **2003**, *68*, 6071-6078.
113. Krizan, T. D.; Martin, J. C. *J. Org. Chem.* **1982**, *47*, 2682-2684.
114. Harfenist, M.; Heuser, D. J.; Joyner, C. T.; Batchelor, J. F.; White, H. L. *J. Med. Chem.* **1996**, *39*, 1857-1863.
115. (a) Fujioka, H.; Murai, K.; Ohba, Y.; Hiramatsu, A.; Kita, Y. *Tetrahedron Lett.* **2005**, *46*, 2197-2199; (b) Fujioka, H.; Murai, K.; Kubo, O.; Ohba, Y.; Kita, Y. *Tetrahedron* **2007**, *63*, 638-643.
116. Cailleau, T. *unpublished work* **2007**.
117. Aurich, H. G.; Biesemeier, F.; Boutahar, M. *Chem. Ber.* **1991**, *124*, *10*, 2329-2334.
118. Neumer, J. F.; *Ger. Offen.* **1972**, 2220383.
119. Dauzonne, D.; Fleurant, A.; Demerseman, P.; Cotrait, M.; Bideau, J. P. *Synth. Commun.*, **1990**, *20*, 3339-3345.
120. Thomas, E. L.; Bozeman, P. M.; Jefferson, M. M.; King, C. C. *J. Biol. Chem.* **1995**, *270*, 2906-2913.
121. Kwok, L. *4th Year Research Project, University of London* **2006**.
122. Nagorski, R. W.; Brown, R. S. *J. Am. Chem. Soc.* **1992**, *114*, 7773-7779.
123. Schlama, T.; Baati, R.; Gouverner, V.; Valleix, A.; Falck, J. R.; Mioskowski, C. *Angew. Chem. Int. Ed.* **1998**, *37*, 2085-2087.
124. With thanks to Asha X, GSK, for her expertise chiral HPLC analysis.

125. (a) Lepore, S. D.; Bhunia, A. K.; Cohn, P. C. *J. Org. Chem.* **2005**, *70*, 8117-8121; (b) Lepore, S. D.; Bhunia, A. K.; Mondal, D.; Cohn, P. C.; Lefkowitz, C. *J. Org. Chem.* **2006**, *71*, 3285-3286.
126. Braddock, D. C. *Research Proposal*, **2007**.
127. Armarego, W. L. F.; Perrin, D. D. *Purification of Laboratory Chemicals* 4th ed.; Butterworth-Heinemann: Oxford, **1996**; p 529.
128. Hunter, S.; Sim, S. K. *Can. J. Chem.* **1972**, *50*, 669-677.
129. Kusakabe, M.; Kitano, Y.; Kobayashi, Y.; Sato, F. *J. Org. Chem.* **1989**, *54*, 2085-2091.
130. Marchi, C.; Fotiadu, F.; Buono, G. *Organometallics* **1999**, *18*, 5, 915-927.
131. As stated by Sigma-Aldrich® catalogue.
132. Reading taken from sample of (–)-(1*S*, 2*S*)-1,2-diphenylethylene diamine purchased from Sigma-Aldrich®.
133. As stated by Sigma-Aldrich® catalogue.
134. Reading taken from sample of (+)-(1*R*, 2*R*)-1,2-diphenylethylene diamine purchased from Sigma-Aldrich®.
135. As stated by Sigma-Aldrich® catalogue.
136. As stated by Sigma-Aldrich® catalogue.
137. Gresher, A.; Stevens, M. F. G.; Turnbull, C. P. *J. Chem. Soc., Perkin Trans.* **1977**, 103-106.
138. Shelly, K. P.; Venimadhavan, S.; Nagarajan, K.; Stewart, R. *Can. J. Chem.* **1989**, *67*, 1274-1282.
139. Schmidt, B.; Wildemann, H. *J. Org. Chem.* **2000**, *65*, 5817-5822.
140. Ahmad, S. M.; Braddock, D. C.; Cansell, G.; Hermitage, S. A.; Redmond, J. M.; White, A. J. P. *Tetrahedron Letters* **2007**, *48*, *34*, 5948-5952.
141. Heasley, G. E.; McCall Bundy, J.; Heasley, V. L.; Arnold, S.; Gipe, A.; McKee, D.; Orr, R.; Rodgers, S. L.; Shellhamer, D. F. *J. Org. Chem.* **1978**, *43*, 2793-2799.
142. Zajc, B.; Zupan, M. *Tetrahedron* **1990**, *46*, 6161-6166.
143. As stated by Sigma-Aldrich® catalogue.
144. Kotsuki, H.; Shimanouchi, T.; Ohshima, R.; Fujiwara, S. *Tetrahedron*, **1998**, *54*, 2709-2722.
145. As stated by Sigma-Aldrich® catalogue.
146. As stated by Sigma-Aldrich® catalogue.
147. Solladié-Carvallo, A.; Lupattalli, P.; Bonini, C. *J. Org. Chem.* **2005**, *70*, 1605-1611.
148. Sels, B. F.; De Vos, D. E.; Jacobs, P. A. *J. Am. Chem. Soc.* **2001**, *123*, 8350-8359.
149. Buckles, R. E.; Forrester, J. L.; Burham, R. L.; McGee, T. W. *J. Org. Chem.* **1960**, *25*, 24-26.
150. Pagni, R. M.; Kabalka, G. W.; Boothe, R.; Gaetano, K.; Stewart, L. J.; Conaway, R.; Dial, C.; Gray, D.; Larson, S.; Luidhardt, T. *J. Org. Chem.* **1988**, *53*, 4477-4482.

8. Appendix

CB0501; (–)-(4*S*,5*S*)-1-[(*R*)-α-acetoxybenzeneacetyl]-4,5-dihydro-2,4,5-triphenylimidazole (176)

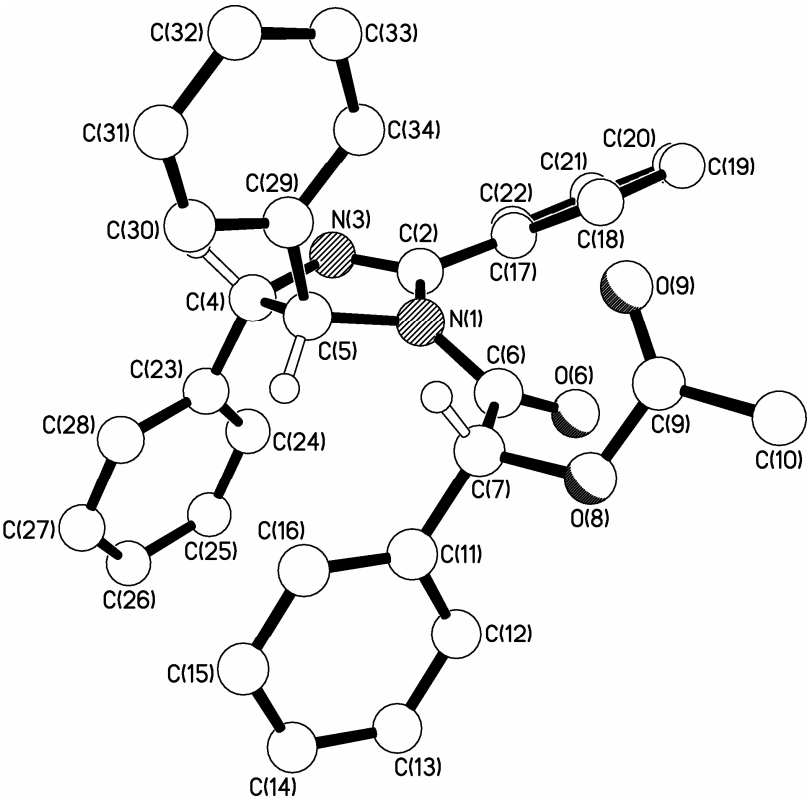

Crystal data and structure refinement for CB0501.

Identification code	CB0501	
Empirical formula	C31 H26 N2 O3	
Formula weight	474.54	
Temperature	173(2) K	
Diffractometer, wavelength	OD Xcalibur PX Ultra, 1.54248 Å	
Crystal system, space group	Orthorhombic, P2(1)2(1)2(1)	
Unit cell dimensions	a = 10.1710(7) Å	α = 90°
	b = 14.6196(9) Å	β = 90°
	c = 17.2572(11) Å	γ = 90°
Volume, Z	2566.1(3) $Å^3$, 4	
Density (calculated)	1.228 Mg/m^3	
Absorption coefficient	0.633 mm^{-1}	

F(000)	1000
Crystal colour / morphology	Colourless blocks
Crystal size	0.22 x 0.21 x 0.15 mm^3
θ range for data collection	3.96 to 68.68°
Index ranges	-12<=h<=12, -17<=k<=17, -20<=l<=20
Reflns collected / unique	53984 / 4696 [R(int) = 0.0280]
Reflns observed [F>4σ(F)]	4638
Absorption correction	Numeric analytical
Max. and min. transmission	0.92271 and 0.87531
Refinement method	Full-matrix least-squares on F^2
Data / restraints / parameters	4696 / 2 / 329
Goodness-of-fit on F^2	1.041
Final R indices [F>4σ(F)]	R1 = 0.0390, wR2 = 0.1005
	R1+ = 0.0390, wR2+ = 0.1005
	R1- = 0.0392, wR2- = 0.1008
R indices (all data)	R1 = 0.0393, wR2 = 0.1009
Absolute structure parameter	x+ = 0.0(2), x- = 1.1(2)
Extinction coefficient	0.0032(3)
Largest diff. peak, hole	0.155, -0.156 $eÅ^{-3}$
Mean and maximum shift/error	0.000 and 0.000

Bond lengths [Å] and angles [°] for CB0501.

N(1)-C(6)	1.375(3)
N(1)-C(2)	1.426(3)
N(1)-C(5)	1.476(2)
C(2)-N(3)	1.275(3)
C(2)-C(17)	1.478(3)
N(3)-C(4)	1.469(3)
C(4)-C(23)	1.513(3)
C(4)-C(5)	1.553(3)
C(4)-C(23')	1.574(4)
C(5)-C(29)	1.519(3)
C(6)-O(6)	1.211(2)
C(6)-C(7)	1.528(3)
C(7)-O(8)	1.445(2)
C(7)-C(11)	1.478(2)
C(7)-C(11')	1.602(4)
O(8)-C(9)	1.358(3)
C(9)-O(9)	1.205(3)
C(9)-C(10)	1.499(3)
C(11)-C(12)	1.3900
C(11)-C(16)	1.3900
C(12)-C(13)	1.3900

C(13)-C(14)	1.3900
C(14)-C(15)	1.3900
C(15)-C(16)	1.3900
C(11')-C(12')	1.3900
C(11')-C(16')	1.3900
C(12')-C(13')	1.3900
C(13')-C(14')	1.3900
C(14')-C(15')	1.3900
C(15')-C(16')	1.3900
C(17)-C(18)	1.388(3)
C(17)-C(22)	1.391(3)
C(18)-C(19)	1.384(3)
C(19)-C(20)	1.380(4)
C(20)-C(21)	1.373(4)
C(21)-C(22)	1.387(3)
C(23)-C(24)	1.3900
C(23)-C(28)	1.3900
C(24)-C(25)	1.3900
C(25)-C(26)	1.3900
C(26)-C(27)	1.3900
C(27)-C(28)	1.3900
C(23')-C(24')	1.3900
C(23')-C(28')	1.3900
C(24')-C(25')	1.3900
C(25')-C(26')	1.3900
C(26')-C(27')	1.3900
C(27')-C(28')	1.3900
C(29)-C(30)	1.380(3)
C(29)-C(34)	1.385(3)
C(30)-C(31)	1.380(3)
C(31)-C(32)	1.372(4)
C(32)-C(33)	1.375(4)
C(33)-C(34)	1.388(3)

C(6)-N(1)-C(2)	125.55(15)
C(6)-N(1)-C(5)	125.57(17)
C(2)-N(1)-C(5)	106.08(15)
N(3)-C(2)-N(1)	114.42(17)
N(3)-C(2)-C(17)	123.2(2)
N(1)-C(2)-C(17)	122.15(17)
C(2)-N(3)-C(4)	108.39(18)
N(3)-C(4)-C(23)	110.71(18)
N(3)-C(4)-C(5)	104.79(15)
C(23)-C(4)-C(5)	116.2(2)
N(3)-C(4)-C(23')	114.6(2)
C(23)-C(4)-C(23')	11.9(2)
C(5)-C(4)-C(23')	104.4(2)
N(1)-C(5)-C(29)	112.50(15)
N(1)-C(5)-C(4)	100.56(15)
C(29)-C(5)-C(4)	113.84(16)
O(6)-C(6)-N(1)	123.2(2)
O(6)-C(6)-C(7)	121.42(19)
N(1)-C(6)-C(7)	115.41(16)
O(8)-C(7)-C(11)	110.33(19)
O(8)-C(7)-C(6)	108.73(16)
C(11)-C(7)-C(6)	111.00(19)

O(8)-C(7)-C(11')	101.5(2)
C(11)-C(7)-C(11')	9.6(2)
C(6)-C(7)-C(11')	111.8(2)
C(9)-O(8)-C(7)	114.47(17)
O(9)-C(9)-O(8)	122.1(2)
O(9)-C(9)-C(10)	126.3(2)
O(8)-C(9)-C(10)	111.6(2)
C(12)-C(11)-C(16)	120.0
C(12)-C(11)-C(7)	118.25(17)
C(16)-C(11)-C(7)	121.75(17)
C(13)-C(12)-C(11)	120.0
C(12)-C(13)-C(14)	120.0
C(15)-C(14)-C(13)	120.0
C(16)-C(15)-C(14)	120.0
C(15)-C(16)-C(11)	120.0
C(12')-C(11')-C(16')	120.0
C(12')-C(11')-C(7)	120.2(3)
C(16')-C(11')-C(7)	119.6(3)
C(11')-C(12')-C(13')	120.0
C(12')-C(13')-C(14')	120.0
C(15')-C(14')-C(13')	120.0
C(14')-C(15')-C(16')	120.0
C(15')-C(16')-C(11')	120.0
C(18)-C(17)-C(22)	119.42(19)
C(18)-C(17)-C(2)	121.57(18)
C(22)-C(17)-C(2)	118.84(18)
C(19)-C(18)-C(17)	119.9(2)
C(20)-C(19)-C(18)	120.3(2)
C(21)-C(20)-C(19)	120.1(2)
C(20)-C(21)-C(22)	120.1(2)
C(21)-C(22)-C(17)	120.0(2)
C(24)-C(23)-C(28)	120.0
C(24)-C(23)-C(4)	122.26(17)
C(28)-C(23)-C(4)	117.55(18)
C(23)-C(24)-C(25)	120.0
C(24)-C(25)-C(26)	120.0
C(27)-C(26)-C(25)	120.0
C(26)-C(27)-C(28)	120.0
C(27)-C(28)-C(23)	120.0
C(24')-C(23')-C(28')	120.0
C(24')-C(23')-C(4)	123.1(3)
C(28')-C(23')-C(4)	116.9(3)
C(23')-C(24')-C(25')	120.0
C(26')-C(25')-C(24')	120.0
C(25')-C(26')-C(27')	120.0
C(28')-C(27')-C(26')	120.0
C(27')-C(28')-C(23')	120.0
C(30)-C(29)-C(34)	119.28(19)
C(30)-C(29)-C(5)	118.30(18)
C(34)-C(29)-C(5)	122.37(18)
C(29)-C(30)-C(31)	120.3(2)
C(32)-C(31)-C(30)	120.5(2)
C(31)-C(32)-C(33)	119.7(2)
C(32)-C(33)-C(34)	120.2(2)
C(29)-C(34)-C(33)	120.0(2)

CB0502b; 1:1 mandelic acid: *iso*-amarine diastereomeric salt (182)

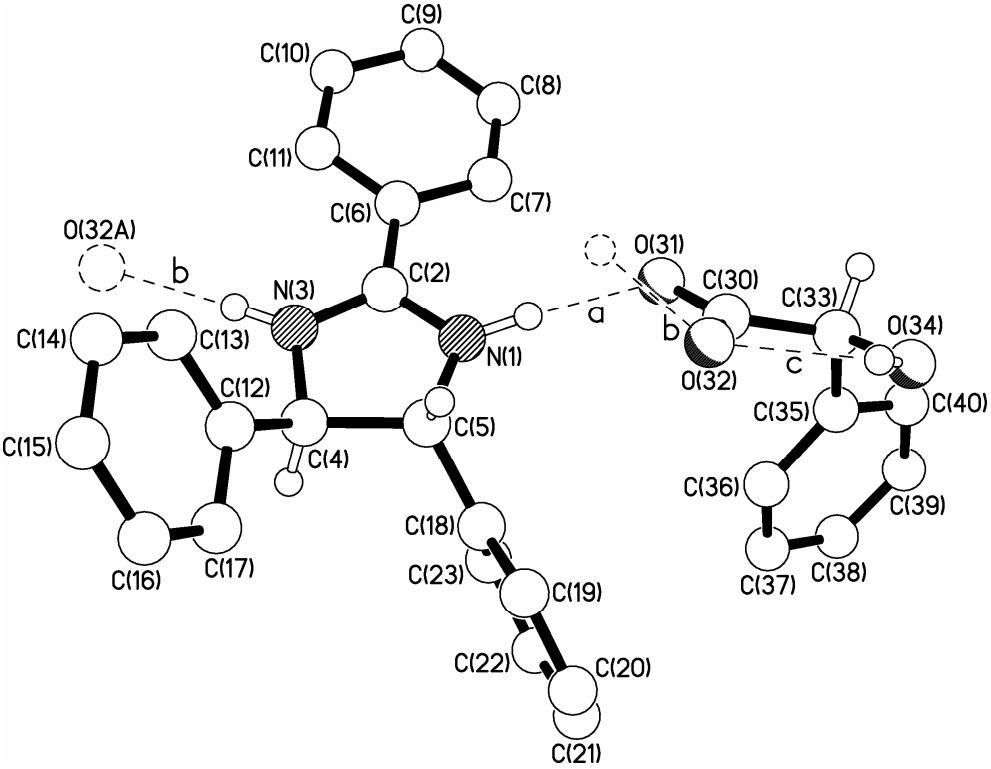

Crystal data and structure refinement for CB0502b.

Identification code	CB0502b	
Empirical formula	C29 H26 N2 O3	
Formula weight	450.52	
Temperature	293(2) K	
Diffractometer, wavelength	OD Xcalibur PX Ultra, 1.54248 Å	
Crystal system, space group	Orthorhombic, P2(1)2(1)2(1)	
Unit cell dimensions	a = 8.6149(5) Å	α = 90°
	b = 16.0588(8) Å	β = 90°
	c = 17.2764(8) Å	γ = 90°
Volume, Z	2390.1(2) $Å^3$, 4	
Density (calculated)	1.252 Mg/m^3	
Absorption coefficient	0.650 mm^{-1}	
F(000)	952	
Crystal colour / morphology	Colourless prisms	
Crystal size	0.14 x 0.07 x 0.06 mm^3	

θ range for data collection	3.76 to 68.71°
Index ranges	-9<=h<=10, -19<=k<=19, -20<=l<=20
Reflns collected / unique	49167 / 4365 [R(int) = 0.0403]
Reflns observed [F>4σ(F)]	3623
Absorption correction	Numeric analytical
Max. and min. transmission	0.96739 and 0.90995
Refinement method	Full-matrix least-squares on F^2
Data / restraints / parameters	4365 / 2 / 317
Goodness-of-fit on F^2	1.069
Final R indices [F>4σ(F)]	R1 = 0.0472, wR2 = 0.1068
	R1+ = 0.0472, wR2+ = 0.1068
	R1- = 0.0472, wR2- = 0.1070
R indices (all data)	R1 = 0.0628, wR2 = 0.1145
Absolute structure parameter	x+ = 0.1(3), x- = 0.9(3)
	Absolute structure indeterminate,
	Assigned by internal reference
Extinction coefficient	0.0018(3)
Largest diff. peak, hole	0.112, -0.104 $eÅ^{-3}$
Mean and maximum shift/error	0.000 and 0.000

Bond lengths [Å] and angles [°] for CB0502b.

N(1)-C(2)	1.310(2)
N(1)-C(5)	1.474(2)
C(2)-N(3)	1.316(2)
C(2)-C(6)	1.469(3)
N(3)-C(4)	1.461(3)
C(4)-C(12)	1.507(3)
C(4)-C(5)	1.566(3)
C(5)-C(18)	1.508(3)
C(6)-C(11)	1.379(3)
C(6)-C(7)	1.386(3)
C(7)-C(8)	1.369(3)
C(8)-C(9)	1.357(3)
C(9)-C(10)	1.371(3)
C(10)-C(11)	1.380(3)
C(12)-C(13)	1.370(3)
C(12)-C(17)	1.375(3)
C(13)-C(14)	1.389(4)
C(14)-C(15)	1.348(4)
C(15)-C(16)	1.355(5)
C(16)-C(17)	1.386(4)
C(18)-C(23)	1.364(3)
C(18)-C(19)	1.374(3)

C(19)-C(20)	1.383(3)
C(20)-C(21)	1.352(4)
C(21)-C(22)	1.351(4)
C(22)-C(23)	1.385(4)
C(30)-O(31)	1.243(2)
C(30)-O(32)	1.244(2)
C(30)-C(33)	1.519(3)
C(33)-O(34)	1.419(3)
C(33)-C(35)	1.504(4)
C(35)-C(36)	1.366(4)
C(35)-C(40)	1.374(3)
C(36)-C(37)	1.384(4)
C(37)-C(38)	1.347(6)
C(38)-C(39)	1.325(7)
C(39)-C(40)	1.405(7)

C(2)-N(1)-C(5)	111.87(14)
N(1)-C(2)-N(3)	111.90(17)
N(1)-C(2)-C(6)	123.88(16)
N(3)-C(2)-C(6)	124.22(16)
C(2)-N(3)-C(4)	111.74(15)
N(3)-C(4)-C(12)	114.41(17)
N(3)-C(4)-C(5)	102.14(14)
C(12)-C(4)-C(5)	113.58(16)
N(1)-C(5)-C(18)	112.77(15)
N(1)-C(5)-C(4)	101.31(14)
C(18)-C(5)-C(4)	115.26(16)
C(11)-C(6)-C(7)	118.60(19)
C(11)-C(6)-C(2)	120.93(17)
C(7)-C(6)-C(2)	120.46(17)
C(8)-C(7)-C(6)	120.2(2)
C(9)-C(8)-C(7)	121.2(2)
C(8)-C(9)-C(10)	119.2(2)
C(9)-C(10)-C(11)	120.7(2)
C(6)-C(11)-C(10)	120.1(2)
C(13)-C(12)-C(17)	118.2(2)
C(13)-C(12)-C(4)	123.6(2)
C(17)-C(12)-C(4)	118.2(2)
C(12)-C(13)-C(14)	121.4(3)
C(15)-C(14)-C(13)	119.7(3)
C(14)-C(15)-C(16)	119.7(3)
C(15)-C(16)-C(17)	121.3(3)
C(12)-C(17)-C(16)	119.6(3)
C(23)-C(18)-C(19)	117.5(2)
C(23)-C(18)-C(5)	121.32(19)
C(19)-C(18)-C(5)	121.1(2)
C(18)-C(19)-C(20)	120.8(2)
C(21)-C(20)-C(19)	120.8(2)
C(22)-C(21)-C(20)	119.1(3)
C(21)-C(22)-C(23)	120.6(3)
C(18)-C(23)-C(22)	121.2(3)
O(31)-C(30)-O(32)	125.64(19)
O(31)-C(30)-C(33)	116.97(19)
O(32)-C(30)-C(33)	117.4(2)
O(34)-C(33)-C(35)	111.01(19)
O(34)-C(33)-C(30)	109.68(19)

C(35)-C(33)-C(30)	112.5(2)
C(36)-C(35)-C(40)	117.0(3)
C(36)-C(35)-C(33)	122.2(2)
C(40)-C(35)-C(33)	120.7(3)
C(35)-C(36)-C(37)	122.7(3)
C(38)-C(37)-C(36)	118.1(5)
C(39)-C(38)-C(37)	121.9(5)
C(38)-C(39)-C(40)	120.0(4)
C(35)-C(40)-C(39)	120.2(4)

CB0601; 2,6-Di-[(4*S*,5*S*)-1-{(*R*)-α-acetoxyphenyl acetyl}-4,5-diphenyl-4,5-dihydroimidazol-2-yl]iodobenzene (245)

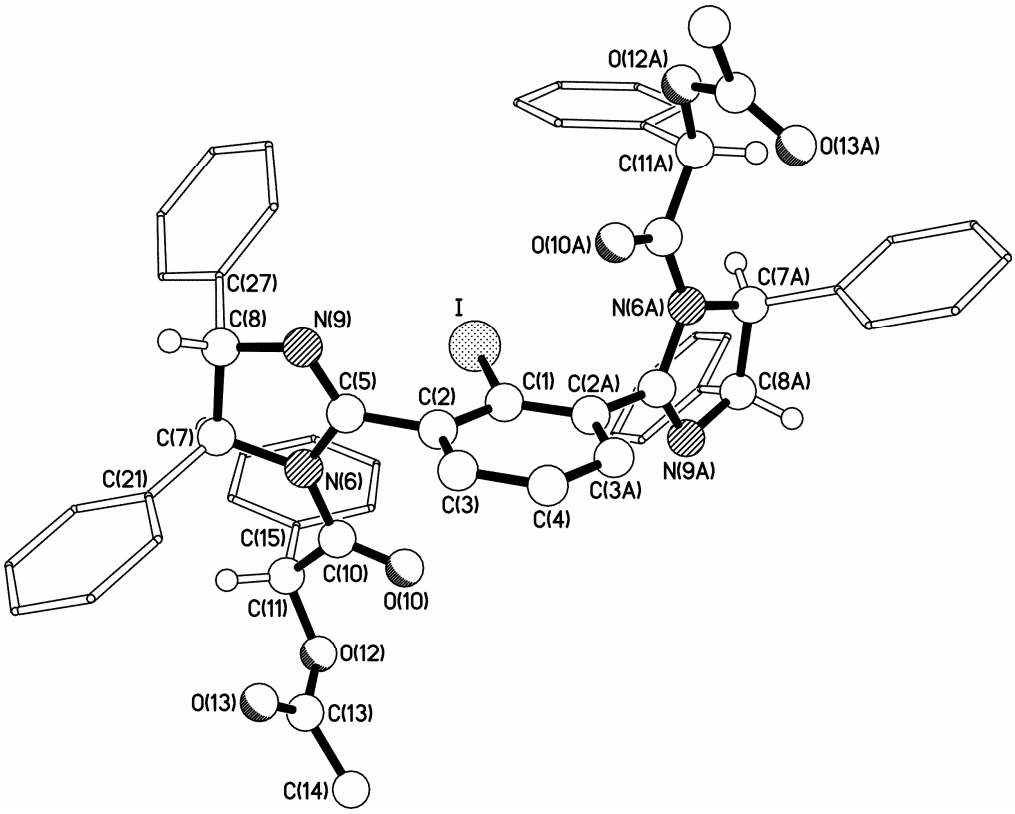

Crystal data and structure refinement for CB0601.

Identification code	CB0601	
Empirical formula	C56 H45 I N4 O6	
Formula weight	996.86	
Temperature	173(2) K	
Diffractometer, wavelength	OD Xcalibur 3, 0.71073 Å	
Crystal system, space group	Monoclinic, P2	
Unit cell dimensions	a = 10.1088(17) Å	α = 90°

	b = 8.9540(15) Å	β = 90.045(8)°
	c = 13.6000(8) Å	γ = 90°
Volume, Z	1231.0(3) $Å^3$, 1	
Density (calculated)	1.345 Mg/m^3	
Absorption coefficient	0.705 mm^{-1}	
F(000)	510	
Crystal colour / morphology	Colourless blocks	
Crystal size	0.30 x 0.26 x 0.25 mm^3	
θ range for data collection	3.76 to 31.97°	
Index ranges	-14<=h<=15, -12<=k<=12, -19<=l<=20	
Reflns collected / unique	19882 / 7620 [R(int) = 0.0360]	
Reflns observed [F>4σ(F)]	7199	
Absorption correction	Analytical	
Max. and min. transmission	0.87259 and 0.83704	
Refinement method	Full-matrix least-squares on F^2	
Data / restraints / parameters	7620 / 1 / 306	
Goodness-of-fit on F^2	1.075	
Final R indices [F>4σ(F)]	R1 = 0.0223, wR2 = 0.0560	
	R1+ = 0.0223, wR2+ = 0.0560	
	R1- = 0.0389, wR2- = 0.1068	
R indices (all data)	R1 = 0.0244, wR2 = 0.0565	
Absolute structure parameter	x+ = 0.000(7), x- = 1.003(7)	
Extinction coefficient	0.0021(10)	
Largest diff. peak, hole	0.449, -0.461 $eÅ^{-3}$	
Mean and maximum shift/error	0.000 and 0.000	

Bond lengths [Å] and angles [°] for CB0601.

I-C(1)	2.0933(16)
C(1)-C(2)#1	1.3962(14)
C(1)-C(2)	1.3962(14)
C(2)-C(3)	1.389(2)
C(2)-C(5)	1.4937(17)
C(3)-C(4)	1.3858(18)
C(4)-C(3)#1	1.3858(18)
C(5)-N(9)	1.2681(18)
C(5)-N(6)	1.4156(15)
N(6)-C(10)	1.3738(15)
N(6)-C(7)	1.4803(15)
C(7)-C(21)	1.5166(19)

C(7)-C(8)	1.5756(18)
C(8)-N(9)	1.4754(19)
C(8)-C(27)	1.514(2)
C(10)-O(10)	1.2079(16)
C(10)-C(11)	1.5443(18)
C(11)-O(12)	1.4375(16)
C(11)-C(15)	1.505(2)
O(12)-C(13)	1.3568(16)
C(13)-O(13)	1.2004(17)
C(13)-C(14)	1.4900(19)
C(15)-C(20)	1.388(2)
C(15)-C(16)	1.395(3)
C(16)-C(17)	1.393(3)
C(17)-C(18)	1.376(4)
C(18)-C(19)	1.358(4)
C(19)-C(20)	1.404(3)
C(21)-C(22)	1.381(3)
C(21)-C(26)	1.392(2)
C(22)-C(23)	1.395(2)
C(23)-C(24)	1.379(3)
C(24)-C(25)	1.371(4)
C(25)-C(26)	1.406(3)
C(27)-C(28)	1.396(3)
C(27)-C(32)	1.397(2)
C(28)-C(29)	1.391(3)
C(29)-C(30)	1.386(4)
C(30)-C(31)	1.383(5)
C(31)-C(32)	1.400(3)

C(2)#1-C(1)-C(2)	120.86(16)
C(2)#1-C(1)-I	119.57(8)
C(2)-C(1)-I	119.57(8)
C(3)-C(2)-C(1)	119.15(13)
C(3)-C(2)-C(5)	120.28(12)
C(1)-C(2)-C(5)	120.52(12)
C(4)-C(3)-C(2)	120.03(14)
C(3)-C(4)-C(3)#1	120.73(18)
N(9)-C(5)-N(6)	115.58(11)
N(9)-C(5)-C(2)	122.49(11)
N(6)-C(5)-C(2)	121.90(10)
C(10)-N(6)-C(5)	125.89(10)
C(10)-N(6)-C(7)	126.22(10)
C(5)-N(6)-C(7)	107.81(9)
N(6)-C(7)-C(21)	112.06(11)
N(6)-C(7)-C(8)	100.79(10)
C(21)-C(7)-C(8)	113.11(11)
N(9)-C(8)-C(27)	111.07(12)
N(9)-C(8)-C(7)	105.68(10)
C(27)-C(8)-C(7)	113.41(13)
C(5)-N(9)-C(8)	108.60(11)
O(10)-C(10)-N(6)	122.99(11)
O(10)-C(10)-C(11)	121.06(11)
N(6)-C(10)-C(11)	115.90(10)
O(12)-C(11)-C(15)	107.82(12)
O(12)-C(11)-C(10)	107.48(11)
C(15)-C(11)-C(10)	110.09(11)

C(13)-O(12)-C(11)	114.03(10)
O(13)-C(13)-O(12)	122.31(12)
O(13)-C(13)-C(14)	125.92(14)
O(12)-C(13)-C(14)	111.77(12)
C(20)-C(15)-C(16)	119.61(18)
C(20)-C(15)-C(11)	120.14(17)
C(16)-C(15)-C(11)	120.26(14)
C(17)-C(16)-C(15)	119.4(2)
C(18)-C(17)-C(16)	120.8(2)
C(19)-C(18)-C(17)	119.97(19)
C(18)-C(19)-C(20)	120.8(2)
C(15)-C(20)-C(19)	119.5(2)
C(22)-C(21)-C(26)	119.18(16)
C(22)-C(21)-C(7)	121.38(13)
C(26)-C(21)-C(7)	119.44(16)
C(21)-C(22)-C(23)	120.77(19)
C(24)-C(23)-C(22)	120.0(2)
C(25)-C(24)-C(23)	119.78(18)
C(24)-C(25)-C(26)	120.70(19)
C(21)-C(26)-C(25)	119.5(2)
C(28)-C(27)-C(32)	118.09(18)
C(28)-C(27)-C(8)	120.38(15)
C(32)-C(27)-C(8)	121.50(17)
C(29)-C(28)-C(27)	121.6(2)
C(30)-C(29)-C(28)	119.9(3)
C(31)-C(30)-C(29)	119.4(2)
C(30)-C(31)-C(32)	121.0(2)
C(27)-C(32)-C(31)	120.1(2)

Symmetry transformations used to generate equivalent atoms:
#1 -x+1,y,-z+1

CB0604; Di(2-bromo-2-phenyleth-1-yl) sulfite (268)

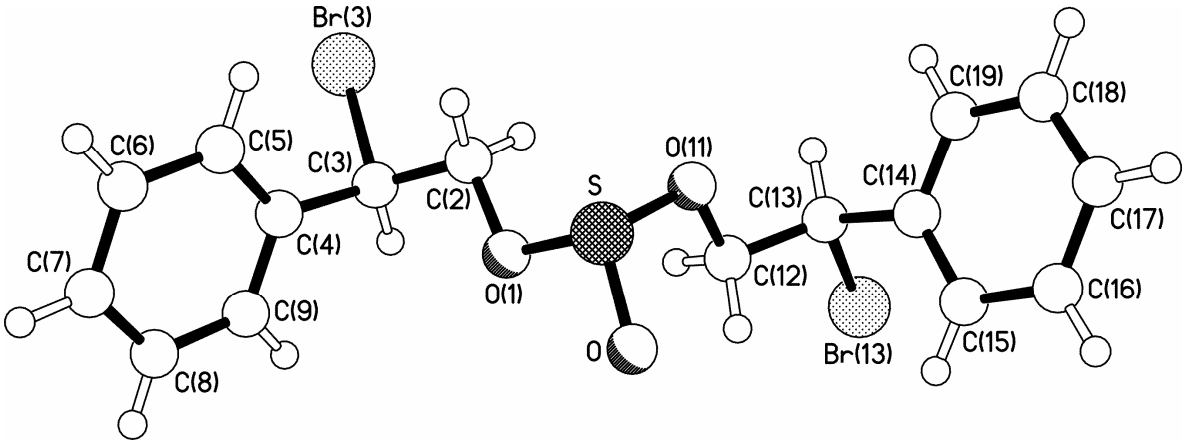

Crystal data and structure refinement for CB0604.

Identification code	CB0604	
Empirical formula	C16 H16 Br2 O3 S	
Formula weight	448.17	
Temperature	173(2) K	
Diffractometer, wavelength	OD Xcalibur PX Ultra, 1.54248 Å	
Crystal system, space group	Monoclinic, I2/a	
Unit cell dimensions	a = 23.8581(2) Å	α = 90°
	b = 5.529 Å	β = 102.5260(10)°
	c = 26.0239(3) Å	γ = 90°
Volume, Z	3351.20(5) $Å^3$, 8	
Density (calculated)	1.777 Mg/m^3	
Absorption coefficient	7.384 mm^{-1}	
F(000)	1776	
Crystal colour / morphology	Colourless platy needles	
Crystal size	0.18 x 0.15 x 0.09 mm^3	
θ range for data collection	3.48 to 71.00°	
Index ranges	-29<=h<=29, -6<=k<=5, -31<=l<=31	
Reflns collected / unique	34847 / 3214 [R(int) = 0.0343]	
Reflns observed [F>4σ(F)]	3080	
Absorption correction	Semi-empirical from equivalents	
Max. and min. transmission	1.00000 and 0.50474	
Refinement method	Full-matrix least-squares on F^2	
Data / restraints / parameters	3214 / 0 / 199	
Goodness-of-fit on F^2	1.112	
Final R indices [F>4σ(F)]	R1 = 0.0549, wR2 = 0.1393	
R indices (all data)	R1 = 0.0566, wR2 = 0.1405	
Largest diff. peak, hole	1.919, -0.646 $eÅ^{-3}$	
Mean and maximum shift/error	0.000 and 0.000	

Bond lengths [Å] and angles [°] for CB0604.

S-O	1.482(6)
S-O(11)	1.618(4)
S-O(1)	1.624(4)
O(1)-C(2)	1.450(7)
C(2)-C(3)	1.451(9)
C(3)-C(4)	1.526(8)
C(3)-Br(3)	1.989(6)
C(4)-C(9)	1.369(9)

C(4)-C(5)	1.379(10)
C(5)-C(6)	1.391(9)
C(6)-C(7)	1.386(8)
C(7)-C(8)	1.372(9)
C(8)-C(9)	1.364(9)
O(11)-C(12)	1.447(7)
C(12)-C(13)	1.476(8)
C(13)-C(14)	1.534(8)
C(13)-Br(13)	1.959(7)
C(14)-C(19)	1.343(9)
C(14)-C(15)	1.397(10)
C(15)-C(16)	1.404(9)
C(16)-C(17)	1.376(9)
C(17)-C(18)	1.364(9)
C(18)-C(19)	1.367(8)

O-S-O(11)	108.3(3)
O-S-O(1)	100.2(3)
O(11)-S-O(1)	99.8(2)
C(2)-O(1)-S	114.4(4)
O(1)-C(2)-C(3)	109.0(5)
C(2)-C(3)-C(4)	114.7(6)
C(2)-C(3)-Br(3)	105.9(4)
C(4)-C(3)-Br(3)	108.9(4)
C(9)-C(4)-C(5)	118.8(5)
C(9)-C(4)-C(3)	113.7(6)
C(5)-C(4)-C(3)	127.5(6)
C(4)-C(5)-C(6)	121.2(5)
C(7)-C(6)-C(5)	118.7(6)
C(8)-C(7)-C(6)	119.5(5)
C(9)-C(8)-C(7)	121.2(6)
C(8)-C(9)-C(4)	120.6(6)
C(12)-O(11)-S	115.6(4)
O(11)-C(12)-C(13)	108.0(5)
C(12)-C(13)-C(14)	113.3(5)
C(12)-C(13)-Br(13)	107.2(5)
C(14)-C(13)-Br(13)	110.0(4)
C(19)-C(14)-C(15)	119.7(5)
C(19)-C(14)-C(13)	115.3(6)
C(15)-C(14)-C(13)	125.0(6)
C(14)-C(15)-C(16)	119.7(6)
C(17)-C(16)-C(15)	118.9(6)
C(18)-C(17)-C(16)	119.6(5)
C(17)-C(18)-C(19)	121.6(6)
C(14)-C(19)-C(18)	120.4(6)

CB0701; (1*R,2*S**)-2-Bromo-1-chloro-1-phenylpropane (274)**

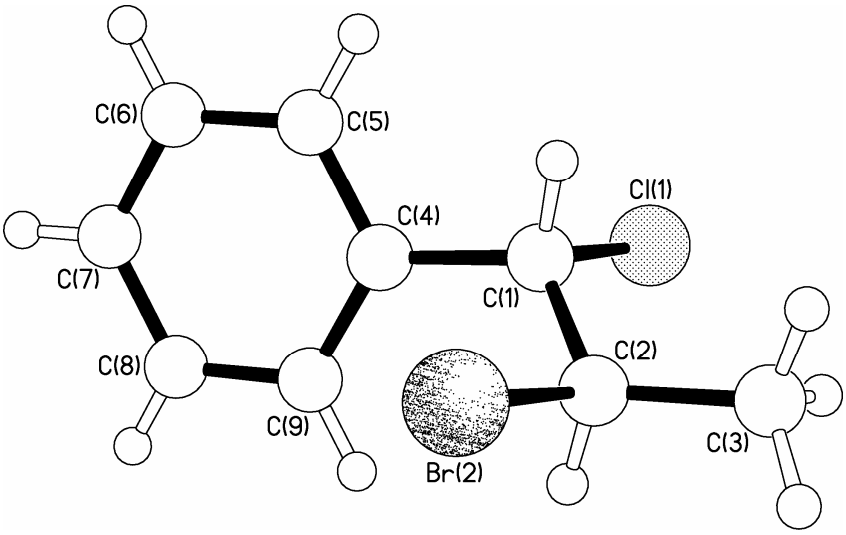

Crystal data and structure refinement for CB0701.

Identification code	CB0701	
Empirical formula	C9 H10 Br Cl	
Formula weight	233.53	
Temperature	173(2) K	
Diffractometer, wavelength	OD Xcalibur PX Ultra, 1.54248 Å	
Crystal system, space group	Monoclinic, I2/a	
Unit cell dimensions	a = 18.7196(5) Å	α = 90°
	b = 5.48830(10) Å	β = 104.159(3)°
	c = 19.2225(5) Å	γ = 90°
Volume, Z	1914.90(8) $Å^3$, 8	
Density (calculated)	1.620 Mg/m^3	
Absorption coefficient	7.877 mm^{-1}	
F(000)	928	
Crystal colour / morphology	Colourless needles	
Crystal size	0.24 x 0.02 x 0.02 mm^3	
θ range for data collection	4.75 to 62.93°	
Index ranges	-20<=h<=21, -6<=k<=5, -22<=l<=21	
Reflns collected / unique	3799 / 1508 [R(int) = 0.0188]	
Reflns observed [F>4σ(F)]	1270	
Absorption correction	Semi-empirical from equivalents	
Max. and min. transmission	1.00000 and 0.67847	

Refinement method	Full-matrix least-squares on F^2
Data / restraints / parameters	1508 / 21 / 131
Goodness-of-fit on F^2	1.101
Final R indices [F>4σ(F)]	R1 = 0.0278, wR2 = 0.0749
R indices (all data)	R1 = 0.0337, wR2 = 0.0773
Largest diff. peak, hole	0.490, -0.228 eÅ^{-3}
Mean and maximum shift/error	0.000 and 0.001

Bond lengths [Å] and angles [°] for CB0701.

C(1)-C(2)	1.480(7)
C(1)-C(4)	1.526(6)
C(1)-Cl(1)	1.830(8)
C(2)-C(3)	1.491(7)
C(2)-Br(2)	1.975(6)
C(4)-C(5)	1.3900
C(4)-C(9)	1.3900
C(5)-C(6)	1.3900
C(6)-C(7)	1.3900
C(7)-C(8)	1.3900
C(8)-C(9)	1.3900
C(1')-C(2')	1.500(8)
C(1')-C(4')	1.520(7)
C(1')-Cl(1')	1.820(8)
C(2')-C(3')	1.608(11)
C(2')-Br(2')	1.960(8)
C(4')-C(5')	1.3900
C(4')-C(9')	1.3900
C(5')-C(6')	1.3900
C(6')-C(7')	1.3900
C(7')-C(8')	1.3900
C(8')-C(9')	1.3900

C(2)-C(1)-C(4)	117.7(4)
C(2)-C(1)-Cl(1)	110.0(6)
C(4)-C(1)-Cl(1)	106.9(5)
C(1)-C(2)-C(3)	117.2(6)
C(1)-C(2)-Br(2)	107.4(3)
C(3)-C(2)-Br(2)	111.6(5)
C(5)-C(4)-C(9)	120.0
C(5)-C(4)-C(1)	116.1(4)
C(9)-C(4)-C(1)	123.9(4)
C(4)-C(5)-C(6)	120.0
C(5)-C(6)-C(7)	120.0
C(6)-C(7)-C(8)	120.0
C(9)-C(8)-C(7)	120.0
C(8)-C(9)-C(4)	120.0
C(2')-C(1')-C(4')	115.4(5)
C(2')-C(1')-Cl(1')	108.3(6)
C(4')-C(1')-Cl(1')	109.5(6)

C(1')-C(2')-C(3')	106.5(7)
C(1')-C(2')-Br(2')	107.3(5)
C(3')-C(2')-Br(2')	106.0(7)
C(5')-C(4')-C(9')	120.0
C(5')-C(4')-C(1')	117.8(5)
C(9')-C(4')-C(1')	122.2(6)
C(4')-C(5')-C(6')	120.0
C(5')-C(6')-C(7')	120.0
C(8')-C(7')-C(6')	120.0
C(7')-C(8')-C(9')	120.0
C(8')-C(9')-C(4')	120.0

CB0703; (2*R*)-5-Bromomethyl-3-oxa-2-methyl-δ-pentano-5-lactone (220)

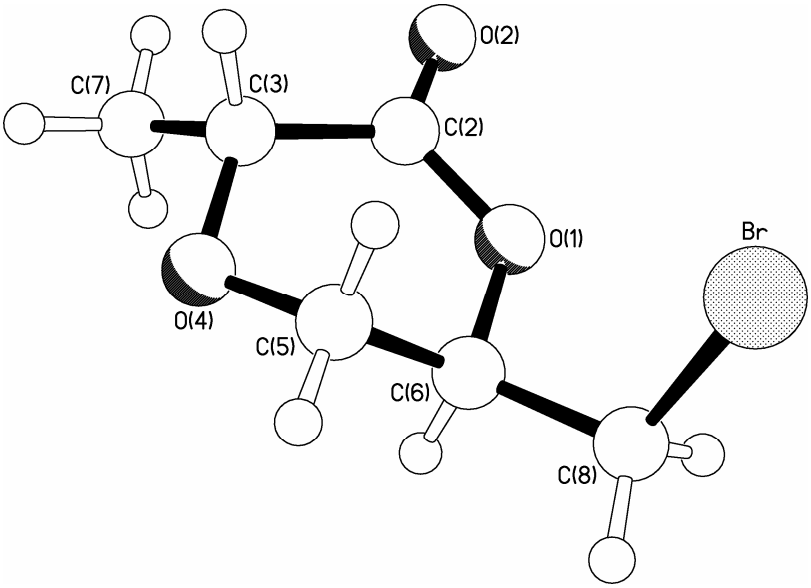

Crystal data and structure refinement for CB0703.

Identification code	CB0703	
Empirical formula	C6 H9 Br O3	
Formula weight	209.04	
Temperature	173(2) K	
Diffractometer, wavelength	OD Xcalibur 3, 0.71073 Å	
Crystal system, space group	Orthorhombic, P2(1)2(1)2(1)	
Unit cell dimensions	a = 6.94127(12) Å	α = 90°
	b = 8.74587(16) Å	β = 90°
	c = 12.6315(2) Å	γ = 90°
Volume, Z	766.83(3) $Å^3$, 4	
Density (calculated)	1.811 Mg/m^3	

Absorption coefficient	5.306 mm^{-1}
F(000)	416
Crystal colour / morphology	Colourless needles
Crystal size	0.34 x 0.14 x 0.03 mm^3
θ range for data collection	3.75 to 32.48°
Index ranges	-10<=h<=10, -13<=k<=13, -18<=l<=18
Reflns collected / unique	25731 / 2658 [R(int) = 0.0697]
Reflns observed [F>4σ(F)]	1876
Absorption correction	Analytical
Max. and min. transmission	0.806 and 0.366
Refinement method	Full-matrix least-squares on F^2
Data / restraints / parameters	2658 / 0 / 91
Goodness-of-fit on F^2	0.973
Final R indices [F>4σ(F)]	R1 = 0.0315, wR2 = 0.0642
	R1+ = 0.0315, wR2+ = 0.0642
	R1- = 0.0596, wR2- = 0.1506
R indices (all data)	R1 = 0.0558, wR2 = 0.0699
Absolute structure parameter	x+ = 0.000(10), x- = ***
Largest diff. peak, hole	0.736, -0.540 $eÅ^{-3}$
Mean and maximum shift/error	0.000 and 0.001

Bond lengths [Å] and angles [°] for CB0703.

O(1)-C(2)	1.345(2)
O(1)-C(6)	1.459(3)
C(2)-O(2)	1.197(3)
C(2)-C(3)	1.514(3)
C(3)-O(4)	1.429(3)
C(3)-C(7)	1.507(4)
O(4)-C(5)	1.425(3)
C(5)-C(6)	1.502(3)
C(6)-C(8)	1.504(3)
C(8)-Br	1.946(2)

C(2)-O(1)-C(6)	120.16(16)
O(2)-C(2)-O(1)	118.40(19)
O(2)-C(2)-C(3)	121.10(19)
O(1)-C(2)-C(3)	120.47(19)
O(4)-C(3)-C(7)	107.58(17)
O(4)-C(3)-C(2)	114.29(17)
C(7)-C(3)-C(2)	111.1(2)
C(5)-O(4)-C(3)	111.36(16)
O(4)-C(5)-C(6)	107.67(18)

O(1)-C(6)-C(5)	109.68(16)
O(1)-C(6)-C(8)	106.92(16)
C(5)-C(6)-C(8)	117.07(19)
C(6)-C(8)-Br	112.93(15)